DISSERTATION

FUNCTIONAL ANALYSES OF ζ-CRYSTALLIN BINDING TO THE 3'-UTR OF GLUTAMINASE (GA) mRNA

Submitted by

Hend M.M. Ibrahim

Department of Biochemistry and Molecular Biology

In partial fulfillment of the requirements

For the Degree of Doctor of Philosophy

Colorado State University

Fort Collins, Colorado

Fall 2006

COLORADO STATE UNIVERSITY

September 12, 2006

WE HEREBY RECOMMEND THAT THE DISSERTATION PREPARED UNDER OUR SUPERVISION BY HEND M. M. IBRAHIM ENTITLED "FUNCTIONAL ANALYSES OF ζ-CRYSTALLIN BINDING TO THE 3'-UTR OF GLUTAMINASE (GA) mRNA" BE ACCEPTED AS FULFILLING IN PART REQUIREMENTS FOR THE DEGREE OF DOCTOR OF PHILOSOPHY.

Committee on Graduate Work

Jim Bamburg

Paul Laybourn

Laurie A. Stargell

Donald Mykles

Advisor- Norman P. Curthoys

Department Head- Marvin R. Paule

ABSTRACT OF DISSERTATION

FUNCTIONAL ANALYSES OF ζ-CRYSTALLIN BINDING TO THE 3'-UTR OF GLUTAMINASE (GA) mRNA

Chronic metabolic acidosis is associated with increased expression of renal glutaminase (GA) that results from selective stabilization of the GA mRNA. LLC-PK_1-$FBPase^+$ cells, a pH-responsive porcine kidney cell line, express four distinct GA mRNAs, that are ~2.5, 3.5, 4.5, and 5.0 kb in length. RNase H mapping indicated that three of the GA mRNAs are generated by the use of alternative polyadenylation sites and they are homologs of the rat kidney glutaminase (KGA) mRNA, while the 4.5 kb GA mRNA contains a different COOH-terminal coding and 3'-untranslated sequence. PCR cloning and sequencing confirmed that the 4.5 kb GA mRNA is the homolog of the human GA mRNA. Sequence analysis established that the 3'-untranslated regions (3'-UTR) of the 4.5 kb GA mRNA contains the 8-base adenylate-uridylate (AU) sequence that functions as a pH-responsive element (pHRE)

The pHRE binds ζ-crystallin /NADPH:quinone reductase (ζ-crystallin) with high affinity and specificity. Analysis of the influence of ζ-crystallin abundance on the GA mRNA level and stability was performed *in vivo*. LLC-PK_1-$FBPase^+$ cells that stably express a β-globin-glutaminase (βG-GA) construct were used to generate stable cell lines that over-express mouse ζ-crystallin. Western analysis established that a 4-fold increase in ζ-crystallin expression was obtained. An adenovirus was also used to over-express mouse ζ-crystallin. This approach produced 100-fold more mouse ζ-crystallin than the endogenous protein. An adenovirus that expresses a short interfering RNA (siRNA)

reduced the expression of ζ-crystallin by 90% compared to the endogenous protein in uninfected or in control cells. GA mRNA level and stability were determined with Northern blot and half-life analyses. No significant changes in the levels or stability of βG-GA mRNA were observed as a result of the increased or reduced abundance of ζ-crystallin. Thus, changes in ζ-crystallin levels are not sufficient to affect the turnover or the pH-responsive stabilization of the GA mRNA. However, the possibility that events promoting modifications of ζ-crystallin may affect its interaction with the GA mRNA or with other factors that affect its stability cannot be excluded. Various kidney cells express multiple isoforms of AUF1, an AU-binding protein that enhances mRNA turnover. RNA gel-shift assays demonstrated that the recombinant p40 isoform of AUF1 binds to the pHRE with high affinity and specificity. Thus, AUF1 may mediate the rapid turnover of the GA mRNA.

Hend M.M. Ibrahim
Department of Biochemistry
and Molecular Biology
Fort Collins, CO 80523
Fall 2006

ACKNOWLEDGMENTS

First of all, I would like to express my deepest sense of gratitude to my supervisor Dr. Norman Curthoys for his patient, guidance, encouragement and excellent advice throughout this study. I appreciate all assistance he provided through my entire graduate career. I would also like to thank my committee members, Dr. James Bamburg, Dr Paul Laybourn, Dr. Laurie Stargell, and Dr. Donald Mykles, for their help, support and ideas.

I am thankful to all previous and current members of Dr. Curthoy's lab for their friendship, support, and research advice especially Lynn Taylor, Dr. Jill Schroeder, Dr. Sachin Hajarnis, Yoen Lee and Dr. Marry Robenson

I would like to thank all people that made this work possible especially Dr. Gul-Shad Ali, Aida Ulloa, Dr. Barbara Sanborn, Dr. Colin Clay, Dr. Jeff Wilusz and Dr. Carol Wilusz for sharing ideas and providing vectors. Special thanks to all members of Biochemistry Department at Zagazig University, Egypt.

I would also like to express my sincere thanks to my Husband Dr. Salah Abdel-Ghany for his love, support, encouragement and valuable advice in science discussion, help in writing my thesis. I am deeply and forever indebted to my daughter (Hadeel) and my son (Ahmad) for being wonderful kids. They always supported me with their love, patient and understanding of how much I was busy.

Finally, I take this opportunity to express my profound gratitude to my beloved parent for their moral support and patience that always was a motivation in my achievements throughout my life. Without their love, advice I would never been where I am today.

TABLE OF CONTENTS

LIST OF FIGURES

ABBREVIATIONS

3'-UTR - 3'-untranslated region

5'-cap - 5'-7-methyl-guanosine cap

+/- S.E. – plus or minus the standard error

ARE - AU-rich element

ATP – adenosine triphosphate

AU-rich - adenylate- and uridylate- rich

b – base

bp – base pair

βG – β-globin

bGH - bovine growth hormone

BCIP - 5-bromo-4-chloro-3-indolyl phosphate, p-toluidine salt

BME - β-mercaptoethanol

BSA – bovine serum albumin

CMV - cytomegalovirus

DEPC - diethyl pyrocarbonate

DNA – deoxyribonucleic acid

Dox - doxycycline

DRB - 5,6-dichlorobenzimidazole 1-β-D-ribofuranoside

dsRNA - double-stranded RNA

DTT - dithiothreitol

EDTA - ethylenediaminetetraacetic acid

EJC - exon junction complex

ELAV - embryonic lethal abnormal visual

EMSA - Electrophoretic Mobility Shift Assay

ErEN - erythroid cell-enriched endoribonuclease

FBPase - fructose 1,6-bisphosphatase

FPLC - fast protein liquid chromatography

G418 – geneticin

Gln - Glutamine

GAPDH - glyceraldehyde-3-phosphate dehydrogenase

GDH - glutamate dehydrogenase

GA - glutaminase

GAC- glutaminase carcinoma isoform

GM-CSF - granulocyte-macrophage colony-stimulating factor

hnRNP - heterogeneous nuclear ribonucleoprotein

IRE - iron-responsive element

IRP - iron regulatory protein

JNK - c-jun N-terminal kinase

kb – kilobase

kDa – kilodalton

KGA - kidney-type glutaminase

LAT2- an isoform of the Na^+-independent system L family of amino acid transporters

LGA - liver-type glutaminase

LLC-PK_1-F^+ cells - LLC-PK_1-$FBPase^+$ cells

Luc - luciferase

MAPK - mitogen-activated protein kinase

mCRD - major protein-coding-region determinant of instability

miRNAs - micro RNAs

MKK - mitogen-activated protein kinase kinase

MOPS - 3-(N-morpholino)propanesulfonic acid

mRNA – messenger ribonucleic acid

mRNP - messenger ribonucleoproteins

NaDC - Na^+/dicarboxylate co-transporter

$Na^+/3HCO_3^-$ co-transporter

NBT - nitroblue tetrazolium

NHE3 - Na^+/H^+ exchanger

NMD - nonsense-mediated decay

NSD - nonstop decay process

nt - nucleotide

oligo - oligodeoxynucleotide

PABP - poly (A) binding protein

PAGE – polyacrylamide gel electrophoresis

PAIP-1 - PABP-interacting protein 1

pβG - β-globin/growth hormone vector

PBS – phosphate buffered saline

pBSSK - pBluescript II SK (-)

PAN1 - PABP-dependent poly (A) nuclease

PARN - poly (A) ribonuclease

PCR – polymerase chain reaction

PEPCK - phosphoenolpyruvate carboxykinase

pH_i - intracellular pH

pHRE - pH-responsive element

PI3-K - phosphatidylinositol 3-kinase

PminCMV - minimal immediate early promoter of cytomegalovirus PMR-1 - polysomal ribonuclease 1

PMSF - phenylmethylsulfonylfluoride

pol II – polymerase II

RISC - RNA-induced silencing complex

RNA – ribonucleic acid

RNAi - RNA interference

RNase – ribonuclease

RSV - Rous sarcoma virus long terminal repeat promoter SAPK - stress-activated protein kinase

SDS - sodium dodecylsulfate

SGLT1 - Na+/glucose cotransporter

siRNAs - Short interfering RNAs

SN1- system N

SR - serine/arginine-rich proteins

$t_{1/2}$ – half-life

TCA - tricarboxylic acid

tet - tetracycline

tetO - tetracycline operator sequence

TetR - tet repressor

TNF-α - tumor necrosis factor alpha

TRE - tetracycline-responsive element

TTP - tristetraprolin

U - units

UV – ultraviolet

VP16 - virion protein 16

WT - wild type

ζ-crys/Nqr - ζ-crystallin/NADPH:quinone reductase

ζ-crystallin - ζ-crystallin/NADPH:quinone reductase

1 INTRODUCTION

1.1 Glutamine

Traditionally, glutamine has been classified as a non-essential amino acid due to its rapid synthesis from glutamate and ammonia in various cells. However, it has recently been re-classified as a conditionally essential amino acid (Neu et al., 1996) due to its efficacy in treating patients who are recovering from trauma, major surgery or sepsis. Glutamine constitutes more than 60% of the free amino acids within the body (Curthoys and Watford, 1995). It is synthesized in mammalian tissues by glutamine synthetase that catalyzes the ATP-dependent conversion of glutamate and an ammonium ion into glutamine. Glutamine synthetase is a cytosolic enzyme that is highly expressed in muscle, lung and adipose tissues. Mitochondrial glutaminase initiates the catabolism of glutamine by catalyzing the hydrolytic cleavage to form glutamate and an ammonium ion. Plasma glutamine is normally maintained at a concentration of 0.5-0.8 mM (Souba, 1991). It plays an important role as a carrier of nitrogen, carbon, and energy between organs. Glutamine has an important role in hepatic urea synthesis, renal ammoniagenesis, gluconeogenesis in both liver and kidney, and as a major respiratory fuel for many cells including those of the small intestine, thymocytes, lymphocytes, macrophages, fetal cells, hair follicles, and many tumor cells (Curthoys and Watford, 1995). In addition to its tissue specific functions, glutamine serves as a precursor for the synthesis of nitrogen containing compounds in all cells. For instance, glutamine is utilized in the synthesis of pyrimidines, purines, glucosamine and other amino acids (Curthoys and Watford, 1995).

1.2 Glutaminase (GA)

Many enzymes can utilize glutamine as a substrate, however, only one produces stoichiometric amounts of glutamate and ammonia, and thus can be classified as a true glutaminase. This enzyme is also known as phosphate-dependant glutaminase, glutaminase I, or mitochondrial glutaminase (Meister, 1975) and catalyses the hydrolysis of glutamine by the following reaction:

$$\text{L-glutamine} + H_2O \text{ ---------> L-glutamate}^- + NH_4^+$$

The body expresses two isoforms of the mitochondrial glutaminase as originally reported by Krebs (Krebs, 1935), the liver-type glutaminase (LGA) and kidney-type glutaminase (KGA). In the rat, LGA is expressed only in periportal hepatocytes of the postnatal liver and is important in coupling ammonia production with urea synthesis. KGA is expressed in kidney, brain, intestine, fetal liver, and lymphocytes. The two isoenzymes have different structural and kinetic properties that contribute to their function and short-term regulation. The two isozymes also differ in their pH optima and their inhibition by the end product of the reaction, glutamate (Meister, 1975). Kidney-type GA is found in association with the inner mitochondrial membrane and free in the mitochondrial matrix (Curthoys, 1984, Shapiro et al., 1982). It requires a polyvalent anion such as phosphate for activity. In the absence of phosphate or other polyvalent anion, GA forms an inactive dimer. In the presence of phosphate, two dimers associate to form the functional tetrameric enzyme (Curthoys, 1984). Kidney type GA has a K_m of 2-5 mM for glutamine, and is strongly inhibited by glutamate (Curthoys, 1984). Both glutamine and glutamate interact at the same active site of the kidney-type GA (Shapiro et al., 1982). The specificity of this site is determined by the phosphate concentration and

the extent of tetramer formation. By contrast, liver-type GA is located in the mitochondrial matrix in loose association with the inner membrane and is only expressed in post-natal liver (Smith and Watford, 1990). It has a K_m of 17 mM for glutamine and glutamate does not inhibit its activity even at a concentration of up to 50 mM (McGivan, 1988).

Kidney-type GA purified from rat brain is composed of 66- and 68-kDa peptides that are present in a 3:1 ratio (Shapiro et al., 1987). The 66- and 68-kDa peptides arise from differential processing of a 74-kDa precursor which is generated from a single mRNA. Incubation of the precursor polypeptide with isolated rat liver mitochondria results in translocation and the synthesis of the mature subunits of GA. *In vitro* transcription and translation of the full length GA cDNA produces a single 74-kDa polypeptide (Shapiro et al., 1991). The 74-kDa precursor is initially processed to a 72-kDa intermediate, which is subsequently cleaved to generate either of the two mature forms of GA (Perera et al., 1990).

The two isoenzymes are subject to long-term regulation. Hepatic glutaminase is increased during starvation, diabetes, and feeding a high-protein diet, whereas kidney-type glutaminase is increased only in kidney in response to metabolic acidosis. The adaptations in hepatic glutaminase are mediated by changes in the rate of transcription, whereas kidney-type glutaminase is regulated at a posttranscriptional level. Kidney-type GA has been purified from different organisms including pig kidney (Kvamme et al., 1970), pig brain (Svenneby et al., 1973), rat kidney (Curthoys and Godfrey, 1976), cow brain (Chiu and Boeker, 1979), rat brain (Haser et al., 1985), and *Ehrlich ascites* tumor cells (Quesada et al., 1988).

1.3 Normal acid base balance

The normal pH of arterial blood is 7.4, whereas the pH of venous blood and interstitial fluids is 7.35 because of the carbon dioxide (CO_2) released from the tissues forms HCO_3^- in these fluids. Acidosis occurs when the pH of arterial blood falls below 7.4, whereas, a pH greater than 7.4 produces an alkalosis. The lower limit of pH at which a person can live for only a few hours is about 6.8 with an upper limit of about 8.0. The intracellular pH (pH_i) is usually lower than plasma pH because the metabolism of the cells produces acid, mainly HCO_3^- and ranges between 6.0 and 7.4. The pH of urine can range from 4.5 to 8.0, depending on the acid-base status of the extracellular fluid.

1.4 Metabolic acidosis

Metabolic acidosis results from a decrease in the bicarbonate (HCO_3^-) concentration in the extracellular fluids. By contrast, respiratory acidosis is caused by excess CO_2. Metabolic acidosis can result from several general causes: failure of the kidneys to recover the bicarbonate that is normally filtered by the glomeruli, excess production of metabolic acids in the body (ketoacidosis, lactic acidosis); ingestion of a high protein diet that results in a net production of acids; or ingestion of metabolic acids or compounds that are rapidly oxidized to acids (acetylsalicylates or methyl alcohol). Metabolic acidosis can also result from specific metabolic conditions or diseases such as renal tubular acidosis, diarrhea, diabetes and chronic renal failure.

1.5 Glutamine metabolism in normal acid base balance

During normal acid base balance, very little of the plasma glutamine is extracted and catabolized by the kidney (Squires et al., 1976). The measured renal arteriovenous difference is less than 3% of the arterial concentration of glutamine. However, approximately 20% of the plasma glutamine is filtered by the glomeruli and enters the lumen of the nephron. The filtered glutamine is reabsorbed by the epithelial cells of the proximal convoluted tubules (Silbernagl, 1980). Most of the glutamine that is transported into the cell is transported across the basolateral membrane via LAT2, an isoform of the Na^+-independent system L family of amino acid transporters (Bode, 2001). Glutamine that is retained in the proximal tubule cells is then transported into the mitochondria via a mersalyl-sensitive electroneutral uniporter (Sastrasinh and Sastrasinh, 1989), where it is deamidated by the mitochondrial glutaminase (GA) to glutamate. Glutamate is then oxidatively deaminated by glutamate dehydrogenase (GDH) to form α-ketoglutarate, which enters the citric acid cycle. Approximately two-thirds of ammonium ions produced as a result of the activities of GA and GDH are trapped in the tubular lumen and excreted into slightly acidified urine (Fig. 1.1).

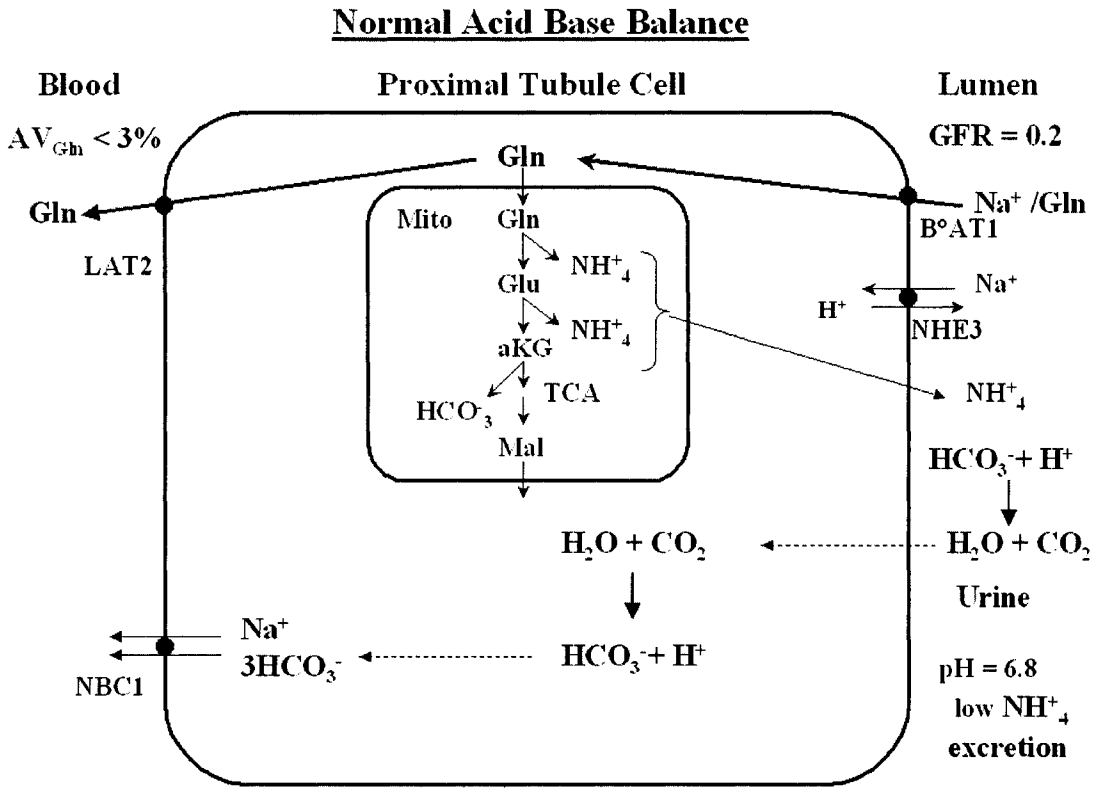

Fig. 1.1: Renal glutamine catabolism and bicarbonate reabsorption during normal acid-base balance. The glomerular filtrate is slightly acidified by the apical NHE3. The translocated H^+ ions titrate most of the filtered bicarbonate ions producing carbonic acid, which is converted to CO_2 and H_2O by the apical carbonic anhydrase. The CO_2 diffuses into the proximal tubule and is hydrated by the cellular carbonic anhydrase to reform bicarbonate ions that are translocated across the basolateral membrane by NBC1. The glutamine filtered by the glomeruli is transported across the apical membrane by B°AT1. Most of the recovered glutamine is then transported across the basolateral membrane by LAT2. A small proportion of the recovered glutamine is transported into the mitochondria where it is catabolized to generate the basal level of ammonium ions that are excreted in the slightly acidified urine. Adapted from 'The Kidney: Physiology and Pathophysiology' 4th Edition. Chapter 67. Renal ammonium ion production and excretion. Curthoys NP

1.6 Acute acidosis

Increased ammoniagenesis and gluconeogenesis from plasma glutamine partially restores acid-base balance during metabolic acidosis (Brosnan et al., 1987). The renal catabolism of glutamine is activated following the onset of metabolic acidosis. The arterial plasma glutamine concentration increases by two fold within 1 to 3 h due to glutamine release from muscle tissue (Hughey et al., 1980). Significant renal extraction of glutamine becomes evident as the arterial plasma concentration is increased. The net glutamine extraction reaches 30% of the plasma level, a level that exceeds the percent filtered by the glomeruli. Thus, the direction of the basolateral glutamine transporter (SN1) must be reversed in order for the proximal convoluted tubule to extract glutamine from both the glomerular filtrate and the venous blood. The transport of glutamine into the mitochondria is also acutely activated (Sastrasinh and Sastrasinh, 1990). Acidification of the urine occurs due to activation of NHE 3 (the apical Na^+/H^+ exchanger) (Peng et al., 2001) and its translocation to the apical membrane (Yang et al., 2000). This adaptation facilitates the rapid excretion of the cellular ammonium ions that are produced from the amide and amine nitrogens of glutamine into the urine (Tannen and Ross, 1979). Lastly, a pH-induced activation of α-ketoglutarate dehydrogenase results in decreases in the concentrations of glutamate and α-ketoglutarate (Lowry and Ross, 1980). Thus, acute acidosis produces an increase in the catabolism of glutamine that results from a rapid activation of the key transport processes, increased glutamine availability, and a decreased concentration of the products of the GA and the GDH reactions. These adaptations result in a rapid and pronounced increase in the excretion of ammonium ions

and titratable acids in the urine which help the partial restoration of acid–base balance (Sleeper et al., 1978) (Fig. 1.2).

1.7 Chronic acidosis

During chronic metabolic acidosis, most of the acute adaptations are partially compensated, but the kidneys continue to extract more than one third of the total plasma glutamine in a single pass. This is associated with increased expression of the genes that encode the mitochondrial glutaminase (GA) (Curthoys and Lowry, 1973), mitochondrial glutamate dehydrogenase (GDH) (Wright and Knepper, 1990a), and the cytoplasmic phosphoenolpyruvate carboxykinase (PEPCK) (Burch et al., 1978) to facilitate the renal catabolism of the absorbed glutamine. The activities of these three enzymes as well as gluconeogenesis are increased only in the proximal tubule cells, which is also the primary site of renal ammoniagenesis (Burch et al., 1978). The decreases in the plasma pH and HCO_3^- concentration during metabolic acidosis produce a comparable and sustained decrease in the intracellular pH (pH_i) within the proximal convoluted tubule (Ackerman et al., 1981; Sahai et al., 1990). Thus, the adaptive increases in gene expression and the activities of the encoded enzymes may be initiated by a decrease in pH_i. The adaptations in GA and PEPCK levels result from increases in the levels of their mRNAs that correlated with increased rates of synthesis of the proteins (Cimbala et al., 1982; Hwang et al., 1991). The increase in the PEPCK mRNA levels is due to enhanced transcription of the PEPCK gene (Hanson and Reshef, 1997) while the increases in the GA mRNA levels are produced by mRNA stabilization (Laterza et al., 1997). The activities of many transporters are also increased during acidosis; the apical Na^+/dicarboxylate co-transporter, NaDC-1 (Aruga et al., 2000), the mitochondrial glutamine transporter

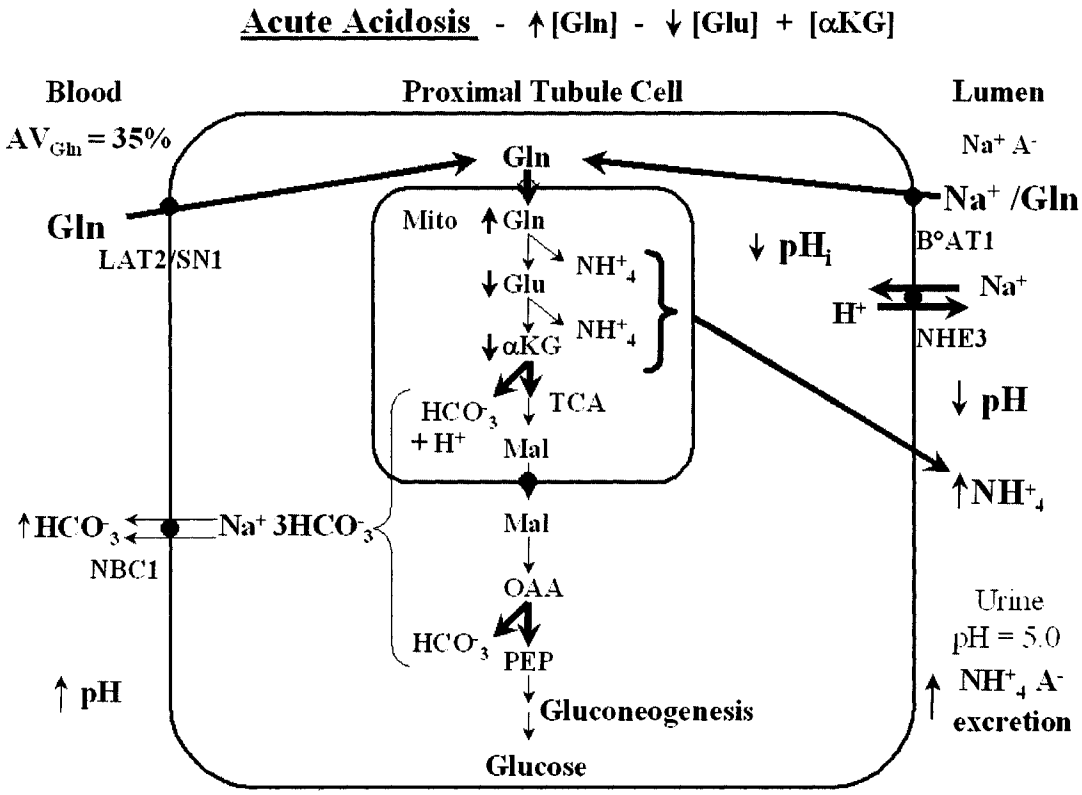

Fig. 1.2: Renal glutamine catabolism and bicarbonate reabsorption during acute acidosis. Acute acidosis produces a decrease in intracellular pH (pH_i) that activates the flux through α-ketoglutarate dehydrogenase and causes translocation and activation of NHE3. The former effect produces a decrease in cellular α-ketoglutarate and glutamate levels that increases flux through glutamate dehydrogenase and glutaminase, respectively. The latter causes a prompt acidification of the urine and facilitates the excretion of ammonium ions. There is a rapid activation of the mitochondrial glutamine transporter and an enhanced transcription of the PEPCK gene. The latter response may contribute to the decrease in cellular α-ketoglutarate and glutamate levels. The combined increases in renal ammonium ion excretion and gluconeogenesis produce a net synthesis of bicarbonate ions.

Adapted from 'The Kidney: Physiology and Pathophysiology' 4th Edition. Chapter 67. Renal ammonium ion production and excretion. Curthoys NP

(Sastrasinh and Sastrasinh, 1990), the basolateral SN1 glutamine transporter (Karinch et al., 2002), the apical Na^+/H^+ exchanger, NHE3 (Preisig and Alpern, 1988), the basolateral $Na^+/3HCO_3^-$ co-transporter, NBC1 (Preisig and Alpern, 1988) and the medullary Na^+K^+-$2Cl^-$ co-transporter (Karim et al., 2003) (Fig. 1.3). The increase in the apical Na^+/H^+ exchanger increases the acidity of the fluid in the tubular lumen and facilitates the excretion of ammonium ion.

During chronic acidosis, the increase in renal amoniagenesis provides an expendable cation that facilitates the excretion of titratable acids while conserving sodium and potassium ions. The α-ketoglutarate generated from glutamine is mainly converted to glucose and to a lesser extent to CO_2. Either process requires the cataplerotic activity of PEPCK to convert intermediates of the tricarboxylic acid cycle to phosphoenolpyruvate (PEP). PEP is either utilized to initiate gluconeogenesis or converted by pyruvate kinase to pyruvate, which then reenters the mitochondria and is oxidized to CO_2. However both pathways generate 2 HCO_3^- ions per molecule of α-ketoglutarate. The increased activity of Na^+/H^+ exchanger also promotes the tubular reabsorption of HCO_3^- ions. The activities of the cytoplasmic citrate lyase and the mitochondrial aconitase are also increased on the onset of acidosis (Aruga et al., 2000). These reactions generate oxaloacetate and isocitrate respectively. The increase in basolateral $Na^+/3HCO_3^-$ co-transporter, NBC1, facilitates the translocation of the reabsorbed and the *de novo*- synthesized HCO_3^- ions into the renal venous blood. The previously mentioned adaptations result in a net production of renal HCO_3^- ions and excretion of acids that contribute to partial restoration acid-base balance.

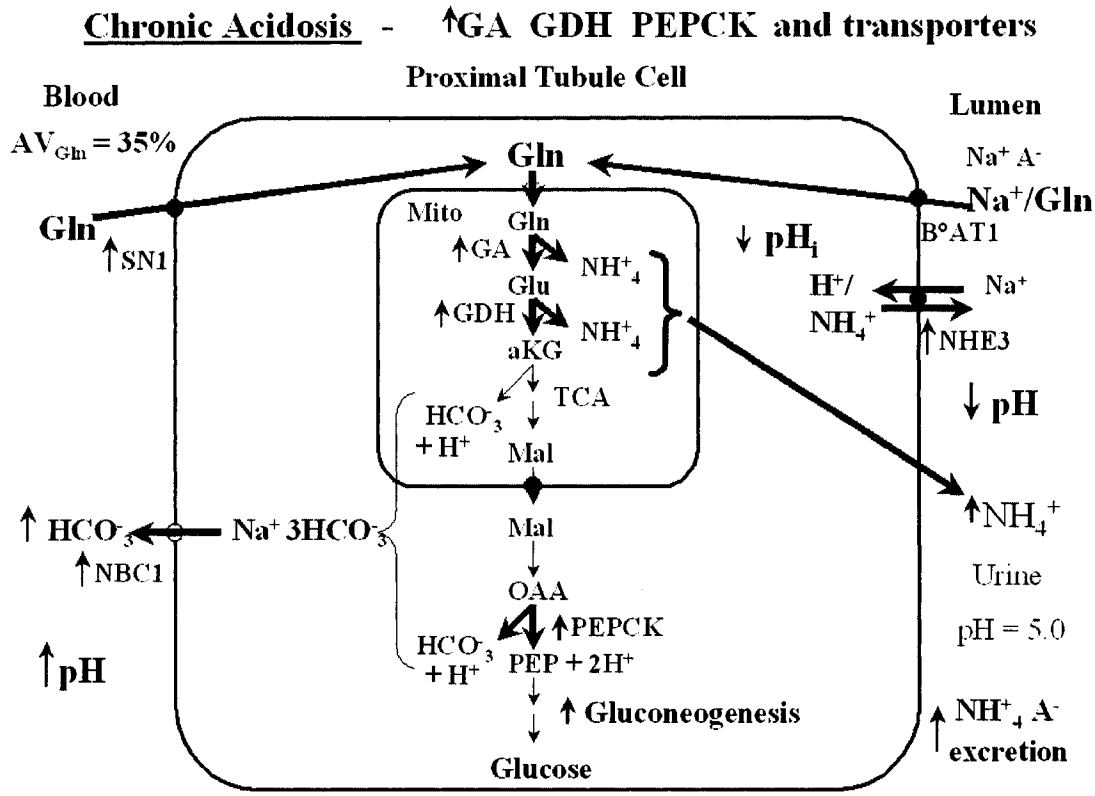

Fig. 1.3: Catabolism of renal glutamine during chronic acidosis. Increased renal catabolism of glutamine is sustained during chronic acidosis by increased expression of the genes that encode glutaminase (GA), glutamate dehydrogenase (GDH), phosphoenolpyruvate carboxykinase (PEPCK), the mitochondrial glutamine transporter, the apical NHE3, the basolateral SN1, and the basolateral NBC1. The increased proteins are indicated by the thicker arrows. Some of the ammonium ions are transported across the apical membrane by NHE3. The combined increases in renal ammonium ion excretion and gluconeogenesis result in a net synthesis of bicarbonate ions.

Adapted from 'The Kidney: Physiology and Pathophysiology' 4th Edition. Chapter 67. Renal ammonium ion production and excretion. Curthoys NP

1.8 mRNA turnover in eukaryotes

Regulation of mRNA turnover is a key mechanism that determines the intracellular abundance of transcripts, thus contributing to the expression of the encoded gene products (Ross, 1995; Guhaniyogi and Brewer, 2001; Wilusz et al., 2001). Eukaryotic mRNAs are synthesized in the nucleus as pre-mRNAs that are processed to mature mRNAs. A 7-methyl guanosine cap is added at the 5'end and a poly (A) tail, containing approximately 200 A's, is added to the 3'end of the pre-mRNA. The introns are then removed by splicing, and the final mature mRNA is exported from the nucleus to the cytoplasm. The nuclear cap binding protein (CBC20/80) binds to the 5'cap, while the nuclear poly (A) binding protein (PABPN1) associates with the 3' poly (A) tail on the mRNA before the export of the mature mRNA to the cytoplasm, (Moore, 2005). During splicing, proteins are deposited at the exon-exon junctions to form the exon junction complex (EJC) (Le Hir et al., 2000). The proteins of the EJC bind in a position-dependent, but sequence-independent manner and some of them remain associated with the mRNA in the cytoplasm. The EJC proteins are involved in mRNA export, mRNA localization, and translational regulation. When present in the 3'-UTRs, the EJC can target the mRNA for degradation via the nonsense mediated decay (NMD) pathway (Tange et al., 2004). The nucleocytoplasmic shuttling hnRNP (heterogenous nuclear proteins) as well as the SR (serine/arginine-rich) proteins are also recruited during transcription and pre-mRNA processing. The hnRNP family of proteins includes hnRNP D (AUF1) (Chen and Shyu, 1995) or hnRNP K (Makeyev and Liebhaber, 2002), which are regulators of the stability of mRNAs.

Once the mRNA reaches the cytoplasm, the start of translation removes most of the nuclear proteins, thus changing the composition of the proteins on the mRNA. In the cytoplasm, the CBC20/80 and PABPN1 are replaced by eIF4E, the cytoplasmic cap binding protein, and by the cytoplasmic poly(A) binding protein (PABPC or Pab1p), respectively. The mRNA can now enter a translationally active pool or a translationally silent state.

mRNAs have limited lifetimes in the cytoplasm. In mammals and yeast two general pathways of mRNA decay have been identified (Parker and Song, 2004) (Fig.1.4). The first step in the general degradation of an mRNA begins with the process of deadenylation, which removes the poly(A) tail. Three different deadenylase complexes have so far been identified. In yeast, the Ccr4/Pop2/Not complex is the predominant deadenylase complex. The Ccr4p, belongs to the ExoIII family of nuclease while, Pop2p belongs to the RNase D family of nuclease. Both of these proteins exhibit deadenylase activity (Daugeron et al., 2001; Tucker et al., 2002). However, they may require other factors such as Not1-Not5p, Caf4, Caf16, Caf40 and Caf130p to deadenylate the RNA (Tucker et al., 2002; Denis and Chen, 2003). The second enzyme complex consists of the Pan2p and Pan3p proteins (Tucker et al., 2001), while the third enzyme is the poly (A) ribonuclease or PARN protein, which may function as a trimer. PARN is not found in the genomes of *S. cerevisiae* and *D. melanogaster,* but is expressed in many eukaryotic organisms. *In vitro* mRNA decay systems indicates that PARN is the major deadenylase in mammalian cells (Gao et al., 2000). The activity of the different deadenylases is dependent upon a variety of factors including the Pab1p or the 7-methylguanosine (m^7Gpp) cap. Binding of Pab1p to the mRNA stimulates Pan2/Pan3 activities (Sachs and

Deardorff, 1992), but inhibits PARN and the Ccr4/Pop2/Not1 complex (Gao et al., 2000; Viswanathan et al., 2003). The cap also stimulates PARN activity (Gao et al., 2000).

After removal of the poly(A) tail, mRNA degradation starts either at the 5'end or at the 3'end of the mRNA. In yeast, the 5'→3' exonucleolytic decay pathway is predominant (Muhlrad et al., 1994) with the 3'→5' exonucleolytic pathway as minor pathway (He et al., 2003). In the 5'→3' decay the decapping activities of Dcp1 and Dcp2 remove the 5'- m^7Gpp cap from mRNA (Steiger et al., 2003). The scavenger-decapping enzyme DcpS is a pyrophosphatase that degrades the released cap to m^7GMP and phosphate (van Dijk et al., 2003). 5'→3' exoribonuclease Xrn1p then rapidly degrades the decapped mRNA. The poly(A) tail controls decapping *in vivo* (Fig 1.4). The poly(A) tail binds the Pabp1, which in turn interacts with eIF4G, a subunit of the cap-binding complex. The cap-binding complex has also been shown to inhibit decapping (Caponigro and Parker, 1995; Wilusz et al., 2001).

In mammalian cells, the 3'→5'decay pathway is the dominant mRNA decay pathway as shown by *in vitro* mRNA decay assays (Mukherjee et al., 2002) with the 5'→3' decay pathway as minor pathway (Fig. 1-4). The cytoplasmic exosome catalyzes the 3'→5' degradation of the deadenylated RNA. The components of the exosome have been identified and purified from yeast and human cells (van Hoof and Parker, 1999; Chen et al., 2001). The exosome is a large complex with ten core proteins that have 3'→5' exonucleolytic activity, and several associated factors that have helicase activity. The exosome is present in both the nucleus and the cytoplasm and is an ATP-dependent activity. The nuclear exosome is involved in the processing of small nuclear and nucleolar RNAs, ribosomal RNAs, and the degradation of pre-rRNA spacers and

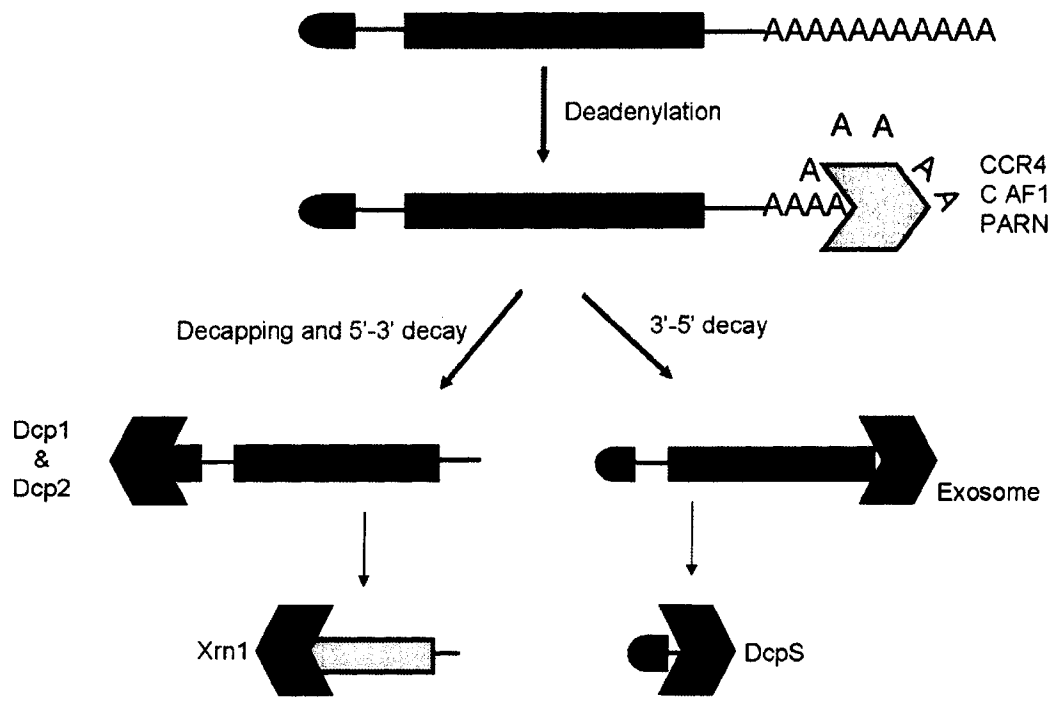

Fig. 1.4: Two pathways to decay mRNA. The first step in decay of mRNAs is removal of the poly(A) tail, which can be catalyzed by several different enzymes. Following deadenylation the body of the mRNA is open to attack from either the 5′ or 3′ ends. A 5′→3′ decay pathway is initiated by removal of the cap structure by the decapping enzymes Dcp1 and Dcp2. The 5′→3′ exonuclease, Xrn1, then degrades the body of the mRNA. Decay from the 3′ end is catalyzed by a large complex of exonucleases termed the exosome, leading to production of m^7GpppX, which can be broken down by the scavenger decapping protein DcpS. In the interests of simplicity we have not depicted any of the mRNA-binding proteins that can dramatically alter the availability of mRNAs for decay. Such proteins can promote interaction of the 5′ and 3′ ends to prevent exonuclease action or act to recruit or inhibit the enzymes themselves. CAF1, CCR4 and PARN are three proteins involved in mRNA deadenylation.

Adapted from (Wilusz and Wilusz, 2004): Bringing the role of mRNA decay in the control of gene expression into focus, Trends in Genetics, 20,491-497.

unspliced pre-mRNAs, while the cytoplasmic exosome is involved in mRNA turnover (Chen et al., 2001). To degrade the cytoplasmic RNA, the cytoplasmic exosome recruits a heterotrimeric complex of Ski2p, Ski3p and Ski8p (Anderson and Parker, 1998; Brown et al., 2000). The Ski2p protein is a member of the DEAD box RNA helicase family and may facilitate the decay process by remodeling the mRNA (Tanner and Linder, 2001). A model of the exosome where the proteins form two complete rings, thus forming a barrel-like structure that sequesters the active sites has been described (Symmons et al., 2002). The exosome may require additional factors to load the mRNAs into the active sites. However, once it is loaded on the mRNA the substrate can be cleaved efficiently and thus prevents premature termination of degradation (van Hoof and Parker, 1999; Parker and Song, 2004).

Other mRNA decay pathways exist in which aberrant transcripts are degraded by the cellular decay machinery. mRNAs that contain a premature translational termination codon are recognized and degraded by a process termed nonsense-mediated decay (NMD). The transcripts are degraded by a deadenylation-independent decapping process or by the cytoplasmic exosome (Lejeune et al., 2003; Mitchell and Tollervey, 2003). Similarly, mRNAs which lack a translation termination codon are recognized and degraded by the cytoplasmic exosome in a process termed the nonstop decay process (NSD) (Frischmeyer et al., 2002; van Hoof et al., 2002).

1.9 AU-Rich Elements (ARE)

The turnover rate of mRNA is determined by both *cis*-elements and *trans*-acting factors (Ross, 1995). Most RNA polymerase II transcripts contain an m7G cap at their 5' end and a poly(A) tail at the 3' end. Specific *cis*-elements in addition to the general cap

and poly(A) tail contribute to the steady state level of mRNA by enhancing degradation or stabilization (Klausner et al., 1993; Ross, 1995). These *cis*-elements can occur anywhere within the mRNA. However, the majority of the resultatory elements are localized to the 3' untranslated region (3'-UTR). In combination with specific *trans*-acting factors, the elements can either stabilize or destabilize the mRNA (Peltz and Jacobson, 1992; Decker and Parker, 1995).

Several proto-oncogene and cytokine mRNAs contain A and U-rich elements (AREs) in their 3'-UTRs which promote rapid degradation of the mRNA (Greenberg and Ausubel, 1993; Decker and Parker, 1995). The half–life of those mRNAs is determined by the AREs within their 3'-UTR (Chen et al., 1995; Ross et al., 1995). Thus mRNAs with short half-lives have adenylate and uridylate (AU) rich elements (ARE) within their 3'-UTRs. AREs can range in size from 50 to 150 nts and have been classified into three classes. Class I AREs contains 1 to 3 scattered copies of the pentanucleotide AUUUA, embedded within a U-rich regions. Examples of these AREs are found in the c-fos and c-myc mRNAs. Class II AREs are only found in cytokine mRNAs such as GM-CSF and TNF-α. They contain multiple overlapping copies (Anderson, 1970) of the AUUUA motif that form a nanomeric sequence, UUAUUUAUU. Class III AREs, such as those present in the c-jun mRNA, lack the AUUUA motif, but contain a U-rich sequence and possibly other unknown features that function as destabilizing elements (Xu et al., 2001).

1.10 RNA binding proteins

RNA binding proteins bind to the AREs and can either stabilize or destabilize the mRNA (Chen and Shyu, 1995), or modulate translation of the mRNA (Ross et al., 1995). A number of ARE binding proteins have been identified such as BRF1 (Stoecklin et al.,

2002), TIA-1, TIAR (Gueydan et al., 1999), KSRP (Min et al., 1997), HuR, tristetraprolin (TTP) and AUF1 (hnRNP D). TIA-1 and the related protein TIAR are translational silencers and are components of stress granules (Zhang et al., 2002). KH-type splicing regulatory protein (KSRP) binds to the ARE of c-Fos and enhances mRNA decay *in vitro* (Chen et al., 2001). KSRP is able to interact with both PARN and the exosome to accelerate turnover (Gherzi et al., 2004).

HuR is a member of the embryonic lethal abnormal vision family (ELVA) of mRNA-binding proteins. It is a 36-kDa protein, containing three RNA recognition motifs, that binds with high affinity to AREs and thus stabilizes specific ARE-containing mRNAs (Peng et al., 1998). Although it is localized mainly in the nucleus, HuR can shuttle between the nucleus and cytoplasm by virtue of its shuttling signal, HNS (HuR nucleocytoplasmic shuttling domain), that is located in the hinge region between its second and third RNA recognition motifs. It is postulated that HuR binds to specific mRNAs in the nucleus, transporting them to the cytoplasm and protecting them from rapid degradation (Atasoy et al., 1998; Brennan and Steitz, 2001).

TTP is the prototype of a group of CCCH tandem zinc finger (TZF) proteins characterized by a CCCH zinc finger motif (Min et al., 1997). TTP binding causes the degradation of the mRNA (Carballo et al., 1998, 2000). TTP enhances mRNA decay at both the deadenylation and 3′→5′ exonucleolytic steps. TTP interacts with the components of the exosome which support that TTP function as destabilizing protein (Chen et al., 2001). TTP exists in variuos phosphorylated forms, which suggests that it may be a target of multiple signaling pathways. It is phosphorylated by ERK-1, p38-MAPK, and MAPK-activated protein kinase 2 (Taylor et al., 1995; Mahtani et al., 2001).

BRF1 and BRF2 are close homologs of TTP and exhibit similar properties (Blackshear, 2002).

AUF1, also known as hnRNPD, is a protein that binds RNA. It exits in four isoforms that are generated by alternative splicing of AUF-1 mRNA (Wagner et al., 1998). The isoforms differ in ARE-binding affinity, nucleocytoplasmic location and ubiquitination. The relative amount of each isoform affects the role of AUF1 on ARE-mediated mRNA decay (Raineri et al., 2004).

1.11 pH-responsive element in the GA 3'-UTR

3'-UTR of GA mRNA has a pH-responsive element that was identified by functional analysis of the 3'-UTR (Hansen et al., 1996). The 3'-UTR of the GA cDNA was cloned into a β-globin/growth hormone (pβG) vector and transfected into the LLC-PK_1-F^+ cells. The stability and levels of the βG mRNA were unaffected when the cells were transferred to acidic medium. The chimeric βG-GA mRNA containing the GA 3'-UTR was destabilized and expressed at lower levels in cells grown in normal medium. However, the βG-GA mRNA was stabilized and increased when the cells were transferred to an acidic medium.

Electrophoretic Mobility Shift Assays (EMSAs) demonstrated that the pH-responsive element of GA mRNA binds to specific proteins in a rat renal cortical cytosolic extracts. (Laterza et al., 1997). Mapping of the GA 3'-UTR identified a 29-base region of the GA 3'-UTR (GA(R2-I)) that contains a direct repeat of two 8-base AREs, UUAAAAUA and UUUAAAUA. Mutations in either element to increase the GC content resulted in a significant decrease in the formation of the RNA-protein complex. When both elements were mutated, the binding was completely abolished (Laterza and

Curthoys, 2000a). Functional studies confirmed that these AREs function as a pH-responsive element (pHRE) (Laterza and Curthoys, 2000a). These studies established that the direct repeat of the AREs are both necessary and sufficient to produce a pH-responsive stabilization of the GA mRNA.

1.12 ζ-crystallin as a pHRE binding protein

Cytosolic extracts of rat renal cortex contain a protein that binds specifically to the GA pHRE. UV-crosslinking studies produced a 48-kDa complex that was visualized by SDS-PAGE (Laterza et al., 1997). Affinity purification of the protein was accomplished using a biotinylated oligoribonucleotide as a ligand (Tang and Curthoys, 2001). The biotinylated RNA protein complex was bound to avidin agarose and packed into a fast protein liquid chromatography (FPLC) column. The eluted protein was identified by mass spectroscopy as ζ-crystallin/NADPH:quinone reductase (ζ-crys/Nqr or ζ-crystallin). The 36-kDa purified protein reacted with anti-ζ-crys/Nqr antibodies on a Western blot and formation of the ζ-crystallin/RNA complex was blocked by the same antibody indicating the specificity of ζ-crystallin binding (Tang and Curthoys, 2001).

ζ-crystallin is a taxon-specific crystallin found in the lens of guinea pig and other hystricomorph rodents and camelids (Huang, 1987; Garland, 1991; Goenka, 2001). In other animals, it is a ubiquitous enzyme that belongs to the protein superfamily of medium-chain alcohol dehydrogenases (Rodokanaki, 1989; Rao and Zigler, 1992; Rao et al., 1997). It has a quinine oxidoreductase activity that reduces various quinones by the sequential transfer of single electrons (Rao and Zigler, 1992). ζ-crystallin gene has two distinct promoters, one responsible for high level expression in the lens and the other for expression in catalytic amounts in other tissues (Lee et al., 1994).

Some proteins have been characterized as functioning both as an enzyme and as an RNA-binding protein (Hentze, 1994). A well-characterized example is the cytoplasmic aconitase which is an iron regulatory protein and an RNA binding protein. Further examples of dual functioning proteins include GDH, glyceraldehyde-3-phosphate dehydrogenase (GAPDH), lactate dehydrogenase, thymidylate synthetase, dihydrofolate reductase, and catalase. By having two different activities, the protein can function as both a post-transcriptional RNA regulator and a metabolic catalyst. Most of the dual function enzymes utilize pyridine nucleotides as substrates and RNA competes with the dinucleotide for the enzyme's binding site. Untill recently there was no evidence that ζ-crystallin functions as an RNA-binding protein, however it was known to bind to the Z-form DNA and single stranded DNA (Rao et al., 1997; Gagna et al., 1998). The DNA is thought to interact with ζ-crystallin in its dinucleotide-binding site, since the DNA binding is effectively competed by the addition of NADPH (Rao et al., 1997).

1.13 LLC-PK$_1$-F$^+$ cells

LLC-PK$_1$-F$^+$ cells are a pH-responsive proximal tubule-like gluconeogenic subline of LLC-PK$_1$ cells (Gstraunthaler and Handler, 1987). The LLC-PK$_1$ cells exhibit a pH-responsive increase in glutamine catabolism but they do not express fructose 1,6-bisphosphatase (FBPase) and thus cannot synthesize glucose from lactate or pyruvate. The LLC-PK$_1$ cells were grown in low glucose medium (< 5 mM) and then selected in glucose free medium, that was supplemented with 10 mM sodium pyruvate. FBPase was expressed in large amounts in the selected cells even when maintained in medium with 5 mM glucose, hence these cells were named LLC-PK$_1$-FBPase$^+$ (LLC-PK$_1$-F$^+$) cells. These cells also exhibit an enhanced rate of glutamine catabolism and ammonia

production (Gstraunthaler, 1994). When the LLC-PK_1-F^+ cells are transferred to acidic medium (pH 6.9 and 9 mM HCO_3^-), the level of ammonium ion production is increased, which correlates to an increase in GA activity. There is also a pH-induced increase in the levels of GDH mRNA in this cell line (Kaiser et al., 1992). The level of PEPCK activity increased 3-fold in the LLC-PK_1-F^+ cells compared to the parental LLC-PK_1 cells (Holcomb et al., 1995). The level of PEPCK mRNA is also increased 3-fold when the LLC-PK_1-F^+ cells are treated with acidic medium (Hwang and Curthoys, 1991). The largest difference between LLC-PK_1-F^+ cells and the rat renal system is in the metabolism of glutamate. Glutamate created by mitochondrial GA in the cell culture system is primarily transaminated to pyruvate to form alanine and α-ketoglutarate and thus only a single ammonium ion is produced per glutamine consumed (Curthoys and Watford, 1995). However, in the rat renal system, GDH is used to deaminate glutamate, producing α-ketoglutarate. This pathway generates two ammonium ions for each catabolized glutamine.

1.14 WKPT cells

WKPT cells are a rat proximal tubule cell line that has high glutaminase (GA) activity. The original cells were initially isolated by micro dissection of rat kidney proximal tubules, grown on 3T3 cell feeder layers, and stably transfected with the SV40 large T-antigen gene using a vector that co-expresses a neomycin resistance gene (Romero et al., 1992). WKPT cells grow in the absence of extracellular glucose, indicating that they are capable of gluconeogenesis. The cells also express a Na/H exchanger activity that is regulated by angiotensin II. Therefore, these cells express a proximal tubular phenotype.

1.15 Short interfering RNAs (siRNAs) and micro RNAs (miRNAs) as regulators of eukaryotic gene expression

A powerful approach to regulating eukaryotic gene expression is the cytoplasmic control of mRNA translation and degradation. miRNAs and siRNAs have emerged as important regulators of translation and mRNA decay. The regulatory pathways mediated by these small RNAs are referred to as RNA interference (RNAi) or RNA silencing. miRNAs and siRNAs can silence cytoplasmic mRNAs by triggering an endonuclease cleavage, promoting translation repression, or accelerating mRNA decapping. These molecules were originally identified in *C. elegans*. More molecules and their possible targets have been identified in the genomes of plants and animals (Bartel and Chen, 2004). Bioinformatics analyses suggest that up to 30% of human genes may be regulated by miRNAs (Lewis et al., 2005).

miRNAs and siRNAs are ~21-26-nucleotide (nt) RNA molecules. Although both types of molecules can function similarly, they are distinguished by their mode of biogenesis (Carmell and Hannon, 2004; Kim, 2005). miRNAs are produced from transcripts that form stem-loop structures (pre-miRNA). These are processed in the nucleus by a complex comprised of at least two components: the RNase III enzyme Drosha, and a protein called Pasha in *Drosophila* or DGCR8 in mammals (Lee et al., 2003; Denli et al., 2004; Gregory et al., 2004; Han et al., 2004; Landthaler et al., 2004). This cleavage is followed by exportin-5-mediated transport to the cytoplasm of a 65-75-nt pre-miRNA, which is further processed by the cytoplasmic RNase III endonuclease complex, Dicer (Yi et al., 2003; Lund et al., 2004). Final processing by Dicer involves

assembly of the miRNA into the RNA-induced silencing complex (RISC), which is the effector of RNAi (Gregory et al., 2005).

siRNAs are produced from long double-stranded RNA (dsRNA) precursors, which can be either endogenously produced or exogenously provided. Processing of siRNAs is also Dicer-dependent and their assembly into the RISC complex is facilitated by the Dicer enzyme complex (Tomari et al., 2004). Gene-specific long double-stranded RNAs have been successfully used in worms and flies for RNAi-mediated gene silencing (Paddison and Hannon, 2002). However, in mammalian cells, double-stranded RNAs >30 bp trigger the antiviral/IFN pathways that results in global shut-down of protein synthesis (Gil and Esteban, 2000; Marcus and Sekellick, 2001). Recently, it was demonstrated that RNAi-mediated gene silencing can be obtained in cultured mammalian cells by delivery of chemically synthesized short (<30 nt) double-stranded siRNA molecules (Elbashir et al., 2001) or by endogenous expression of short hairpin RNAs (shRNAs) bearing a fold-back stem-loop structure (Brummelkamp et al., 2002; Elbashir, 2002; Paddison et al., 2002; Sui et al., 2002).

An important feature of miRNA/siRNA function is the specificity of their interactions with their target mRNAs and how each interaction leads to discrete downstream consequences. Some essential principles of this interaction have been characterized. First, base-pairing between the 5' end of the miRNA (residues 2-7) and the mRNA target plays a primary role in establishing interactions, with the important feature being the thermal stability of the miRNA:mRNA interaction (Doench and Sharp, 2004). Moreover, the 5' portion of related miRNAs is the most highly conserved. Second, the 3'

portion of the miRNA can also contribute to efficient repression, and it has been suggested to work as a modulator of suppression (Doench and Sharp, 2004; Kiriakidou et al., 2004; Kloosterman et al., 2004). Third, for efficient endonuclease cleavage, base-pairing is needed at the site of cleavage, between bases 10 and 11 (Elbashir et al., 2001; Haley and Zamore, 2004; Martinez, 2004). Fourth, while only one complementary site is generally sufficient to direct repression by cleavage, multiple sites are generally required for efficient translational repression (Doench et al., 2003; Zeng et al., 2003; Doench and Sharp, 2004; Kiriakidou et al., 2004). Fifth, the interaction of miRNA and Argonaute (a component of the RISC complex) with the mRNA may be influenced by other sequence-specific RNA-binding proteins, thus providing an additional level of specificity to miRNA:mRNA interactions. This possibility is suggested by the observations that an RNA-binding protein, GW182, interacts with Argonaute proteins and is required for efficient miRNA-mediated repression in animals (Ding et al., 2005; Jakymiw et al., 2005; Liu et al., 2005) and that the RNA-binding protein TTP collaborates with a miRNA to affect the decay rate of some mRNAs (Jing et al., 2005). Surprisingly, in this latter case, the sequence within miRNA that is important for pairing with the target mRNAs is from nucleotide 11 to 18. This study suggests that miRNAs could have more far reaching and general effects on gene regulation. Finally, because effective repression of the LIN-14 mRNA by the LIN-14 miRNA appears to require a bulge in the miRNA:mRNA duplex (Ha et al., 1996), the specific conformation of the miRNA:mRNA duplex may be important in function, perhaps to allow the recruitment of additional RNA-binding proteins in specific contexts.

2 STATEMENT OF PROBLEM

During normal acid base balance, mRNAs that encode the mitochondrial glutaminase (GA), glutamate dehydrogenase (GDH) and the cytosolic phosphoenolpyruvate carboxykinase (PEPCK) are degraded rapidly (Laroia et al., 1999; Hajarnis et al., 2005). However, metabolic acidosis is associated with an increase in the levels of the GA, GDH and PEPCK mRNAs. These adaptations are associated with increased renal ammoniagenesis and gluconeogenesis that play a critical role in restoring acid-base balance. The increase in PEPCK is caused by a rapid increase in the transcription. However, increases in GA and GDH are primrily due to post-transcriptional regulation. The 3'-untranslated region (3'-UTR) of the GA mRNA contains a direct repeat of eight-base, AU-rich sequences (UUAAAAUA and UUUAAAUA) that function as pH-response elements (pHRE). The elements bind ζ-crystallin /NADPH:quinone reductase (ζ-crystallin) with high affinity and specificity. Thus, it may function as a pHRE binding protein (pHRE-BP).

LLC-PK_1-$FBPase^+$ cells, a pH-responsive porcine kidney cell line, express four distinct GA mRNAs, that are ~2.5, 3.5, 4.5, and 5.0 kb in length. RNase H mapping indicated that three of the GA mRNAs are generated by use of alternative polyadenylation sites and are homologs of the rat KGA mRNA, while the 4.5 kb GA mRNA contains a different COOH-terminal coding and 3'-untranslated sequences. PCR cloning and sequencing of the 4.5 kb GA mRNA and its 3'-untranslated region will be performed to determine if it contains one or more pHREs.

The cellular activities of RNA-binding proteins can be regulated by their abundance, cellular localization, post-translational modifications, and the availability of

specific regulatory molecules. Identification of ζ-crystallin as a potential pHRE-binding protein required the characterization of the process by which this binding activity is enhanced during acidosis and the mechanism by which this interaction leads to cell-specific stabilization of the GA mRNA.

It was hypothesized that during normal acid-base balance, the pHRE either did not bind or bound ζ-crystallin with low affinity. This would allow the pHRE to bind a protein that recruits a deadenylase and the exosome or a specific exo-ribonuclease to degrade the GA mRNA. However, during metabolic acidosis, ζ-crystallin binds with greater affinity to the pHRE. The increased binding protects the GA mRNA from ribonucleolytic digestion and thereby increases its stability. Therefore, the onset of metabolic acidosis may activate a signal transduction pathway that results in increased expression and/or post-translational modification of ζ-crystallin.

More than 15 proteins are known to bind to AU-rich elements (AREs) (Hollams et al., 2002). Only a few of them have been shown to regulate mRNA stability. These include the ARE/poly-(U)-binding/degradation factor 1 (AUF-1) (Zhang et al., 1993; Blaxall, 2002), the embryonic lethal abnormal vision (ELAV) proteins (also named Hu proteins), especially HuR (Brennan and Steitz, 2001), the KSRP, (Chen et al., 2001; Gherzi et al., 2004) and the TTP family of zinc-finger RNA-binding proteins (Lai et al., 1999; Linker et al., 2005).

In an attempt to identify other proteins that may interact with the pHRE in the 3'-UTR of the GA mRNA and play a role in its regulation, RNA Electrophoretic Mobility Shift Assays (RNA-EMSA) has been performed. A [^{32}P]-labeled 29-nt GA element (R2I) encoding the direct AU-repeat will be used for binding and competition assays to

determine if the pHRE of GA exhibit a specific binding to any of the previously mentioned RNA binding proteins.

To test the hypothesis that increased binding of ζ-crystallin may promote the stabilization of the GA mRNA, experiments have been performed to determine if over-expression of ζ-crystallin stabilizes and increases the level of GA mRNA. Similarly decreased expression of ζ-crystallin may increase GA mRNA turnover or prevent the pH-responsive stabilization. A tetracycline responsive expression system was used to determine the *in vivo* decay of a chimeric βglobin-GA (βG-GA) mRNA (Schroeder et al., 2005). LLC-PK_1-F^+ cells that stably express the tTA protein, a recombinant transcriptional activator protein was stably transfected by pTRE2-βG -GA-bGH (Schroeder et al., 2005). A homogeneous population of βG-GA mRNA is synthesized using a transcriptional pulse. After creating a transcriptional pulse, a pH-responsive stabilization of the βG-GA mRNA will be tested. These cell lines have been used to overexpress and knockdown ζ-crystallin to examine the effect on GA mRNA half-life. Post-translational modification of ζ-crystallin may also be a contributing factor in GA mRNA regulation. Experiments will also be performed to address this question using 2D gel electrophoresis technique.

Data from this work will provide further information about mechanism of GA mRNA stability and turn over during metabolic acidosis. This information will also contribute to understand the mechanisms of cellular regulation that activate renal catabolism of glutamine and ammoniagenesis during metabolic acidosis. This may also lead to pharmacological approaches to stimulate renal ammoniagenesis and/or

gluconeogenesis to combat metabolic acidosis caused by starvation, dietary stress, renal nephropathies and diabetes mellitus.

3 MATERIALS

Materials

Male Sprague-Dawley rats (140-160 g) were purchased from Charles River. Slide-a-lyzer cassettes were obtained from Pierce. Microcon columns were obtained from Millipore. [α-^{32}P]UTP and [α-^{32}P]dCTP (specific activity 3000 Ci/mmol) were purchased from ICN Biochemicals or Amersham Pharmacia Biotech. Oligolabelling kit was from Pharmacia Biotechnology. Restriction enzymes, RNase T1, T7 RNA polymerase, an RNA standard, and yeast tRNA were acquired from Roche, New England Biolabs and MBI Fermentas. GENECLEAN kits were obtained from Bio101, Inc. The PCRScript cloning kit was obtained from Stratagene. Chemicals for acrylamide gels, Micro Bio-spin chromatography columns, and protein standards were purchased from Bio-Rad. RNasin was obtained from Promega. GelBond PAG films were purchased from Intermountain Scientific. DNA preparation kits were from Promega or Qiagen. GeneScreen Plus was purchased from New England Nuclear. Gel-blotting paper was purchased from Schleicher and Schuell. An RNA standard, DMEM/F12, DME base medium, and Geneticin (G418) were products of Gibco-BRL. Tissue culture plates were purchased from Dow Corning. Guanidine thiocyanate and sodium-N-lauryl sarcosine were obtained from Fluka. MOPS was obtained from Research Organics. TRIzol Reagent was obtained from Invitrogen. Other chemicals were acquired from Sigma, Mallinckrodt, or Fisher.

3.1 Buffers and Solutions

Krebs-Henseleit Saline Buffer (KHS)

118 mM Sodium Chloride
4.8 mM Potassium Chloride
1.2 mM Sodium Phosphate

1.2 mM Magnesium Phosphate

2.5 mM Calcium Chloride

25 mM Sodium Bicarbonate

5.5 mM Glucose

1.0 mM Acetoacetate

1.0 mM Alanine

0.1 mM Myoinositol

1.0 mM Glutamine

pH to 7.4

Rat Renal Cortex Cytoplasmic Extraction Buffer

40 mM Hepes

100 mM Potassium Acetate

10 mM Magnesium Acetate

1 mM Dithiothreitol (DTT)

0.01 mM Leupeptin

0.01 mM Antipain

5 μg/ml Phenylmethylsulfonylfluoride (PMSF)

pH to 7.4

1X Binding Buffer for FPLC

10 mM Hepes

1 mM DTT

0.5% Igepal CA630

pH to 7.4

100X Binding Buffer for FPLC

10 mM Hepes

1 mM DTT

0.5% Igepal CA630

0.5 M Potassium Acetate

50 mM Magnesium Acetate

pH to 7.4

1X Dialysis Buffer, pH 7.4

10 mM Hepes

25 mM Potassium Acetate

2.5 mM Magnesium Acetate

1 mM DTT

pH to 7.4

Lower Tris Stock

18.17 g Tris Base

4 ml 10% Sodium Dodecylsulfate (SDS)

pH to 8.6, adjust to 100 ml

Upper Tris stock

6.06 g Tris Base

4 ml 10% SDS

pH to 6.6, adjust to 100 ml

2X Sample Buffer

10 ml Glycerol

5 ml β-Mercaptoethanol (BME)

30 ml 10% SDS

12.5 ml Upper Tris Stock

5 ml 0.05% Bromophenol Blue

adjust to 100 ml

4X Reservoir Buffer Stock

12 g Tris base

57.6 g Glycine

pH 8.5

adjust to 1 L

After dilution add 1/100 volume of 10% SDS

Annealing Buffer

50 mM Sodium Chloride

66 mM Tris-HCl

6.6 mM Magnesium Chloride

pH to 7.5

50X TAE Buffer

2.0 M Tris-acetate, pH 8.0

100 mM Ethylenediaminetetraacetic acid (EDTA)

10X Stop Buffer

2 ml 0.25 M EDTA

2.5 ml Glycerol

0.5 ml Nanopure Water

25 mg Bromophenol Blue

5X TBE Buffer

450 mM Tris, pH 8.2

550 mM Boric Acid

10 mM EDTA

Type III Buffer (6X)

0.25% Bromophenol Blue

0.25% Xylene Cyanol

30% Glycerol

Elution Buffer

0.5 M Ammonium Acetate

10 mM Magnesium Acetate

1 mM EDTA

0.1% SDS

Water-saturated Phenol

0.1% 8-Hydroxyquinoline (v/v) to phenol was added and thoroughly mixed with an equal volume of nanopure water, dissolved and equilibrated at 50°C

DEPC-treated Water

0.1% (v/v) Diethyl Pyrocarbonate (DEPC), incubate at 37 °C overnight and then autoclave

10X Binding Buffer

100 mM Hepes

25 mM Magnesium Acetate

250 mM Potassium Acetate

pH to 7.4

2X HBSP, pH 7.0

1.5 mM Sodium Phosphate

10 mM Potassium Chloride

280 mM Sodium Chloride

12 mM Glucose

50 mM Hepes

65 μM 5,6-Dichlorobenzimidazole 1-β-D-ribofuranoside (DRB)

4.2 mg/ml dissolved in 95% ethanol

Use 40 μl 4.2 mg/ml DRB/8ml medium to obtain 65 μM

10X MOPS Buffer

0.2 M MOPS (3-(N-morpholino) propanesulfonic acid)

10 mM Sodium Acetate

10 mM EDTA, pH to 7.0

Northern Loading Buffer

33.75% Formaldehyde (37% v/v)

10% Glycerol

10% 0.1 % Bromophenol Blue

20% 10X MOPS

RNA Agarose Gel Running Buffer

10% v/v 10X MOPS

8% v/v Formaldehyde (37% v/v)

20X SSC

3.0 M Sodium Chloride

0.1 M Sodium Citrate

Hybridization Buffer

250 mM Sodium Chloride

50% v/v Formamide

25 mM Sodium Phosphate, pH 7.2

1 mM EDTA

7% w/v SDS

Northern Wash Solutions

Wash 1: 2X SSC

0.5% w/v SDS

Wash 2: 25 mM Sodium Phosphate, pH 7.2

0.5% w/v SDS

1 mM EDTA

Wash 3: 25 mM Sodium Phosphate, pH 7.2

5% w/v SDS

1 mM EDTA

SDS lysis buffer

2%SDS

10mM Tris 7.5

10mM NaF

5mM DTT

2mM EGTA

1mM Na vanadate

urea lyses buffer

8 M urea

4% IGEPAL

0.018 M DTT

urea/thiourea lyses buffer

7 M urea,

2 M thiourea

4% IGEPAL

0.018 M DTT

protease inhibitors

0.01 mM Leupeptin

0.01 mM Antipain

5 μg/ml Phenylmethylsulfonylfluoride (PMSF)

phosphatase inhibitors

10mM NaF

2mM EGTA

1mM Na vanadate

2D rehydration buffer

8M urea	12g
2% IGEPAL	0.5mL

add water to 25mL

store in 1mL aliquots at –20°C

2x 2D re-hydration buffer

make just enough for what you need, do not refreeze

the final 1x solution should be 0.5% IPG buffer and 18mM DTT

for making 400ul of the 2x 2D re-hydration buffer use:

4ul pH 3-10 IPG buffer

14ul fresh 1M DTT

Blue 2D re-hydration buffer

Add a few grains of bromophenol blue to an aliquot of 2D re-hydration buffer

SDS equilibration buffer

50mM Tris pH 8.8	3.35mL 1.5M Tris pH8.8
6M urea	36g

30% glycerol	30mL
2% SDS	20mL 10% SDS
bromophenol blue	small scoop

add water to 100mL (it takes ~25mL)

store in 20mL aliquots at –20°C

2mg/ml DTT

PBS+

PBS with

0.5 mM $MgCl_2$

0.9 mM $CaCl_2$

4 METHODS

METHODS

4.1 Culture of LLC-PK$_1$-F$^+$ cells

LLC-PK$_1$-F$^+$ cells were obtained from Gerhard Gstraunthaler (Gstraunthaler and Handler, 1987) and cultured in a 50:50 mixture of Dulbecco's modified Eagle's and Ham's F-12 medium containing 5 mM glucose and 10% fetal bovine serum at 37 °C in a 5% CO_2 atmosphere. The cells were grown either in normal medium (pH 7.4) that contains 25 mM sodium bicarbonate or in acidic medium (pH 6.9) that contains 10 mM sodium bicarbonate. Acidic medium was also supplemented with 15 mM sodium chloride to maintain an equivalent osmolarity and sodium ion concentration.

4.2 Stable pTet-Off cell lines

LLC-PK$_1$-F$^+$ cell lines expressing the tTA protein were produced by stably transfecting the pTet-off plasmid, encoding the tTA protein, into LLC-PK$_1$-F$^+$ cells. Clonal cell lines were made by transfection of 3-d post-split cells with calcium phosphate precipitated DNA (Chen and Okayama, 1987). Cell lines were selected by J. Schroeder, E. Anderson and N.P. Curthoys. A luciferase assay was used to determine the doxycycline responsiveness of the stable cell lines. The cells were transiently transfected by calcium phosphate precipitation of pTRE2-Luc (CLONTECH Laboratories) at 3 d post-split. The fold-induction of TRE2-Luc expression was calculated as the ratio of luciferase activities measured in cells grown in absence and presence of 0.5 μg/ml doxycycline. Protein concentration was used to normalize the luciferase activity of the samples.

4.3 pTRE2-βG-GA construct

pTRE2 was digested with *Mlu*I and *Sap*I to remove the β-globin sequence. A segment of pβG-GA (Schroeder et al., 2006) containing the β-globin coding region, 960 bp of the GA 3'-UTR, and a segment of the bovine growth hormone (bGH) 3'-untranslated region containing the polyadenylation site was PCR amplified with primers containing unique *Mlu*I and *Sap*I restriction sites. This fragment was cloned into pCR-Script SK (+) at the *Srf*I site, amplified, and then ligated into the pTRE2 fragment to create pTRE2-βG-GA.

4.4 Stable TRE-βG-GA cell lines

Clonal lines were made by stable transfection of pTRE2-βG-GA and pTK-Hyg, which confers antibiotic resistance to hygromycin B, into the LLC-PK_1-F^+ cells that stably express the tTA protein. These cell lines were developed and tested for tetracycline-responsiveness.

4.5 pcDNA 3.1 expression plasmids

pcDNA 3.1/Neo-ζ-crystallin was created by ligation of an *Xba*I/*Dra*I fragment (ζ-crystallin coding region) of PMLR107 plasmid into the *Nhe*I/*EcoR*V fragment of pcDNA 3.1/Neo. pcDNA 3.1/Zeo-ζ-crystallin was created by cloning the same fragment from PMLR107 plasmid into pcDNA 3.1/Zeo. pcDNA 3.1/Hygro-ζ -crystallin plasmid was created by cloning of a 2-kb *Bgl*II/*Xba*I fragment from pcDNA 3.1/Zeo-ζ-crystallin plasmid into the *Bgl*II/*Xba*I fragment of pcDNA 3.1/Hygro.

4.6 Selection of stable cell lines over-expressing zeta-crystallin

pcDNA 3.1/Neo-ζ-crystallin and pcDNA 3.1/zeo-ζ-crystallin plasmids were used to select clonal lines of LLC-PK_1-F^+ and TRE-βG-GA clonal cells that over-express ζ-crystallin, respectively. This was done by transfection of 2-d post-split cells with calcium phosphate precipitated DNA (Chen and Okayama, 1987). Fresh medium was added 1 h before the addition of 20 μg of calcium phosphate precipitated DNA. After 24 h, the transfection medium was removed, and the cells were washed two times with phosphate-buffered saline before fresh pH 7.4 medium containing 0.8 mg/ml neomycin or 2 mg/ml zeocin was added. The medium was changed every two days. After 10-15 days, neomycin resistant colonies were grown on larger plates. The selection with zeocin required about 21-30 days to form colonies. Following the initial split, the cells were grown in pH 7.4 medium containing 0.2 mg/ml of the appropriate antibiotic.

4.7 Western blot analyses

Samples containing 15 μg of protein were mixed with an equal volume of 2X SDS sample buffer containing 10% (v/v) glycerol, 5% (v/v) β-mercaptoethanol, 3% (w/v) SDS, 184 mM Tris-HCl (pH 6.8), and 0.2% (w/v) bromophenol blue. The samples were heated in boiling water for 5 min, loaded on a 10% SDS-polyacrylamide gel, transferred to a PVDF membrane, and incubated with 1:5000 dilution of anti-ζ-crystallin/NADPH: quinone reductase antiserum. The membrane was then incubated with a 1:20,000 dilution of secondary antibody conjugated to Alexa fluor. Images were visualized and quantified using an Odyssey Infra-red imaging system.

4.8 Test of TRE-βG-GA- stable cell lines for tetracycline-responsiveness

The isolated cell lines were tested for tetracycline-responsiveness by maintaining the cells for 48 h in pH 7.4 medium in the presence or absence of 0.5 μg/ml Dox. Total RNA was harvested from the cells and analyzed on a Northern blot. The level of βG-GA mRNA was divided by the corresponding level of 18S rRNA to correct for errors in sample loading. For each clonal cell line, the reported data are the ratio of βG-GA mRNA levels in cells –Dox to cells +Dox.

4.9 Creation of a transcriptional pulse

Cells were grown in medium containing 0.2 mg/ml G-418 and 0.2 mg/ml hygromycin B and 50 ng/ml Dox, the minimal amount of Dox needed to shut off transcription, for 48 h. The cells were washed twice with PBS and then grown for 3 h in fresh medium minus Dox and then RNA was isolated. As controls, RNA was also isolated from cells that were maintained in the presence and absence of Dox. The RNAs were subjected to Northern blot analysis. The percent induction was calculated as the level of TRE-2-βG-GA mRNA present following a 3 h pulse divided by the level present in the cells minus Dox times 100.

4.10 Functional studies using pTRE2-βG-GA

Half-life analysis using Dox to inhibit transcription

Cells infected with adenovirus were grown without antibiotics after splitting. Cells expressing the TRE2-βG-GA mRNA were split 1:10 and grown to 60-70% confluence in pH 7.4 medium containing 0.2 mg/ml G-418 and 0.2 mg/ml hygromycin B or zeocin. The cells were then maintained in pH 7.4 medium without antibiotics for 12 h

and subsequently treated for 24 h in normal or acidic medium. At time zero, 1 μg/ml Dox was added to each plate. At 0, 3, 6, and 9 h post-Dox treatment, total cellular RNA was isolated. Control plates minus Dox were harvested 9 h post-mock Dox treatment. RNAs were subjected to Northern blot analysis.

Half-life analysis using a transcriptional pulse

The cells were split 1:10 and grown for 3-5 days in pH 7.4 medium without antibiotics but with 50 ng/ml Dox. They were then maintained in pH 7.4 or pH 6.9 medium for 24 h. For some of the experiments, cells were treated with acidic medium for only 10 h. The cells were washed two times with PBS and incubated in medium without Dox for 3 h to create a transcriptional pulse. Fresh medium containing 1 μg/ml Dox was added and RNA was isolated at 0, 3, 6, and 9 h after Dox re-addition. Controls grown in the presence or absence of Dox were harvested after the last time point. RNAs were subjected to Northern blot.

4.11 Isolation of total RNA

Total RNA was isolated using TRIzol reagent (Invitrogen). The pellets were re-suspended in 50 μl of Formazol and dissolved by heating at 55 °C for 15 min. The RNA concentration was determined by measuring the absorbance of the RNA at 260 nm using a Beckman Spectrophotometer.

4.12 Preparation of cDNA probes for Northern analyses

A 507-bp fragment of rabbit β-globin cDNA was excised by restricting pRSV-βG (Gorman et al., 1983) with *Hind*III and *Bgl* II. A 2.0-kb fragment of the 18S ribosomal RNA cDNA from *Acanthamoeba castellanii* was excised by restricting pAr2 (D'Alessio

et al., 1981) with *Hind*III and *EcoR*I. A 1.1-kb fragment of the coding region of both KGA and GAC was excised by restricting pGA104 plasmid with *EcoR*I (Shapiro et al., 1991). A 0.8-kb fragment containing the 3'UTR of rat KGA was excised by restricting pGA104 with *Nhe*I. A 0.95-kb *Hind*III fragment of pGA105 containing the 3'UTR of rat GAC, a 1.4-kb *EcoR*I fragment of pF3/4391 (Elgadi et al., 1999) containing the 3'UTR of pig 4.5-kb GA cDNA, and a 2.4-kb *Nhe*I and *Not*I fragment of pGA201 (Porter et al., 1995) containing the 3'UTR of pig 4.5-kb GA cDNA were also prepared. The DNA fragments were separated on 1% agarose gels, excised, and purified using the GENECLEAN kit.

4.13 Northern analyses

Samples containing 15 μg of total RNA were combined with 2X loading buffer and 1.5 μl of 0.4 mg/ml ethidium bromide. The RNA samples were heated at 70 °C for 10 min and then placed on ice for 10 min. The samples were loaded onto a 1% agarose gel containing 20 mM MOPS, 1 mM EDTA, and 1 mM sodium acetate, pH 7.0. The samples were electrophoresed for either 6-7 h at 70 V or for 16 h at 20 V. The gel was washed with nanopure water for 20 min, incubated with 50 mM sodium hydroxide for 20 min, and then neutralized in 0.25 M sodium phosphate, pH 6.5, for 30 min. RNA was transferred to GeneScreen Plus by a standard capillary transfer protocol using 25 mM sodium phosphate, pH 6.5. The completeness of transfer was determined by UV-illumination of the membrane. The transferred RNA was cross-linked to the GeneScreen Plus membrane by UV-irradiation for 3 min.

The membrane was prehybridized for 1-2 h at 43 °C in hybridization solution prepared as previously described (Amasino, 1986) in a Biometra hybridization oven. A

^{32}P-labelled cDNA probe (>10^9 cpm/mg) was added and hybridized to the membrane under the same conditions for 14-20 h. Following hybridization, membranes were washed two times for 20 min at 53°C in each of the three Northern washing solutions described in the Materials section. The blots were exposed to a PhosphorImager screen and the intensity of the resulting digital image of each band was quantified using Molecular Dynamics Software. The level of experimental mRNA was divided by the corresponding level of 18S rRNA (determined by re-hybridizing the same blot with the 18S cDNA probe) to correct for errors in sample loading.

For half-life studies, the log of normalized data was then plotted versus the time of treatment with Dox. The values are averages of data obtained from replicate experiments. The line represents the best-fit of the data points as determined by the KaleidaGraph program that weights each data point based upon its standard deviation.

4.14 Cloning of porcine ζ-Crystallin coding region from LLC-PK$_1$-F$^+$ cells

Total RNA from LLC-PK$_1$-F$^+$ cells was isolated using TRIzol reagent (Invitrogen). First-strand cDNA was synthesized from 1 μg of DNase1-treated total RNA using *Moloney murine leukemia virus* reverse transcriptase (Promega) and oligo (dT) primers according to the manufacturer's instructions. The ζ-crystallin coding sequence was amplified by PCR using 3 μl cDNA as a template. Sense and antisense primers used for ζ-crystallin amplification were NFPZC ($^{5'}$ATGGCNACTGGNCAGAAGTTGATGAGNGC$^{3'}$) and NRPZC ($^{5'}$TCATAAGAGNAGAATCATTTTNCC$^{3'}$), respectively. The PCR reactions were performed in a final volume of 25 μl using Expand Long template PCR system (Roche). The reaction mixtures were heated at 94 °C for 2 min and 35 cycles of amplification were

performed in a thermocycler. Each cycle consisted of 45 sec of denaturation at 94 °C, 1 min of annealing at 50 °C, and 2 min of extension at 68 °C. The PCR product was gel extracted and cloned into the pGEM-TEasy cloning vector (Promega, Madison, WI) and sequenced using a Prism 377 DNA Sequencer (Applied Biosystems). The cDNA sequence was deposited in the GenBank database with accession number DQ841573.

4.15 shRNA design, cloning and screening (Construction of ZC-103 pre-miRNA expression cassette)

Design of shRNA sequences

The siDesign Center of the Dhramacon website (http://www.dharmacon.com) was used to select 19-nt siRNA sequences for ζ crystallin. Porcine ζ-crystallin coding sequence was used for the search. The search was also run with different organisms (human, rat, cow) for the Blast search and comparison. The four sequences that had the highest scores and exceeded the minimum score of 6 were selected (Khvorova et al., 2003). BLAST searches of potential sequences were performed in the Gene Bank (http://www.ncbi.nlm.nih.gov/BLAST/Blast.cgi). Sequences with high homology to other proteins were avoided. Sequences containing a TTT repeat were not considered.
The following steps were used to place the siRNA sequence into a miRNA 30 (miR30) backbone (Zeng et al., 2003; Boden, 2004).

1. The position of the selected siRNA (19 nt) in the ζ-crystallin cDNA sequence was found.
2. (X) and (Y) bases were aded before and after the 19 nt in the ζ-crystallin cDNA to yield (XN19Y).

3. An adenine (A) was added before X (AXN19Y) to mismatch with a C base in the stem of miR30.
4. GCG was added before A. The First G will mismatch with a T base.
5. The miR30 loop sequence CTGTGAAGCCACAGATGGG was added after the Y base (GCGAXN19Y**CTGTGAAGCCACAGATGGG**).
6. The inverted complement of sequence (XN19Y) was added after the loop sequence (GCGAXN19Y **CTGTGAAGCCACAGATGGG*YN19X***).
7. Then CTGC was added at the 3' end to create A/C and G/T mismatches (GCGAXN19Y**CTGTGAAGCCACAGATGGG*YN19X***CTGC).
8. A termination sequence was added at the 3' end (TTTTTT).

(GCGAXN19Y**CTGTGAAGCCACAGATGGG*YN19X***CTGC**TTTTTT**).

9. A *BamH*I site was added at the 3' end GGATCC.

(GCGAXN19Y**CTGTGAAGCCACAGATGGG*YN19X***CTGC**TTTTTT**GGATCC).

10. Six bases (CGGGCC) were added as flanking sequence to help the restriction enzyme to bind

(GCGAXN19Y**CTGTGAAGCCACAGATGGG*YN19X***CTGC**TTTTTT**GGATCC CGGGCC).

11. To the 5' end, a *BseR*1 site (GAGGAGN10) with 10 bases that include pSHAG complementary sequence (CACCG) were added.

(GAGGAGCTAGCCACCGGCGAXN19Y**CTGTGAAGCCACAGATGGG*YN19X*** CTGC**TTTTTT**GGATCCCGGGCC).

12. A *Kpn*1 site (GGTACC) was added as flanking 5' sequence

(GGTACCGAGGAGCTAGCCACCGGCGAXN19Y**CTGTGAAGCCACAGATG**

GG*YN19X*CTGC**TTTTTT**GGATCCCGGGCC).

The total length of the sequence was 109 bases. The sequence was entered as a DS gene file and saved as a sense siRNA sequence. The sense siRNA sequence was reverse complemented and saved as the anti-sense siRNA sequence. An siRNA design folder was created that has the perminant sequences for the 3'end and the 5'end and the hairpin loop. After selection of the desired 21 siRNA sequence, one can simply add the 5' end of the siRNA and the hairpin loop, the complementary sequence and the 3'end sequence to the 3'end. The design and the cloning steps can be modified to synthesize two oligos that have the *Bser*I and *BamH*I sites. These oligos have to be annealed and phosphorylated then cloned into the pSHAG vector. Screening for the correct clones and design instructions are included in the lab protocol books.

Primers for shRNA/ZC103-pre-miRNA

The sense primer corresponds to nucleotides 1 to 68 (5' to 3') of the sense strand. The antisense primer corresponds to nucleotides 1 to 68 (5' to 3') of the anti-sense strand. The sense and antisense primers used to synthesize the ZC103-pre-miRNA are pzc103FP ($^{5'}$GGTACCGAGGAGCTAGCCACCGGCGAGGACAATCAGGTTCTAAT CAACTGTGAAGCCACAGATGGGTT$^{3'}$) and pzc103RP ($^{5'}$GGCCCGGGATCCAAAAAAGCA GGGACAATCAGGTTCTAATCAACCCATC TGTGGCTTCACAGTTGATT$^{3'}$) respectively, in which the underlined bases are complementary.

Annealing and extension of the forward and reverse primers

Oligonucleotides were diluted to 20 pmol/μl in annealing buffer. Oligonucleotides were annealed and extended using the following profile, 95 °C for 5 min, 50 °C for 30 sec, 68 °C for 20 min and the Expand High Fidelity PCR System (Roche). Products were gel purified, restricted with *BseR*I and *BamH*I and ligated into pSHAG-U6-MCS. When necessary, the PCR products can be re-amplified with forward and reverse primers. pSHAG-U6-FF-luc (Paddison and Hannon, 2002) that encodes an shRNA targeting the luciferase gene was used as a control vector.

pSHAG1

pSHAG1 was constructed in the pENTER/D topo backbone (Invitrogen) as described previously (Paddison and Hannon, 2002) and obtained from Dr. Sanborn. More details are available on Dr. Hannon's web site: (http://katahdin.cshl.org:9331/RNAi_web/scripts/main2.pl). The pSHAG1 plasmid contains the *att*L1 and *att*L2 recombination sites, a U6 promoter and a kanamycin selection gene.

Cloning shRNA sequences into pSHAG1 vector

One μg of pSHAG1 was digested with *BseR*I and *BamH*I restriction enzymes for 2 h at 37 °C. The digest was run on a 1% agarose gel and a 3-kb band was excised and purified using the QIAquick Gel Extraction Kit (Qiagen). DNA was eluted in 30-50 μl. The DNA concentration was determined either by spectrometry or by quantification against a lambda *Sty*I standard. DNA was stored at -20 °C until used for the ligation step. The annealed and extended product of ZC103 shRNA was digested with *BseR*I and *BamH*I. The digested product was purified using QIAquick Gel Extraction Kit (Qiagen) and ligated with *BseR*I/*BamH*I digested pSHAG1 vector.

Ligation was performed using, 4.0 µl 5X Ligase Buffer, 5.0 µl annealed ZC-shRNA oligo, (20 ng/µl) 1.0 µl pSHAG vector, 1.0 µl T4 DNA ligase (Ferments) (5 units/µl) and 9.0 µl ddH_20. A ratio of 3:1 of shRNA:pSHAG1 plasmid was used. The ligation reaction was mixed and incubated in a thermocycler at 14 °C for 16 h. Then 5 µl of the ligation reaction was used for transformation of XL1-Blue competent cells. Transformation reaction was plated into LB+Kanamycin (50 µg/ml) plates and incubated at 37 °C for 16 h. Colonies were picked and grown overnight as minipreps using the QIAprep Spin Miniprep Kit (Qiagen). DNA was eluted in 50 µl water. Clones were initially screened for restriction sites included in the cloned shRNA sequence. Positive clones were digested with *BseR*I and *BamH*I to produce the 81 bp band and digested with *Not*I and *BamH*I enzymes to produce a 360 bp band. pSHAG and pSHAG-Ffl plasmids were also digested as controls. The clones identified as potential positives were sequenced using M13F (M13 forward) primer.

4.16 psiCHECK™-2 vector

psiCHECK-2 Vector is designed to provide a quantitative and rapid approach for initial optimization of RNA interference (RNAi). The vector enables monitoring of changes in expression of a target gene fused to a *Renilla* luciferase reporter gene. The gene of interest is cloned into a multiple cloning region located downstream of the *Renilla* translational stop codon. Initiation of the RNAi process by expression of an shRNA towards the gene of interest results in cleavage and subsequent degradation of the fusion mRNA. Therefore, the decrease in *Renilla* luciferase activity provides a convenient measure of the RNAi effectiveness.

4.17 Screening shRNA sequences using luciferase assays

A 1 kb ζ-crystallin cDNA coding region fragment was obtained by *Not*I digest of the pZC7 plasmid. The 1-kb fragment was ligated into *Not*I digested and phosphorylated psi-CHECK-2 vector using a 3:1 ratio of the vector to the insert to produce psiCHECK-2-ZC. ZC-shRNA sequence was checked to insure that it is not complementary to the cDNA for either Firefly-luciferase or *Renilla*-Luciferase. The cells were plated in 6-well plates. Two days post split or when 70% confluent, the cells were transfected with the luciferase expressing plasmid, psi-CHECK-2, with or without pSHAG-shRNA. The pSHAG1 plasmid was added as carrier DNA to insure that the same amount of DNA was added to all wells. Lipofectamine 2000 in a 1:1 ratio with DNA was used for transfection (Invitrogen). psiCHECK-2 plasmid was used at a concentration of 0.005-0.01 μg/μl and shRNA plasmid at 0.08 μg/μl . The transfected cells were grown for 72 h. The samples were analyzed using the Dual-Luciferase Reporter Assay system (Promega). The shRNA for Firefly-luciferase expressing pSHAG1 (pSHAG-Ffl) was obtained from Hannon's lab and used as a control to knockdown firefly-luciferase activity from pMAMneo-LUC where. Cells were transiently co-transfected with 0.2 μg of the various pMAMneo-LUC plasmid and 0.005-0.01 μg of pRL-null (Promega) per well using lipofectamine 2000. The experimental samples were either co-transfected with 1.0 μg per well of pSHAG-Ffl or pSHAG1. When psiCHECK-2 plasmids used, the *Renilla* luciferase activities obtained from the various psiCHECK-2 constructs were divided by the corresponding firefly luciferase activities to correct for differences in transfection efficiency. Whereas, for cells cotrnsfected with pMAMneo-LUC, the firefly luciferase activities were divided by the corresponding *Renilla* luciferase activities to correct for differences in transfection

efficiency. In a single experiment, each transfection was performed in triplicate. For comparative purposes, the mean of the ratio of luciferase activities measured with the control construct was normalized to a value of one. A normalized value of the experimental construct of less than one indicates a decrease in the stability of the chimeric mRNA.

4.18 Shuttle vectors

pAdTrack-RFA plasmid (containing *att*R recombination sites) was provided by Dr. Colin Clay. This plasmid is constructed from pAdTrack plasmid by using the Gateway Vector Conversion System (Invitrogen). This system is designed to convert any vector into a Gateway destination vector using a restriction endonuclease and ligase. The system has a Gateway cassette containing *att*R recombination sites flanking a *ccd*B gene and a chloramphenicol-resistance gene that are blunt-end cloned into the multiple cloning site of the vector.

4.19 shRNA-pSHAG/pAdTrack-RFA constructs (shRNA-pAd-Track-RFA plasmid)

The Gateway LR Clonase II enzyme mix (Invitrogen) was used to catalyze the *in vitro* recombination between an entry clone, 65 ng/μl of pSHAG1-ZC-premiRNA, and the destination vector, 200 ng/μl pAdTrack-RFA plasmid to generate an expressing shRNA clone.

4.20 Electrocompetent BJ5183 cells pre-transformed with pAdEasy1

To avoid rearrangements of the AdEasy vector, electrocompetent BJ5183 cells were prepared from a freshly transformed stock. Electrocompetent cells (BJ5183) were transformed with ~50 ng pAdEasy1 DNA (Adenovirus backbone) using 100 µl sample and settings of 2.25 kV, 200 Ω and 25 µF. The freshly-transformed BJ5183 cells are made competent by the protocol outlined in the AdEasy manual. These cells were prepared and kindly provided by Alisa Shaw from the Bamburg lab.

4.21 Recombination of Adenoviral shuttle plasmid (shRNA-pAdTrack-RFA) into pAdEasy1 using BJ5183 *E. coli*

Four µg of DNA (shuttle or shRNA shuttle vector) were digested overnight in a 100 µl reaction with 4 µl of *Pme*I. Quality of the DNA and a complete digest are important for this step. The digest was phenol/chloroform extracted and DNA was precipitated with ethanol. The DNA was electrophoresed into BJ5183/AdEasy electrocompetent cells using 40 µl cold water, 40 µl cells, 3 µl *Pme*I-cut DNA in a pre-chilled 0.1 cm gap cuvette. The cells were shocked at 2.25 kV, 25 uF, 200 Ω using a time constant of ~4.7 millisecond. The cuvette was returned to ice briefly and cells were re-suspended into 1 ml of LB medium then transferred to a sterile eppendorf tube to be incubated for 45-60 min at 37 °C without shaking. The cells were spin for 1 min at 14,000 rpm, then re-suspended in ~150 µl LB medium. Cells were spread on two LB-kanamycin (LB-KAN) plates, with ~10% on one plate, ~90% on the other and grown 24 h at 37 °C. Selected colonies (2-4) were inoculated into 10 ml of LB-KAN and grown overnight.

Qiagen miniprep DNA was isolated and eluted with 70 °C preheated water. 20 µl of DNA (shRNA-Adenovirus) was digested with *Pac*I and analyzed on a 0.6% agarose gel. A positive recombinant was transformed into XL-Blue cells using 10-15 µl of DNA (shRNA-Adenovirus) that was isolated from BJ5183 cells. The Transformed cells were plated on one LB-KAN plate for 20 h. Then, 2-4 small colonies were inoculated into 10 ml of LB-KAN and grown overnight. Qiagen miniprep DNA was isolated. DNA was digested with *Pac*I and ran on a 0.6% gel. A glycerol stock of the purified, positive recombinant was prepared and stored frozen.

4.22 Virus production in HEK 293 cells

HEK293 cells were stably transformed by sheared Ad type 5 DNA (Graham, 1977). They express the E1 gene of adenovirus so they can produce packaged infectious adenoviral particles when transfected with E1-deleted pAdEasy-1 recombined DNA. They were cultured in a 50:50 mixture of Dulbecco's modified Eagle's and Ham's F-12 medium containing 5 mM glucose and 10% fetal bovine serum at 37°C in a 5% CO_2 atmosphere. These cells must split regularly when they reach a maximum confluency of 75%. The number of passages should not exceed 20 before transfection with the pAdEasy-1 recombined DNA.

Transfection of Viral DNA into HEK 293

A 20 µl sample containing 5 µg of recombined DNA (shRNA-Adenovirus) was digested in a 100 µl reaction with 4 µl of *Pac*I overnight. The digest was extracted using Phenol/chloroform extraction method and DNA was precipitated with ethanol. HEK 293 cells were transfected with *Pac*I digested DNA using the following steps:

- ~$4x10^5$ HEK 293 cells were plated in a T25 flask the day before the transfection to produce cells that are 50-70% confluent.
- 230 µl of the Optimem medium was added to the 20 µl of *Pac*I-digested DNA (solution A).
- 20 µl of Lipofectamine was added to 230 µl of Optimem (solution B).
- Solutions A and B were combined, mixed gently, and incubated for 20 min.
- The medium was removed from the 293 cells and the cells were rinsed once with Optimem medium, then 2.5 ml of Optimem was added.
- The DNA/Lipofectamine mixture was added to the 2.5 ml of Optimem and the cells were agitated gently but thoroughly and returned to the incubator for 4 h.

- The transfection medium was removed and replaced with 6 ml of HGDMEM (High Glucose Dulbecco's Modified Eagle's Medium)/10% FBS (this is counted as day 0).
- The transfection efficiency was checked on day one or two. The confluence of the cells, the number of fluorescent cells per 10X field, as well as the percentage of transfected cells were monitored.
- Signs of virus propagation, a clear increase of fluorescent cells per 10X field or the formation of plaques/fluorescent streaks, occur between day 4 and day 20. With a very high transfection efficiency, the cells must be harvested early (day 4 or 5) due to the absence of non-transfected cells that are necessary to sustain the infection. After 5 days, 3 ml of medium

was removed and replaced with 3 ml of fresh medium to maintain pH and provide nutrients.

Harvesting virus

After propagating, the cells were scraped off the dish into medium with a cell scraper and transferred to a 50-ml conical tube. The cells were centrifuged at 2,500 rpm for 3 min. The medium was removed except for 2 ml that was used to re-suspend the cells by vortexing. The cell suspension was frozen in a dry ice/100% ethanol bath. The cell suspension was thawed quickly in a 37 °C bath but without warming the virus. The cell suspension was vortexed. The freeze/thaw cycles were repeated for 4 times and the cells were centrifuged at 3,000 rpm for 4 min. The supernatant containing the virus was used as the cell lysate for further viral amplification.

The first amplification

Approximately $4x10^5$ HEK 293 cells were plated in a T25 flask the day before the infection. The cells should be ~70% confluent on the day of infection. The HEK 293 cells were infected with 0.5 ml the transfection cell lysate. Virus production was monitored and harvested as described above. Virus should propagate in 2 to 5 days. The majority of the cells should be infected and rounded at the time of harvesting.

The second amplification

3-$4x10^6$ HEK 293 cells were plated in a T75 flask the day before the infection. To prevent trypsin toxicity, the cells need to be pelleted and re-suspended after trypsin addition. Cells should be ~70% confluent at the time of infection. The cells were infected with 0.1 ml of the first amplification cell lysate. All of the cells should round up and start detaching on the 2nd day. To achieve the highest titer, cells should be harvested when

they are rounding but before lysis starts. The cells were scraped into medium and centrifuged at 2,500 rpm for 3 min. The cell pellet were re-suspended in 4-6 ml of medium and subjected to 4 freeze/thaw cycles. The cells were centrifuged at 3,000 rpm for 4 min and the cell lysate was divided into small aliquots. This lysate was used for adenovirus titering by E2 immunostaining.

Adenovirus titration by E2 immunostaining

The E2a protein is required for viral replication and is controlled by the E1a gene product. E1a gene is deleted in the replication deficient pAd-Easy-1 virus. A simple method to test for viral infectivity is to infect permissive 293 cultured cells with adenovirus and wait till the expression of the E2a protein is high and then fix and stain the cells with the monoclonal antibody to E2a. This assay requires fixation and staining of the cells at exactly 16 h after viral infection. The timing is important as 16 h allow the production of the E2a antigen in all the infected cells without packaging or release of virus to infect additional cells which usually happens 18-24 h after infection

Day 1

HEK293 cells were plated in 12-well plates by adding 2.5 x 10^5 cells per well.

Day 2

When cells reached 70-95% confluent, 1:10^4, 10^5, and 10^6 dilutions of the virus were made in DMEM medium without serum. The virus stock to be tittered was mixed very well before starting the dilution. The medium was aspirated from the 293 cells and 0.5 ml diluted virus was added per well. The solutions were added down the sides of the wells to avoid detachment of cell patches. The cells were incubated for 45 min with

occasional rocking. The virus solutions were removed and replaced with 1 ml DMEM containing 2% FBS to each well. The cells were incubated for 16 h.

Day 3

The medium was removed and the cells were washed once with PBS+ (PBS containing 0.5 M $MgCl_2$ and 0.9 M $CaCl_2$). The cells were fixed in 1 ml of 4% formaldehyde in PBS+ for 5 min at room temperature (for 10 ml: 1 ml 10X PBS + 7 ml H_2O + 2 ml 20% formaldehyde + 10 µl of 0.5 mM $MgCl_2$ and 0.9 mM $CaCl_2$). 1 ml was used per well. Once the fixation solution has been added to the cells, the plates were transferred to the regular fume hoods. The cells were washed once with 1 ml of PBS+ and permeabilized in 90% methanol/10% PBS+ for 2 min at room temperature. The cells were washed once in PBS+ then washed once with 1 ml of PBS+ containing 1% BSA (fraction V). Then 1 ml of B6-8 monoclonal antibody (anti-E2) primary antibody diluted 1:5 in 1%BSA/PBS+ was added and incubated for 45 min at room temperature. The cells were washed twice with PBS+ and once with 1%BSA/PBS+.

The goat anti-mouse IgG-alkaline phosphatase (Sigma) secondary antibody was diluted 1:1000 in 1%BSA/PBS+ then 0.5 ml was added per well and incubated for 45 min at room temperature. The cells were washed 3 times with PBS+, then washed once with 50 mM Tris pH 9.5, 100 mM NaCl, 1 mM $MgCl_2$ (pH of this solution should be measured before adding the $MgCl_2$). 44 µl of Nitro-Blue Tetrazolium Chloride (NBT)/ and 33 µl of 5-Bromo-4-Chloro-3'-Indolyphosphate p-Toluidine (BCIP) were added to 10 ml pH 9.5 Tris buffer). Then 0.5 ml was added to each well and incubated at room temperature for 30-60 min (longer time may be needed for clear color development). The nuclei of infected cells appeared very dark brown. Using a 20X objective on the Nikon

37623 microscope, the number of infected cells was counted in at least 5 fields. The number of Focus Forming Units/ml (FFU) can be calculated as follows, number of positive cells/field x 1361 x 2 x dilution = titer. 1361 is the conversion factor for comparing the area of the field of view with the 20X objective versus the area of a well in the 12-well plate. This factor may differ for different microscopes. We multiplied by 2 to account for only using 0.5 ml of virus per well.

4.23 MOI (Multiplicity Of Infection)

MOI is defined as the number of infectious viral particles added per cell. To determine the viral stock volume needed to produce specific MOI, we used the equation:

Viral stock volume (μl) = number of cells x desired MOI/viral titer.

4.24 Synthesis of the biotinylated DNA probe

The following deoxyoligonucleotide was synthesized by Macromolecular Resources (CSU, http://macromolecular.colostate.edu/synthesis.html): $^{5'}$TTAATTAACCCTCACTAAAGGG$^{3'}$ with a biotin molecule at the 5'end. The underlined sequence is the initial sequence that is transcribed from the T3 promoter of pBSK (-). A sample containing 280 pmol of the Biotinylated DNA, 140 pmol of GA25-BssHII RNA, 2 μl of 500 mM KCl, 2 μl of 100 mM Hepes (pH 7.4), 1 μl of RNAsin (40 U/μl) was diluted to a final volume of 20 μl with DEPC- treated H_2O. The resulting DNA/RNA hybrid was incubated at room temperature for 1 h, and then kept on ice until incubation with the rat renal cytoplasmic extract.

4.25 Affinity purification of the ζ-crystallin

Cytosolic extracts from rat renal cortex were prepared as described previously (Tang and Curthoys, 2001). A 300-µl sample of the rat renal cortical cytosolic extract prepared in 1X binding buffer [10 mM Hepes, (pH 7.4), 25 mM potassium acetate, 2.5 mM magnesium acetate] was incubated for 10 minutes on ice with 0.4% Nonidet P-40, 75 µg t-RNA, 2.2 mM DTT (Dithiothreitol) and 240 units of RNAsin. Then, 20 µl of biotinylated DNA and GA25-BssHII RNA hybrid was added. The hybrid/extract mix was incubated on ice for an additional 20 min. A protein liquid chromatography column was packed with 0.5 ml of avidin agarose and washed extensively with 1X binding buffer. The total sample was loaded at a flow rate of 0.1 ml/min, and the column was then washed at flow rate of 0.05 ml/min with 24 ml of binding buffer in which the concentrations of the potassium acetate and magnesium acetate were linearly increased 4-fold. The bound proteins were then eluted with 9 ml of buffer in which the potassium acetate and magnesium acetate concentrations were linearly increased from 4 to 20-fold. Fractions (0.5-ml) were collected and assayed by RNA gel shift analysis. 10 µl of the collected fractions were separated on a 10% SDS- polyacrylamide gel and stained with 0.1% silver nitrate.

4.26 Silver staining

Following electrophoresis, the protein was fixed by incubating the gel twice in 50% methanol and 10% glacial acetic acid (10-15 min each) with shaking. The gel was re-hydrated in a re-hydration solution (10% methanol, 10% glacial acetic acid) for 5 min, washed twice with distilled water, and then incubated with 40 µM DTT for 10 min followed by a brief rinse with distilled water. A 0.1% silver nitrate solution was added for

10 min, then a 242 mM sodium carbonate and 0.017 % formaldehyde solution was added for 5-15 min to stain the proteins. The duration of the staining depends on the intensity of the protein bands. The staining reaction was stopped by addition of 100 ml of 57.5 mM citric acid. The gels were dried and visualized using a light box.

4.27 Chloroform/ methanol precipitation of proteins

The protein fractions (0.15 ml) were mixed sequentially with 600 µl of methanol, 150 µl of chloroform, 450 µl of water in the previous order. The samples were vortexed after each addition and then centrifuged at 14,000 xg for 5 min. The upper phase was discarded without disturbing the interphase. Methanol (0.45 ml) was added and the samples were vortexed and centrifuged for 5 min at 14,000 x g. The supernatant was removed and the protein pellets were air-dried and re-suspended in 30 µl of water.

4.28 2-Dimensional gel electrophoresis

Two dimension gel electrophoresis separates proteins in the first-dimension by isoelectric focusing (IEF), according to their isoelectric points (pI), and in the second-dimension according to their molecular weights (MW) by SDS-PAGE. Each spot on the resulting 2-D gel corresponds to a single protein species.

4.29 Iso-electric focusing

The IPGphore isoelectric focusing system from Amersham was used for the first dimension separation. It utilizes IPG immobilin dry strips with a pH range of 3-10. The rat kidney tissue was lysed using urea lyses buffer with protease and phosphatase inhibitors. The protein concentration was determined using a modified Bradford filter paper assay (Minamide and Bamburg, 1990). The strip holders were rinsed with nanopure

water and dried. The samples, 15 µg of rat kidney cytosolic extract or 10 µl of the affinity purified protein fraction, were added to urea rehydration buffer. Following addition of IPG buffer, the samples were applied to the center of the strip holder in a total volume of 125 µl. Immobiline DryStrip pH 3-10, with the gel side down, was added into the solution to distribute the solution as evenly as possible under the strip. A thin layer of mineral oil was used to cover the strip. The strips were re-hydrated on the IPGphor apparatus for at least 12 h. The first dimension protocol used for IEF was as follow, 50 uA/strip at 20 °C, 1 h at 500V, 1 h at 1000V and 2 h at 8000V. The voltage did not reach the full 8000V.

4.30 SDS-PAGE

The second dimension SDS-PAGE was performed using 10% SDS-PAGE using the 2D gel prep combs. The gel stacker was rinsed with water and wells were filled with SDS running buffer to make sure there are no air bubbles. The Immobiline strip was removed from the holder and placed in 5 ml of SDS equilibration buffer for 15 min on the shaker. The ends of the strip were trimmed to fit in the well. The strip was placed in the well so that it is in contact with the bottom of the well. The strips were loaded with the + end (pointy, pH 3) farthest away from the molecular weight standard to help in marking the gel. The excess SDS running buffer was removed from the well. Then, 5 µl of the protein molecular weight standard was loaded into the marker well. The gel was run and the protein was transferred to PVDF membrane (Amersham) for 1.5 h at 100 volt in the cold room.

5 RESULTS

5.1 mRNA Decay studies using a Tetracycline-Responsive Expression System

The tetracycline- responsive expression system was developed to control the expression of a single gene in mammalian cells by using low, non-toxic levels of tetracycline (Gossen and Bujard, 1992). Previously, functional studies were performed using 5,6-dichlororibofuranosylbenzimidazole (DRB) as an inhibitor to shut-off pol II transcription. However, with prolonged inhibition of general pol II transcription, cell function and viability were affected. The tetracycline-responsive promoter system allows the *in vivo* decay of a specific mRNA to be studied without the potential artifacts that are caused by the general inhibition of pol II transcription (Xu et al., 1998).

In this system a tetracycline-controlled transcriptional activator (tTA) protein is negatively regulated by tetracycline (Fig 5.1). The tTA protein interacts specifically with an inducible promoter, which controls the transcription of the gene of interest (βG-GA). The inducible promoter consists of a minimal CMV promoter, preceded by seven copies of a tetracycline-resistance operator (*tet*O) from *E. coli* (Gossen and Bujard, 1992) that forms a tetracycline-responsive element (TRE). tTA is a fusion of the *E. coli* DNA-binding domain of the Tet repressor (TetR) to the activation domain from herpes simplex virus protein 16 (VP16AD). This fusion converts tTA from a repressor into a transcriptional activator. In the absence of tetracycline, tTA binds to the TRE and strongly activates the minimal promoter, leading to rapid transcription of the gene of interest. However, in the presence of tetracycline a conformational change in the Tet

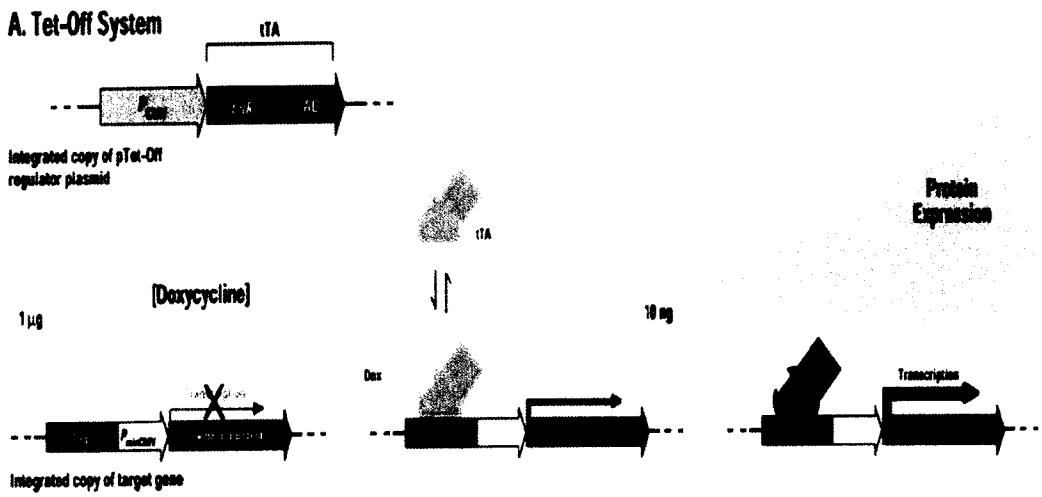

Adopted from CLONTECH Laboratories Inc. 1999

Fig. 5.1: Schematic representation of the Tet-Off System for regulating gene expression . A stable cell line that expresses high levels of the tTA protein was selected. The chimeric tTA protein contains a Tet-binding domain fused to a strong transcriptional activation domain. βG-GA was cloned upstream of a promoter that contains multiple tetracycline-responsive elements (TREs) and the minimal immediate early promoter of cytomegalovirus (PminCMV). In the absence of doxycycline (Dox), the tTA protein binds to the TREs and strongly activates transcription. In the presence of >25 ng/ml Dox, the tTA protein no longer binds to the TRE and transcription is turned off. Thus, by removing and then adding Dox to the cell culture medium, a transcriptional pulse can be created.

repressor domain prevents tTA from binding to the TRE and transcription is inhibited. Thus, gene expression can be controlled by adding or removing tetracycline, or more effectively by using the tetracycline analog, doxacycline (Dox). A tetracycline-regulated gene expression system that controls expression of βG-GA in LLC-PK_1-F^+ cells was established previously (Schroeder et al., 2006). The necessary elements are contained in two vectors. Therefore, a stable cell line expressing high levels of the chimeric tetracycline-controlled transcriptional activator protein (tTA) was initially created. The second component of the tetracycline-responsive system, the pTRE2 vector containing the βG-GA gene, was subsequently integrated into the cells selected for high expression of tTA (Fig 5.2).

5.2 Characterization of βG-GA cells that over-express ζ-crystallin

From previous studies it was hypothesized that increased binding of ζ-crystallin may promote the stabilization of the GA mRNA. Thus, over-expression of ζ-crystallin may stabilize and increase the level of GA mRNA, while decreased expression of ζ-crystallin may increase GA mRNA turnover or prevent the pH-responsive stabilization. To test this hypothesis and to study the mechanism by which ζ-crystallin can stabilize GA mRNA, a system that over-expresses ζ-crystallin was developed using clonal lines that express the βG-GA reporter construct. The pcDNA 3.1/Zeo-ζ-crystallin plasmid was used to select βG-GA clonal cells that over-express mouse ζ-crystallin (ζ^+ cells). Whereas, pcDNA 3.1/Zeo plasmid was used to select for control cells (ζ^- cells) that

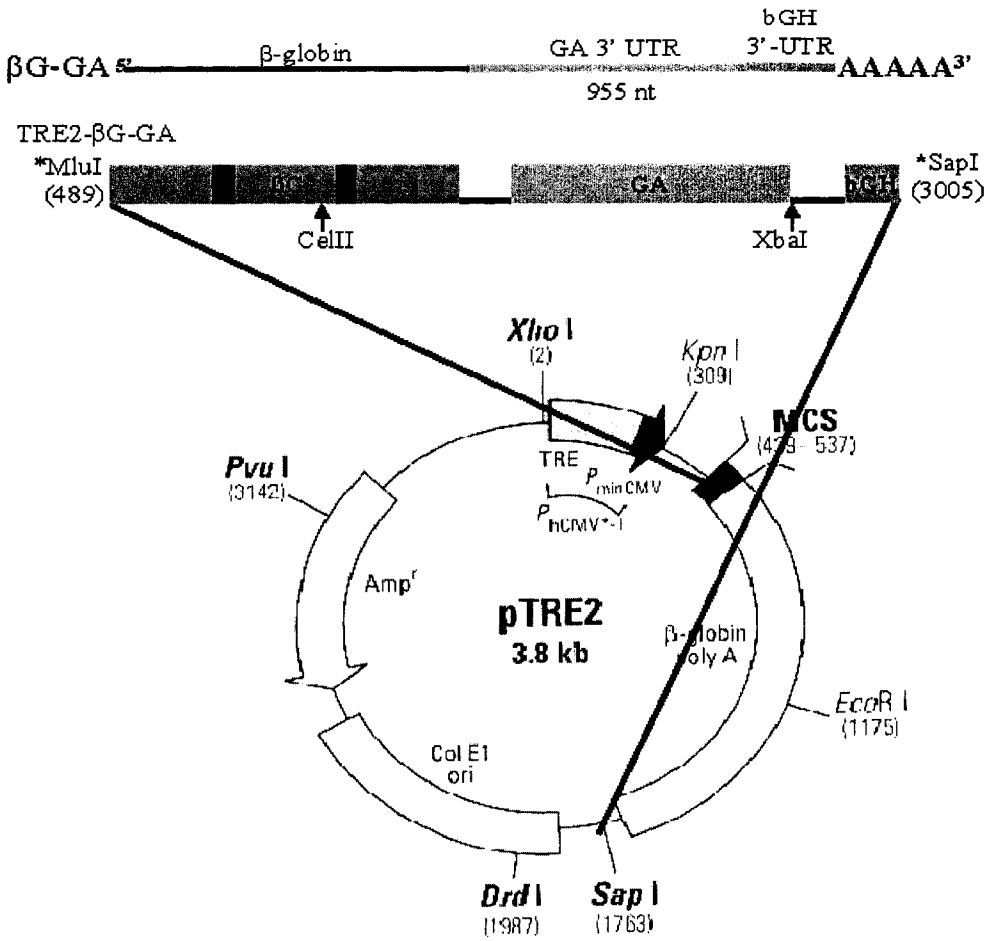

Adopted from CLONTECH Laboratories Inc. 1999

Fig. 5.2: Schematic representation of the pTRE2-βG-GA-bGH. The pTRE2 vector contains a tetracycline-responsive element (TRE) upstream of a minimal CMV promoter (P_{minCMV}), a multicloning site (MCS), and the 3'-coding and 3'-untranslated regions of the rabbit β-globin gene (β-globin polyA). To generate pTRE2-βG-GA-bGH, the βG coding region, the GA 3'-UTR, and the bovine growth hormone polyadenylation signal were PCR amplified from pβG-GA with primers that add *Mlu*I and *Sap*I sites on to the 5' and 3' ends of the PCR fragment, respectively. The PCR fragment was cloned into the *Srf*I site of pCR-Script SK (+) and an *Mlu*I/*Sap*I fragment was excised and inserted into the *Mlu*I and *Sap*I sites of pTRE2.

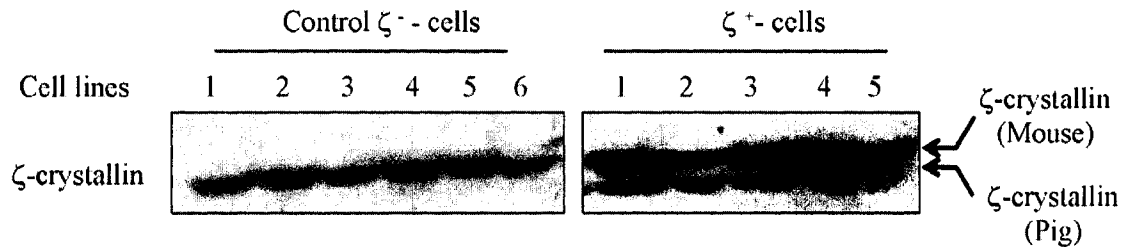

Fig. 5.3: Selection of clonal cell lines that over-express mouse ζ-crystallin. Western blot analysis of ζ-crystallin in LLC-PK_1-F^+ cells that express the TRE-βG-GA-bGH gene. Cells were selected following transfection with either pcDNA 3.1/Zeo (Control cells) or pcDNA 3.1/Zeo-ζ-crystallin(Cells over-expressing mouse ζ-crystallin). Cell extracts were separated by 10% SDS-PAGE and probed with antibodies specific for ζ-crystallin.

express only the endogenous ζ-crystallin (Fig 5.3). The selected clonal lines were tested by Western blot analyses to determine the level of expression of mouse ζ-crystallin compared to the endogenous protein (Fig 5.3). The clonal lines expressed various levels of ζ-crystallin with a maximum of a 5-fold increase compared to the endogenous level of ζ-crystallin. The cell lines were tested for tetracycline-responsive βG-GA expression by culturing the cells in the presence or absence of 0.5 μg/ml Dox. Total RNA was harvested and used for Northern blot analysis. The level of βG-GA mRNA was divided by the corresponding level of 18S rRNA to correct for errors in sample loading. For each cell line, the reported data were normalized to the +Dox values (Figs 5.4A and 5.5A). Cell lines were judged based on whether βG-GA transcription was efficiently inhibited by the presence of Dox and whether in the absence of Dox there was a high level of transcription.

ζ^--5 (control) and ζ^+- 4 (overexpress ζ-crystallin) cell lines showed the strongest tetracycline-responsive expression. The level of mRNA in the presence of Dox was almost undetectable, whereas, a high level of transcription was observed in the absence of Dox (Figs 5.4B and 5.5B). A 23-fold increase in the level of βG-GA mRNA was detected from both cell lines grown in the absence Dox. This fold–change exceeded the levels observed for the other cell lines and therefore these two cell line were used in all further experiments. The level of the mouse ζ-crystallin in ζ^+- 4 cells was 4-fold greater than the level of endogenous ζ-crystallin in the ζ^--5 cells (Fig 5.3).

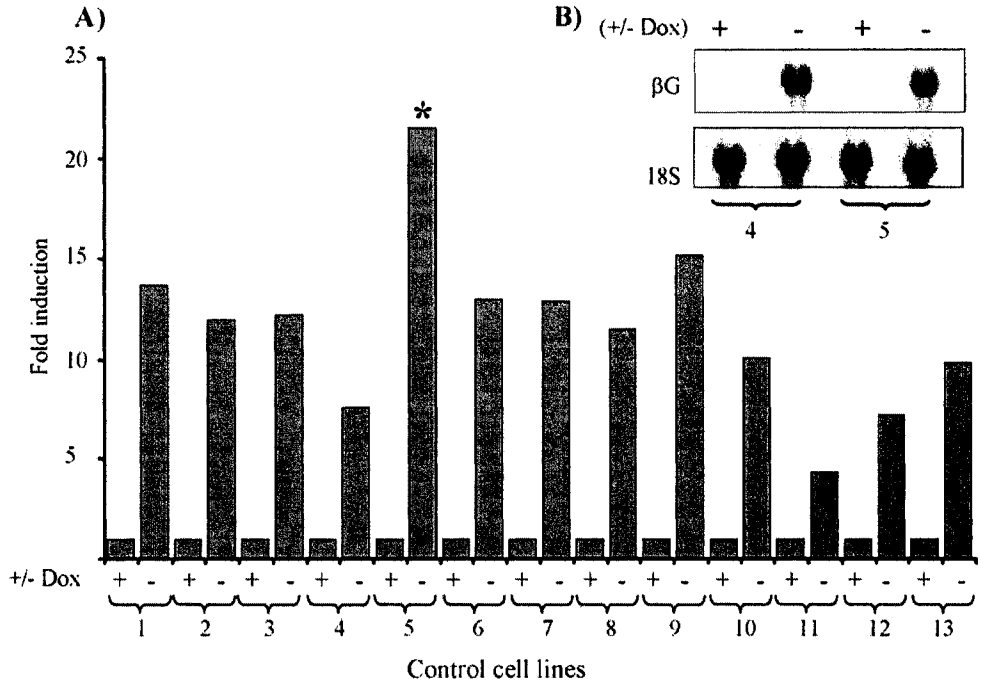

Fig. 5.4: Characterization of LLC-PK$_1$-F$^+$ cell lines that stably express pTRE2-βG-GA and pcDNA 3.1/Zeo.

Panel A. Cells lines were characterized by growing the cells for 48 h in pH 7.4 medium in the presence or absence of 0.5 μg/ml doxycycline (Dox). Total RNA was harvested from the cells and used for Northern blot analysis. The level of βG-GA mRNA was quantified and normalized to the corresponding level of 18S rRNA to correct for errors in sample loading. For each cell line, values + Dox were set equal to 1.

Panel B. Northern blot analysis of βG-GA mRNA levels expressed in two of the cell lines 4 and 5 of LLC-PK$_1$-F$^+$ expressing pTRE2-βG-GA and pcDNA 3.1/Zeo and maintained in the presence or absence of Dox. Line selected for further analysis is indicated by an asterisk (*).

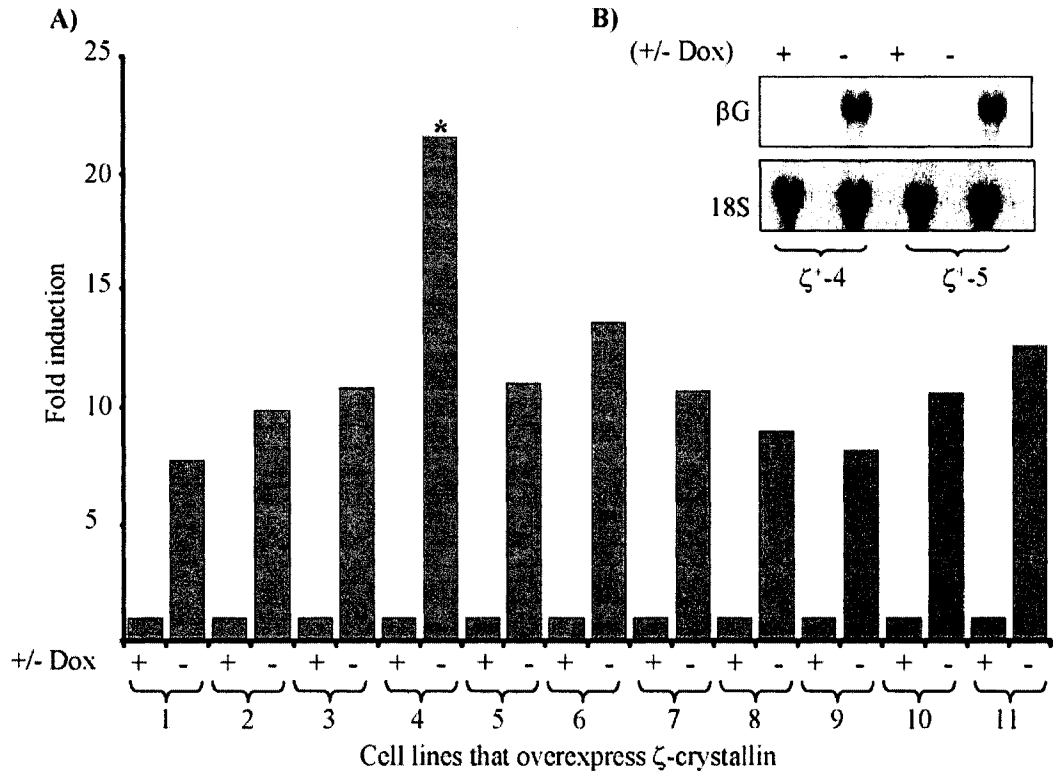

Fig. 5.5: Characterization of LLC-PK$_1$-F$^+$ cell lines that stably express pTRE2-βG-GA and pcDNA 3.1/zeocin-ζ-crystallin.

Panel A. The selected cell lines were grown for 48 h in pH 7.4 medium in the presence or absence of 0.5 μg/ml Doxycycline (Dox). Total RNA was harvested and used for Northern blot analysis. The level of βG-GA mRNA was divided by the corresponding level of 18S rRNA to correct for errors in sample loading. For each cell line, the reported data were normalized to the +Dox values.

Panel B. Northern blot analysis of the βG-GA mRNA levels expressed in two of the clonal lines (ζ$^+$-4 and ζ$^+$-5) of LLC-PK$_1$-F$^+$ expressing pTRE2-βG-GA and pcDNA 3.1/zeocin-ζ-crystallinand maintained in the presence or absence of Dox.Line selected for further analysis is indicated by an asterisk (*).

5.2.1 Creating a transcriptional pulse of βG-GA in selected clonal cell lines

A transcriptional pulse was developed to study the decay of βG-GA mRNA. The cells were initially cultured in medium containing 50 ng/ml Dox for 48 h or until 60% confluent. This level of Dox (50 ng/ml) was sufficient to completely turn off transcription but allowed rapid activation of transcription when the cells were washed to remove Dox. Removing the Dox for 3 h (transcriptional pulse) provided a population of mRNA that is nearly homogeneous in poly(A) tail length. Subsequently, high levels of Dox (1 μg/ml) were added into the medium to rapidly inhibit transcription of the TRE-βG-GA gene, so that decay of βG-GA mRNA can be monitored over time.

5.2.2 Stability of βG-GA mRNA synthesized by transcriptional pulse did not change with ζ-crystallin overexpression

A transcriptional pulse was used to determine the half-life of βG-GA mRNA without disrupting the transcription of other mRNAs in the cell. Both the ζ^--5 (control) and ζ^+-4 (overexpress ζ-crystallin) cells were maintained in normal medium with 50 ng/ml Dox until 60% confluent. Before initiating the pulse, the cells were incubated with either normal (pH 7.4) or acidic (pH 6.9) medium for 24 h, followed by a 3 h transcriptional pulse, that was stopped with the addition of 1 ug/ml Dox. RNA was isolated at 0, 3, 6, 9 and 12 h. The half-life of βG-GA mRNA isolated from cells grown in normal medium was 5.9 h and 5.3 h for the ζ^- -5 and ζ^+-4 cells, respectively (Figs 5.6 and 5.7). However, when the cells were maintained in acidic conditions, the half-life of the βG-GA mRNA was stabilized to 13 h and 12 h in the ζ^--5 and ζ^+-4 cells, respectively (Figs 5.6 and 5.7).

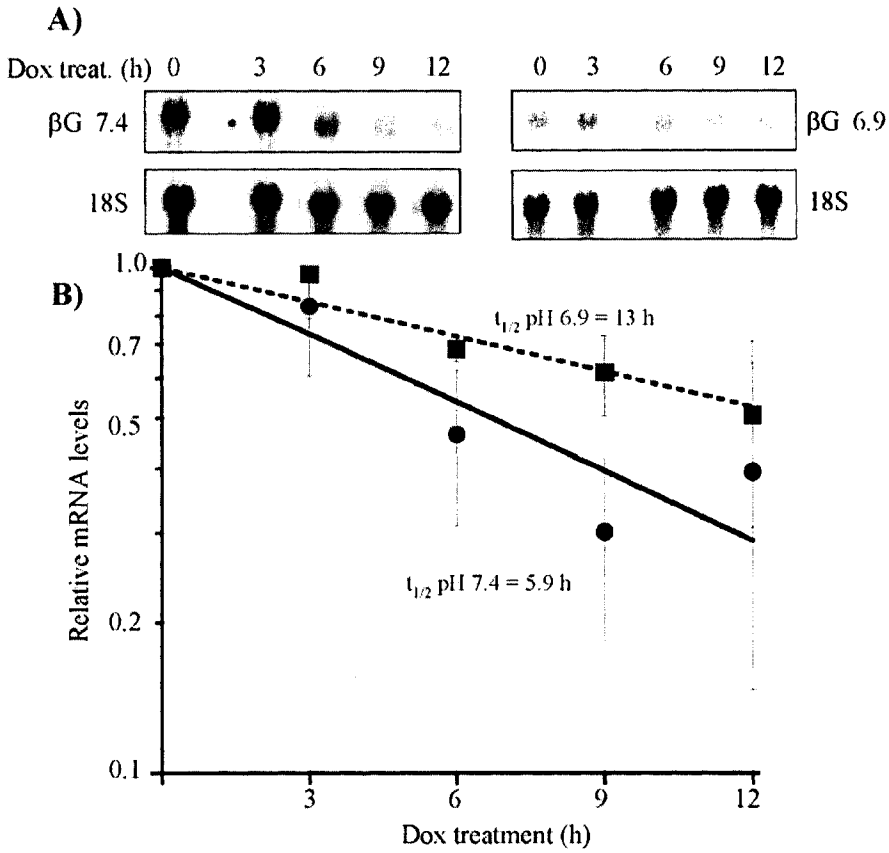

Fig. 5.6: -GA mRNA half-life in cells selected with pcDNA 3.1/Zeo (control cells) using Pulse-Chase analysis.

Panel A: Northern blot analysis of βG-GA mRNA levels. Cells were grown in medium containing 50 ng/ml Dox until 60% confluent and then either normal (pH 7.4) or acidic (pH 6.9) medium containing 50 ng/ml Dox was added for 24 h. Cells were then washed with phosphate-buffered saline (PBS) and incubated in medium minus Dox for 3 h to create a transcriptional pulse. RNA was isolated at various intervals after addition of fresh medium containing 1 μg/ml Dox. The levels of the chimeric mRNA and the 18S rRNA were quantified by Northern analysis.

Panel B: Quantification of the relative levels of βG-GA mRNA. The level of βG-GA mRNA was divided by the corresponding level of 18S rRNA to correct for errors in sample loading. The log of normalized data obtained from cells maintained at pH 7.4 (•) or treated with pH 6.9 (■) medium was then plotted versus time of Dox treatment. The reported data are the mean of triplicate samples ± S.E. The line represents the best-fit of the data points as determined by the KaleidaGraph program that weights each data point based upon its standard deviation.

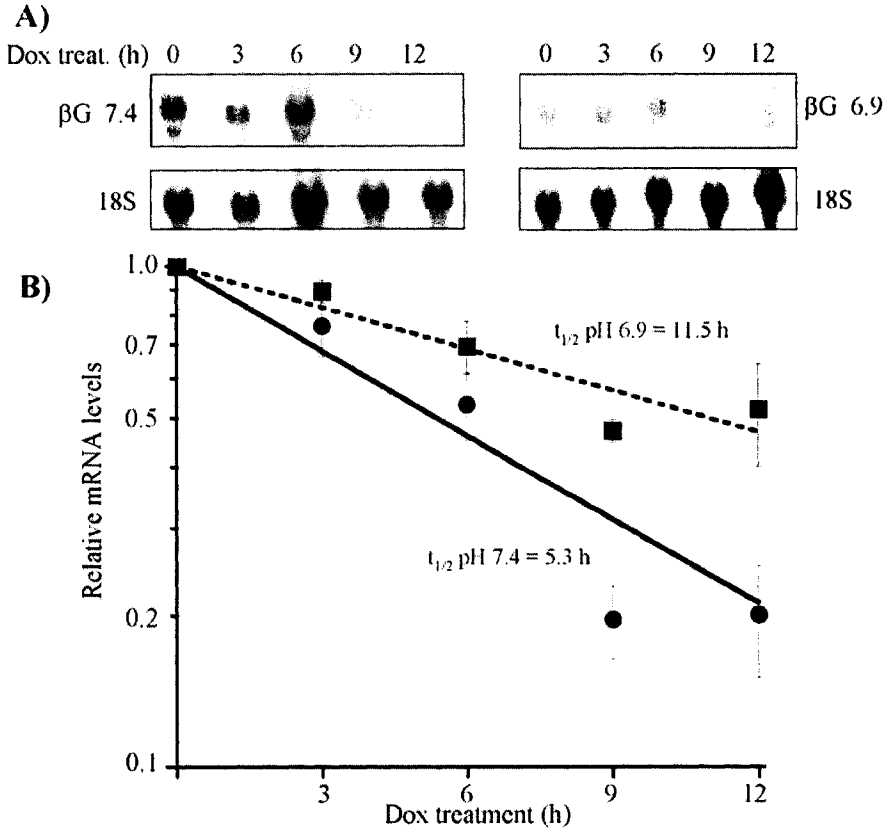

Fig. 5.7: 4-fold overexpression of ζ-crystallin did not affect βG-GA mRNA half-life using Pulse-Chase analysis.

Panel A: Northern blot analysis of βG-GA mRNA levels. Cells were grown in medium containing 50 ng/ml Dox until 60% confluent and then either normal (pH 7.4) or acidic (pH 6.9) medium containing 50 ng/ml Dox was added for 24 h. Cells were then washed with phosphate-buffered saline (PBS) and incubated in medium minus Dox for 3 h to create a transcriptional pulse. RNA was isolated at various intervals after addition of fresh medium containing 1 μg/ml Dox. The levels of the chimeric mRNA and the 18S rRNA were quantified by Northern analysis.

Panel B: Half-life analysis of βG-GA mRNA. The level of βG-GA mRNA was divided by the corresponding level of 18S rRNA to correct for errors in sample loading. The log of normalized data obtained from cells maintained at pH 7.4 (•) or treated with pH 6.9 (■) medium was then plotted versus time of treatment with Dox. The reported data are the mean of triplicate samples ± S.E. The line represents the best-fit of the data points as determined by the KaleidaGraph program.

These data replicate previous results obtained by pulse-chase analysis of the turnover of the βG-GA mRNA in LLC-PK_1-F^+ cells. Therefore, co-expression of the pcDNA3.1-Zeo or pcDNA3.1-Zeo-ζ-crystallin plasmids had no effect on the basal or pH-responsive turnover of the βG-GA mRNA. Furthermore, neither half-life was affected by the 4-fold overexpression of mouse ζ-crystallin.

5.2.3 pH-responsive stabilization of βG-GA mRNA does not occur in the absence of a pulse

J Schrouder (Schroeder., 2002) showed previously that cells grown in the absence of Dox and then treated with 1 μg/ml Dox failed to exhibit a pH-responsive stabilization of the βG-GA mRNA. In this experiment, βG-GA cells were grown minus Dox until 60% confluent and then the medium was replaced with either normal (pH 7.4) or acidic (pH 6.9) medium for 24 h before the addition of 1 μg/ml Dox. RNA was isolated at 0, 3, 6, and 9 h after treatment. Northern analysis indicated that the βG-GA mRNA turned over with a half-life of 2 h in cells treated with either normal or acidic medium. The level of βG-GA mRNA transcribed in the absence of Dox was 10-fold greater than the maximal level synthesized during the pulse-chase procedure. Therefore, the high level of βG-GA mRNA may exceed the level of the cellular factors that are responsible for a pH-responsive stabilization of the mRNA. In such case, the mRNA would not be stabilized under acidic conditions since the cells lack a sufficient level of stabilizing factors. In order to test this hypothesis, the effect of over expression of ζ-crystallin on the stability of βG-GA mRNA was determined using the no-pulse protocol.

5.2.4 Over-expression of ζ-crystallin did not restore the pH-responsive stabilization of βG-GA mRNA in the absence of a pulse

Both the ζ^--5 and ζ^+-4 cells were maintained in normal medium and in the absence of Dox for 48 h or until 60% confluent. The medium was changed to either normal or acidic medium without Dox for 24 h, followed by addition of 1 μg/ml Dox. RNA was isolated at 0, 3, 6, 9 and 12 h. The half-life of βG-GA mRNA isolated from cells grown in normal medium was 2.5 h and 2.6 h for the ζ^--5 and ζ^+-4, respectively (Fig 5.8). When the cells were treated with acidic medium, the half-life of the βG-GA mRNA was 2.4 h and 2.6 h for for ζ^-- 5 and ζ^+-4, respectively (Fig. 5.8).

A 4-fold increase in mouse ζ-crystallin expression in βG-GA cells did not restore the pH responsive stabilization of the βG-GA mRNA. Therefore, either the level of βG-GA mRNA that is transcribed with no-pulse still exceeds the level of ζ-crystallin that is required for the pH-responsive stabilization of the βG-GA mRNA or an additional or alternative stabilizing factor is limiting and not sufficient to stabilize the high level of βG-GA mRNA.

5.3 Cloning and identification of porcine ζ-crystallin from LLC-PK$_1$-F$^+$ cells

To test the hypothesis that decreased expression of ζ-crystallin may increase GA mRNA turnover or prevent the pH-responsive stabilization, an siRNA was used to reduce expression of ζ-crystallin. In the previous experiments recombinant mouse ζ-crystallin was used for overexpression. Designing and identification of an siRNA specific for ζ-crystallin in LLC-PK$_1$-F$^+$ cells required the initial determination of the nucleotide

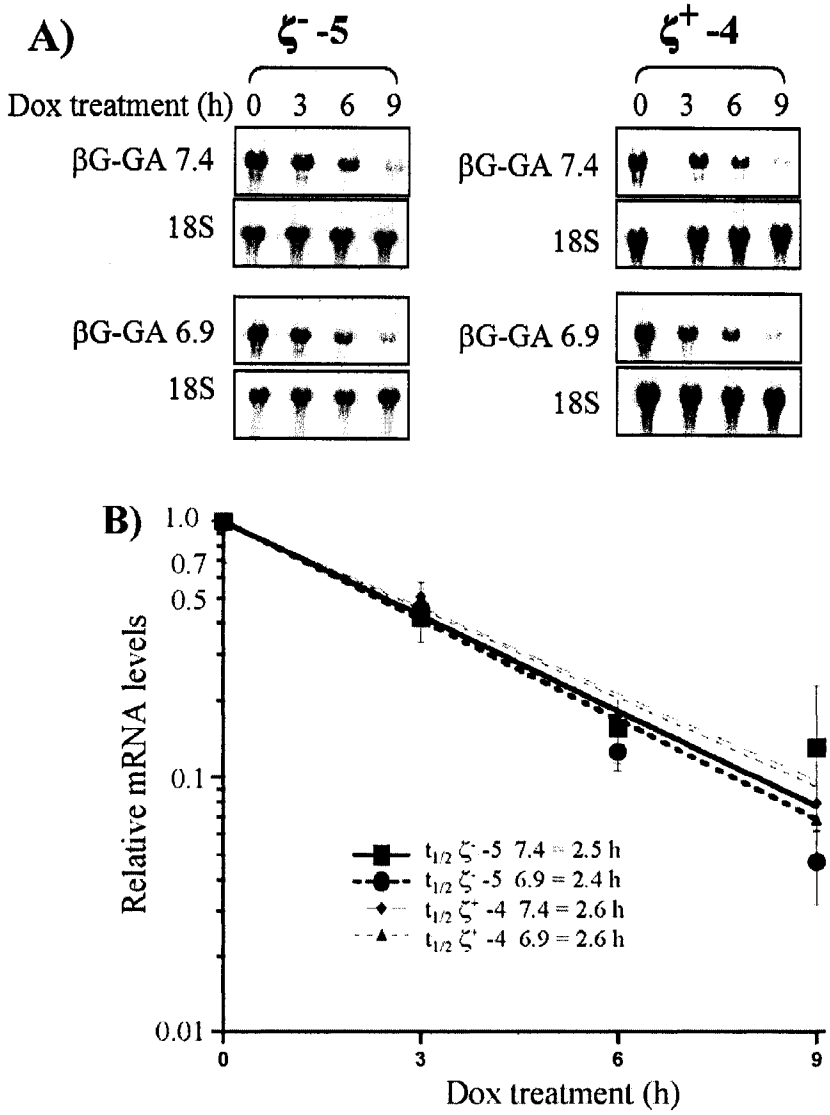

Fig. 5.8: 4-fold over-expression of ζ-crystallin is not sufficient to stabilize βG-GA mRNA in LLC-PK$_1$-F$^+$ cells without a transcriptional pulse.

Panel A Both the ζ$^-$-5 and ζ$^+$-4 cells were maintained in normal medium and in the absence of Dox for 48 h or until 60% confluent. The medium was changed to either normal or acidic medium without Dox for 24 h, followed by addition of 1 μg/ml Dox. RNA was isolated at 0, 3, 6, 9 and 12 h and analyzed by Northern analysis.

Panel B: Quantification of the relative levels of βG-GA mRNA. The level of βG-GA mRNA from ζ$^-$-5 (control) or from ζ$^+$-4 cells (over-express ζ-crystallin 4-fold) was divided by the corresponding level of 18S rRNA to correct for errors in sample loading. The log of normalized data was then plotted versus time of Dox treatment. The reported data are the mean +/- of data obtained from 3 separate determinations. The line represents the best-fit of the data points as determined by the KaleidaGraph program.

sequence of porcine ζ-crystalllin.

Degenerative primers were designed based upon conserved sequences within the mouse, human and rat ζ-crystallin cDNA. They were used to RT-PCR amplify and clone cDNAs from poly(A) RNA isolated from LLC-PK_1-F^+ cells. A PCR fragment containing 990 bp of the coding region of ζ-crystallin was obtained and cloned into the pGEM-T-Easy vector (pZC7 plasmid). Sequence analysis and alignment established that the porcine ζ-crystallin is 75.4, 74.5 and 85.1 % identical to the mouse, rat and human sequences, respectively, whereas the amino acid sequence has a 76.7, 77.2 and 84.5 % identity to the respective sequences (Figs 5.9 A & B). The amino acids sequence analysis of the various ζ-crystallins was performed using the MEGALIGN and EDITSEQUENCE programs (DNASTAR. Inc). This analysis identified potential protein kinase c and casein kinase II phosphorylation sites that are conserved in all species.

5.4 Design and selection of ζ-crystallin siRNA

The coding region sequence of the porcine ζ-crystallin was used to design an siRNA to clone it into pSHAG1 vector. The porcine ζ-crystallin coding region was also cloned in psiCHECK-2 vector. To design a ζ-crystallin specific siRNA for LLC-PK_1-F^+ cells, a structural motif described by (Boden, 2004) containing a loop structure (miB-*tat*) identical to that of endogenously produced miR-30 RNA was used (Fig. 5.10). The motif or cassette consisted of a U6 (Pol III) promoter followed by a short hairpin DNA sense and antisense sequence, separated by a miR-30 loop. The sequence encoding the ζ-

```
ATG GCG ACT GGG CAG AAG TTG ATG AGC GCT ATT AGA GTT TTT AAA TTT GGT GGA CCA GAA
 M   A   T   G   Q   K   L   M   S   A   I   A   V   F   L   F   G   G   P   E

GTG ATG AAA CTC CAG TCG GAT GTT GCC ATA CCA ATT CCA AAG GAC AAT CAG GTT CTA ATC
 V   M   K   L   Q   S   D   V   A   I   P   I   P   K   D   N   Q   A   L   I

AAA GTC CAC GCA TGT GGT GTC AAC CCA GTG GAC ACG TAT ATT CGC TCT GGT ACT CAC AAT
 K   V   H   A   C   G   V   N   P   V   D   T   Y   I   R   S   G   T   H   N

ATG AAA CCA CTT CTA CCC TAT ACT CCT GGT TTA GAT GTG GCT GGA ATA GTA GAA GCT GTC
 M   K   P   L   L   P   Y   T   P   G   L   D   V   A   G   I   V   E   A   V

GGA GAG CAT GTA TCT TCT TTC AAG AAA GGT GAC AGA GTT TTC ACA GTC AGC ACT CTC TCC
 G   E   H   V   S   S   F   K   K   G   D   R   V   F   T   V   S   T   L   S

GGG GGC TAC GCA GAG TAT GCT TTA GCA GCC GAC GAC ACT GTT TAC ATG CTG CCA GAA AAA
 G   G   Y   A   E   Y   A   L   A   A   D   D   T   V   Y   M   L   P   E   K

CTG GAC TTT AAA CAA GGA GCT GCC ATT GGG ATC CCA TAT TTT ACT GCT TGT CTT GCT CTG
 L   D   F   K   Q   G   A   A   I   G   I   P   Y   F   T   A   C   L   A   L

CTC CAC AGT GCC TGT GTG AAA GCT GGA GAA ATT GTT CTG ATT CAT GGG GCT AGT GGA GGG
 L   H   S   A   C   V   K   A   G   E   I   V   L   I   H   G   A   S   G   G

GTT GGA ATA GCA GCG TGC CAA ATT GCT AGA GCT TAT GGC TTA AAG GTT TTG GGC ACA GCT
 V   G   I   A   A   C   Q   I   A   R   A   Y   G   L   K   V   L   G   T   A

GGT ACT GAG GAA GGA CAA AAT ATT GTT TTG CAA AAT GGA GCC CAT GAA GTG TTT AAT CAC
 G   T   E   E   G   Q   N   I   V   L   Q   N   G   A   H   E   V   F   N   H

AGA GAA GTT AAT TAT ATT GAC AAA ATT AAG AAA TCT GTT GGT GAA AAA GGA ATT GAT GTG
 R   E   V   N   Y   I   D   K   I   K   K   S   V   G   E   K   G   I   D   V

ATT ATT GAA ATG TTA GCT AAT GTA AAT CTT AGC AAT GAT TTG AAT CTT TTG TCA CAT GGA
 I   I   E   M   L   A   N   V   N   L   S   N   D   L   N   L   L   S   H   G

GGA CGA GTA ATA ATT GTT GGC TCC AGA GGT CCT ATT GAA ATA AAC CCT CGG GAC ACT ATG
 G   R   V   I   I   V   G   S   R   G   P   I   E   I   N   P   R   D   T   M

ACA AAG GGA TCT AGC ATA AAA GGA GTT GCT CTC TAT TCA TCA ACC AAG GAG GAA TTT CAG
 T   K   G   S   S   I   K   G   V   A   L   Y   S   S   T   K   E   E   F   Q

CAG TTG GCA GCA GCC CTT CAA GCT GGA ATG GAA GTT GGT TGG TTG AGA CCT GTG ATA GGT
 Q   L   A   A   A   L   Q   A   G   M   E   V   G   W   L   R   P   V   I   G

CCT GTG TAT CCA CTG GAG AAG GCG GCC CAG GCT CAT GAA GAC ATC ATT CAC AGC CGT GGG
 P   V   Y   P   L   E   K   A   A   Q   A   H   E   D   I   I   H   S   R   G

GCT ACT GGG AAA ATG ATT CTT CTC TTA TGA
 A   T   G   K   M   I   L   L   L   *
```

Fig. 5.9A: DNA sequence and predicted amino acid sequence of porcine ζ-crystallin. Start codon is underlined and stop codon is marked by asterisk (*).

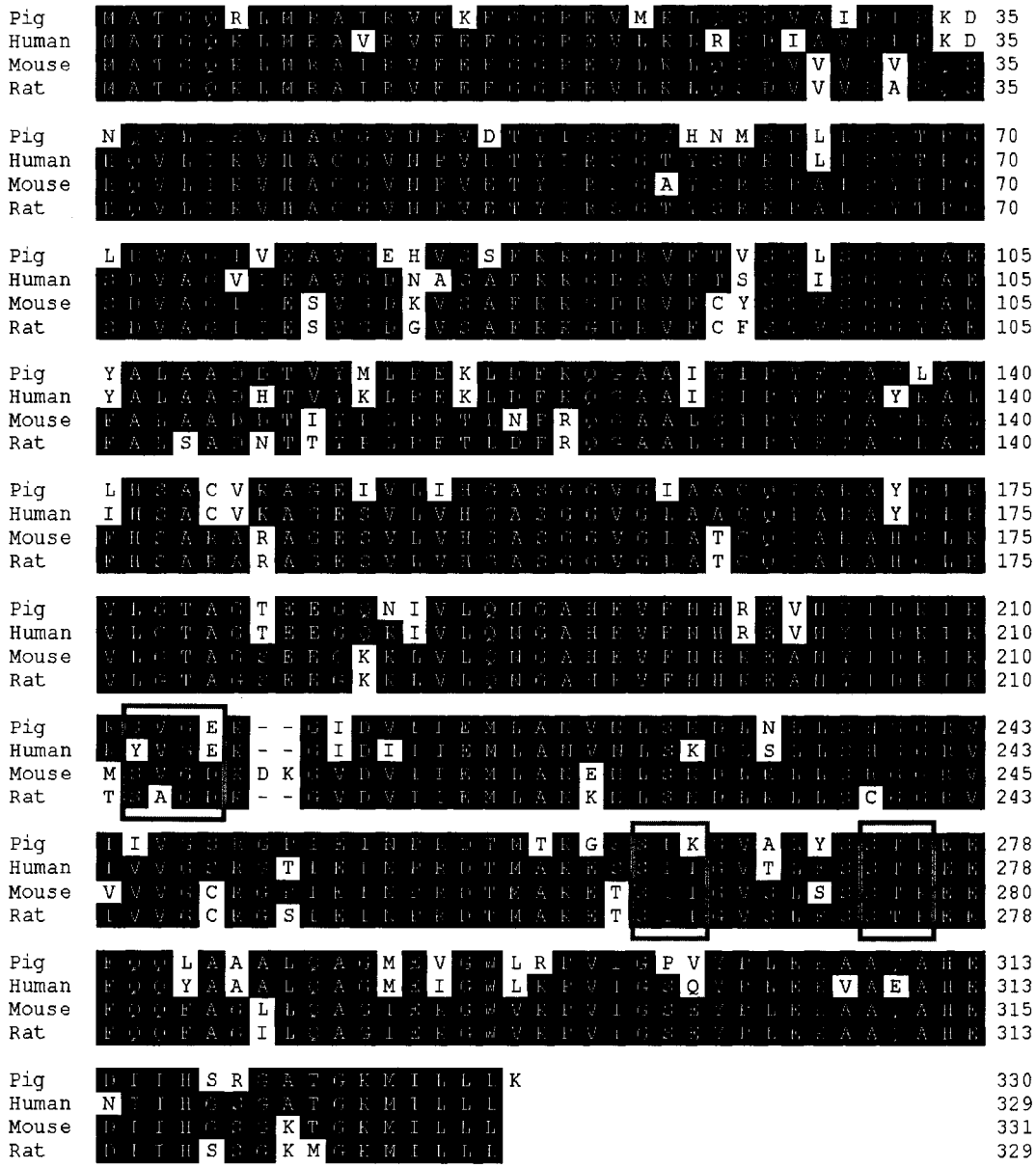

Fig. 5.9B: ζ-crystallin is highly conserved. Predicted amino acids of ζ-crystallin from pig, human, rat and mouse were aligned using MEGALIGN and EDITSEQUENCE programs (DNASTAR. Inc.). Potential phosphorylation sites that are conserved in four species are boxed.

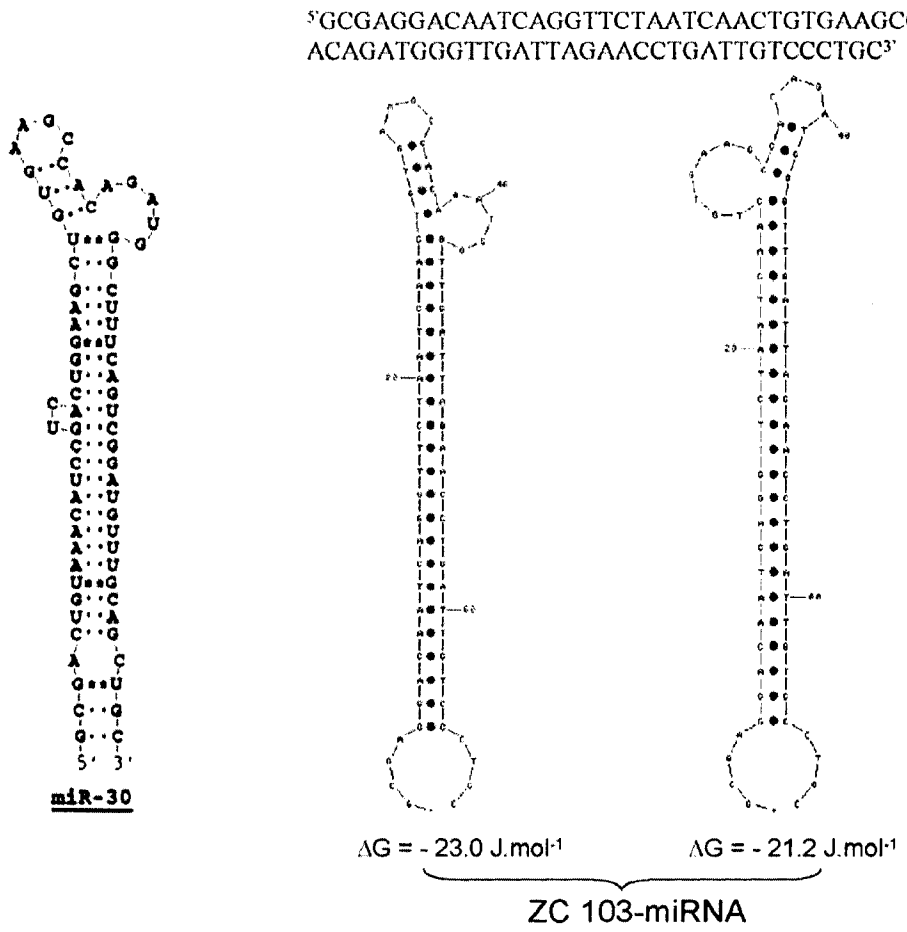

Fig. 5.10: Structure of miR-30 and ZC103-miRNA. The coding region sequence was scanned for 21nt stretches that had favorable predicted secondary structure features such as free energy (ΔG) of the target site, total numbers of unpaired nucleotides, and major loop size. ΔG and the secondary structure of ZC103-miRNA were predicted using the scitool form IDT website http://www.idtdna.com/Home/Home.aspx . The two ZC103-miRNA structures represent the favorable secondary structures that can be produced by this sequence. The sequence encoding the ζ-crystallin siRNA was incorporated into a human miR-30 pre-microRNA (pre-miRNA) backbone and delivered as pre-miRNA precursor (ZC 103-miRNA).

crystallin siRNA was incorporated into a human miR-30 pre-microRNA (pre-miRNA) backbone and delivered as a pre-miRNA precursor (ZC103-miRNA). The coding region sequence was scanned for 21-nt stretches that had predicted secondary structure features such as a favorable free energy (ΔG) of hybridization to the target site, total number of unpaired nucleotides, and major loop size. A control vector (pSHAG-Ffl) was obtained from the Hannon lab which encodes an shRNA that is specific for the firefly luciferase.

The porcine ζ-crystallin coding region was cloned into the psiCHECK-2 vector. The psiCHECK-2 vector provides a quantitative and rapid approach for initial optimization of RNA interference (RNAi) (Fig 5.11A). This vector enables monitoring of changes in expression of a ζ-crystallin gene fused to a *Renilla* luciferase reporter gene. The ζ-crystallin gene was cloned into a multiple cloning region located downstream of the *Renilla* translational stop codon. Initiation of the RNAi process by expression of a shRNA towards the ζ-crystallin gene should result in cleavage and subsequent degradation of the fusion mRNA. Therefore, the decrease in *Renilla* activity provides a convenient measure of the RNAi effectiveness.

5.4.1 Cloning ζ-miRNA sequences into pSHAG1 vector

A ζ-crystallin specific construct (ZC103-miRNA) was cloned into the pSHAG1 vector (Fig. 5 .11B) to produce pSHAG-ZC103-miRNA. The insertion of ZC103-miRNA into the pSHAG1 plasmid was confirmed by restriction analysis and by sequencing. pSHAG-Ffl plasmid that has the shRNA for Firefly luciferase was co-transfected with pMAMneo-LUC (expresses firefly luciferase) and the pRL-null (expresses Renilla

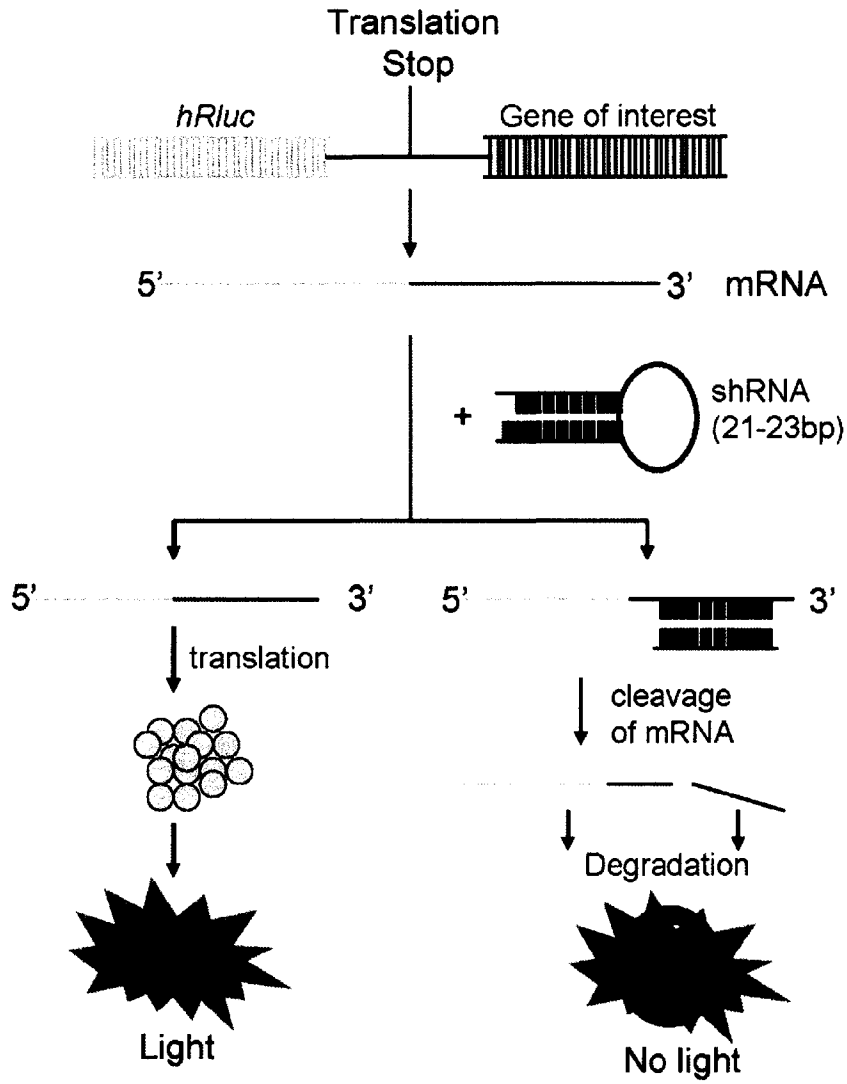

Fig. 5.11A: Use of the psiCHECK-2 vector to screen for siRNA efficiency. psiCHECK-2 Vector is designed to provide a rapid and quantitative approach for initial optimization of RNA interference (RNAi). The vector enables monitoring of changes in expression of a target gene fused to a *Renilla* luciferase reporter gene. The gene of interest is cloned into a multiple cloning region located downstream of the *Renilla* translational stop codon. Initiation of the RNAi process by expression of a shRNA towards the gene of interest results in cleavage and subsequent degradation of the fusion mRNA. Therefore, the decrease in *Renilla* activity provides a convenient measure of the RNAi effectiveness

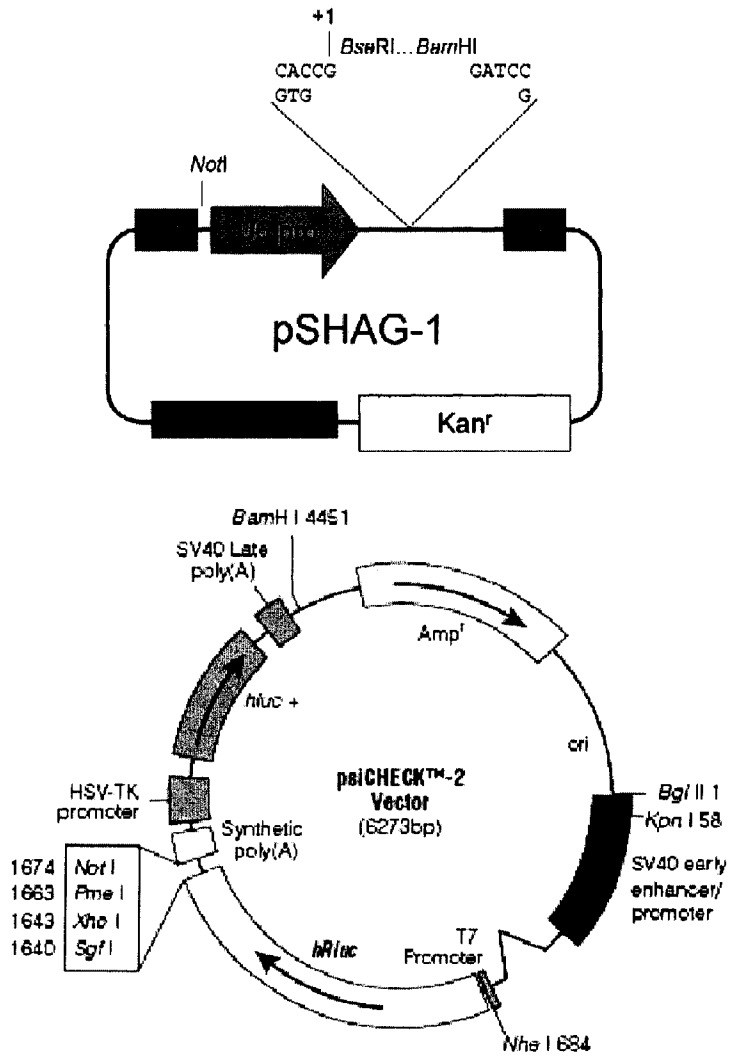

Fig.5.11B: Schematic representation of the pSHAG1 and psiCHECK2. ZC103-miRNA was cloned into the pSHAG1. The coding region of ζ-crystallin was cloned into the psiCHECK-2. pSHAG1 plasmid contains the *att*L1 and *att*L2 recombination sites, a U6 promoter and a kanamycin selection gene. psiCHECK-2 vector provides a quantitative and rapid approach for initial optimization of RNA interference (RNAi). This vector enables monitoring of changes in expression of a ζ-crystallin gene fused to a *Renilla* luciferase reporter gene.

luciferase) plasmids as a control to test the efficiency of siRNA processing in the LLC-PK_1-F^+ cells.

5.4.2 Cloning of ζ-crystallin coding region into psiCHECK-2 vector

The coding region of ζ-crystallin was cloned into the psiCHECK-2 vector (Fig. 5.11B) in either the sense (psiCHECK-ZC1) or anti-sense (psiCHECK-ZC2) direction. The insertion and orientation of ζ-crystallin coding region into the psiCHECK-2 plasmid was confirmed by restriction analysis and sequencing. Digestion with *BamH*I produced 3347 bp and 3884 bp fragments for the psiCHECK-ZC1 (sense), whereas it produced 3167 bp and 4046 bp fragments for psiCHECK-ZC2 (antisense).

5.4.3 Screening siRNA sequences using luciferase assays

As a control to test the efficiency of siRNA processing in LLC-PK_1-F^+ cells, cells were transiently transfected with pMAMneo-LUC and the pRL-null plasmids in the absence or presence of a pSHAG-Ffl plasmid that encodes the shRNA for Firefly luciferase. The resulting firefly luciferase activity was standardized against the corresponding Renilla luciferase activity and then normalized. The data are the mean +/- S.E. of 3 separate transfections (n = 3). The relative luciferase activities were reduced to about 20% of the original activity when a pSHAG-Ffl plasmid was cotransfected (Fig 5.12).

psiCHECK-2, psiCHECK-ZC1 or psiCHECK-ZC2 plasmid was transiently co-transfected with pSHAG-ZC103-miRNA (encodes ζ-crystallin siRNA) into LLC-PK_1-F^+ cells. Dual luciferase assay was used to test the efficiency of siRNA in cleavage and

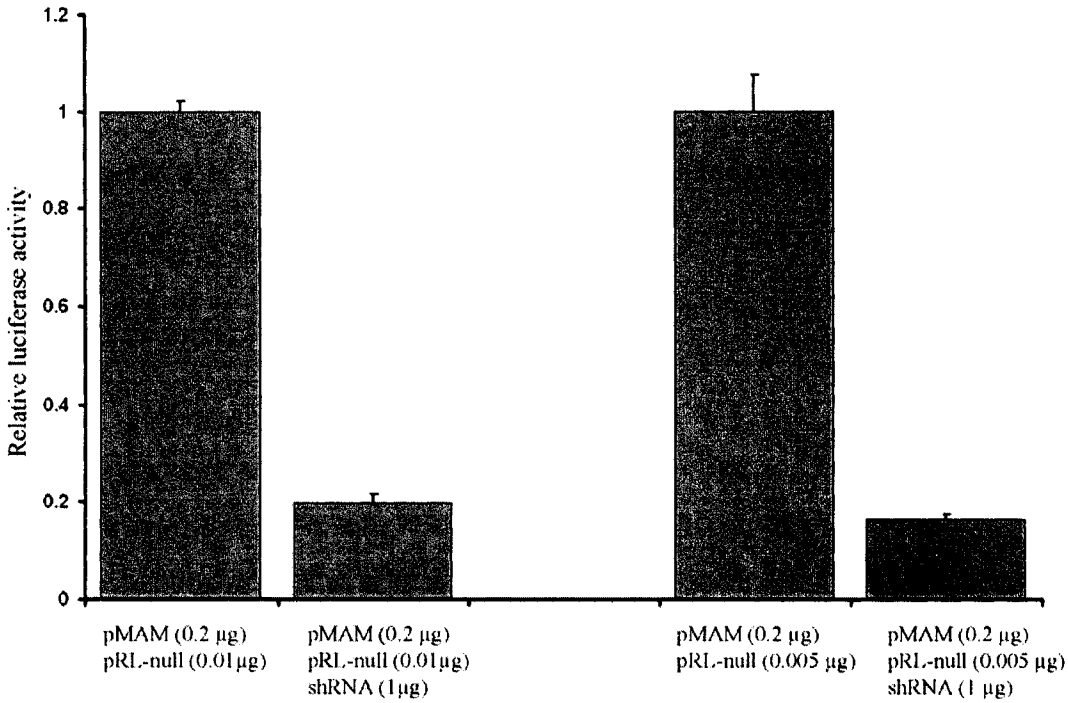

Fig. 5.12: Effect of co-expression of the Firefly luciferase-shRNA on the activities of pMAMneo-LUC reporter plasmid. LLC-PK_1-F^+ cells were transiently transfected with pMAMneo-LUC and the pRL-null plasmids in the absence or presence of a pSHAG-Ffl plasmid that encodes the shRNA for Firefly luciferase. The resulting firefly luciferase activity was standardized against the corresponding Renilla luciferase activity and then normalized. The data are the mean +/- S.E. of 3 separate transfect ions (n = 3).

degradation of the fusion ζ-crystallin mRNA. The decrease in Renilla activity provides a convenient measure of the RNAi effectiveness. The resulting Renilla luciferase activity was standardized against the corresponding firefly luciferase activity and then normalized. Co-transfection of the pSHAG-ZC103miRNA reduced the relative luciferase activity of psiCHECK-ZC1 (ζ-crystallin coding region in the sense orientation) by 87%, whereas, the activity of the psiCHECK-ZC2 plasmid (ζ-crystallin coding region in the anti-sense orientation) was reduced by 70% of the original activity. The relative luciferase activity of the psiCHECK-2 plasmid was not affected by co-transfection of ZC103-miRNA (Fig 5.13). These findings indicated the specificity of the siRNA sequence and its efficiency in knocking down ζ-crystallin.

5.5 Construction of shuttle vector that contains the ZC-miRNA (miRNA-pAd-Track-RFA plasmid)

The Gateway LR Clonase II enzyme mix (Invitrogen) was used to catalyze the *in vitro* recombination between pSHAG1-ZC-miRNA and pAdTrack-RFA plasmid to generate the miRNA-pAd-Track-RFA plasmid. The recombination accomplished the insertion of the ZC-miRNA into the pAdTrack vector (Fig. 5.14). The insertion of the shRNA sequence was confirmed by restriction analysis with *XbaI* and *XhoI* which produced 8320-bp and 400-bp fragments from the recombined miRNA-pAd-Track-RFA plasmid, whereas the non-recombined vector, pAd-Track-RFA, produced 1711-bp and 8320-bp fragments. Sequence analysis of the miRNA-pAd-Track-RFA plasmid using

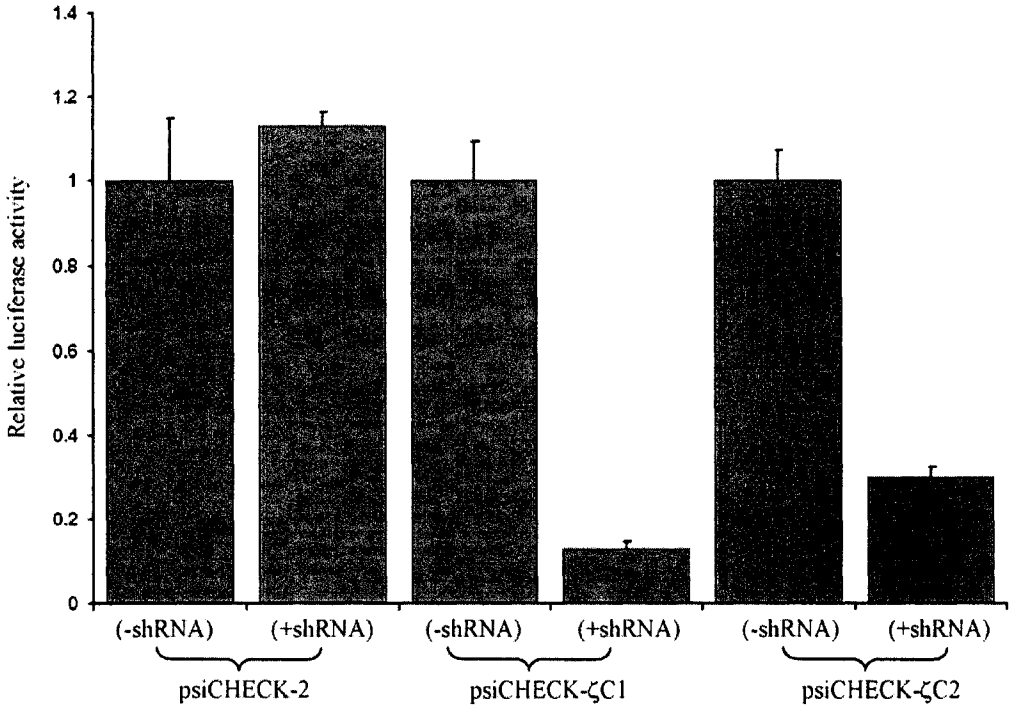

Fig. 5.13: Effect of co-expression of the ζ-crystallin-shRNA on the activities of the psi-CHECK-2 constructs. LLC-PK_1-F^+ cells were transiently transfected with the psi-CHECK-2 constructs in the absence or presence of a pSHAG-shRNA plasmid that encodes the shRNA for ζ-crystallin. The resulting Renilla luciferase activity was standardized against the corresponding firefly luciferase activity and then normalized. The data are the mean +/- S.E. of 3 separate transfect ions (n = 3).

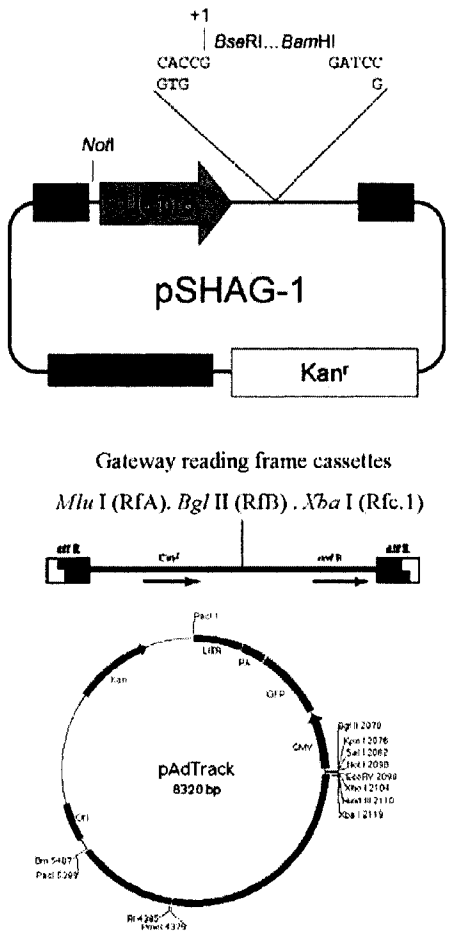

*att*B1-gene-*att*B2 x *att*P1-*ccd*B-*att*P2 ⇔ *aat*L1-gene-*att*L2 x *att*R1-*ccd*B-*att*R2
(expression clone) (pDONR) (entry clone) (destination vector)

Fig. 5.14: Construction of shuttle vector that contains the ZC-miRNA (miRNA-pAd-Track-RFA plasmid). *in vitro* recombination of pSHAG1 (containing L1 and L2 recombination site) and pAD-Track-RFA (containing *att*R recombination sites). pAD-Track-RFA is constructed from pAdTrack plasmid by using the Gateway Vector Conversion System (Invitrogen). This system is designed to convert any vector into a Gateway destination vector using restriction endonuclease and ligase. The system has a Gateway cassette containing *att*R recombination sites flanking a *ccd*B gene and a chloramphenicol-resistance gene that are blunt-end cloned into the multiple cloning site of the vector. The Gateway LR Clonase II enzyme mix (Invitrogen) was used to catalyze the *in vitro* recombination between an entry clone, pSHAG1-ZC-premiRNA, and the destination vector, pAdTrack-RFA plasmid to generate an expressing siRNA clone.

forward primer (serial number 55592) 5'-GGG CCA TTT ACC GTA AGT TAT G-3' (~67 bp before BglII site of MCS) and a reverse primer (serial number 55724): 5'-CTC ACA ATG CTT CCA TCA AAC G -3' (~92 bp from XbaI site of MCS) were used to confirm the insertion.

5.6 Generation of recombinant and replication deficient Adenoviruses for controlled expression of ζ-crystallin in βG-GA expressing cells

Adenoviruses can be produced as high-titer replication-deficient viruses that can be used to infect many cells. Thus adenoviruses were used to overexpress and to knockdown ζ-crystallin in LLC-PK_1-F^+ cells that stably express the TRE-βG-GA gene. Adenovirus offer three main advantages for our system: a high titer, a high infection efficiency and the lack of integration into the host cell genome. Since the adenoviral DNA remains episomal, none of the host cell genes are interrupted. Type 5 Adenovirus (Ad5) is a virus that is used for generating most of the recombinant adenoviruses. Ad 5 virus has a double stranded genomic DNA of approximately 36 kb. The viral genome is grouped into 3 transcriptional units including the early (E1, E2, E3, E4), intermediate, and late units. Production of recombinant adenovirus utilizes deletion of certain viral genes and their replacement with the gene of interest. Deletion of E1 and E3 genes are the most commonly used deletions to produce Ad-Easy-1 virus. E1 gene is necessary for viral replication so its deletion will produce a replication incompetent virus in normal cells. Providing the E1 gene in *trans* will produce the replication competent virus from the E1-deleted adenoviral vectors. E3 gene is not necessary for either viral replication or infection. Up to 7.5 kb of foreign DNA can be inserted into Ad vectors after deletion of

E1 and E3 genes (Leber, 1996). Recombinant Ad vectors were generated in bacterial cells as described by (He et al., 1998). This is accomplished by homologous recombination between pAdEasy-1 plasmid, containing E1 and E3 deleted adenovirus genome and a transfer (shuttle) plasmid that has the gene or sequence of interest flanked by regions of homologous sequences to the viral genome (Fig 5.15). This recombination step is performed in bacterial cells (BJ5183 *E.coli* cells) that are recombination competent. A recombinant adenoviral plasmid is isolated from the BJ5183 cells and then linearized (by *Pac*I restriction enzyme) and transfected into a mammalian packaging cell line, 293 cells (E1-transformed human embryonic kidney cells), to produce packaged and infectious but replication-incompetent viral particles.

Two shuttle vectors (pShuttle and pAdTrack plasmids) were used to clone the ζ-crystallin coding region or ζ-crystallin siRNA behind its own promoter, respectively. Identification of the infected cells can be monitored when using pAdTrack plasmid because it also contains a green fluorescent protein (GFP) gene under the control of cytomegalovirus (CMV) immediate-early promoter.

The pShuttle plasmid was used for generation of virus that over-express ζ-crystallin (ζ-cryst) and as a control (shuttle) adenovirus (provided by the Bamburg Lab), whereas a modified pAdTrack plasmid (pAdTrack-RFA plasmid) was used for generation of adenovirus that expresses shRNA for ζ-crystallin (shRNA) or its control (GFP) adenoviruses. The ZC103-miRNA was first cloned into the pSHAG1 plasmid and then it was inserted into the pAdTrack-RFA transfer vector using the LR *in vitro* recombination

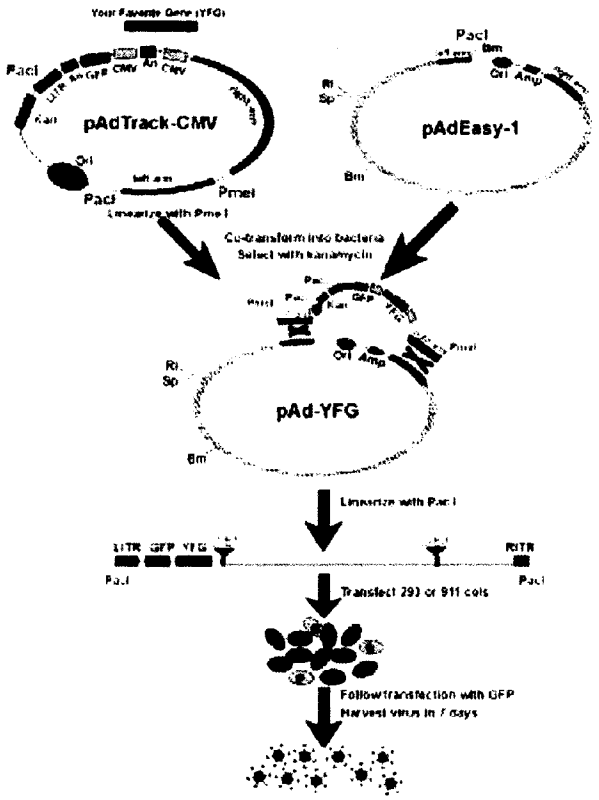

Adopted from He *et al.*, (http://www.coloncancer.org/adeasy/protocol2.htm)

Fig. 5.15: Schematic outline of the AdEasy system. The gene of interest is first cloned into a shuttle vector, e.g., pAdTrack-CMV or Shuttle vectors. The resultant plasmid is linearized by digesting with restriction endonuclease *Pme*I, and subsequently co-transformed into *E. coli* BJ5183 cells with an adenoviral backbone plasmid, e.g., pAdEasy-1. Recombinants are selected for kanamycin resistance. The recombinant adenoviral plasmid is then digested with *Pac*I and transfected into 293 cells where they are packaged into virus particles.

kit. For generation of control virus, the pSHAG1 plasmid was recombined *in vitro* with the pAdTrack-RFA vector. The correct recombination was tested by restriction digest with *XbaI* and *XhoI* where the correct plasmid should produce 0.4 kb and 8.5 kb bands. Incorrect clones would produce 1.7 kb with the 8.5 kb bands. Next the shuttle plasmids were digested with *PmeI* and then used to transform the AdEasier-1 cells (also known as BJAdEasy Cells or AdEasier Cells) using electroporation. AdEasier-1 cells are BJ5183 derivatives which already contain the AdEasy-1 plasmid. BJ5183 cells have a relatively high frequency of homologous recombination so unwanted rearrangements and/or recombinations of the pAdEasy-1 sequences in AdEasier-1 cells can happen. Colonies were immediately picked and characterized by restriction analysis using PacI. The correct adenoviral plasmid should produce a 30-kb band and either a 4.5-kb or 3-kb band depending on whether the homologous recombination occurred between the left flanking regions or at the origin of replication. The pShuttle and pAdTrack vectors contain a kanamycin resistance gene whereas the pAdEasy-1 provides resistance to ampicillin. The recombinant adenoviral plasmids obtained from the BJ5183 cells were used to re-transform and select XL-1 blue cells using kanamycin to obtain a higher titer plasmid that can be used for transfection of 293 cells. Following transfections of the plasmids into a mammalian packaging cell line (293 cells), viral production was followed by monitoring expression of the virally encoded green fluorescent protein or observing signs of viral infection such as rounding of cells or formation of plaques (clear areas) that are surrounded by GFP expressing or rounded cells. This system was used to generate and test the recombinant adenoviruses for expression of ζ-crystallin protein or its siRNA.

5.7 Over-expression of ζ-crystallin using adenovirus

The previous experiments using the pcDNA3.1 expression plasmids produced a 4- to 5- fold over-expression of ζ-crystallin compared to the endogenous ζ-crystallin. With that level of ζ-crystallin expression no significant difference in the stability of βG-GA mRNA were observed. Higher levels of ζ-crystallin expression may be required to affect the pH-responsive stabilization of the GA-mRNA. Adenovirus has been used to express high levels of exogenous proteins in a wide range of cells with an infection efficiency of 90% or greater (Davidson, 1993; Bilang-Bleuel et al., 1997; Soudais C, 2001; Minamide, 2003). A recombinant adenoviral plasmid that expresses mouse ζ-crystallin, (ζ-crystallin adenovirus) and its control pAd-Shuttle adenovirus were used. These viruses had a titer of 1.8×10^{10} and 7.1×10^{9}, respectively.

Over-expression of ζ-crystallin using recombined adenovirus required characterization of the optimal MOI of the virus and the time required to obtain maximal infectivity with minimal cell toxicity. Such conditions often depend on the toxicity of the encoded protein and the specific adenovirus used. For this analysis, 5×10^{5} βG-GA cells were passaged 2 d before adding the ζ-crystallin adenovirus. The virus was added using MOI of 10, 20, 30, 40 and 50 for three days. MOI was calculated as described in the methods. Cell extracts were harvested daily, separated by 10% SDS-PAGE and probed with antibodies that are specific for ζ-crystallin. The ζ-crystallin levels were calculated by normalizing the data to the levels of ζ-crystallin expressed in the un-infected cells maintained in normal (pH 7.4) medium. With an MOI of 30, the ζ-crystallinvirus produced a 100-fold increase in ζ-crystallin on the 2nd and 3rd d post-infection (Fig. 5.16)

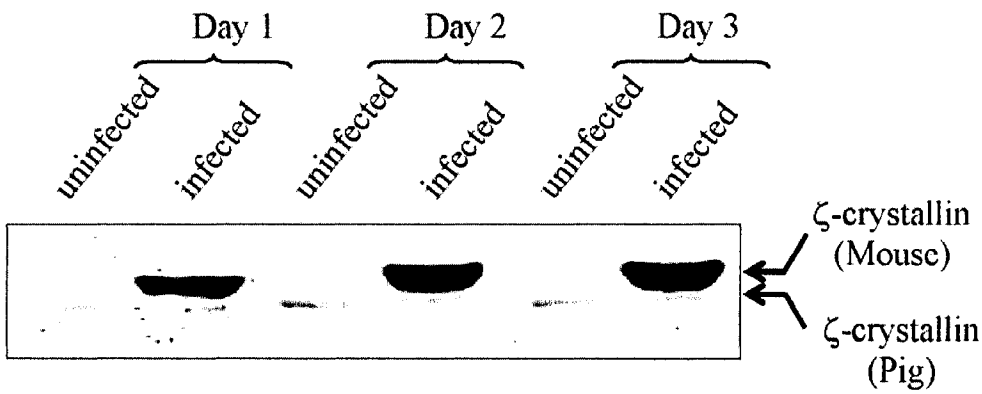

Fig. 5.16: Over-expression of ζ-crystallin using ζ-crystallin-Adenovirus. LLC-PK$_1$-FBPase$^+$ cells that stably express pTRE-βG-GA were infected with ζ-crystallin expressing adenoviruses (infected) and extracts were prepared on various days post-infection. Extracts from uninfected cells was used for comparison. Cell extracts were separated by 10% SDS-PAGE and probed with antibodies specific for ζ-crystallin. The lower faint band represents the endogenous ζ-crystallin and the upper dark band represents the recombinant ζ-crystallin (mouse).

A 48 h infection with this MOI was selected for further experiments to study the effect of ζ-crystallin over-expression on the level and stability of the βG-GA mRNA.

5.7.1 Characterization of βG-GA cells that over-express ζ-crystallin using the ζ-crystallin adenovirus

ζ-crystallin adenovirus was used with an MOI of 30 to infect βG-GA cells. The shuttle adenovirus was used as a control. The infected cells were subjected to Western Blot analyses to determine the level of over-expression of mouse ζ-crystallin. The cells were also tested for tetracycline-responsive βG-GA expression by culturing the cells in the presence or absence of 50 ng/ml Dox and quantifying βG-GA mRNA expression by Northern analysis.

The infected cells maintained the tetracycline-responsive expression. The level of mRNA observed in the presence of Dox was almost undetectable, but an average of a 40 fold increase in transcription was observed in the absence of Dox in the infected, the infected control, and the uninfected cells (Fig 5.17).

5.7.2 Adenoviral over-expression of ζ-crystallin did not restore the pH-responsive stabilization of βG-GA mRNA in the absence of pulse

In the initial experiments, a 4-fold over-expression of the mouse ζ-crystallin did not restore the pH responsive stabilization of the βG-GA mRNA. However, cells infected with ζ-crystallin adenovirus expressed 100-fold more ζ-crystallin than the control or un-infected cells. These cells were used to test the ability of a very high level of ζ-crystallin expression to stabilize the βG-GA mRNA in cells grown in normal medium. This was

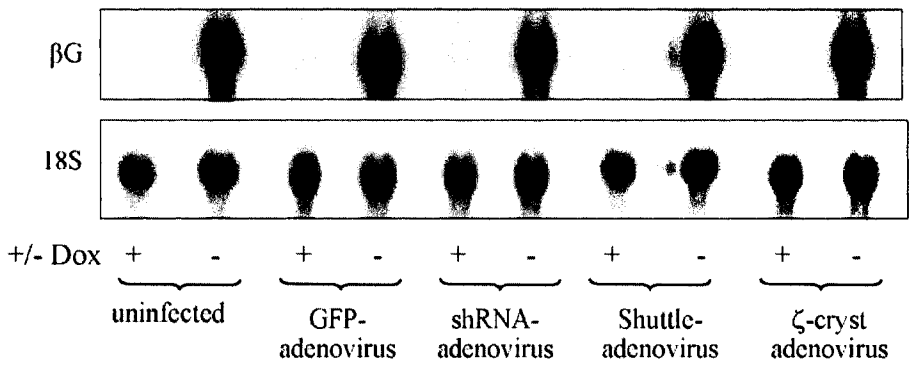

Fig. 5.17: Tetracyclin responsiveness of TRE-βG-GA gene in cells infected with adenovirus. Northern blot analysis of the βG-GA mRNA levels expressed in LLC-PK_1-F^+ cells maintained in the presence or absence of Dox. Cells were grown in pH 7.4 medium in the presence or absence of 50 ng/ml Doxycycline (Dox). Samples from uninfected cells were compared to samples from cells infected with various adenovirus constructs. Total RNA was harvested from the cells of four days post-infection and used for Northern blotting. The level of βG-GA mRNA was divided by the corresponding level of 18S rRNA to correct for errors in sample loading.

done to test the hypothesis that an increased binding of ζ-crystallin was required for the pH-responsive stabilization of the GA mRNA. Approximately $5x10^5$ βG-GA cells were split and grown in normal medium for 2 d before the addition of the ζ-crystallin adenovirus. The virus was added using an MOI of 30 and cells were grown for 48 h in before addition of 1 ug/ml Dox. RNA was isolated 0, 3, 6, 9 h later and subjected to northern analysis. This analysis showed that the βG-GA mRNA turned over with a half-life of about 3.2 h, 4.7 h and 3.8 h for uninfected, contol infected and ζ-crystallin adenovirus infected cells, respectively (Fig. 5.18), in cells maintained in normal conditions. No change in the half life was observed, even with very high levels of ζ-crystallin expression. Therefore, an increase in the level of ζ-crystallin is not sufficient to stabilize the βG-GA mRNA under normal conditions. Other factors or a modification of ζ-crystallin must contribute to the pH-responsive stabilization of the GA-mRNA.

5.7.3 Creating a transcriptional pulse of βG-GA in cells infected with Adenovirus

A transcriptional pulse was developed to study the decay of βG-GA mRNA. The conditions used for creating a pulse of βG-GA mRNA were the same as described previously except that the treatment minus Dox was performed for 4 h instead of 3 h. Fresh medium was added 1 hour before infection and the cells were allowed to grow for 48 h or 72 h for cells infected with ζ-crystallin and siRNA adenovirus, respectively. When the cells were grown for 72 h, the medium was also changed after 48 h. To study the pH-responsive stabilization of the βG-GA mRNA in the adenovirus infected cells, the medium was changed to acidic medium 10 h before induction of the transcriptional pulse

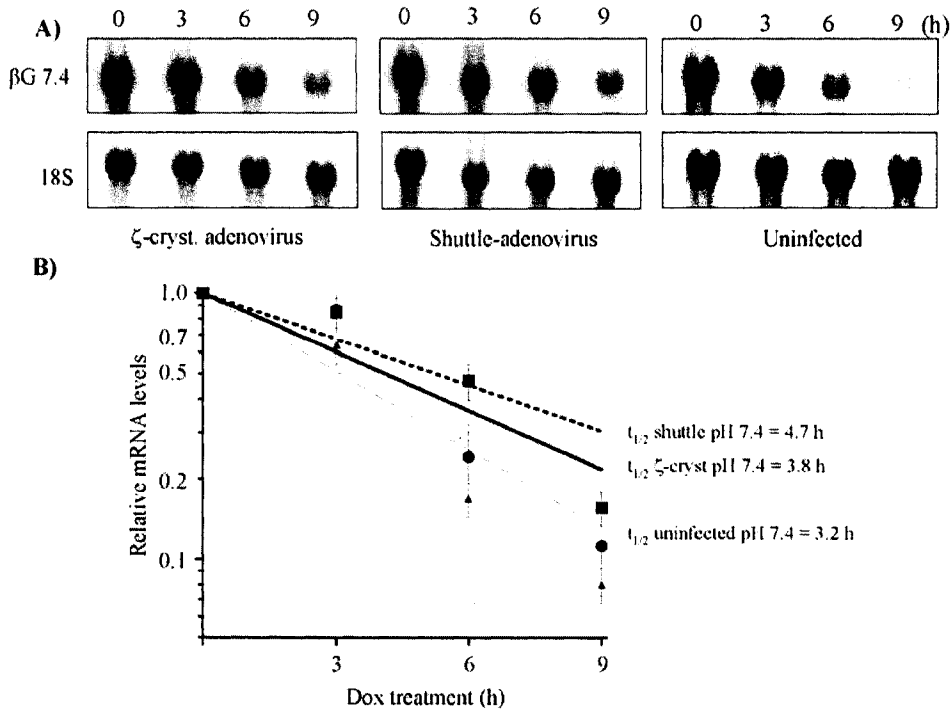

Fig. 5.18: Effect of adenoviral expression of ζ-crystallin on the half-life of βG-GA mRNA in LLC-PK$_1$-F$^+$ cells.

Panel A: Cells were infected with ζ-crystallin adenovirus at a MOI of 30 or the shuttle adenovirus (control) at a MOI of 30 for 2 d after splitting. The cells were cultured in normal (pH 7.4) medium minus Dox for 2 d then treated with 1 μg/ml Dox for 0, 3, 6, and 9 h. RNA samples from infected and uninfected cells were also harvested and analyzed by Northern analysis.

Panel B: Quantification of the relative levels of βG-GA mRNA. The level of βG-GA mRNA from uninfected (▲) or from cells infected with ζ-crystallin virus (•) or shuttle virus (■) was divided by the corresponding level of 18S rRNA to correct for errors in sample loading. The log of normalized data was then plotted versus time of Dox treatment. The reported data are the mean +/- of data obtained from 3 separate determinations. The line represents the best-fit of the data points as determined by the KaleidaGraph program.

5.7.4 Effect of ζ-crystallin over-expression on the stabilization of βG-GA mRNA synthesized with a transcriptional pulse

A transcriptional pulse was used to determine the half-life of βG-GA mRNA in cells infected with either the shuttle virus (control) or ζ-crystallin adenovirus. This analysis allowed us to study the effect of 100-fold over-expression of ζ-crystallin on the pH-responsive stabilization of the βG-GA mRNA. When the cells were transferred to acidic medium for 10 h before the pulse, the measured half-lives of βG-GA mRNA were 13.8 h, 15.7 h and 14.7 h for uninfected, control infected and ζ-crystallin infected cells, respectively (Fig 5.19). Therefore, the pH-responsive stabilization of the βG-GA mRNA in the infected cells was not significantly different in the uninfected cells or in cells that over-expressed ζ-crystallin by 100-fold.

Furthermore, these experiments produced the same pH-responsive stabilization of the βG-GA mRNA as observed in previous studies of cells that expressed only the endogenous ζ-crystallin (Schroeder, 2003) or in the ζ^+ cells that over-expressed ζ-crystallin by 4-fold.

5.8 Knock-down of ζ-crystallin using an siRNA adenovirus in the βG-GA cells

5.8.1 Expected effect of ζ-crystallin knockdown on the βG-mRNA

If increased binding of ζ-crystallin to the 3'-UTR of βG-GA mRNA was the sole mediator of the pH-responsive stabilization, then inhibition of ζ-crystallin expression

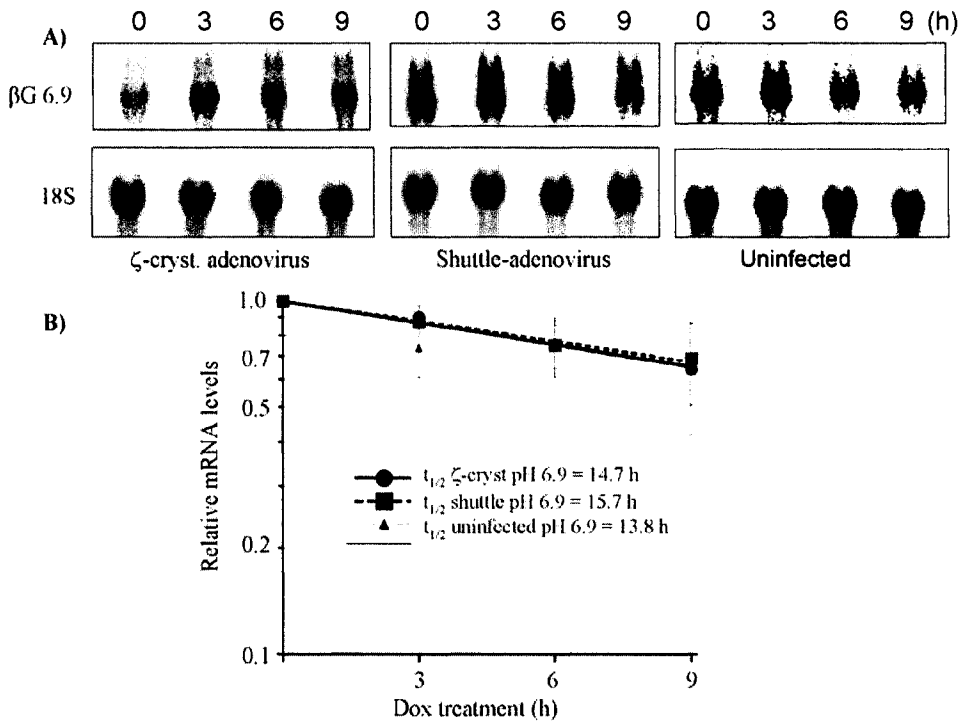

Fig. 5.19: Effect of adenoviral expression of ζ-crystallin on the pH-responsive stabilization of the βG-GA mRNA.

Panel A: LLC-PK$_1$-F$^+$ cells were infected with ζ-crystallin adenovirus (over-expressing ζ-crystallin) at MOI 30 or with shuttle adenovirus (control) at a MOI of 30 for 2 d after splitting in normal (pH 7.4) medium with 50 ng/ml Dox. Cells were grown for 48 h post-infection in normal medium with 50 ng/ml Dox and then maintained in pH 6.9 medium for 10 h plus Dox. Cells were washed twice with PBS and incubated in pH 6.9 medium minus Dox for 3 h to create a transcriptional pulse. Fresh pH 6.9 medium containing 1 μg/ml Dox was added and RNA was isolated at 0, 3, 6, and 9 h after Dox re-addition. Samples from uninfected cells were also harvested for half-life analysis.

Panel B: The level of βG-GA mRNA was divided by the corresponding level of 18S rRNA to correct for errors in sample loading. The log of normalized data was then plotted versus time of Dox treatment. The reported data are the mean ± SE of data obtained from 3 separate determinations. The line represents the best-fit of the data points as determined by the KaleidaGraph program

would inhibit this response. RNA interference was performed to specifically knock down ζ-crystallin expression, through the use of an adenovirus-based short hairpin siRNA (siRNA adenovirus) targeted against a sequence located in the coding region of the porcine ζ-crystallin mRNA. The negative control adenovirus contained a scrambled siRNA sequence that was introduced into an adenovirus that encodes GFP. The strategy used to achieve intracellular synthesis of siRNA involved the incorporation of a ζ-crystallin siRNA sequence into the stem of the human *miR-30* miRNA (ZC103-miRNA). This procedure efficiently produced active ζ-crystallin specific siRNA in βG-GA cells under the control of the human U6 pol III promoter. In co-transfection experiments, we found that luciferase activity of ζ-crystallin containing reporter construct was effectively suppressed by 90% using ζ-crystallin-miRNA.

Before using a recombined adenovirus to knockdown ζ-crystallin, the optimal MOI of the virus and the time required to obtain maximal infectivity and knockdown with minimal cell toxicity have to be characterized. Approximately, $2x10^4$ βG-GA cells were cultured in 12-well plates for 1 day before adding the GFP or siRNA viruses. The virus was added using an MOI of 5, 10, 20, 30, 40 and 50 for 4 d. MOI was calculated as described in the Methods. Cell infection was followed with the aid of the green fluorescent protein. The cells expressing GFP were examined 24, 48, 72 and 96 h after infection. Fixed exposure time on a digital camera with a 10X objective was used to record both phase and fluorescence images of random fields (Fig 5.20). Very high infectivity of the virus was observed with MOI of 5. The effecacy of the siRNA in

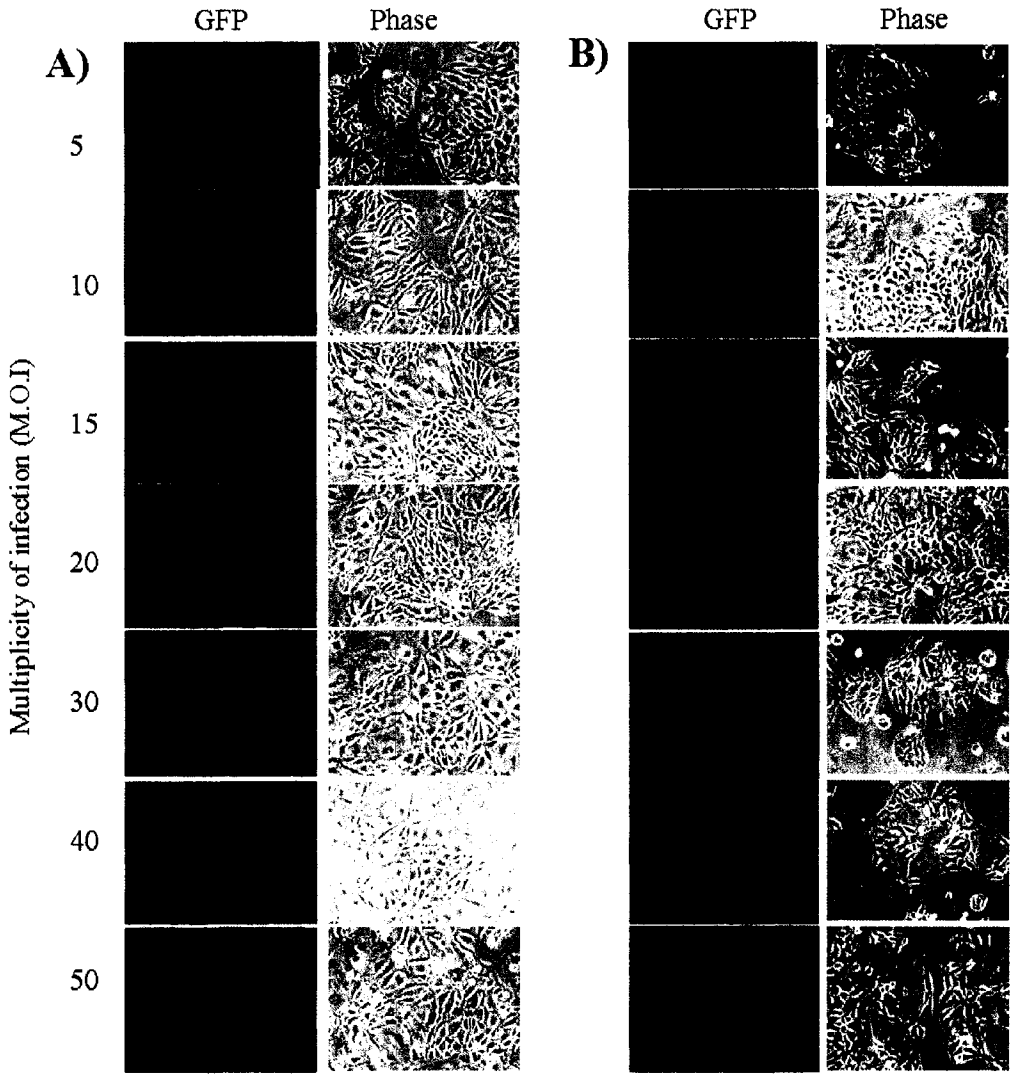

Fig. 5.20: 90% infectivity of adenoviruses in LLC-PK$_1$-F$^+$ cells obtained with various multiplicity of infection (MOI). Adenoviruses were generated using the pAdeasy system and titered. Infections were carried out using the shRNA expressing virus (Panel A) or the GFP expressing control virus (Panel B). Infections were performed using various MOI for each virus. The efficiency of infection was detected by observing the GFP expression in the infected cells using fluorescence microscope.

reducing ζ-crystallin expression was tested by western blot analysis to determine the most effective MOI to be used for further analysis. $5x10^5$ of βG-GA cells were plated for 2 d before adding the siRNA virus. Cell extracts were harvested daily and analyzed by western blot analysis using antibodies specific for ζ-crystallin. The ζ-crystallin levels were calculated by normalizing the data to the levels of ζ-crystallin expressed in the un-infected cells maintained in normal (pH 7.4) medium. The siRNA adenovirus when used at an MOI of 20 was able to reduce ζ-crytsallin expression to 13% and 7% of the endogenous level at 72 h and 96 h post infection, respectively (Fig 5.21). An MOI of 20-30 and a cell infection for 72 h were used in further experiments to study the effect of ζ-crystallin knockdown on the level and stability of the βG-GA mRNA. The cells were also tested for tetracycline-responsive βG-GA expression by culturing the cells in the presence or absence of 50 ng/ml Dox and quantifying βG-GA mRNA expression by Northern analysis. The infected cells maintained the tetracycline-responsive expression. The level of mRNA observed in the presence of Dox was almost undetectable, but an average of a 40 fold increase in transcription was observed in the absence of Dox in the infected, the infected control, and the un-infected cells (Fig 5.17).

5.8.2 Effect of ζ-crystallin knockdown on the turn over of βG-GA mRNA with no pulse

Approximately $5x10^5$ βG-GA cells were grown in normal medium for 2 d before the addition of the siRNA virus. The virus was added using an MOI of 30 and cells were grown for 72 h in before addition of 1 μg/ml Dox. RNA was isolated at 0, 3, 6, 9 h and subjected to Northern analysis. This analysis showed that the βG-GA mRNA turned over with a half-life of approximately 3.2 h, 3 h and 2.5 h for uninfected, GFP adenovirus (control) and siRNA adenovirus infected cells, respectively (Fig. 5.22). No significant

stabilization of the message was produced even when the ζ-crystallin expression was reduced to 10% of the original level

5.8.3 Effect of ζ-crystallin knockdown on βG-GA mRNA synthesized with a transcriptional pulse

The protocol to produce a transcriptional pulse was used to study the effect of ζ-crystallin knockdown on the half-life of βG-GA mRNA under normal and acidic conditions. Both the GFP virus (control) and siRNA virus (kockdown ζ-crys) infected cells were maintained in normal medium containing 50 ng/ml Dox for 48 h before the medium was changed to either normal or acidic medium for 10 h followed by a 4 h transcriptional pulse. The half-life of βG-GA mRNA cultured in normal conditions was 5.6 h and 4.6 for h for the control and siRNA infected cells, respectively (Fig. 5.23) compared to 5.7 h in the un-infected cells. However, when the cells were transferred to acidic medium, the half-lives of the βG-GA mRNA were increased to 16 h and 14.5 h for the control and siRNA infected cells, respectively (Fig. 5.24).

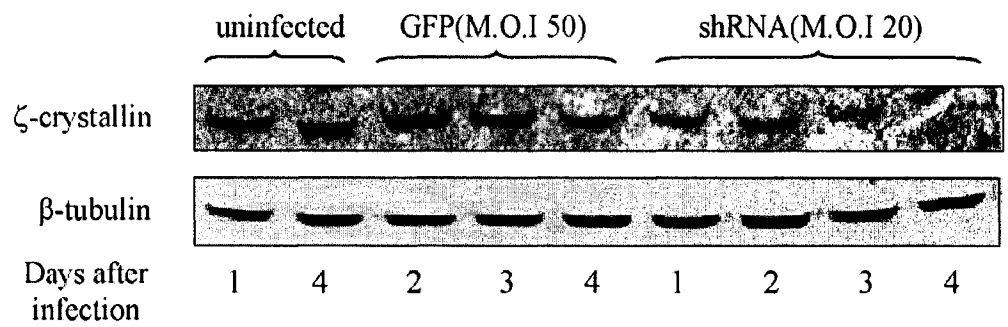

Fig. 5.21: Western blot analysis of the effect of shRNA-adenovirus on the level of ζ-crystallin. LLC-PK_1-FBPase$^+$ cells that stably express pTRE-βG-GA were infected with the GFP (control) expressing adenoviruses or the shRNA adenovirus. Cells were harvested on various days post infection and extracts were analyzed by Western blots using antibodies specific for ζ-crystallin. Western blot with anti-β-tubulin antibody was used as an internal loading control.

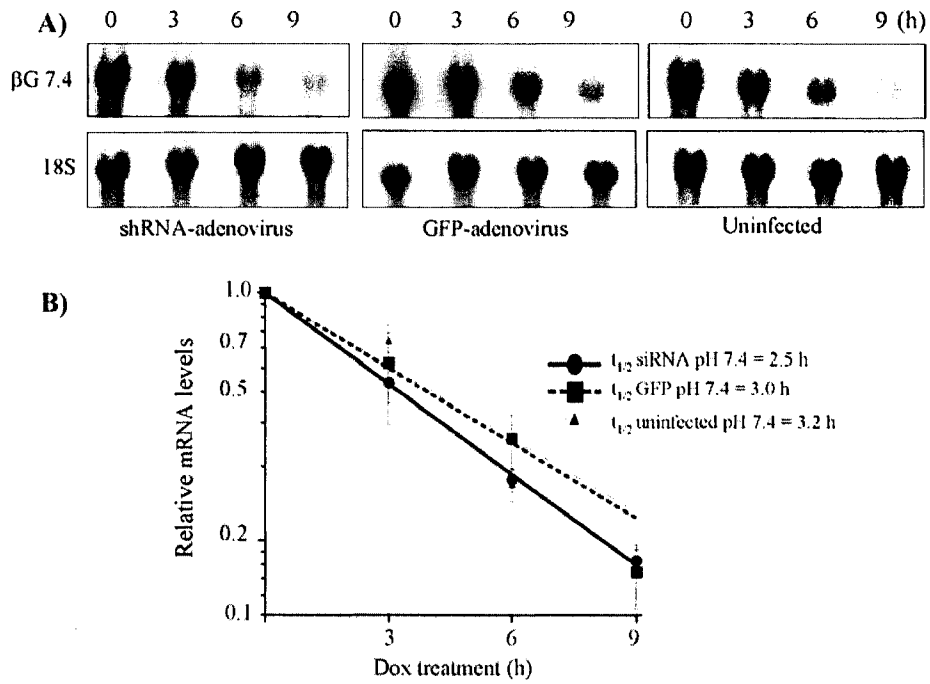

Fig. 5.22: No change in the half-life of βG-GA mRNA analyzed without a transcriptional pulse using sh-RNA adenovirus to knockdown of ζ-crystallin.
Panel A: Northern blot analysis of βG-GA mRNA levels. After 2 d post splitting, LLC-PK_1-F^+ cells were infected with shRNA adenovirus or GFP adenovirus (control) at a MOI of 30. The cells were cultured in normal (pH 7.4) medium minus Dox for 3 d then treated with 1 μg/ml Dox for 0, 3, 6, and 9 h. RNA samples were also isolated from uninfected cells and analyzed by Northern blotting.
Panel B: Relative levels of βG-GA mRNA. The level of βG-GA mRNA was divided by the corresponding level of 18S rRNA to correct for errors in sample loading. The log of normalized data was then plotted versus time of Dox treatment. The reported data are the mean ± SE of data obtained from 3 separate determinations. The line represents the best-fit of the data points as determined by the KaleidaGraph program.

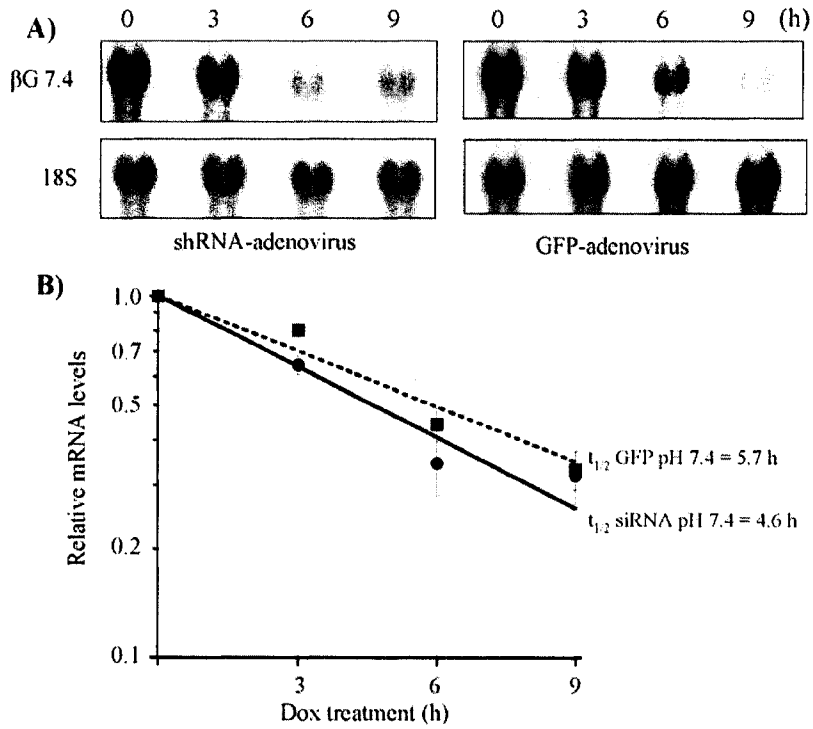

Fig. 5.23: No change in the half-life of βG-GA mRNA analyzed with a transcriptional pulse using sh-RNA adenovirus to knockdown of ζ-crystallin.
Panel A: After second post splitting in normal (pH 7.4) medium containing 50 ng/ml Dox, LLC-PK_1-F^+ cells were infected with siRNA adenovirus or GFP adenovirus (control) at a MOI of 30. After 72 h, the cells were washed two times with PBS and incubated in medium without Dox for 3 h to create a transcriptional pulse. Fresh medium containing 1 μg/ml Dox was added and RNA was isolated at 0, 3, 6, and 9 h after Dox re-addition.
Panel B: The level of βG-GA mRNA was divided by the corresponding level of 18S rRNA to correct for errors in sample loading. The log of normalized data was then plotted versus time of Dox treatment. The reported data are the mean ± SE of data obtained from 3 separate determinations. The line represents the best-fit of the data points as determined by the KaleidaGraph program.

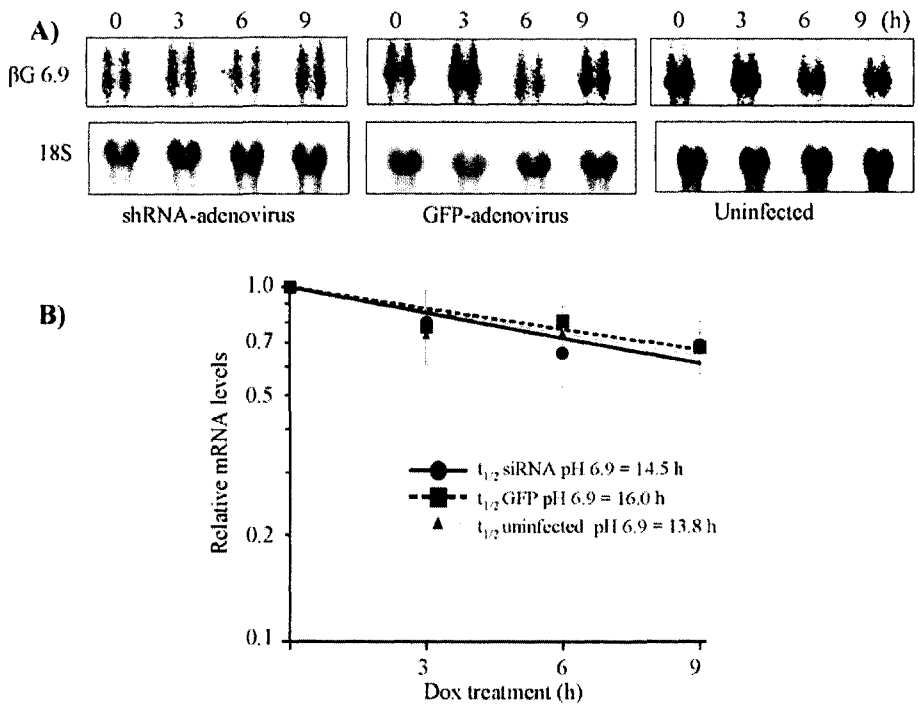

Fig. 5.24: sh-RNA adenoviral knockdown of ζ-crystallin does not affect the pH-responsive stabilization of βG-GA mRNA using a transcriptional pulse.
Panel A: Northern blot analysis of βG-GA mRNA levels. At 2 d after splitting in normal (pH 7.4) medium containing 50 ng/ml Dox, LLC-PK_1-F^+ cells were infected with siRNA adenovirus or GFP adenovirus (control) at a MOI of 30. After 72 h, the cells were transferred to pH 6.9 medium containing 50 ng/ml Dox for 10 h. The cells were washed twice with PBS and incubated in pH 6.9 medium minus Dox for 3 h to create a transcriptional pulse. Fresh pH 6.9 medium containing 1 μg/ml Dox was added and RNA was isolated at 0, 3, 6, and 9 h after Dox re-addition. Samples from uninfected cells were also harvested for half life analysis.
Panel B: Relative levels of βG-GA mRNA. The level of βG-GA mRNA was divided by the corresponding level of 18S rRNA to correct for errors in sample loading. The log of normalized data was then plotted versus time of Dox treatment. The reported values are the mean ± SE of data obtained from 3 separate determinations. The line represents the best-fit of the data points as determined by the KaleidaGraph program.

5.9 Effect of acidosis on ζ-crystallin expression

The effect of acidosis on the level of ζ-crystallin expression in the LLC-PK_1-F^+ cells (control) and ζ^+ (overexpressing ζ-crystallin) cells was determined by western blot analysis. The cells were maintained in normal medium until 70% confluent. The medium was changed to either normal (pH 7.4) or acidic (pH 6.9) medium for 24 h. The extracts were prepared and samples were fractionated by SDS-PAGE and probed with ζ-crystallin specific antibody. Treatment with acidic medium had no effect on the level of ζ-crystallin expression in either cell line (Fig. 5.25).

5.10 Affinity purification of the pHRE binding proteins

A new approach was used to purify the proteins that bind to the R2I-BssHII RNA (Fig. 5.26). A 5'- biotinylated deoxy oligonucleotide (Biotinylated T3 promoter) that is complementary to the sequence transcribed from the T7 promoter within the pBluescript II-SK (-) plasmid was synthesized by Macromolecular Resources. The R2I-BssHII RNA was transcribed from pBSSK-R2I that had been digested with BssHII. The resulting RNA contains the pHRE sequence (UUUAAAUAUUAAAAUA) followed by the sequence complementary to the biotinylated DNA. The biotinylated DNA and the transcribed RNA were incubated to form a RNA-DNA hybrid. A cytoplasmic extract from rat kidney cortex was incubated with a slight excess of the affinity ligand. The resulting complex was then applied to a fast protein liquid chromatography (FPLC) column that had been packed with avidin-agarose and equilibrated with binding buffer. The column was washed extensively and then proteins were eluted with binding buffer in which the

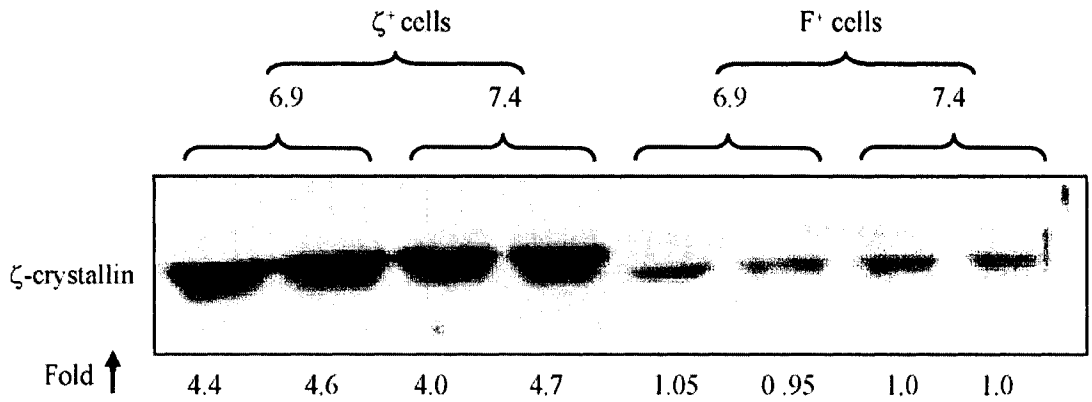

Fig. 5.25: Effect of acidosis on the level of ζ-crystallin protein in F^+ cells. Western blot analysis of endogenous levels of ζ-crystallin in LLC-PK_1-FBPase$^+$ cells and ζ^+ cells that stably express pcDNA 3.1/Neo-ζ-crystallin construct. Cells were grown for 5 days. About 24 h prior to harvest, cells were transferred to normal (pH 7.4) or acidic (pH 6.9) medium. Cell extracts were separated by 10% SDS-PAGE and probed with antibodies that are specific for ζ-crystallin. The ζ-crystallin levels were calculated by normalizing the data to the levels of ζ-crystallin expressed in F^+ cells maintained in normal (pH 7.4) medium.

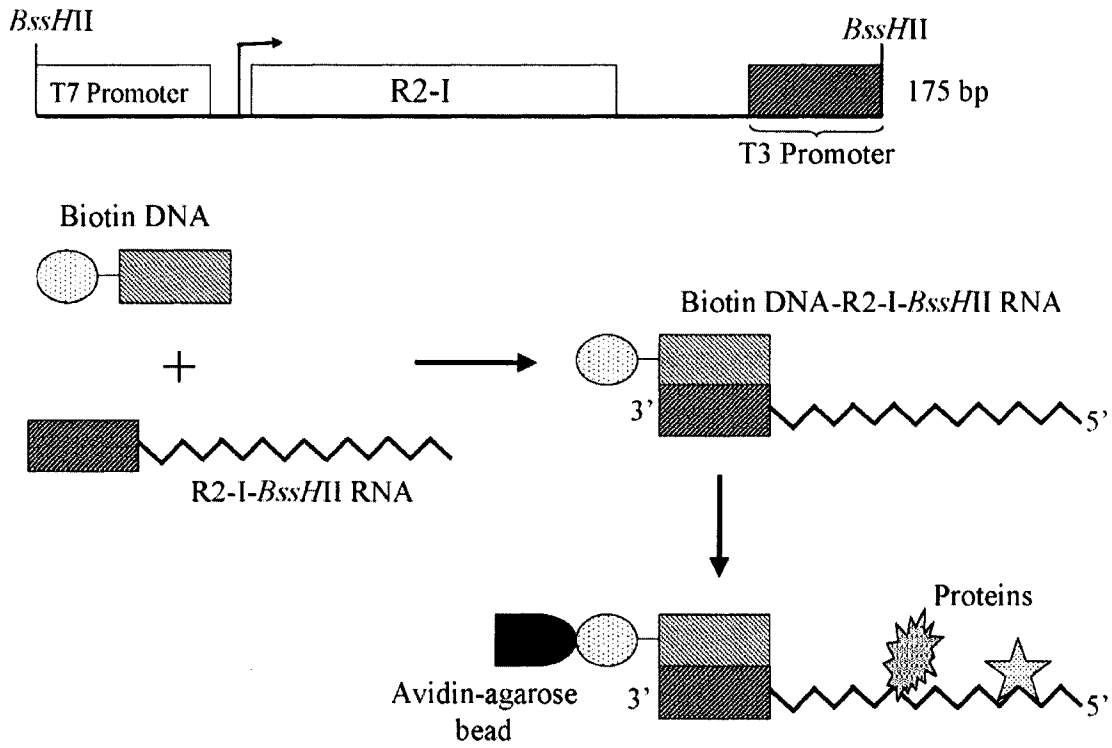

Fig. 5.26: Schematic of the RNA affinity purification protocol used to isolate the pHRE RNA binding proteins. R2-I containing plasmid digested with *BssH*II to produce a 119-bp (R2-I-*BssHII*) DNA template. The synthesis of the R2-I-*BssHII* RNA is under the control of the T7 promoter. The sequences at the 3'end of this RNA are complementary to the T3 promoter, indicated by the hatched box. A DNA sequence, which contains the T7 promoter sequences, was synthesized with a biotin at the 5'end. The biotinylated DNA probe was then mixed with the R2-I-*BssH*II RNA, to form a DNA:RNA hybrid. This DNA:RNA hybrid was incubated with rat renal cytosolic extracts and applied to an avidin agarose column. The proteins bound to the RNA were eluted with a salt gradient.

concentrations of potassium acetate and magnesium acetate were gradually increased. Aliquots from each of the collected fractions were analyzed by SDS-PAGE. Silver staining detected a number of proteins in each of the fractions (Fig. 5.27A). ζ-crystallin was previously identified as 36-kDa pHRE binding protein. Its RNA binding activity and specificity were analyzed using an RNA electrophoretic mobility shift assay with [^{32}P]-labeled R2I RNA as the probe. The eluted fractions produced the RNA protein complex that was observed previously with the kidney extracts (Fig. 5.28).

During the affinity purification of the 36-kDa ζ-crystallin, a second protein (pHRE-BP2) was eluted from the pHRE RNA affinity ligand with the final elution buffer. The unidentified protein was named, pHRE-BP2. It has an approximate subunit molecular weight of about 42-kDa. Previous experiments by J.Schroeder indicated that pHRE-BP2 is not an isoform of ζ-crystallin.

5.10.1 Identifiction of pHRE-BP2

Sequences identical to the pHRE were identified in the 3'UTRs of the mRNAs that encode actin and actin depolymerizing factor (ADF), an actin-assembly regulatory protein. Experiments demonstrated that the ADF mRNA is also increased when the porcine cells were transferred to acidic medium and that the AU-sequence from the ADF mRNA binds purified ζ-crystallin with high affinity. Previous studies established that synthesis of actin and ADF are autoregulated by the actin monomer pool and that ADF activity is pH-regulated (Bernstein et al., 2000). These observations suggested that during normal acid-base balance, ζ-crystallin may be sequestered by binding to monomeric

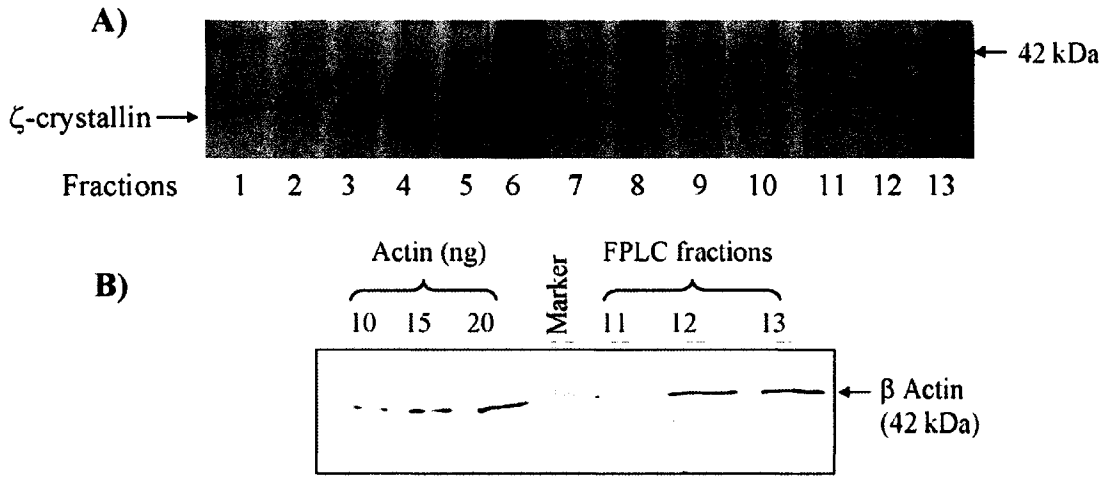

Fig. 5.27: Protein elution profile from an FPLC affinity column.

Panel A: Fractions 1-9 were collected during elution using a linear gradient of 4X to 20X binding buffer. Fractions 10-13 were collected by washing with 20X binding buffer. The fractions were dialyzed overnight against 1X binding buffer and then separated by 10% SDS-PAGE and stained with 0.1% silver nitrate.
Panel B: Western blot analysis of eluted 42 kDa protein. Aliquots of the protein fractions (0.1 ml) were precipitated with chloroform/methanol. The protein pellets were re-suspended in 10 µl and loaded on a 10% SDS gel. Proteins were detected with western blot analysis using antibodies specific for β-actin. Rabbit muscle actin was used as a positive control.

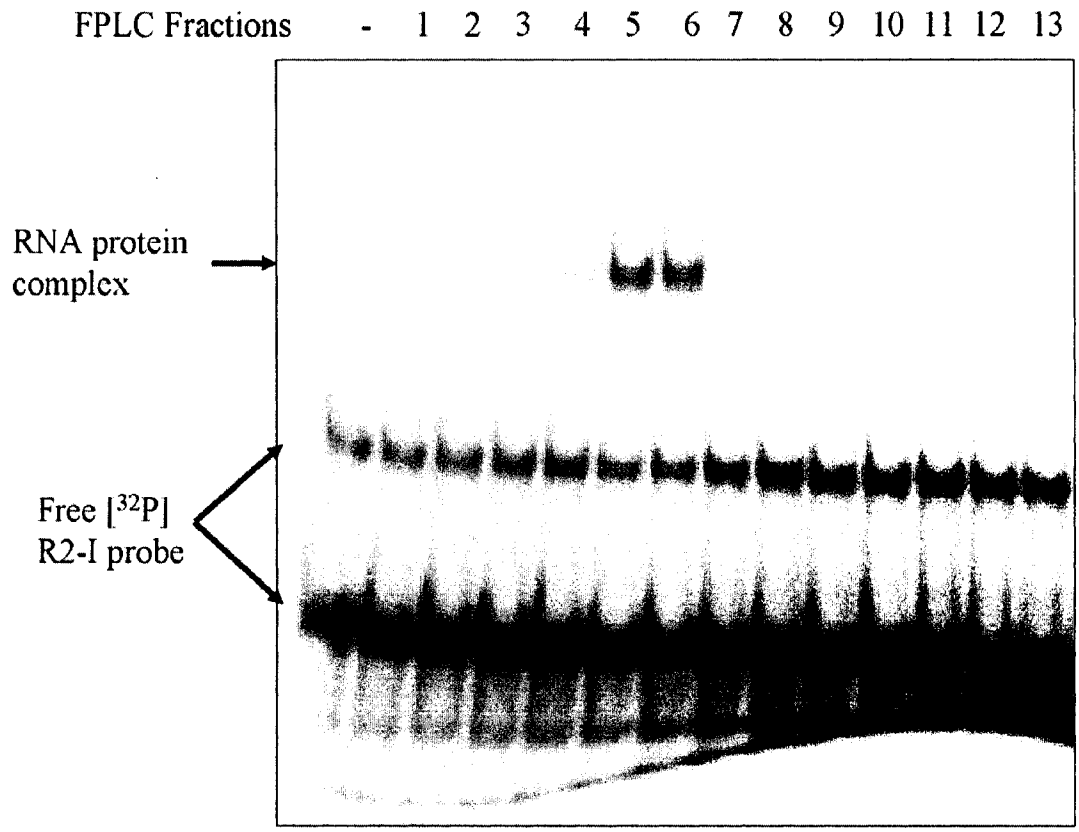

Fig. 5.28: Binding activity in the fractions obtained by affinity purification with R2-I-*BssH*II RNA.
The fractions (F1-F13) were incubated with [^{32}P]-labeled R2-I RNA. The resulting RNA protein complexes were resolved on a native gel and imaged on a PhosphorImager.

actin. However, a decrease in intracellular pH would enhance actin polymerization and release of ζ-crystallin so that it now binds to and stabilizes multiple mRNAs. Therefore, the co-elution of actin in affinity purified FPLC fractions was determined by separating 10 µl samples of the concentrated FPLC fractions on 10% SDS-PAGE. Western blot analysis was performed using antibodies against actin. Actin, a 42-kDa protein, was identified as one of the proteins in the eluted fractions. Rabbit muscle actin was used as a positive control (Fig. 5.27B).

5.11 2-D gel analysis of ζ-crystallin

Two-dimensional gel electrophoresis (2-DE) was used to determine if rat kidney cortex contains multiple isoforms of ζ-crystallin. Proteins were extracted from rat kidney cortex in 8M urea lysis buffer and focused on IPG strips (pH 3-10). Separation in a second dimension was achieved using 10% SDS-PAGE. The gels were electroblotted to a polyvinylidene difluoride (PVDF) membrane and subjected to Western analysis using a ζ- crystallin specific antibody. This analysis produced multiple spots (about 12 spots). The spots migrated as 3 different but similar molecular weight species (A, B, C) (Fig. 5.29). Affinity purified proteins from rat kidney cortex were diluted into 8M urea lysis buffer and focused on the IPG strips (pH 3-10) and then separated in the second dimension using 10% SDS-PAGE. Immunoblot analysis of gels using ζ-crystallin antibodies visualized only 3 spots. Alignment of the two membranes indicates that the 3 proteins may have a molecular weight equivalent to the B group of proteins in the crude extract (Fig. 5.30). Further analysis is needed to characterize the potential isoforms of ζ-crystallin.

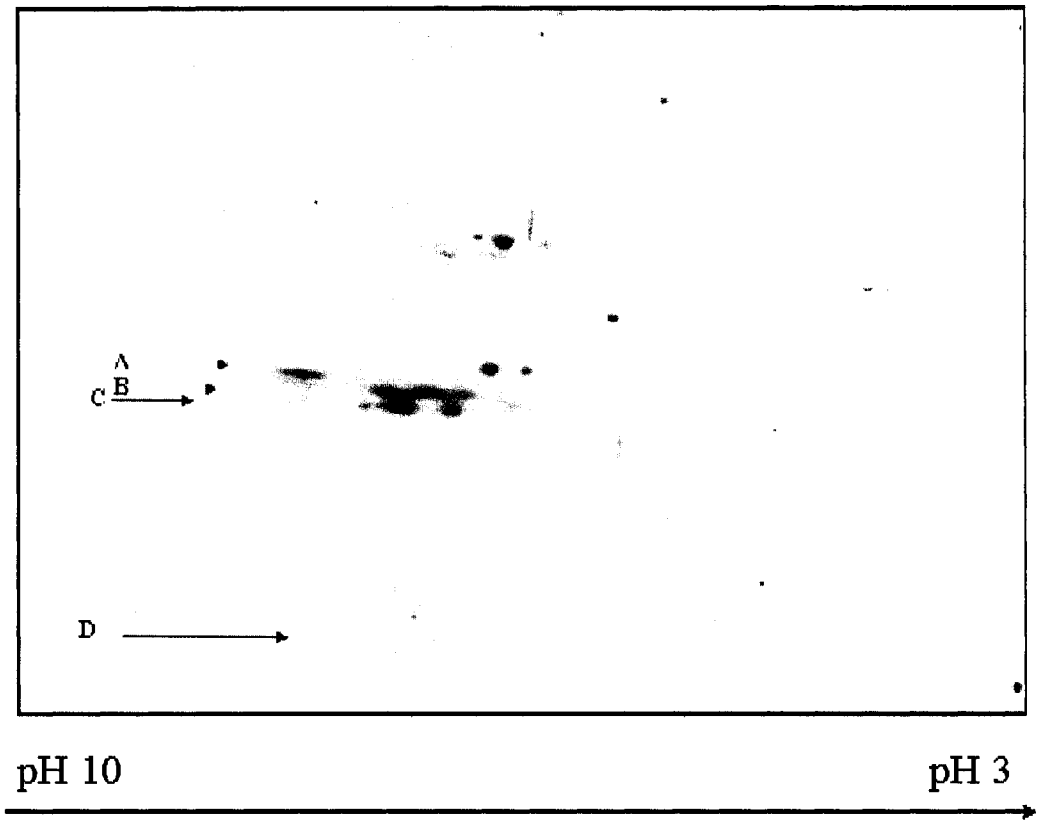

Fig. 5.29: Two-dimensional gel electrophoresis and Western blot analysis of ζ-crystallin from rat renal cytosol.
15 μg of rat renal cytosolic proteins were separated on a 7 cm IPG strip (pH 3–10) and then fractionated by 10% SDS gel electrophoresis. Proteins were detected with western blot analysis using antibodies specific for ζ-crystallin. Lettered spots were used for comparison with the spots obtained from RNA affinity purified proteins.

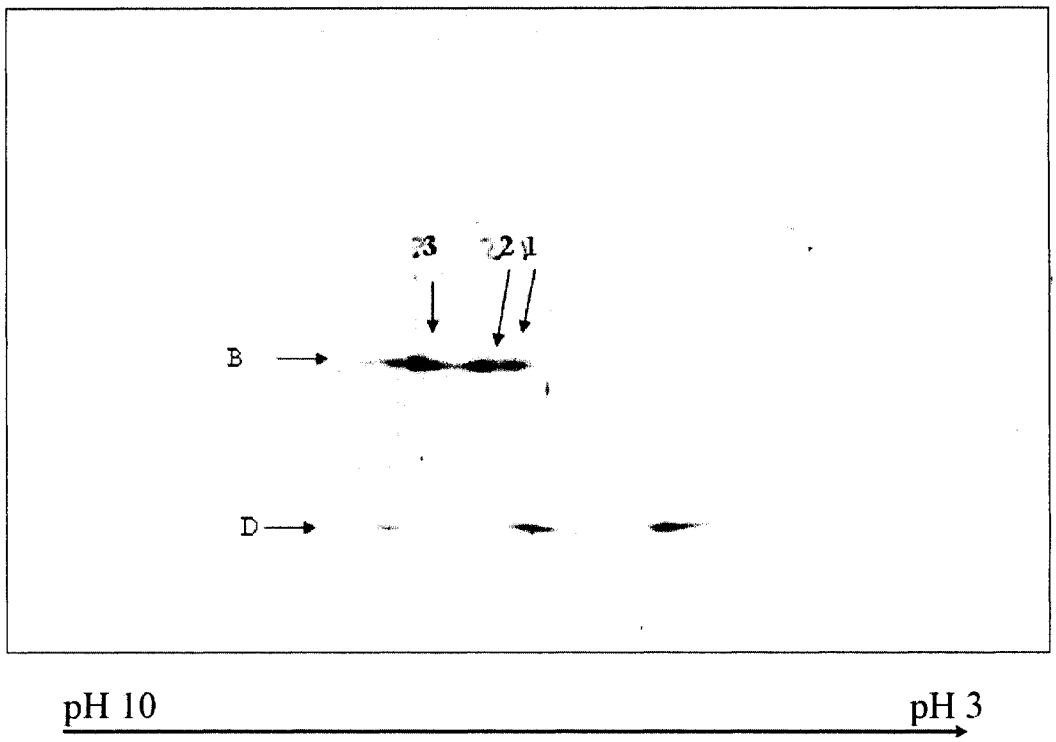

Fig. 5.30: Two-dimensional gel electrophoresis of affinity purified ζ-crystallin: 10 µl of fraction 5 from an FPLC affinity column (Fig. 5.27) were separated on a 7 cm IPG strip (pH 3–10) and then fractionated by 10% SDS gel electrophoresis. Proteins were detected with Western blot analysis using antibodies specific for ζ-crystallin. Lettered spots were used for comparison with the spots obtained from rat renal cytosolic extract.

6 DISCUSSION

The turnover of mRNA in eukaryotic cells is highly regulated and plays an important role in the post-transcriptional regulation of gene expression. During acidosis modulation of mRNA stability is an important control mechanism for regulation of glutaminase (GA) mRNA (Hansen et al., 1996). During normal acid base balance, the mRNAs that encode the mitochondrial glutaminase (GA), glutamate dehydrogenase (GDH) and the cytosolic phosphoenolpyruvate carboxykinase (PEPCK) are rapidly degraded (Laroia et al., 1999; Hajarnis et al., 2005). However, metabolic acidosis is associated with an increase in the levels of the GA, GDH and PEPCK mRNAs. The increase in PEPCK is caused by a rapid increase in transcription, but the increases in GA and GDH are mainly due to post-transcriptional regulation.

The rate of mRNA decay is determined by *cis*-acting sequences within the mRNA, which are recognized by *trans*-acting factors. The best-characterized *cis*-acting sequences responsible for mRNA decay in mammalian cells are the AU-rich elements (AREs) present within the 3'-UTRs of short-lived mRNAs, whose expression have to be finely regulated (Bakheet et al., 2001; Linker et al., 2005). The AREs enhance deadenylation and subsequent degradation of mRNAs (Shyu et al., 1991; Xu et al., 1997) and have also been described to stimulate 5'-decapping (Gao et al., 2001). AREs are the targets of specialized RNA binding proteins (RBPs) that govern the half-lives and translation rates of mRNAs (Chen and Shyu, 1995; Wilusz and Wilusz, 2004; Mazan-Mamczarz et al., 2006). Such ARE-RBPs include proteins that promote mRNA decay (including AU-binding factor 1 [AUF1], the tristetraprolin (TTP) family of zinc-finger RNA-bps (Carballo et al., 1998; Stoecklin et al., 2002; Lai et al., (1999), K-homology splicing regulatory protein (KSRP), and butyrate response factor 1 (BRF1), proteins that

promote mRNA stabilization and modulate translation (such as the Hu proteins: HuR, HuB, HuC, and HuD) and proteins that suppress translation, including the T-cell-restricted intracellular antigen 1 (TIA-1) and the TIA-1-related protein TIAR (Zhang, 1993; Antic and Keene, 1997; Gueydan et al., 1999; Loflin et al., 1999; Piecyk, 2000; Brennan and Steitz, 2001; Carballo et al., 2001; Stoecklin et al., 2002).

The 3'-untranslated region (3'-UTR) of the GA mRNA contains AU-sequences that are important for the regulation of GA mRNA stability and that function as pH-responsive elements (pHRE) (Laterza and Curthoys, 2000a). The pHRE is a direct repeat of two 8- nucleotide AU-sequences (UUAAAAUA and UUUAAAUA).

In the rat, both the KGA and GAC mRNAs contain multiple pHRE sequences. Thus both mRNAs may be stabilized and increased during chronic acidosis. However, in the pig and human, only the GAC variant of the KGA mRNA contains multiple pHRE sequences. In an attempt to isolate proteins interacting with the pHRE in the 3'-UTR of the GA mRNA, an RNA-affinity purification using the pHRE (R2-I) RNA was performed (Tang and Curthoys 2001). This method resulted in the identification of ζ-crystallin/NADPH:quinone reductase and the T cell intracellular antigen-1-related (TIAR) proteins as RBPs that interact with the pHRE of GA mRNA. ζ-Crystallin was not previously known to function as an RNA-binding protein. It has a NADPH-dependent quinone oxidoreductase activity that reduces various quinones through the sequential transfer of single electrons (Rao et al., 1992). It is expressed at enzymatic levels in various tissues of different species (Rao and Zigler, 1992; Gonzalez et al., 1994b; Gonzalez et al., 1994a). Identification of ζ-crystallin/NADPH:quinone reductase as a pHRE-binding protein was expected to facilitate the characterization of the process by

which this binding activity is enhanced during acidosis and the mechanism by which this interaction leads to the cell-specific stabilization of the GA mRNA.

This study also determined that AUF1 is a protein that binds to the pHREs within the GA mRNA and may enhance its rate of degradation. Recombinant p40 AUF1 exhibits specific binding to the pHRE within the GA(R2-I) RNA. Scatchard analysis demonstrated that the interaction between recombinant p40 AUF1 and the GA(R2-I) RNA has a K_d of 2 μM. Binding of ζ-crystallin and AUF1 to the GA mRNA may have critical role for acidosis induced GA mRNA stabilization. Thus, the further characterization of potential role of AUF1 in the regulation of GA gene expression is necessary.

It was hypothesized that during normal acid-base balance, AUF1 preferentially binds to the pHRE and recruits the protein complexes that accounts for the rapid removal of the poly(A) tail and promotes the subsequent degradation of the GA mRNA. The onset of acidosis is likely to activate a specific signaling mechanism (Feifel et al., 2002; Li et al., 2004) that results in covalent modification of ζ-crystallin and/or AUF1 and the preferential binding of ζ-crystallin to the pHRE. As a result, the interaction of the deadenylase with the poly(A) tail is reduced. This results in the prolonged maintenance of the poly(A) tail and the increased stability of the GA mRNA.

As the cellular activity of RNA-binding proteins is regulated by their abundance, cellular localization, post-translational modifications and/or availability of specific regulatory molecules, the work in this thesis tested the effect of ζ-crystallin abundance on the GA mRNA level and stability. To analyze the influence of ζ-crystallin expression *in vivo*, first LLC-PK_1-$FBPase^+$ cells that stably express the Tet-βG-GA construct were

used to generate stable cell lines that over-express mouse ζ-crystallin by 4-fold. Previous studies using Northern analysis indicated that the fully-induced βG-GA mRNA turned over with a half-life of 2 h in cells treated with either normal or acidic medium. Due to the loss of the pH-responsive stabilization, it was hypothesized that the high level of βG-GA mRNA may exceed the level of the cellular factors that are responsible for a pH-responsive stabilization of the mRNA. In such a case, the mRNA would not be stabilized under acidic conditions since there is not a sufficient level of stabilizing factors present in the cell. In order to test this hypothesis, the effect of over expression of ζ-crystallin on the stability of βG-GA mRNA was determined using the no-pulse protocol. Our data indicated that a 4-fold increase in mouse ζ-crystallin expression in βG-GA cells did not restore the pH responsive stabilization of the βG-GA mRNA. The half-life of βG-GA mRNA with normal and acidic conditions was about 2.5 h. Therefore, either the level of βG-GA mRNA that is transcribed with no-pulse still exceeds the level of ζ-crystallin that is required for the pH-responsive stabilization of the βG-GA mRNA or an additional or alternative stabilizing factor is limiting and not sufficient to stabilize the high level of βG-GA mRNA.

When the transcriptional pulse protocol was used the half-life of βG-GA mRNA in cells grown in normal medium was 5.9 h and 5.3 h for the control (ζ^--5) and ζ-crystallin over-expressing (ζ^+-4) cells, respectively (Figs. 5.6 and 5.7). However, when the cells were maintained in acidic conditions, the half-life of the βG-GA mRNA was stabilized to 13 h and 12 h, respectively (Figs. 5.6 and 5.7). These data establish that a 4-fold over-expression of ζ-crystallin had no effect on the stability of βG-GA mRNA.

To test the ability of very high levels of ζ-crystallin expression to stabilize the βG-GA mRNA in cells grown in normal medium, an adenovirus was used to over-express mouse ζ-crystallin approximately 100-fold (Fig. 5.16). This analysis showed that the βG-GA mRNA turned over with a half-life of 3.2 h, 4.7 h and 3.8 h for uninfected, contol infected and ζ-crystallin adenovirus infected cells, respectively (Fig. 5.19) in cells maintained in normal conditions. Thus, no change in the half-life was observed, even with very high levels of ζ-crystallin expression. Therefore, an increase in the level of ζ-crystallin is not sufficient to stabilize the βG-GA mRNA in cells grown in normal medium. Other factors or a modification of ζ-crystallin must contribute to the pH-responsive stabilization of the GA-mRNA.

The cellular expression of short interfering RNA (siRNA) or short hairpin RNA (shRNA) homologous to a specific gene decreased the protein expression by the selective degradation of its RNA. The microRNAs (miRNA) have been used to successfully deliver an siRNA (Boden, 2004). By incorporating sequences encoding siRNA targeting the ζ-crystallin into a human miR-30 pre-microRNA (pre-miRNA) backbone, we were able to express a ζ-crystallin siRNA in βG-GA cells. As a control to test the efficiency of siRNA cascade in LLC-PK_1-F^+ cells, cells were transiently transfected with pMAMneo-LUC and the pRL-null plasmids in the absence or presence of a pSHAG-Ffl plasmid that encodes the shRNA for Firefly luciferase. psiCHECK-2, psiCHECK-ZC1 or psiCHECK-ZC2 plasmid was transiently co-transfected with pSHAG-ZC103-miRNA (encoding a ζ-crystallin siRNA) into LLC-PK_1-F^+ cells. Dual luciferase assay was used to test the efficiency of siRNA in cleavage and degradation of the fusion ζ-crystallin mRNA. Co-transfection of the pSHAG-ZC103miRNA reduced the relative luciferase activity of

psiCHECK-ZC1 (ζ-crystallin coding region in the sense orientation) by 87%, whereas, the activity of the psiCHECK-ZC2 plasmid (ζ-crystallin coding region in the anti-sense orientation) was reduced by 70% of the original activity. The relative luciferase activity of the psiCHECK-2 plasmid was not affected by co-transfection of ZC103-miRNA (Fig. 5.13). A recombinant adenovirus was used to transfer ζ-crystallin microRNA (ZC103-miRNA) expression cassettes genetically into the cells. ζ-crystallin expression was suppressed by >90% in the cells compared to control cells (Fig 5.21).

We determined the effect of ζ-crystallin knockdown on the pH-responsive stabilization of βG-GA mRNA with no pulse. This analysis showed that the βG-GA mRNA turned over with a half-life of 3.2 h, 3 h and 2.5 h in uninfected, GFP adenovirus (control) and siRNA adenovirus infected cells, respectively (Fig 5.22). Therefore, no significant change in the half-life was observed when the level of ζ-crystallin expression was reduced up to 90% with siRNA.

The protocol to produce a transcriptional pulse was also used to study the effect of ζ-crystallin knockdown on the half-life of βG-GA mRNA under normal and acidic conditions. The half-life of βG-GA mRNA cultured in normal conditions was 5.6 h and 4.6 h in the control and siRNA infected cells, respectively (Fig 5.23) compared to 5.7 h in the un-infected cells. However, when the cells were transferred to acidic medium, the half-lives of the βG-GA mRNA were increased to 16 h and 14.5 h for the control and siRNA infected cells, respectively compared to 13.8 h in the uninfected cells (Fig 5.24).

In summary, no changes in the levels or stability of βG-GA mRNAwere observed as a result of increases or reductions in the abundance of ζ-crystallin. This indicated that ζ-crystallin activity is independent of its abundance. However, we could not exclude that

covalent modifications of ζ-crystallin may play an essential role in defining its biological activity.

The amino acid sequence alignments of human, porcine, rat, and mouse ζ-crystallin identified conserved potential phosphorylation sites. ζ-crystallin contains protein kinase C phoshorylation and casein kinase II phosphorylation sites. Western blot analysis using whole cell lysates revealed no obvious increase in total ζ-crystallin expression during acidosis compared to its level during normal acid base balance in various cell lines, so we hypothesize that acidosis could induce post-translational modifications or affect the cellular localization of ζ-crystallin.

To test the possibility of post-translational modifications, 2-D gel analysis was used. ζ-crystallin from normal extracts and purified fractions produced multiple spots on 2-D gels which may indicate different isoforms or post-translational modifications. The nature of these modifications and its effect on cellular localization are unknown. Further studies, during normal acid base balance and acidosis, to address the subcellular localization of ζ-crystallin will also be needed to test the possibility of its regulation in response to metabolic acidosis.

A more complex mechanism that involves modification of ζ-crystallin may be involved. ζ-crystallin may bind and then recruit other proteins that stabilize or destabilize the GA mRNA. If ζ-crystallin functions as a bridging factor, the recruited proteins may be the limiting factor for this response. Alternatively, if post-translational modification of ζ-crystallin is involved traces of the modified ζ-crystallin may be sufficient to exhibit its effect. In this case, overexpression or knockdown to even 10% of the original level may still have no effect.

The results reported above indicate that 10 to 100- fold change in the level of ζ-crystallin have no effect on GA mRNA expression or stability. The effect of acidosis on the level of endogenous ζ-crystallin was examined. As shown in Fig. 5.25 incubation of cells with acidic medium did not change the expression of the endogenous ζ-crystallin. The enhanced expression of GA mRNA during acidosis does not require enhanced ζ-crystallin expression. Therefore, post-translational modification or a change in ζ-crystallin localization need to be further investigated. In summary, these data imply that an interplay of different proteins in a complex network could be necessary to explain changes in GA mRNA expression during acidosis.

KSRP has been shown to recruit the exosome to ARE-containing mRNAs to enable exosome-mediated degradation (Jeon, 1995; Gherzi et al., 2004). The exosome is a complex of 10 different proteins that catalyze the 3'– > 5' degradation of ARE-containing mRNAs in mammalian cells (Lai et al., 1999; Gao et al., 2001; Blaxall, 2002). Therefore, it will be important to examine the interaction of ζ-crystallin with the exosome in cells by co-immunoprecipitation experiments. These analyses should examine the protein–protein interaction with the various subunits of the exosome.

Another possible mechanism for involvement of ζ-crystallin in the regulation of GA mRNA is under investigation in collaboration with the Bamburg lab. They have identified identical AU-sequences in the 3'UTRs of the mRNAs that encode actin and actin depolymerizing factor (ADF), an actin-assembly regulatory protein. Previous experiments have demonstrated that the ADF mRNA is also increased when the porcine cells were transferred to acidic medium and that the AU-sequence from the ADF mRNA binds purified ζ-crystallin with high affinity. Previous studies established that synthesis

of actin and ADF are autoregulated by the actin monomer pool and that ADF activity is pH-regulated (Bernstein et al., 2000). These observations suggested that during normal acid-base balance, ζ-crystallin may be sequestered by binding to monomeric actin. However, a decrease in intracellular pH would enhance actin polymerization and release ζ-crystallin so that it now binds to and stabilizes multiple mRNAs. This hypothesis is being tested by Hui Hung in the Bamburg lab. However, Western blot analysis of RNA affinity purified proteins has also identified β-actin as a potential pHRE binding protein (Fig.5.27). Post-translational modification may also change the activity and/or the affinity of ζ-crystallin to bind the actin monomers. Further studies are needed to determine if there is a common mechanism regulating mRNA stability during pH-mediated gene expression and the autoregulation of actin expression by the actin monomer pool (Fig. 6.1).

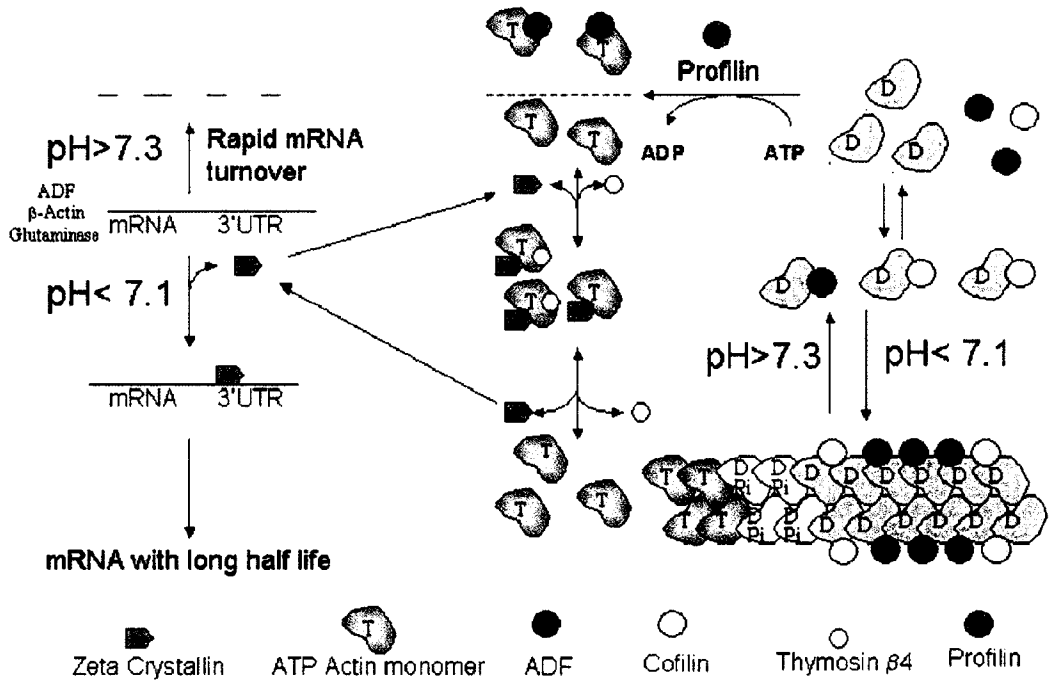

Fig. 6.1: Proposed model for regulation of mRNA stability by the actin monomer pool.

A common mechanism for pH-dependent mRNA stability and actin autoregulation has been proposed. During normal acid-base balance, actin monomer pool may be bind and sequester ζ-crystallin. However, the onset of acidosis would enhance actin polymerization and ζ-crystallin will be released so that it can binds to and stabilizes multiple mRNAs. Post-translational modification may be also necessary for changing the activity and/or the affinity of ζ-crystallin to the monomeric actin. Adopted from Dr. Bamburg's proposed model.

Another protein that was identified by RNA affinity purification is the T-cell restricted intracellular antigen-related protein (TIAR), a well-known RNA-binding protein that contains three RNA recognition motifs (Dember, 1996). It also binds to the AU-rich element that mediates the translational regulation of tumor necrosis factor α mRNA (Gueydan et al., 1999). This effect of TIA-1 and TIAR may be due to their ability to recruit mRNAs to stress granules that function as a storage site for inactive mRNAs. In addition, knocked-out for TIA-1 in Mouse embryonic fibroblasts (MEFs) or RNA interference (RNAi)-mediated knockdown of endogenous TIA-1, TIAR, or HuR in HeLa cells resulted in a decrease in β-F_1-ATPase protein expression (Izquierdo, 2006), suggesting that the 3 proteins function to stabilize the mRNA that encodes the β subunit of the F_1-ATPase.

The affinity purified TIAR failed to bind to either the R-2I or the longer R-2H RNA. Specific antibodies to TIAR did not block formation of specific complexes that are formed by incubating either RNA with a cytosolic extract of rat kidney cortex. Thus, it was concluded that TIAR probably does not function as a pHRE-binding protein (Tang and Curthoys, 2001). Purification of TIAR by the pHRE-affinity ligand (Tang and Curthoys, 2001) was explained by the fact that it is a well known RNA-binding protein that has broad specificity for AU-rich sequences. However, it remains possible that the purified TIAR is irreversibly denatured by the high salt concentration contained in the elution buffer.

Recent studies by Linker *et al.*, (Linker et al., 2005) demonstrated that overexpression of TTP resulted in a marked increase in iNOS expression, without any direct binding of TTP to the human iNOS mRNA. TIAR may affect the GA mRNA by a

similar mechanism. Therefore, it will be valuable to study the effect of TIAR, TTP, AUF1 and HuR over-expression on the level and stability of the GA mRNA.

7 CONCLUSIONS AND FUTURE DIRECTIONS

The current study has increased our knowledge regarding the the *trans*-acting factors that may regulate the turnover of the GA mRNA in the kidney cortex during normal acid-base balance and during metabolic acidosis. The reported data provide an experimental test of the previous hypothesis for the regulation of GA mRNA stability during acidosis. It was proposed that during normal acid-base balance, ζ-crystallin is not bound to the pHRE and instead the pHRE recruits a specific deadenylase or endoribonuclease to initiate the rapid decay of the GA mRNA. However, during metabolic acidosis, ζ-crystallin binds to the GA pHRE with greater affinity, thus protecting the mRNA from ribonucleolytic digestion and increasing the stability of the GA mRNA (Fig. 7.1). Our studies indicate that the previously proposed hypothesis was over simplified and other proteins like AUF1 have a role in this regulation. Our study has generated a different prospective for studying the regulatory mechanism of GA mRNA stabilization. The results of this study are summarized below. To have additional insights in the regulation of GA mRNA, some additional experiments based on the conclusions of this study are proposed.

ζ-crystallin and AUF1 bind within the GA 3'-UTR

Previous RNA gel shift assays revealed that proteins from a rat renal cortical cytosolic extract bind to the GA 3'-UTR. The binding was narrowed to the R2-I, segment of the 3'-UTR, that contains the pHRE. Affinity purification of the proteins that bind to the R2-I RNA identified ζ-crystallin as an RNA binding protein. Further studies using RNA gel shift and immunoblocking assays confirmed that ζ-crystallin binds to the pHRE with high affinity and specificity.

Recent experiments (Schroeder et al., 2006) have indicated that the 3'-UTR of the GA mRNA contains additional instability element(s) that may also participate in the pH-responsive stabilization. This study identified AUF1, a protein that binds to various AREs and promotes mRNA degradation (DeMaria and Brewer, 1996; Wilson and Brewer, 1999a), as a pHRE binding protein. It was found that anti-AUF1 antibodies produce a slight supershift of the GA (R2-I) RNA/protein complex formed with a cytosolic extract of rat kidney and that recombinant p40 AUF1 exhibits specific binding to the GA (R2-I) RNA. Analysis using the mutated GA (R2-I) RNAs indicates that a single 8-base AU-element is sufficient for AUF-1 binding. The same element also binds ζ-crystallin with high affinity and specificity (Tang and Curthoys, 2001), suggesting that the two proteins may compete for binding. Scatchard analysis also demonstrated that the interaction between recombinant p40 AUF1 and the GA (R2-I) RNA has a K_D of 2 μM. Fluorescence anisotropy measurements indicated that recombinant p40 AUF1 binds to the ARE of TNFα mRNA with a 50-fold greater affinity (Wilson et al., 2003). However, this analysis also demonstrated that the affinity of the interaction between AUF1 and the ARE is affected by phosphorylation of AUF1. Affinity purified ζ-crystallin was also shown to bind to the GA(R2-I) RNA with a K_D of 20-40 nM (Laterza and Curthoys, 2000a). However, recombinant ζ-crystallin bound the GA (R2-I) RNA with an affinity similar to that of the recombinant p40 AUF1. Thus, it will be important to determine if the onset of acidosis alters the phosphorylation states of AUF1 and/or ζ-crystallin and if these changes affect their relative binding interaction with the pHRE.

Proposed model for the decay of the GA mRNA

Based upon the combined observations and results obtained from this thesis, a revised model for the degradation of the renal GA mRNA is proposed. This model assumes that the pHRE and possibly additional instability elements within the 3'-UTR are involved in the decay and the stabilization of the GA mRNA. During normal acid-base balance, AUF1 and ζ-crystallin interact and bind to multiple binding sites within the GA 3'-UTR. Accessory proteins may modulate the activity of the two proteins. Degradation begins with the recruitment of a deadenylase complex to the poly (A) tail. The poly(A) is removed by a combination of processive and distributive mechanisms (Schroeder et al., 2006). AUF1 and/or ζ-crystallin then recruit the exosome, which then rapidly degrades the deadenylated GA mRNA from the 3'→ 5' end.

The onset of acidosis activates a signaling pathway that leads to phosphorylation or dephosphorylation of AUF1 and ζ-crystallin or other accessory proteins. This phosphorylation event may change the activity or the affinity of the proteins to bind the GA mRNA. This may lead to formation of a new protein complex on the mRNA that blocks recruitment or inhibits the activity of the deadenylase complex and prevents the recruitment of the exosome, thus stabilizing the GA mRNA (Fig. 7.2)

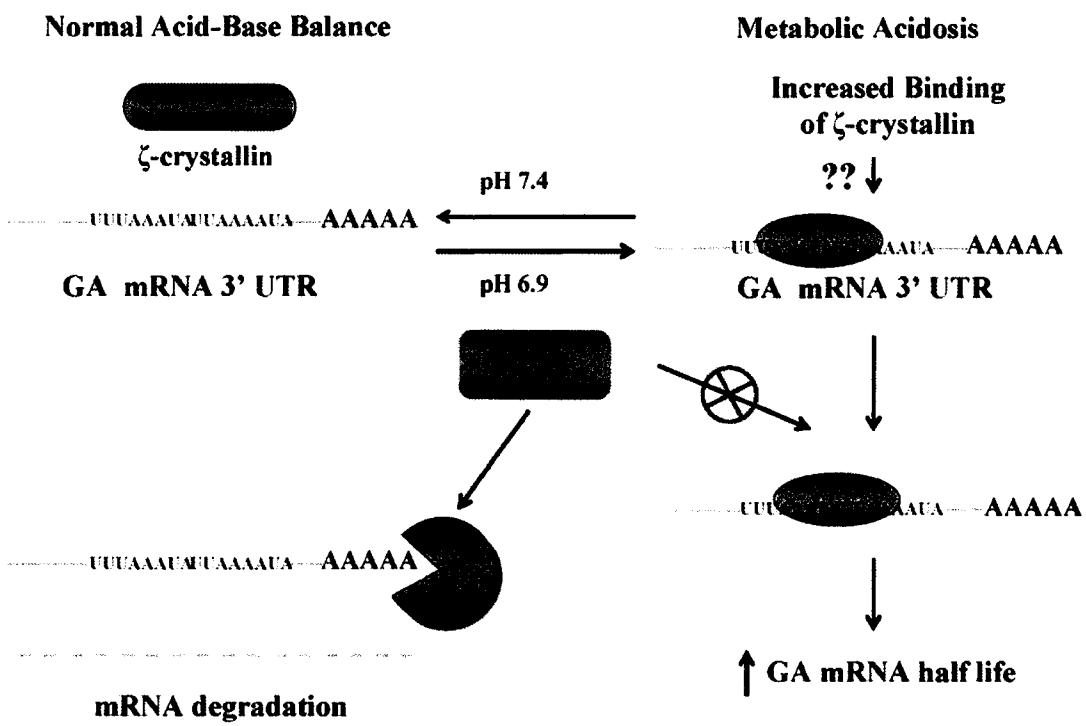

Fig. 7.1: Previously proposed model for the mechanism of renal GA mRNA stabilization during acidosis:
During normal acid-base balance, ζ-crystallin is not bound to the pHRE. The pHRE will recruit a specific deadenylase or endoribonucleaseto initiate the deadenylation and the rapid decay of the GA mRNA. However, during metabolic acidosis, ζ-crystallin binds to the GA pHRE with greater affinity, thus protecting the mRNA from ribonucleolytic digestion and increasing the stability of the GA mRNA.

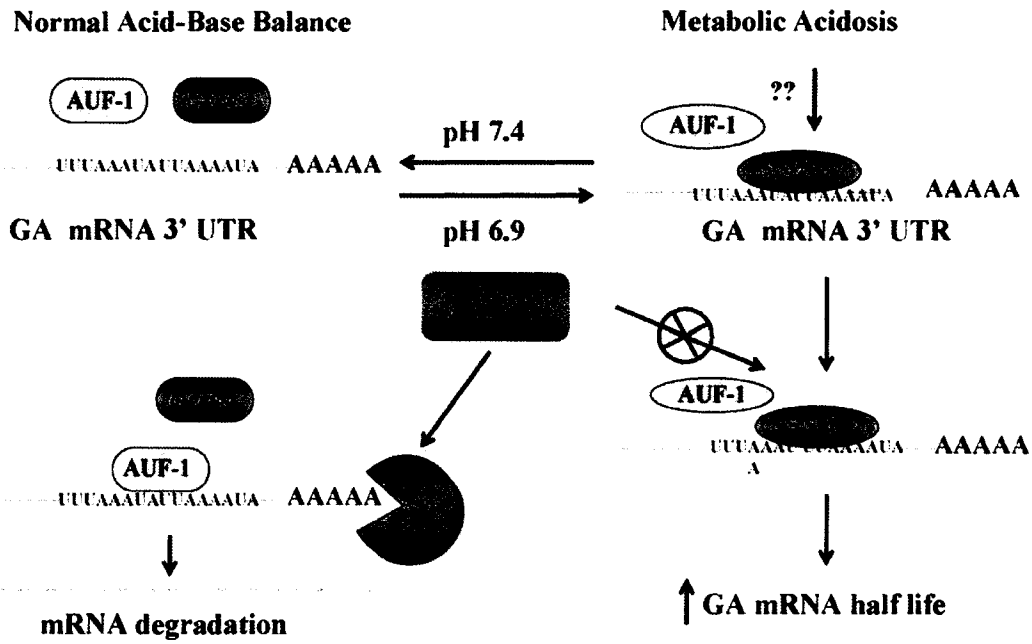

Fig. 7.2: New proposed model for the mechanism of renal GA mRNA stabilization during acidosis:
During normal acid-balance, AUF1 and/or ζ-crystallin bind to the pHRE within the GA 3'-UTR. Accessory proteins may also modulate the activity of the two proteins. Degradation begins with the recruitment of a deadenylase complex to the poly(A) tail. AUF1 and/or ζ-crystallin then recruit the exosome to intiate 3'→ 5' degradation of the deadenylated GA mRNA. However, the onset of acidosis may activate a signaling pathway that leads to phosphorylation or dephosphorylation of AUF1 and/or ζ-crystallin or may be other accessory proteins. This phosphorylation event may be essential for the change in the activity or the affinity of the proteins that bind the GA mRNA. A new protein complex may be assembled on the mRNA that blocks recruitment or inhibits the activity of the deadenylase complex and prevents the recruitment of the exosome, thus stabilizing the GA mRNA.

Suggested future experiments

It will be interesting to examine the *in vivo* binding of GA mRNA 3' UTR to various known RNA binding proteins, particularly ζ-crystallin, AUF1 and TIAR using Ribonomics (Tenenbaum, 2002) or RNA CHIP assay (Niranjanakumari et al., 2002). These techniques involve immunoprecipitation of the protein of interest followed by RT-PCR amplification of the bound RNA using specific primers. This approach may identify the cellular protein(s) that bind(s) to the pHRE and mediate(s) the pH-responsive stabilization of the GA mRNA.

It will be important to perform co-immunoprecipitation experiments to examine the interaction of ζ-crystallin and AUF1 with the various subunits of the exosome in cells. These analyses should characterize the protein–protein interactions that recruit the exosome as some RNA binding proteins are known to recruit the exosome to ARE-containing mRNAs and thereby enable exosome-mediated degradation of the mRNA (Chen et al., 2001; Gherzi et al., 2004).

AUF1, ζ-crystallin and/or other accessory proteins may undergo post-translational modification that affects their funcion. Identification of other proteins involved in the regulation of GA mRNA and characterization of the potential covalent modification that affects their function will be essential to understand the mechanism that mediates the pH-responsive stabilization of the GA mRNA.

Complexity and species variation of the kidney-type glutaminase gene

L. David Porter, Hend Ibrahim, Lynn Taylor and Norman P. Curthoys

Physiol Genomics 9:157-166, 2002. First published Apr 16, 2002;
doi:10.1152/physiolgenomics.00017.2002

Physiol Genomics 9: 157–166, 2002.
First published April 16, 2002; 10.1152/physiolgenomics.00017.2002.

Complexity and species variation of the kidney-type glutaminase gene

L. DAVID PORTER, HEND IBRAHIM, LYNN TAYLOR, AND NORMAN P. CURTHOYS
Department of Biochemistry and Molecular Biology,
Colorado State University, Fort Collins, Colorado 80523-1870

Received 12 February 2002; accepted in final form 15 April 2002

Porter, L. David, Hend Ibrahim, Lynn Taylor, and Norman P. Curthoys. Complexity and species variation of the kidney-type glutaminase gene. *Physiol Genomics* 9: 157–166, 2002. First published April 16, 2002; 10.1152/physiolgenomics.00017.2002.—Increased expression of rat kidney-type glutaminase (KGA) during metabolic acidosis results from selective mRNA stabilization. This process is mediated by an 8-base AU-sequence that functions as a pH-response element (pHRE). LLC-PK$_1$-FBPase$^+$ cells, a pH-responsive porcine kidney cell line, express four distinct GA mRNAs. RNase H mapping indicated that three of the GA mRNAs are generated by use of alternative polyadenylation sites and are homologs of the rat KGA mRNA, while the fourth contains a different COOH-terminal coding and 3′-untranslated sequence. PCR cloning and sequencing established that the latter GA mRNA is the homolog of the human GAC mRNA. A rat GAC cDNA was also cloned from a rat kidney library. The 3′-untranslated regions of the GAC mRNAs, but not the porcine or human KGA mRNAs, contain identifiable pHREs. The human KGA gene spans 82 kb and is composed of 19 exons. The unique sequence from the hGAC cDNA is contained in a single exon. Thus in humans, alternative splicing of the initial transcript could produce two GA mRNAs, only one of which may be increased during acidosis.

pH-response element; metabolic acidosis; mRNA stabilization; LLC-PK$_1$-FBPase$^+$ cells; COOH-terminal domains; RNase H mapping

IN RAT KIDNEY, AMMONIUM IONS are derived primarily from glutamine that is extracted from the plasma (29). Both basal and enhanced catabolism of glutamine during metabolic acidosis occur primarily within the proximal convoluted tubule (11, 26). The latter process is sustained, in part, by the increased expression of the genes that encode various transport proteins and the key enzymes of glutamine metabolism (7). For example, the level of the mitochondrial glutaminase (GA) is increased 8- to 20-fold within the rat renal proximal convoluted tubule during chronic acidosis (6, 33). This increased expression results from an increased rate of GA synthesis (31) that correlates with an increased level of the GA mRNA (17, 32). However, the apparent rate of transcription of the GA gene is not increased in acute (16) or chronic acidosis (17). These observations led to the suggestion that increased expression of the GA gene may result from the selective stabilization of the GA mRNA.

LLC-PK$_1$-FBPase$^+$ cells, a pH-responsive porcine proximal tubule-like cell line (12), have been used to characterize the mechanism of the adaptive increase in GA activity. Through the analysis of the turnover of various chimeric β-globin (βG) constructs, it was demonstrated that the 3′-untranslated region of the rat kidney-type glutaminase (rKGA) mRNA contains a pH-response element (pHRE) (14). RNA gel shift analyses were used to characterize and map the specific binding of a rat renal protein to two adjacent 8-base AU-sequences within the 3′-untranslated region of the rKGA mRNA (20). Further studies with various βG-GA reporter constructs (18, 19) established that a single 8-base AU-sequence was both necessary and sufficient to produce a mRNA that is selectively stabilized by the transfer of LLC-PK$_1$-FBPase$^+$ cells to an acidic media (pH 6.9, 10 mM HCO_3^-). The protein in rat kidney cortex that binds to the pHRE was recently identified as ζ-crystallin/NADPH-quinone reductase (30).

The pattern of GA mRNA expression in the porcine LLC-PK$_1$-FBPase$^+$ cells is complex. At least four distinct GA mRNAs are differentially expressed as a function of cell growth and development (25). Treatment with cycloheximide or prolonged maintenance in the same medium can be used to substantially increase the levels of the various GA mRNAs in LLC-PK$_1$-FBPase$^+$ cells. An initial GA cDNA that contains 528 bp of coding sequence and a 2.7-kb 3′-untranslated region was cloned from a porcine kidney cDNA library and shown by sequence comparison to encode the homolog of the rat kidney-type GA (rKGA) mRNA (25). However, probes derived from the 3′-untranslated region of the porcine KGA (pKGA) cDNA hybridized only with the 5.0- and 3.5-kb GA mRNAs (13, 25). In contrast, probes derived from the coding region of the rKGA or pKGA cDNAs hybridized to all four GA mRNAs. Furthermore, only the 4.5-kb GA mRNA, which apparently contains a unique 3′-untranslated region, is increased when confluent cultures of LLC-PK$_1$-FBPase$^+$ cells were transferred to acidic medium (13). The two- to threefold increase in the level of the 4.5-kb GA mRNA was shown to correlate with a similar increase in the stability of the 4.5-kb GA mRNA. In contrast, the

Article published online before print. See web site for date of publication (http://physiolgenomics.physiology.org).

Address for reprint requests and other correspondence: Norman P. Curthoys, Dept. of Biochemistry and Molecular Biology, Colorado State Univ., Fort Collins, CO 80523-1870 (E-mail: ncurth@lamar.colostate.edu).

stability of the 5.0-kb GA mRNA was not affected by treatment with acidic media. Thus it is important to determine the relationship and the structural differences among the multiple GA mRNAs that are expressed in the LLC-PK_1-FBPase$^-$ cells.

The human (h) homolog of the rKGA cDNA has also been cloned and characterized (8, 15). However, the 3′-untranslated region of the hKGA mRNA lacks an identifiable pHRE. An isoform of the hKGA cDNA, termed hGAC, was also cloned from a human colon carcinoma cDNA library (8). The 5′-coding region of the hGAC cDNA is identical to the corresponding sequence within the hKGA cDNA. However, the hGAC cDNA encodes a distinct COOH-terminal sequence and contains a different 3′-untranslated region, suggesting that the two mRNAs may be produced by alternative splicing. The 3′-untranslated region of the hGAC mRNA contains four separate 8-base AU sequences that are identical to either of the 8-base elements that were identified as pHREs within the rKGA mRNA. Furthermore, Northern analysis indicated that both the hKGA and hGAC mRNAs are expressed in human kidney tissue (8).

In the current study, RNase H mapping was used to further characterize the structural relationship between the multiple GA mRNAs expressed in LLC-PK_1-FBPase$^+$ cells. In addition, reverse transcriptase and polymerase chain reactions (RT-PCR) were used to amplify and sequence additional segments of the 5.0-kb and 4.5-kb GA mRNAs. These analyses established that the 4.5-kb GA mRNA has a COOH-terminal coding sequence that is identical to the hGAC cDNA and a 3′-untranslated region that contains three putative pHREs. Thus this mRNA is the porcine homolog of the hGAC cDNA. Finally, analysis of the current human genome database indicates that the unique sequence within the hGAC cDNA is derived from a single exon within the hKGA gene.

MATERIALS AND METHODS

Materials. [α-^{32}P]dATP and [α-^{32}P]dCTP (specific activity of 3,000 Ci/mmol), Hot Tub DNA polymerase and the random oligolabeling kit were obtained from Amersham Pharmacia Biotech. GeneScreen Plus and the restriction enzymes were products of New England Nuclear and Boehringer-Mannheim, respectively. The Reverse Transcription System and the pGEM-T Easy vector were obtained from Promega. Ex Taq DNA polymerase was purchased from TaKaRa Biomedicals (Otsu, Japan). Retrotherm reverse transcriptase, Hybridase thermostable RNase H, and RNase H from *Escherichia coli* were obtained from Epicentre Technologies (Madison, WI). Formazol (formamide) was purchased from Molecular Research Center. Oligo(dT)-cellulose spin columns were from 5 Prime-3 Prime. Agarose (MEEO) and Sequenase were products of United States Biochemicals. Oligodeoxynucleotides were synthesized by Macromolecular Resources (Ft. Collins, CO). Unless designated otherwise, the oligonucleotides contained sequences that are complementary to the sequence starting with the designated 5′ base of the rat GA cDNA (27). All other biochemicals were purchased from Sigma or Fluka.

Cell culture. The LLC-PK_1-FBPase$^+$ cells were originally isolated by Gstraunthaler and Handler (12) and were obtained from Edward Nord (SUNY Stony Brook). The cells were cultured in a 50:50 mixture of Dulbecco's modified Eagle's and Ham's F-12 media as described previously (25). To increase the levels of the various GA mRNAs, cells were grown under standard conditions for 7 days and then maintained in the same medium for 4 days or treated with 0.5 mM cycloheximide for 16 h.

RNase H and Northern analysis. Total RNA was isolated from cultured cells using the acid guanidinium thiocyanide: phenol:chloroform protocol (4). The isolated RNA samples were dissolved in Formazol and stored at −70°C. Poly(A)$^+$ RNA was prepared using oligo(dT)-cellulose spin columns. RNase H digestions were performed as described previously (24). RNA samples were subjected to electrophoresis on a 1% agarose-formaldehyde gel. The cDNA probes used for hybridization included sequences that correspond to the coding region (r1500) of the rat GA mRNA and the 3′-untranslated region (p2400) of the porcine GA mRNA. The r1500 cDNA is an *Acc*I restriction fragment of the rat pGA104 plasmid (27). The p2400 probe is an *NheI*/*Not*I restriction fragment of the porcine pGA201 plasmid (25). The cDNA probes were radiolabeled by random primer labeling using either [α-^{32}P]dATP or [α-^{32}P]dCTP (10). The hybridization solution containing 5–10 ng/ml of the ^{32}P-labeled cDNA probe was prepared as described (3), except that the formamide concentration was 40% and no polyethylene glycol was added. Hybridizations were carried out in glass bottles rotated overnight at 43°C in a hybridization oven. Membranes were initially washed in 300 mM NaCl, 30 mM sodium citrate, and 0.5% sodium dodecyl sulfate (SDS) at 43°C. The final wash was performed at either 56°C or 48°C using 50 mM sodium phosphate, pH 7.2, and 0.1% SDS or at 48°C using 45 mM NaCl, 4.5 mM sodium citrate, and 0.1% SDS. For low-abundance mRNAs, a stronger signal was obtained by relaxing the stringency of the final wash without changing the pattern or the relative intensities of the observed bands. The Northern blots were imaged on a PhosphorImage Analyzer (Molecular Dynamics) following a 1- to 3-day exposure or by autoradiography at −70°C for 3–21 days.

Isolation and amplification of a 5′ segment of the 5.0-kb GA mRNA. Total poly(A)$^+$ RNA isolated from LLC-PK_1-FBPase$^+$ cells that had been maintained in the same medium for 4 days was used as the starting material for the isolation and amplification of a 5′ segment of the porcine 5.0-kb GA cDNA. The purification protocol is diagrammed in Fig. 3*A*. Approximately 10 μg of poly(A)$^+$ RNA was spin dialyzed into 26 μl of water using a 30-kDa cutoff microconcentrator. Then 1 μl of 50 μM oligonucleotide 3082 and 3 μl of 10× RNase H buffer (0.5 M Tris·HCl, pH 7.4, 1.0 M NaCl, 20 mM $MgCl_2$, 10 mM dithiothreitol) were added, and the sample was incubated at 48°C. The reaction was initiated by addition of 1.0 U of Hybridase RNase H and incubated for 15 min (24). The reaction was terminated by adding 300 μl of water and 330 μl of 2× oligo(dT) column binding buffer (1.0 M LiCl, 100 mM sodium citrate, and 0.2% SDS) and the diluted sample was heated at 60°C for 3 min. The sample was then cooled to room temperature and applied twice to an oligo(dT) column. The final flow-through fraction containing the poly(A)$^-$ RNA was collected and precipitated with an equal volume of isopropanol. The poly(A)$^-$ RNA was then resuspended in 50 μl of Formazol. The column was washed and eluted per the manufacturer's instructions to recover the poly(A)$^+$ fraction. The fractionation was confirmed by Northern analysis.

The RT-PCR protocol employed Retrotherm, a heat-stable reverse transcriptase, to increase the priming stringency and the efficiency of polymerization through regions of possible mRNA secondary structure. The isolated poly(A)$^-$ RNA fraction was spin-dialyzed into 16.5 μl of water, and 25 pmol of

oligonucleotide 1952 was added. The sample was held at 56°C in the thermocycler while 1 μl of dNTPs (4 mM each), 1 μl each of *solution A* (0.2 M Tris·HCl, pH 8.3, and 1.0 M KCl) and *solution B* (30 mM $MgCl_2$ and 15 mM $MnSO_4$), and 2 U of reverse transcriptase were added. The reaction temperature was then increased slowly over a 10-min period to 70°C. After 5 min at 70°C, the first-strand synthesis was considered complete. The reaction was subsequently heated to 95°C for 2 min and then held at 80°C as 20 μl from this sample was directly pipetted into the succeeding PCR reaction mix. This mix was preincubated at 80°C and consisted of 62 μl of water, 1 μl of 50 μM oligonucleotide 574-forward, 1 μl of 50 μM oligonucleotide 1689, 10 μl of 10× Hot Tub polymerase reaction buffer, and 4 μl of dNTPs (4 mM each). The Hot Tub polymerase (1.6 U) was added last. Second-strand synthesis was performed during the first amplification cycle. Amplification was carried out for 35 cycles as follows: 94°C for 30 s, 50°C for 30 s, and 70°C for 150 s. The final cycle was followed by an incubation at 70°C for 3 min and the sample was then stored at 4°C until analyzed by Southern blotting.

Isolation and amplification of a 5′ segment of the 4.5-kb GA mRNA. The isolation and amplification of the corresponding 5′ segment of the 4.5-kb GA mRNA was accomplished using the above protocol with modifications as outlined below and in Fig. 3*B*. Total RNA from starved LLC-PK_1-FBPase$^+$ cells was used for RNase H digestion with oligonucleotide 1952. After digestion, the sample was passed over an oligo(dT) column. The 5′ segments from the cleaved GA mRNAs eluted with the poly(A)$^-$ RNAs in the flow-through fraction, whereas the intact 4.5-kb GA mRNA eluted from the column with the poly(A)$^+$ RNAs. This poly(A)$^+$ fraction was used for the detailed RNase H mapping of the intact 4.5-kb GA mRNA. To remove background poly(A)$^+$ RNAs, a second RNase H digest using oligonucleotide 1689 was performed, and this sample was applied to a second oligo(dT) column. Now the 5′ segment from the 4.5-kb GA mRNA was eluted in the poly(A)$^-$ flow-through fraction, while the poly(A)$^+$ RNAs were retained on the column. The purified 5′ segment was amplified by RT-PCR using oligonucleotides 574-forward and 1476.

Dideoxy sequencing of RT-PCR products. The two RT-PCR products were purified by agarose gel electrophoresis and sequenced without subcloning. Approximately 1 μg of extracted cDNA was transferred to 20 mM Tris·HCl, pH 9.0, by spin dialysis. An 8-μl sample containing the cDNA and 25 pmol of primer were heat denatured at 95°C for 1 min and then set on ice. DNA sequencing was performed using the Sequenase kit (United States Biochemicals).

RT-PCR amplification and cloning of the 3′ end of the 4.5-kb GA mRNA. The reverse transcription reactions were carried out using 1 μg of total RNA isolated from LLC-PK_1-FBPase$^+$ cells and the Reverse Transcription System from Promega. This kit utilizes an oligo$(dT)_{15}$ primer and the AMV reverse transcriptase. The PCR amplification reactions utilized the Ex Taq DNA polymerase. The initial PCR reaction used the F1 and B2 primers that were described previously (8). The second PCR reaction utilized the complement of the B2 sequence as the forward primer and a reverse primer, 5′-CAAAATGTAGGCATACTGG-3′, that is complementary to sequence located near the 3′ end of the hGAC cDNA. The resulting PCR fragments were cloned into the pGEM-T Easy vector. The resulting plasmids were sequenced using a Prism 377 DNA Sequencer (Applied Biosystems) and primers designed with Omiga software.

Analysis of human GA genes. The human KGA (15) and rat liver-type GA (LGA) (5) cDNA sequences were used in a BLAST search of the human genome database located within the website: **http://www.ensembl.org**. The COOH-terminal cDNA sequence unique to the human GAC (8) sequence was used in a similar BLAST search.

RESULTS

RNase H mapping. Previous studies (13, 25) indicated that the 4.5- and 5.0-kb GA mRNAs from LLC-PK_1-FBPase$^+$ cells contain divergent sequences within their 3′ ends. Thus RNase H digestions were used to confirm these results and to more precisely map the region where the two porcine GA mRNAs diverge (Fig. 1). Samples of total RNA containing elevated amounts of the two GA mRNAs were isolated from cycloheximide-treated LLC-PK_1-FBPase$^+$ cells and incubated with one of three oligonucleotides (2072, 1952, and 1689) that are complementary to sequences within the COOH-terminal coding region of the rat kidney GA cDNA (27). Following RNase H digestion, the samples were probed with a cDNA (p2400) that is specific for the 3′-untranslated region of the 5.0-kb GA mRNA. Treatment with each of the oligonucleotides resulted in site-specific cleavage of the 5.0-kb GA mRNA. The sizes of the resulting bands (2.8, 2.9, and 3.1 kb, respectively) correspond closely to the expected lengths of the 3′ fragments as determined from the sequence of the pKGA cDNA (25). The blot was then stripped and reprobed with the r1400 probe that is derived from coding region of the rKGA cDNA and that hybridizes to both the 4.5- and 5.0-kb GA mRNAs. Again, the 5.0-kb GA mRNA was cleaved by all three oligonucleotides to produce the corresponding 2.2-, 2.1-, and 1.9-kb 5′ fragments, respectively. The r1400 probe also hybridized weakly to the 3.1-kb 3′ fragment that was produced following hybridization and digestion with oligonucleotide 1689. In contrast, the 4.5-kb GA mRNA was cleaved only when incubated with oligonucleotide 1689. The unexpected formation of fragments that are less than 1.9-kb in length may result from the low stringency of the oligonucleotide binding during the 37°C digestion with the *E. coli* RNase H. However, the resulting data establish that the sequence divergence between the two porcine GA mRNAs occurs ~150–350 nucleotides upstream of the 3′ end of the coding sequence.

A more thorough mapping analysis (Fig. 2) was performed using a total of 13 oligonucleotides that span the entire length of the 5.0-kb GA mRNA and a thermostable RNase H to achieve increased stringency (24). Each of the tested oligonucleotides cleaved at the corresponding sites in the 2.5-kb, 3.5-kb, and 5.0-kb GA mRNAs. Thus both of the smaller and less abundant GA mRNAs may be derived by use of alternative polyadenylation signals that occur at appropriate positions within the 5.0-kb GA cDNA sequence. This analysis also suggested that much of the coding sequence of the 4.5-kb GA mRNA is identical to that of the other GA mRNAs. However, this mRNA must contain unique sequences within the 3′ end of the coding region and throughout the entire 3′-untranslated region.

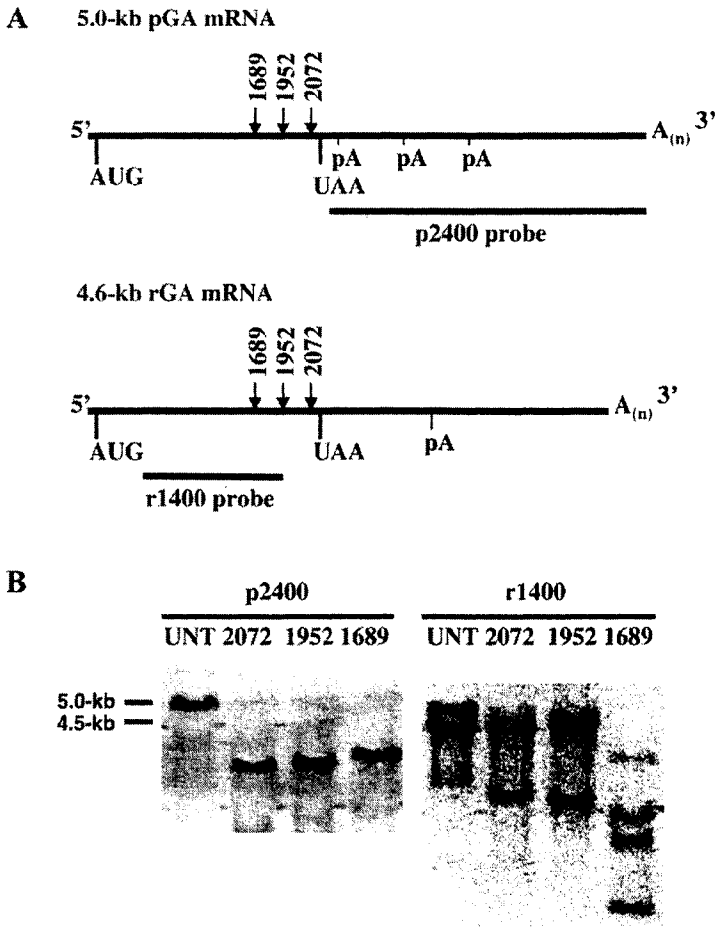

Fig. 1. RNase H mapping of the porcine 5.0-kb and 4.5-kb glutaminase (GA) mRNAs. *A*: the p2400 probe was obtained from the 3′-untranslated region of a porcine GA cDNA, whereas the r1400 probe was derived from the coding region of a rat GA cDNA. *B*: samples containing 20 μg of total RNA isolated from LLC-PK$_1$-FBPase$^+$ cells pretreated with cycloheximide were either untreated (UNT) or incubated with the indicated oligonucleotide. RNase H treatment was performed at 37°C for 15 min. The p2400 probe hybridizes specifically with the 5.0-kb GA mRNA, whereas the r1400 probe hybridizes to both GA mRNAs.

Sequence analysis. RNase H digestion and fractionation on oligo(dT)-cellulose were used to selectively purify the 5′ ends of the 5.0- and 4.5-kb GA mRNAs (Fig. 3, *A* and *B*). The oligonucleotide 3888 was used to selectively cleave the 5.0-kb GA mRNA. Following purification on oligo(dT)-cellulose, the poly(A)$^-$ fraction was shown by Northern analysis to contain only the 5′ end of the 5.0-kb GA mRNA (L. D. Porter, data not shown). This fraction was used to RT-PCR amplify and sequence the segment of the 5.0-kb GA mRNA between oligonucleotides 574 and 1689 (Fig. 4). Subsequently, oligonucleotide 2144 was incubated with total RNA and used to cleave the 5.0-, 3.5-, and 2.5-kb GA mRNAs. After fractionation on oligo(dT)-cellulose, Northern analysis verified that the poly(A)$^+$ fraction contained the intact 4.5-kb GA mRNA and the 3′ ends of the three other GA mRNAs (L. D. Porter, data not shown). This fraction was digested with oligonucleotide 1689 and rechromatographed on oligo(dT)-cellulose. The poly(A)$^-$ fraction, which contained only the 5′ end of the 4.5-kb GA mRNA, was used to RT-PCR amplify and sequence the segment between oligonucleotides 574 and 1476 (Fig. 4). The two amplified segments contained identical sequences, confirming the results of the RNase H mapping analysis and suggesting that the 4.5- and 5.0-kb porcine GA mRNAs may be derived from a single kidney-type GA gene.

Elgadi et al. (8) cloned a GA cDNA from a human colon carcinoma cDNA library that they termed hGAC. The 5′ end of the hGAC cDNA is identical to that of the human kidney-type GA cDNA (8, 15). However, the hGAC cDNA contains a unique COOH-terminal coding sequence and a distinct 3′-untranslated region. Since KGA cDNA coding sequences are highly conserved among species, it was probable that the unique sequence found in the hGAC cDNA would also be conserved. Thus specific primers corresponding to sequences from the hGAC cDNA were used to RT-PCR amplify and clone cDNAs from poly(A)$^+$ RNA isolated from LLC-PK$_1$-FBPase$^+$ cells (Fig. 3*C*). The initial PCR fragment (464 bp) spanned the region where the 4.5- and 5.0-kb GA mRNAs diverge. The sequence of

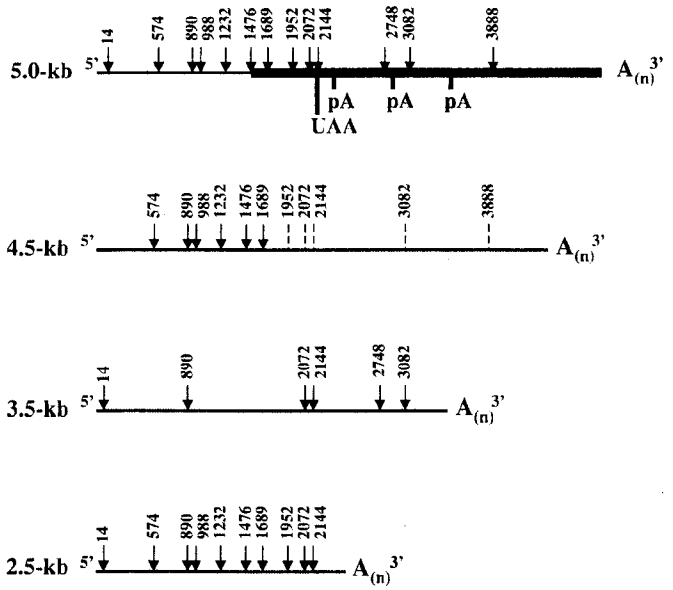

Fig. 2. Composite RNase H map of the porcine GA mRNAs. Solid arrows or dashed lines indicate oligonucleotides that either promote cleavage with RNase H or do not hybridize to the individual GA mRNAs, respectively. The bold line indicates the portion of the 5.0-kb GA cDNA that was previously sequenced (25). The fine lines indicate previously unknown cDNA sequence.

the initial 364 bp of this fragment was 100% identical to sequence contained in the 5.0-kb GA cDNA, but only 96% identical to the corresponding segment of the hGAC cDNA (Fig. 4). All of the nucleotide substitutions in this region occur within wobble positions. Thus the two sequences encode an identical amino acid sequence. By contrast, the nucleotide sequence of the remaining 100 bp was highly divergent from the adjacent sequence in the porcine 5.0-kb GA cDNA, but was 100% identical to the corresponding sequence in the hGAC cDNA. Thus the remainder of the 3′ end of the 4.5-kb GA cDNA was amplified by RT-PCR, cloned, and sequenced. From the point of divergence to the 3′ end, the sequence of the isolated porcine cDNA is 77% identical to the 3′ end of the hGAC cDNA (Fig. 4). All of the differences in DNA sequence within the unique coding regions of the hGAC and the porcine 4.5-kb GA cDNAs occur within wobble positions. Thus the corresponding mRNAs encode identical COOH-terminal domains (Fig. 5). This level of identity clearly establishes that the porcine 4.5-kb GA mRNA is the homolog of the hGAC mRNA. Furthermore, the 3′-untranslated regions of both the 4.5-kb porcine GA and the hGAC mRNAs contain multiple pHREs (Fig. 4). In contrast, both the hKGA (8, 15) and the 5.0-kb porcine GA mRNA (25) lack the pHRE sequence identified in the rKGA mRNA. If the 2.5- and 3.5-kb porcine GA mRNAs are formed by use of alternative polyadenylation sites within pKGA transcript, then they will also lack a pHRE sequence.

RNase H experiments performed with total RNA from normal rat kidney and with poly(A)$^+$ RNA isolated from acidotic rat kidney established the presence of a 4.4-kb GA mRNA that was not cleaved when incubated with oligonucleotides 4008, 2958, 2458, or 1952, but was cleaved with oligonucleotides 1689, 1476, and 574 (L. D. Porter, data not shown). This data strongly supports the previously reported evidence (9) for the presence of a rat homolog of the hGAC mRNA. We had previously cloned a number of GA cDNAs from a rat kidney library (27). One of these clones (rat pGA105) contained a divergent sequence that was previously assumed to result from an artifact of cloning. When fully sequenced, this clone was found to diverge at the same position as the hGAC and the porcine 4.5-kb GA cDNAs. The final 147 bp of the 3′ coding sequence of the rat pGA105 cDNA is 90.5% and 91.2% identical to the unique COOH-terminal coding sequences within the human and porcine GAC cDNAs, respectively. Thus rat kidney also expresses a GAC variant of the rKGA mRNA. The rGAC mRNA encodes a COOH-terminal domain that contains five conservative amino acid substitutions compared with the corresponding human and porcine GAC proteins (Fig. 5). Thus multiple mammalian species express two distinct classes of kidney-type GA that differ in their COOH-terminal domains.

GA genome. Analysis of the current human genome database suggested that the two kidney-type GA mRNAs are produced by alternative splicing of an initial transcript of a single gene. The kidney-type GA gene is located on chromosome 2 (1). Sequences corresponding to the two GA cDNAs are located on four separate contigs and are distributed into 19 exons (Fig. 6). The entire gene spans 82 kb. Each of the identified junctions contains a sequence that fits to the consensus sequence for 5′ and 3′ splice sites. The hGAC mRNA is formed by joining exons 1–15, whereas the hKGA mRNA is derived from exons 1–14 and 16–19. Thus all of the sequence that is unique to the hGAC mRNA is contained in exon 15.

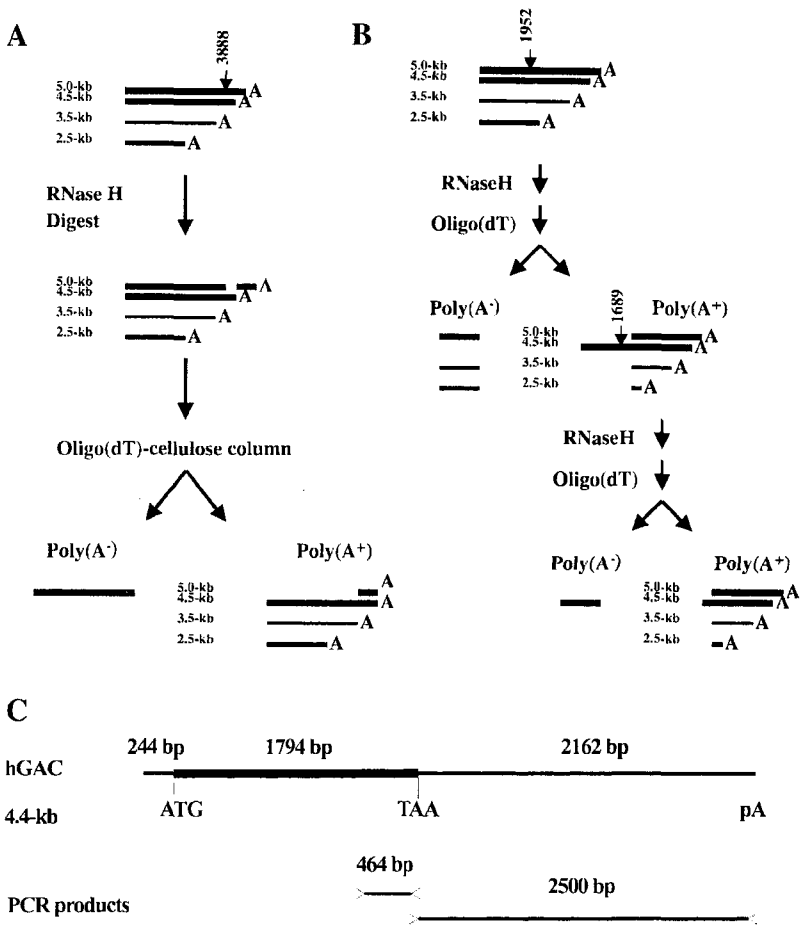

Fig. 3. Schematic diagrams of the protocols used to isolate the 5′ segments of the 5.0-kb GA mRNA (*A*) and of the 4.5-kb GA mRNA (*B*). *C*: schematic diagram of the PCR amplification of the 3′ end of the 4.5-kb GA cDNA. Forward (>) and reverse (<) primers were selected from known sequences within the hGAC cDNA (8).

The rat LGA is derived from a separate but closely related gene (5). In humans, the LGA gene is located on chromosome 12 (1). The hLGA gene sequence within the human genome database is located on two nonoverlapping contigs. The missing overlap contains ~600 bp of the first intron. Thus all of the cDNA sequence was identified in 18 exons that span ~18 kb. The lengths of exons 3–17 within the hLGA and hKGA genes are identical. The nucleotide sequences of the segments of the two cDNAs derived from these exons have a 69% identity. However, the amino sequences encoded by the same exons have a 77% identity. In contrast, the COOH-terminal amino acid sequence encoded by exon 18 of the hLGA gene shares very little identity with the COOH-terminal sequence of either the hKGA (33%) or the hGAC protein (14%). This difference further suggests that the COOH-terminal domain may impart different properties and functions to the various GA proteins.

DISCUSSION

Multiple isoforms of the kidney-type GA mRNA are expressed in various cell lines (24) and in different

Fig. 4. Comparison of the sequences of the porcine 4.5-kb GA and the hGAC cDNAs. The composite sequence determined for the porcine 4.5-kb GA cDNA (*top* line) is aligned with the corresponding sequence for the hGAC cDNA (*bottom* line), which is numbered as previously reported (8). The identified coding regions are shown in upper case letters, whereas the 3′-untranslated regions are shown in lower case letters. For the hGAC sequence, only the base substitutions are shown. Hyphens indicate nucleotides where the bases are identical, and blank spaces indicate regions where corresponding bases are absent in either sequence. Potential pH-response elements and polyadenylation signals within the 3′-nontranslated regions of the two cDNAs are indicated in bold underscore and bold italic, respectively.

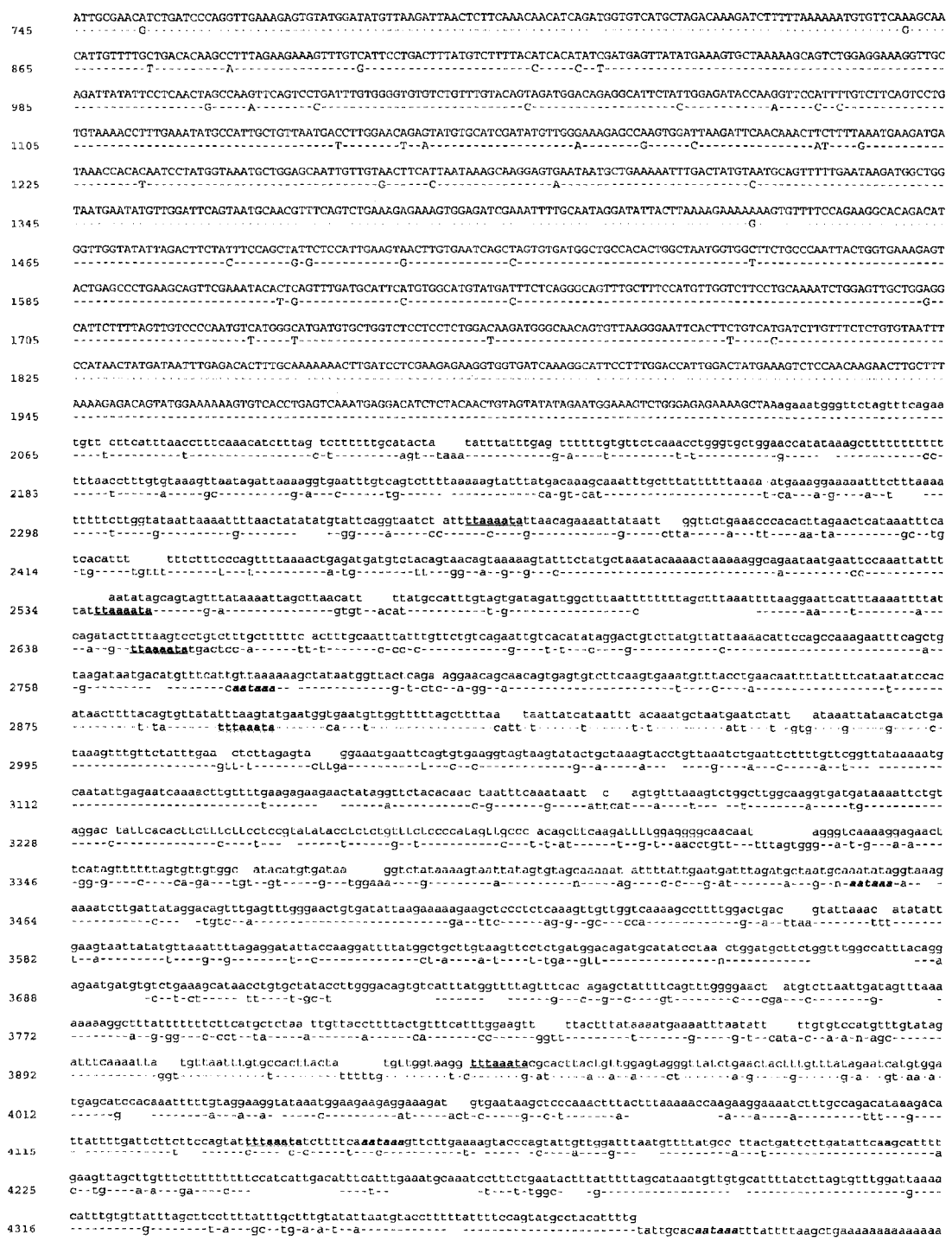

```
531  DNLRHFAKKL DPRREGGDQR VKSVINLLFA AYTGDVSALR  hKGA
571  RFALSAMDME QRDYDSRTAL HVAAAEGHVE VVKFLLEACK  hKGA
611  VNPFPKDRWN NTPMDEALHF GHHDVFKILQ EYQVQYTPQG  hKGA
651  DSDNGKENQT VHKNLDGLL                         hKGA
```

Fig. 5. Comparison of the COOH-terminal sequences of various kidney-type GA proteins. An underscore indicates regions where the amino acid sequence is identical to the human kidney-type glutaminase (hKGA) protein, whereas a hyphen indicates an amino acid that is identical to the divergent COOH-terminal sequence of the hGAC protein.

tissues (8, 16). The abundance of a particular GA mRNA variant may differ significantly depending upon the tissue type or the developmental or metabolic state of the tissue. The relative abundance of each isoform can be determined only if the structural basis for each type of GA mRNA is known. All of the KGA and GAC isoforms share a common sequence within their 5′ end but diverge significantly within the 3′-coding and 3′-untranslated regions. This variation has complicated the cloning of GA cDNAs. Given the length of the GA mRNA, it has not been possible to isolate a full-length GA cDNA to assure accurate cloning of the original mRNA. Instead, all of the reported GA cDNAs have been constructed from overlapping, but arbitrarily combined sequence segments. Thus, to obtain definitive information regarding putative isoforms of GA mRNAs, RNase H mapping was employed to characterize the relationship between the various GA mRNAs

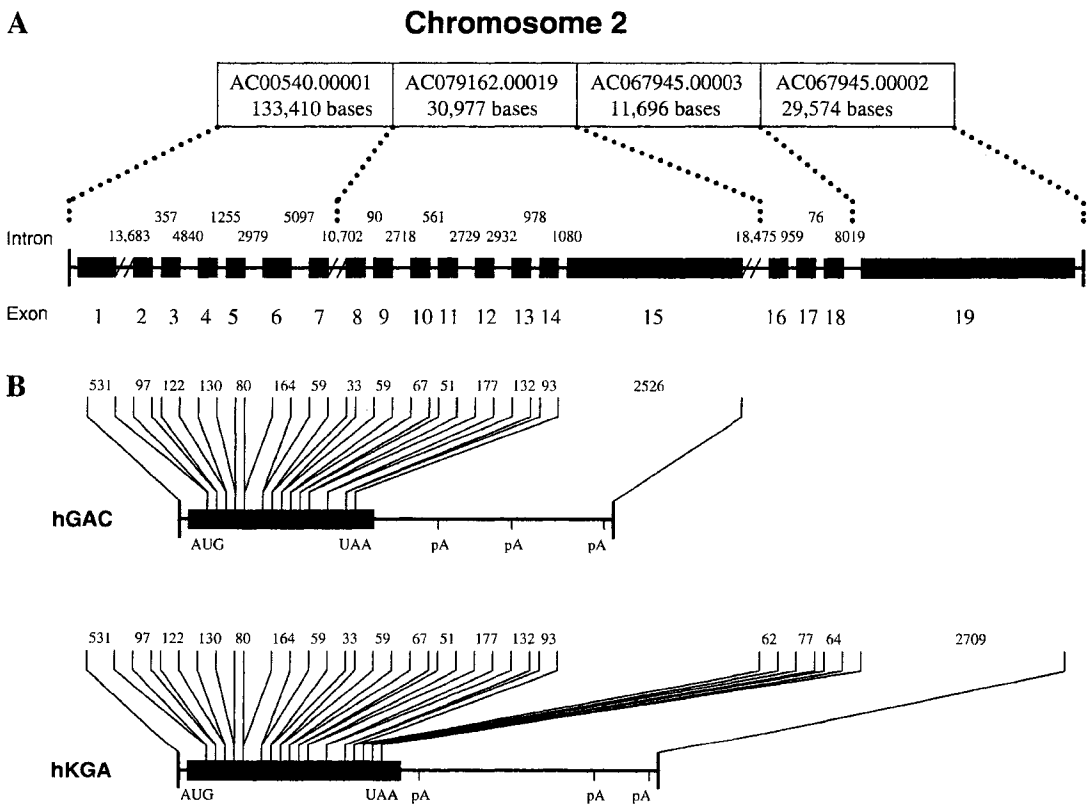

Fig. 6. Genomic structure of the hKGA gene. *A*: identified exons are shown as solid boxes and are drawn to scale. The introns are shown as lines, with lengths noted in bp. *B*: differential splicing of the exons to form hGAC and hKGA mRNAs. The lengths of exons are noted in bp.

that are expressed in the porcine renal LLC-PK_1-$FBPase^+$ cell line. From the results of this analysis, a protocol was developed (Fig. 2), using a modification of a previous strategy (21), to isolate similar segments from the coding regions of two specific GA mRNAs. Subsequent sequencing analysis confirmed the previously hypothesized relationship between 4.5-kb and 5.0-kb porcine GA mRNAs (25).

The KGA and GAC mRNAs are frequently expressed in the same cell line or tissue (8). The two GA mRNAs are sufficiently similar in size that they are difficult to resolve by agarose gel electrophoresis (13, 25). Thus reports in the literature that have used only a probe that hybridizes to the shared coding sequence should be interpreted with this in mind. However, the methods and probes developed in this study extend the previous techniques (8) that can be employed to detect and quantify the two GA mRNA variants.

Four GA mRNAs, that are ~2.5, 3.5, 4.5, and 5.0 kb in length, are expressed in LLC-PK_1-$FBPase^+$ cells (25). The two larger mRNAs predominate except when the LLC-PK_1-$FBPase^+$ cells are starved for nutrients by maintaining them in the same medium for 4 days. Under these conditions, very high levels of the 2.5-kb GA mRNA are selectively expressed. When $poly(A)^+$ RNA isolated from pig kidney was probed with a porcine GA cDNA that contained the shared coding sequence, all four GA mRNAs were detected (data not shown). However, the 5.0-kb GA mRNA was predominant. The RNase H experiments reported in this study suggest that the two smaller GA mRNAs are produced from the same initial transcript by use of appropriately positioned alternative polyadenylation sites. However, both the RNase H mapping and the sequence analysis indicate that the 4.5-kb GA mRNA is the homolog of the hGAC mRNA (8). The genome analysis indicates that the GAC mRNA is produced by alternative splicing of a distinct exon within the GA gene. The finding that the unique sequence within the hGAC mRNA constitutes a single exon within the human hKGA gene provides strong evidence in support of the conclusion that the hKGA and hGAC mRNAs are formed by alternative splicing of the initial transcript of the same gene. In many well-conserved gene families, the number and lengths of the component exons are also conserved between species. Given the high percent identity between the hGAC cDNA and the porcine and rat homologs, it is highly likely that the exon arrangement present in the hKGA gene is conserved in the porcine and rat KGA genes.

An alternative splicing reaction could generate two distinct isoforms of the GA protein. Currently, the only evidence that the GAC mRNA encodes an active GA protein is the high GA activity measured in TSE cells that express only the hGAC mRNA (8). Translation of the rKGA mRNA yields a 74-kDa precursor protein that is translocated into the mitochondrial matrix and processed to yield the 68- and 66-kDa peptides that constitute the mature rat renal GA (23, 26). Assuming that the precursor translated from the GAC mRNA is similarly processed, the mature GAC protein would contain 60-kDa and/or 58-kDa peptides. In addition, the two proteins would contain distinct COOH-terminal domains. The sequence of the LGA is very homologous to the KGA protein except within the NH_2- and COOH-terminal regions (5). The COOH terminus of the hLGA protein mediates its association with two PDZ domain-containing proteins, α1-syntrophin, and a glutaminase interacting protein termed GIP (22). The recombinant GIP protein inhibits GA activity when added to crude rat liver extracts (2). These observations suggest that the COOH-terminal domains of the various GA isoenzymes may constitute sites for selective protein-protein interactions. Thus alternative splicing may result in the formation of two KGA isoforms that contain distinct COOH-terminal protein interactive domains. Selective interactions of the GA protein with a membrane anchoring protein could account for its loose association with the inner surface of the mitochondrial inner membrane (28). Alternatively, selective association of either KGA protein with the mitochondrial glutamine transporter or the subsequent enzymes of glutamine metabolism could facilitate the acute activation of renal glutamine catabolism that precedes increased expression of the GA protein during the rapid onset of an acute acidosis (7).

Increased expression of rat renal GA during chronic acidosis results from selective stabilization of the rKGA mRNA (14, 20). This process is mediated by 8-base AU sequences that function as pHREs (18, 19). In the rat, both the KGA and GAC mRNAs contain multiple pHRE sequences. Thus both mRNAs may be stabilized and increased during chronic acidosis. However, in the pig and human, only the GAC variant of the KGA mRNA contains multiple pHRE sequences. Based upon the rat model, one would hypothesize that only the pGAC and hGAC mRNAs would be increased within the proximal tubule of their respective species during chronic acidosis. Such an induction could be mediated by cell-specific alternative splicing such that only the GAC mRNA is produced within the proximal tubule cells. Alternatively, only the KGA mRNA may be constitutively expressed in multiple segments of the nephron during normal acid-base balance, and the onset of acidosis could lead to a cell-specific change in splicing that results in formation of the pH-responsive GAC variant solely within the proximal tubule. Either mechanism would result in the cell-specific induction of GA activity.

Based upon nucleotide and protein sequence homology, it was previously concluded that the rat LGA and KGA proteins were derived from separate, but structurally related genes (5). A comparison of the composition of the two genes established that the extensive region of high homology within both genes is encoded by 15 exons. Furthermore, the lengths of the 15 corresponding exons within the two genes are identical. These observations support the previous conclusion. They also suggest that the separate genes probably arose from gene duplication followed by divergent evolution. During evolution, significant differences in the composition and lengths of the introns arose. In addi-

tion, different 5′- and 3′-exons were added to the two genes to encode different NH_2-terminal mitochondrial targeting signals and COOH-terminal protein interacting domains, respectively. Finally, an alternative 3′-exon was inserted within the KGA gene to allow for the formation of the GAC isoform of the KGA protein.

The nucleotide sequences for the pGAC and rGAC cDNAs have been deposited in the GenBank under accession numbers AF490841 and AY083459, respectively.

This work was supported, in part, by National Institute of Diabetes and Digestive and Kidney Diseases Grant DK-37124.

REFERENCES

1. **Aledo JC, Gomez-Fabre PM, Olalla L, and Marquez J.** Identification of two human glutaminase loci and tissue-specific expression of the two related genes. *Mamm Genome* 11: 1107–1110, 2000.
2. **Aledo JC, Rosado A, Olalla L, Campos JA, and Marquez J.** Overexpression, purification, and characterization of glutaminase-interacting protein, a PDZ-domain protein from human brain. *Protein Expr Purif* 23: 411–418, 2001.
3. **Amasino RM.** Acceleration of nucleic acid hybridization by polyethylene glycol. *Anal Biochem* 152: 304–307, 1986.
4. **Chomczynski P and Sacchi N.** Single-step method of RNA isolation by acid guanidinium thiocyanate-phenol-chloroform extraction. *Anal Biochem* 162: 156–159, 1987.
5. **Chung-Bok MI, Vincent N, Jhala U, and Watford M.** Rat hepatic glutaminase: identification of the full coding sequence and characterization of a functional promoter. *Biochem J* 324: 193–200, 1997.
6. **Curthoys NP and Lowry OH.** The distribution of glutaminase isoenzymes in the various structures of the nephron in normal, acidotic and alkalotic rat kidney. *J Biol Chem* 248: 162–167, 1973.
7. **Curthoys NP and Gstraunthaler G.** Mechanism of increased renal gene expression during metabolic acidosis. *Am J Physiol Renal Physiol* 281: F381–F390, 2001.
8. **Elgadi KM, Meguid RA, Qian M, Souba WW, and Abcouwer SF.** Cloning and analysis of unique human glutaminase isoforms generated by tissue-specific alternative splicing. *Physiol Genomics* 1: 51–62, 1999.
9. **Elgadi KM, Souba WW, and Abcouwer SF.** Evidence for a new glutaminase isoenzyme in rat tissues. *Surg Forum* 44: 52–54, 1988.
10. **Feinberg AP and Vogelstein B.** A technique for radiolabeling DNA restriction endonuclease fragments to high specific activity. *Anal Biochem* 137: 266–267, 1984.
11. **Good DW and Burg MB.** Ammonia production by individual segments of the rat nephron. *J Clin Invest* 73: 602–610, 1984.
12. **Gstraunthaler G and Handler JS.** Isolation, growth and characterization of a gluconeogenic strain of renal cells. *Am J Physiol Cell Physiol* 252: C232–C238, 1987.
13. **Gstraunthaler G, Holcomb T, Feifel E, Liu W, Spitaler N, and Curthoys NP.** Differential expression and acid-base regulation of glutaminase mRNAs in gluconeogenic LLC-PK_1-FBPase$^+$ cells. *Am J Physiol Renal Physiol* 278: F227–F237, 2000.
14. **Hansen WR, Barsic-Tress N, Taylor L, and Curthoys NP.** The 3′-nontranslated region of the rat renal glutaminase mRNA contains a pH-responsive stability element. *Am J Physiol Renal Fluid Electrolyte Physiol* 271: F126–F131, 1996.
15. **Holcomb T, Taylor L, Trohkimoinen J, and Curthoys NP.** Isolation, characterization and expression of a human brain mitochondrial glutaminase cDNA. *Mol Brain Res* 76: 56–63, 2000.
16. **Hwang JJ and Curthoys NP.** Effect of acute alterations in acid-base balance on rat renal glutaminase and phosphoenolpyruvate carboxykinase gene expression. *J Biol Chem* 266: 9392–9396, 1991.
17. **Hwang JJ, Perera S, Shapiro RA, and Curthoys NP.** Mechanism of altered renal glutaminase gene expression in response to chronic acidosis. *Biochemistry* 30: 7522–7526, 1991.
18. **Laterza OF and Curthoys NP.** Specificity and functional analysis of the pH-responsive element within renal glutaminase mRNA. *Am J Physiol Renal Physiol* 278: F970–F977, 2000.
19. **Laterza OF and Curthoys NP.** Effect of acidosis on properties of the glutaminase mRNA pH-response element binding protein. *J Am Soc Nephrol* 11: 1583–1588, 2000.
20. **Laterza OF, Hansen WR, Taylor L, and Curthoys NP.** Identification of an mRNA-binding protein and the specific elements that may mediate the pH-responsive induction of renal glutaminase mRNA. *J Biol Chem* 272: 22481–22488, 1997.
21. **MacDonald CC and Williams DL.** RNase H/oligonucleotide-directed mRNA purification (ROMP) of ApoII mRNA. *Nucleic Acids Res* 21: 765–766, 1993.
22. **Olalla L, Aledo JC, Bannenberg G, and Marquez J.** The C-terminus of human glutaminase L mediates association with PDZ domain-containing proteins. *FEBS Lett* 488: 116–122, 2001.
23. **Perera S, Chen TC, and Curthoys NP.** Biosynthesis and processing of renal mitochondrial glutaminase in cultured proximal tubules epithelial cells and in isolated mitochondria. *J Biol Chem* 265: 17764–17770, 1990.
24. **Porter D and Curthoys NP.** Use of thermostable and *Escherichia coli* RNase H in RNA mapping studies. *Anal Biochem* 247: 279–286, 1997.
25. **Porter D, Hansen WR, Taylor L, and Curthoys NP.** Differential expression of multiple glutaminase mRNAs in LLC-PK_1-F^+ cells. *Am J Physiol Renal Fluid Electrolyte Physiol* 269: F363–F373, 1995.
26. **Sajo IM, Goldstein MB, Sonnenberg H, Stinebaugh BJ, Wilson DR, and Halperin ML.** Sites of ammonia addition to tubular fluid in rats with chronic metabolic acidosis. *Kidney Int* 20: 353–358, 1981.
27. **Shapiro RA, Farrell L, Srinivasan M, and Curthoys NP.** Isolation, characterization, and in vitro expression of a cDNA that encodes the kidney isoenzyme of the mitochondrial glutaminase. *J Biol Chem* 266: 18792–18796, 1991.
28. **Shapiro RA, Haser WG, and Curthoys NP.** The orientation of phosphate-dependent glutaminase on the inner membrane of rat renal mitochondria. *Arch Biochem Biophys* 243: 1–7, 1985.
29. **Squires EJ, Hall DE, and Brosnan JT.** Arteriovenous differences for amino acids and lactate across kidneys of normal and acidic rats. *Biochem J* 160: 125–128, 1976.
30. **Tang A and Curthoys NP.** Identification of ζ-crystallin/NADPH:quinone reductase as a renal glutaminase mRNA pH-response element binding protein. *J Biol Chem* 276: 21375–21380, 2001.
31. **Tong J, Harrison G, and Curthoys NP.** The effect of metabolic acidosis on the synthesis and turnover of rat renal phosphate-dependent glutaminase. *Biochem J* 233: 139–144, 1986.
32. **Tong J, Shapiro RA, and Curthoys NP.** Changes in the levels of translatable glutaminase mRNA during onset and recovery from metabolic acidosis. *Biochemistry* 26: 2773–2777, 1987.
33. **Wright PA and Knepper MA.** Phosphate-dependent glutaminase activity in rat renal cortical and medullary tubule segments. *Am J Physiol Renal Fluid Electrolyte Physiol* 259: F961–F970, 1990.

Role of deadenylation and AUF1 binding in the pH-responsive stabilization of glutaminase mRNA

Jill M. Schroeder, Hend Ibrahim, Lynn Taylor and Norman P. Curthoys

Am J Physiol Renal Physiol 290:733-740, 2006. First published Oct 11, 2005;
doi:10.1152/ajprenal.00250.2005

AJP - Renal Physiology publishes original manuscripts on a broad range of subjects relating to the kidney, urinary tract, and their respective cells and vasculature, as well as to the control of body fluid volume and composition. It is published 12 times a year (monthly) by the American Physiological Society, 9650 Rockville Pike, Bethesda MD 20814-3991. Copyright © 2005 by the American Physiological Society. ISSN: 0363-6127. ESSN: 1522-1466. Visit our website at http://www.the-aps.org/.

Am J Physiol Renal Physiol 290: F733–F740, 2006.
First published October 11, 2005; doi:10.1152/ajprenal.00250.2005.

Role of deadenylation and AUF1 binding in the pH-responsive stabilization of glutaminase mRNA

Jill M. Schroeder, Hend Ibrahim, Lynn Taylor, and Norman P. Curthoys

Department of Biochemistry and Molecular Biology, Colorado State University, Fort Collins, Colorado

Submitted 14 June 2005; accepted in final form 11 October 2005

Schroeder, Jill M., Hend Ibrahim, Lynn Taylor, and Norman P. Curthoys. Role of deadenylation and AUF1 binding in the pH-responsive stabilization of glutaminase mRNA. *Am J Physiol Renal Physiol* 290: F733–F740, 2006. First published October 11, 2005; doi:10.1152/ajprenal.00250.2005.—During chronic metabolic acidosis, increased expression of renal glutaminase (GA) results from selective stabilization of the GA mRNA. This response is mediated by a direct repeat of an 8-base adenylate-uridylate (AU) sequence that binds ζ-crystallin and functions as a pH response element (pH-RE). A tetracycline-responsive promoter system was developed in LLC-PK_1-F^+ cells to perform pulse-chase analysis of the turnover of a chimeric β-globin (βG) mRNA that contains 960 bp of the 3′-UTR of GA mRNA including the pH-RE. The βG-GA mRNA exhibits a 14-fold increase in half-life when the LLC-PK_1-F^+ cells are transferred to acidic medium. RNase H cleavage and Northern blot analysis of the 3′-ends established that rapid deadenylation occurred concomitantly with the rapid decay of the βG-GA mRNA in cells grown in normal medium. Stabilization of the βG-GA mRNA in acidic medium is associated with a pronounced decrease in the rate of deadenylation. Mutation of the pH-RE within the βG-GA mRNA blocked the pH-responsive stabilization, but not the rapid decay, whereas insertion of only a 29-bp segment containing the pH-RE was sufficient to produce both a rapid decay and a pH-responsive stabilization. Various kidney cells express multiple isoforms of AUF1, an AU-binding protein that enhances mRNA turnover. RNA gel-shift assays demonstrated that the recombinant p40 isoform of AUF1 binds to the pH-RE with high affinity and specificity. Thus AUF1 may mediate the rapid turnover of the GA mRNA, whereas increased binding of ζ-crystallin during acidosis may inhibit degradation and result in selective stabilization.

renal ammoniagenesis; metabolic acidosis; posttranscriptional regulation

AS PART OF THE ADAPTIVE RESPONSE to metabolic acidosis, renal extraction and catabolism of plasma glutamine are rapidly increased (3). This adaptation results in a large increase in the renal synthesis of ammonium and bicarbonate ions. The ammonium ions are preferentially excreted in the urine where they provide an expendable cation that facilitates the excretion of acidic anions. In contrast, the bicarbonate is added to the renal venous blood to partially compensate for the systemic acidosis. Renal catabolism of glutamine is initiated by a phosphate-activated mitochondrial glutaminase (5). During chronic acidosis, increased catabolism of glutamine is sustained, in part, by an 8- to 20-fold increase in the level of the mitochondrial glutaminase that occurs solely within the proximal convoluted tubule (4, 36).

During acidosis, the increased synthesis of the renal glutaminase (GA) protein (29) occurs without increasing the rate of transcription of the GA mRNA (14, 15). Experiments that characterized the half-life of a chimeric β-globin-glutaminase (βG-GA) mRNA in LLC-PK_1-F^+ cells, a pH-responsive line of porcine proximal tubule-like cells (11), established that the 3′-untranslated region (3′-UTR) of the GA mRNA contains a pH-responsive instability element (12). RNA gel-shift analysis demonstrated the presence of a protein in rat renal cortical cytosolic extracts that binds to the 3′-UTR of the GA mRNA with high affinity and specificity (20). This binding interaction was mapped to a direct repeat of an 8-base AU sequence. Functional studies established that this sequence was both necessary and sufficient to impart a pH-responsive stabilization to a chimeric βG mRNA (21). Subsequent studies identified ζ-crystallin/NADPH quinone reductase as the primary protein in rat renal extracts that binds to the pH response element (pH-RE) (28).

The rapid degradation of mammalian mRNAs is frequently initiated by the binding of proteins (25) that recruit a poly(A)-specific ribonuclease (9) and the exosome (30) to remove the poly(A) tail and accomplish a rapid 3′→5′ exonucleolytic degradation, respectively. In the current study, a tetracycline-responsive promoter (23) was used to perform a pulse-chase analysis of the decay of newly synthesized βG-GA mRNA. The resulting data demonstrate that the pH-responsive stabilization of the βG-GA mRNA is associated with a proportional decrease in the rate of deadenylation. Additional studies established that recombinant AUF1, an AU-binding protein that enhances mRNA turnover (32), also binds to the pH-RE with high affinity and specificity. Therefore, the enhanced binding of ζ-crystallin to this site during acidosis (18) may block AUF1 binding and prevent the AUF1-mediated deadenylation and degradation of the GA mRNA.

MATERIALS AND METHODS

Materials. Male Sprague-Dawley rats were purchased from Charles River. [α-^{32}P]dCTP (specific activity 3,000 Ci/mmol) was purchased from MP Biomedicals or Amersham Pharmacia Biotechnology. The animal protocols used in this study were received and approved by The University Animal Care and Use Committee as protocol 93-25DA-12. The oligolabeling kit was from Ambion. Restriction enzymes, RNase T1, T7 RNA polymerase, and yeast tRNA were acquired from Roche, New England Biolabs and MBI Fermentas. RNase H was purchased from Epicentre Technologies. GENECLEAN kits were obtained from Bio101. The pCRScript cloning kit was obtained from Stratagene. Micro Bio-spin columns and chemicals for acrylamide gels were purchased from Bio-Rad. RNasin was obtained from Promega. DMEM/F12 medium, Geneticin (G418), and hygromycin B were products of Sigma and Mediatech. A polyclonal antibody vs. AUF1 was obtained from Upstate. An expression plas-

Address for reprint requests and other correspondence: N. P. Curthoys, Dept. of Biochemistry and Molecular Biology, Colorado State Univ., Campus Delivery 1870, Fort Collins, CO 80523-1870 (e-mail: Norman.Curthoys@ColoState.edu).

The costs of publication of this article were defrayed in part by the payment of page charges. The article must therefore be hereby marked "*advertisement*" in accordance with 18 U.S.C. Section 1734 solely to indicate this fact.

mid that encodes the p40 isoform of AUF1 was obtained from Dr. J. Wilusz. All other biochemicals were acquired from Sigma.

Synthesis of pTRE2 constructs. pTRE2 (Clontech) contains a tetracycline-responsive element (TRE) that includes seven direct repeats of a 42-bp sequence containing the tet operator positioned upstream of a minimal CMV promoter, a multicloning site, and the 3′-coding and 3′-untranslated regions of the rabbit β-globin gene. pTRE2 was digested with *MluI* and *SapI* to remove the β-globin sequence. A segment of pβG-GA (12) containing the β-globin coding region, 960 bp of the GA 3′-UTR, and a segment of the bovine growth hormone (bGH) 3′-untranslated region containing the polyadenylation site was PCR amplified with primers containing unique *MluI* and *SapI* restriction sites. This fragment was cloned into pCR-Script SK(+) at the *SrfI* site, amplified, and then ligated into the pTRE2 fragment to create pTRE2-βG-GA. The pβG and pβG-GA(R2-I) plasmids (27) were digested with *CelII* and *XbaI* and the isolated fragments were inserted into pTRE2-βG-GA that had been digested with *CelII* and *XbaI*. This procedure removed the GA 3′-UTR or replaced it with a 29-bp sequence containing the pH response element, respectively. The pβG-mGA plasmid (19) was digested with *NheI* and *NotI* and the isolated fragment was inserted into pTRE2-βG-GA that had been digested with *NheI* and *NotI* to produce a construct containing the GA 3′-untranslated region in which the pH response element was mutated to include GC bases.

Selection of stable cell lines. LLC-PK_1-F′ cells (11) were grown in a 50:50 mixture of DMEM and Ham's F-12 medium containing 5 mM glucose and 10% fetal bovine serum at 37°C in a 5% CO_2 atmosphere. Normal medium (pH 7.4) contained 25 mM sodium bicarbonate, whereas acidic medium (pH 6.9) contained 10 mM sodium bicarbonate supplemented with 15 mM sodium chloride to maintain an equivalent osmolarity and sodium ion concentration. Clonal lines of LLC-PK_1-F^+ cells that stably express the tTA protein were produced by calcium phosphate transfection (1) of 3-day postsplit cells with the pTet-off plasmid and selection with medium containing 0.8 mg/ml G418. After 14–21 days, colonies were selected and expanded in medium containing 0.2 mg/ml G418. The expanded cell lines were grown for 3 days on six-well plates using medium containing 1 μg/ml doxycycline (Dox) and then transiently transfected with pTRE2-Luc. Approximately 16 h later, the medium was replaced with fresh medium with or without 1 μg/ml Dox and the cells were cultured for an additional 32 h. Cell extracts were prepared and assayed using the reagents contained in the Luciferase Assay System (Promega). The firefly luciferase activities obtained for the various stable Tet-Off clonal lines were standardized per microgram of protein (24). The fold-induction of the TRE2-Luc gene was calculated as the mean of the ratio of the specific luciferase activities measured in triplicate cultures grown in the absence and presence of Dox.

Clonal cell lines that stably express the various βG-GA constructs were prepared by cotransfection of LLC-PK_1-F^+ cells that express the tTA protein with the appropriate TRE2 plasmid and pcDNA3.1/Hygro (Invitrogen). At 48 h posttransfection, selection medium containing 0.2 mg/ml G418 and 0.8 mg/ml hygromycin was added. After 14–21 days, individual colonies were isolated and expanded. The cell lines were tested for responsiveness by growing the cells for 48 h in the presence or absence of 0.5 μg/ml Dox, a tetracycline analog. Total RNA was harvested and analyzed by Northern blotting.

Half-life analysis. For pulse-chase analysis, the stably transfected LLC-PK_1-F^+ cells were split 1:10 and grown for 5–7 days in normal medium containing 0.2 mg/ml G418 and 0.2 mg/ml hygromycin B. The cells were then grown for 48 h in pH 7.4 or 6.9 medium containing antibiotics and 25 ng/ml Dox. The cells were washed two times with phosphate-buffered saline and incubated in normal or acidic medium with antibiotics but without Dox for 3 h to create a transcriptional pulse. Then, fresh medium containing antibiotics and 1 μg/ml Dox was added and total RNA was isolated at 0, 3, 6, and 9 h using the TRIzol reagent (Invitrogen). Control cells were grown for 48 h in the presence or absence of Dox. Alternatively, the stably transfected LLC-PK_1-F^+ cells were grown for 5–7 days and then maintained in normal or acidic medium minus Dox for 24 h. Subsequently, 1 μg/ml Dox was added to each plate and total RNA was isolated at 0, 3, 6, and 9 h post-Dox addition. Control plates containing no Dox were harvested at 0 and 9 h.

Northern blot analysis. A 507-bp fragment of rabbit β-globin cDNA was excised by restricting pRSV-βG (10) with *HindIII* and *BglII*. A 2.0-kb fragment of the 18 S ribosomal RNA cDNA from *Acanthamoeba castellanii* was obtained by restricting pAr2 (6) with *HindIII* and *EcoRI*. A 228-bp bGH fragment was excised from pCRScript-bGH with *SphI*. The fragments were separated on 1% agarose gels, excised, and purified using the GENECLEAN kit. The synthesis of oligolabeled cDNA probes and Northern blot analysis was performed as described previously (27). The blots were exposed to a PhosphorImager screen and quantified using Molecular Dynamics Software. The level of the chimeric β-globin mRNA was divided by the level of the corresponding 18S rRNA to correct for errors in sample loading. The log of normalized data was then plotted vs. the time of addition of Dox.

RNase H treatment. A 26-nt deoxyoligonucleotide (GA oligo), which is complementary to the 3′-end of the GA sequence encoded by pTRE2-βG-GA (bp 2514–2539 of the GA cDNA), was synthesized by Macromolecular Resources (Fort Collins, CO). The sequence of the GA oligo is 5′-GACCGACAGCTACACACCACAGAGAG-3′. A 30-mer of oligo dT deoxyoligonucleotide was used to degrade the poly(A) tail of the mRNA. RNA samples, which were stored in Formazol, were precipitated with 4 vol of ethanol and a final concentration of 0.2 M sodium chloride and resuspended in 25 μl of DEPC-treated water. RNase H treatment was performed as described previously (26). Briefly, 10 μg RNA, 1.0 μl containing 50 pmol of GA oligo, and 1.0 μl containing 50 pmol of oligo-dT (if needed) in 12.5 μl were incubated at 55°C for 1 min. Next, 1.5 μl of 10× RNase H buffer (0.5 M Tris, pH 7.4, 1.0 M NaCl, 20 mM $MgCl_2$, and 10 mM dithiothreitol) and 1.0 μl of freshly diluted RNase H (1 U/μl) were added and the sample was incubated at 62°C for 15 min. Then, 25 μl of denaturing buffer (20 μl Formazol, 3 μl 10× MOPS, and 6 μl 37% formaldehyde solution) were added and the mixture was incubated at 55°C for 5 min and then transferred to ice. RNase H-treated RNAs were mixed with 10 μl of an RNase H gel loading buffer (50% glycerol, 1 mM EDTA, 0.25% bromophenol blue, 0.25% xylene cyanol, and 100 μg/ml ethidium bromide) and subjected to Northern blot analysis using a 1.2% agarose gel. The blot was hybridized with the bGH probe.

Western blotting. Cytosolic extracts of rat renal cortex and of various cell lines were prepared as described previously (19). The samples were separated by electrophoresis on a 10% SDS-polyacrylamide gel, transferred to a nitrocellulose membrane, and incubated with a 1:1,000 dilution of AUF1 antibody. The membrane was then incubated with a 1:15,000 dilution of horseradish peroxidase (HRP)-conjugated secondary antibody. Images were developed with Dura reagent (Pierce Chemicals) and visualized by brief exposure to X-ray film.

RNA EMSA. ^{32}P-labeled and -unlabeled GA(R2-I) and mutated forms of GA(R2-I) RNAs were synthesized as described previously (19). An aliquot containing ~1–8 μg of rat renal cortical protein or 12.5–100 ng of recombinant AUF1 was preincubated for 10 min at room temperature in binding buffer containing 0.5% Nonidet P-40, 1 mM dithiothreiotol, 2 μg yeast t-RNA, 40 U of RNAsin, 10% glycerol, and 10–70 fmol of ^{32}P-labeled RNA. The indicated excess of unlabeled RNA was added, and the reaction mixture was incubated at room temperature for 20 min. The samples were then loaded and subjected to electrophoresis for ~2 h at 10 mA using a 90 mM Tris, 110 mM boric acid, and 2 mM EDTA running buffer. Gels were dried and exposed overnight to a PhosphorImager screen. In the antibody supershift experiments, the anti-AUF1 antibody was preincubated with the rat renal cytosolic extract for 10 min at room temperature and then for 1 h on ice before the binding buffer was added.

Statistical analyses were performed using a paired Student's *t*-test.

RESULTS

Effect of medium pH on deadenylation of βG-GA mRNA. Clonal cell lines that stably express the tTA protein, a tetracycline-responsive transcription factor, were isolated by transfection of LLC-PK_1-F^+ cells with pTet-off and selection with G418. Their Dox responsiveness was tested by transient expression of pTRE2-Luc in cells that were maintained in the presence or absence of Dox. The 8C line of LLC-PK_1-F^+ cells showed the greatest induction of luciferase activity. With the use of 0.3 μg of pTRE2-Luc DNA, they produced a 200-fold difference in luciferase activity when grown in the presence and absence of 1 μg/ml Dox. Therefore, the 8C line of LLC-PK_1-F^+ cells was used for the subsequent experiments. Clonal cell lines that stably express pTRE2-βG-GA were isolated by cotransfection of the 8C cells with pcDNA3.1/Hygro and selection with hygromycin. The isolated cell lines were tested for Dox-responsive βG-GA expression by culturing the cells in the presence or absence of Dox and quantifying βG-GA mRNA expression by Northern blot analysis. Cell lines were evaluated based on the level of βG-GA mRNA expressed in the presence of Dox and the increased expression produced by removal of Dox. The selected 8C-2A cell line exhibited a 50-fold difference in the levels of βG-GA mRNA when grown in the presence or absence of 0.5 μg/ml Dox (Fig. 1).

Previous experiments characterizing the half-lives of various βG-GA chimeric mRNAs used the Rous sarcoma virus long-terminal repeat (RSV) promoter to drive transcription (20). The level of βG-GA mRNA transcribed from the tetracycline-responsive promoter in the absence of Dox was far greater than the level of mRNA synthesized from the RSV promoter (Fig. 1). To create a level of βG-GA mRNA similar to that produced with the RSV promoter, transcription was initially inhibited by adding 25 ng/ml Dox for 48 h. Dox was then removed from the selected cells to create a pulse of transcription and RNA was isolated at various times. The level of βG-GA mRNA produced by a 3-h transcriptional pulse was comparable to the level of βG-GA mRNA produced by the RSV promoter (Fig. 1). Therefore, a 3-h transcriptional pulse should provide a level of newly synthesized and adenylated βG-GA mRNA that is sufficient to follow decay and deadenylation.

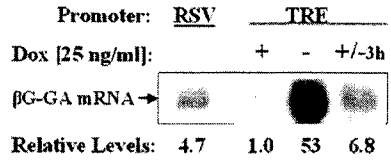

Fig. 1. Comparison of β-globin-glutaminase (βG-GA) mRNA expression from a Rous sarcoma virus (RSV) promoter and the tetracycline-responsive promoter. RNA was isolated from LLC-PK_1-F^+ cells that were stably transfected with βG-GA constructs that are driven by a RSV long-terminal repeat or a promoter containing multiple tetracycline-responsive elements (TRE). Cells expressing pTRE-βG-GA were grown in the presence (+) or absence (−) of 25 ng/ml doxycycline (Dox) for 48 h or in the presence of Dox and then maintained for 3 h in medium minus Dox (±3 h). Isolated RNAs were subjected to Northern blot analysis and the levels of βG-GA mRNA were quantified by PhosphorImager analysis. The relative levels were calculated by normalizing the data to the levels of βG-GA mRNA expressed in cells maintained in the presence of Dox for 48 h.

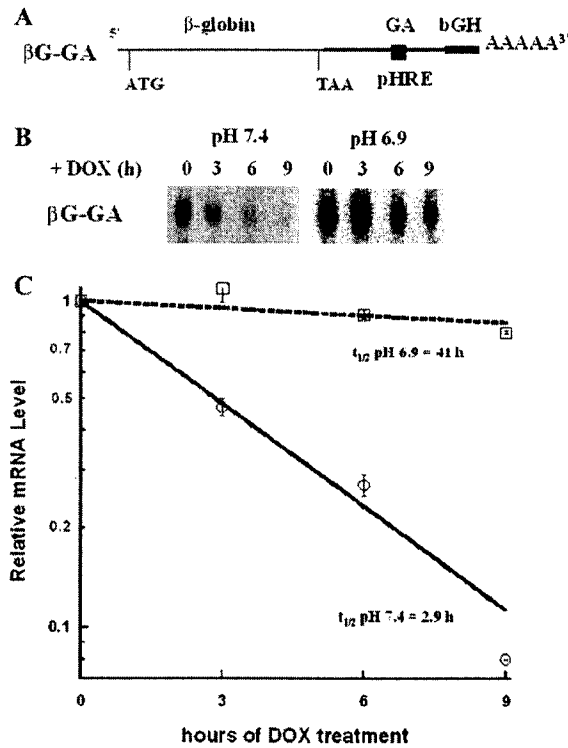

Fig. 2. Pulse-chase analysis of the half-life ($t_{1/2}$) of βG-GA mRNA. *A*: βG-GA mRNA contains the coding region of the β-globin mRNA, a 960-bp segment of 3′-UTR of the GA mRNA containing the pH response element (pHRE), and a short segment of the 3′-UTR of bovine growth hormone (bGH) mRNA that contains a polyadenylation site. *B*: Northern blot analysis of βG-GA mRNA isolated from LLC-PK_1-F^+ cells that stably express pTRE2-βG-GA. Cells were maintained in either normal (pH 7.4) or acidic (pH 6.9) medium containing 25 ng/ml Dox for 48 h. The cells were then washed with phosphate-buffered saline and incubated in medium minus Dox for 3 h to create a transcriptional pulse. RNA was isolated at 0, 3, 6, and 9 h after addition of fresh medium containing 1 μg/ml Dox. *C*: relative levels of βG-GA mRNA were determined by PhosphorImager analysis. The level of βG-GA mRNA was divided by the corresponding level of 18S rRNA to correct for errors in sample loading. The log of the normalized data was then plotted vs. time of treatment with Dox. Values are means ± SE of data obtained from 3 separate determinations. The line represents the best-fit of the data points as determined by a KaleidaGraph program that weights each data point based on its standard deviation.

To perform a pulse-chase analysis, the selected cells were maintained in normal or acidic medium containing 25 ng/ml Dox for 48 h. A 3-h pulse was created by removing Dox and then chased for 0, 3, 6, and 9 h following addition of 1 μg/ml Dox. The half-life of βG-GA mRNA in cells cultured in normal medium was 2.9 h. However, when the cells were maintained in acidic conditions, the βG-GA mRNA was significantly stabilized and now decayed with a half-life of ~40 h (Fig. 2). An oligonucleotide (GA oligo), which specifically hybridizes to the 3′-end of the GA sequence, was used along with RNase H to cleave the βG-GA mRNA and to produce a short 3′-fragment (Poly A^+) that contains the poly(A) tail (Fig. 3*A*). Oligo(dT) was also added to an aliquot of the zero-time RNA sample to remove the poly(A) tail from the βG-GA

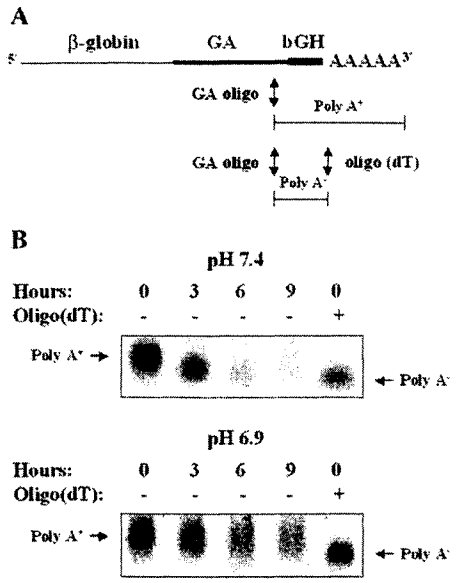

Fig. 3. Effect of medium pH on deadenylation of βG-GA mRNA. *A*: treatment of βG-GA mRNA with RNase H in the presence of the GA oligo produces a 3′-fragment (Poly A^+) that contains 330 nt plus the poly(A) tail. When oligo(dT) was also added, a fully deadenylated 330-nt RNA fragment is produced (Poly A^-). *B*: RNAs isolated from cells grown in normal (pH 7.4) or acidic (pH 6.9) medium and analyzed in Fig. 2 were treated with RNase H and the GA oligo in the absence (−) or presence (+) of oligo(dT). The resulting 3′-fragments were quantified by Northern analysis using a ^{32}P-labeled cDNA that specifically hybridizes to the segment of bGH contained in the 3′-fragments.

mRNA, creating a 330-nt deadenylated RNA fragment (Poly A^-). The 3′-fragments were detected by Northern blot analysis using a ^{32}P-labeled cDNA probe that specifically hybridizes to the bGH sequence within the 3′-end of the βG-GA mRNA.

The adenylated and the fully deadenylated RNA fragments were easily resolved, making it feasible to monitor the extent of deadenylation of the βG-GA mRNA. The 3′-ends of the βG-GA mRNAs harvested from cells maintained in normal medium appear to exhibit a synchronous or nonprocessive pattern of deadenylation (Fig. 3*B*). However, the 3′-fragments containing the shortened poly(A) tail decay at a rate similar to that observed with the full-length mRNA. If complete removal of the poly(A) is required to initiate decay, then a portion of the βG-GA mRNA must undergo a more rapid and processive deadenylation to form a transient, but fully deadenylated, intermediate that is rapidly degraded and does not accumulate. As a result, the synchronous deadenylation of the βG-GA mRNAs would appear to occur concomitantly with the decay of the body of the chimeric mRNA. When the cells were treated with acidic medium, the rates of synchronous deadenylation (formation of shorter 3′-fragments) and processive deadenylation (decay of 3′-fragments) of the βG-GA mRNA were significantly inhibited. Therefore, the pH-responsive stabilization correlates with a decrease in both the rate and the extent of deadenylation of the βG-GA mRNA.

Functional analysis of the pH-RE. As reported previously (20), the chimeric β-globin mRNA lacking sequence from the GA 3′-UTR is extremely stable. However, the insertion of a 29-bp segment containing the pH-RE is sufficient to create a labile mRNA that decayed with a half-life of 3.0 h in LLC-PK_1-F^+ cells that were maintained in normal medium (Fig. 4). When transferred to acidic medium, the βG-GA(R2-I) mRNA decayed with a half-life of ~17 h. Thus this segment functions both as an instability element and as a pH-RE. In contrast, the βG-mGA mRNA, which contains the GA 3′-UTR in which the AU-rich pH-RE was mutated to the Mut3 sequence shown in Fig. 8*A*, is degraded rapidly in cells that are grown in either normal or acidic medium (Fig. 5). Thus the 3′-UTR must contain multiple instability elements that contribute to the rapid turnover of the GA mRNA.

Binding of AUF1 to the pH-RE. AUF1 binds to various AU-rich elements (AREs) and enhances the mRNA degradation (32). Previous studies (19, 27) demonstrated that GA(R2-I), a 29-bp RNA segment that contains the pH-RE and surrounding sequence within the GA mRNA, forms a specific complex when incubated with a cytosolic extract of rat kidney

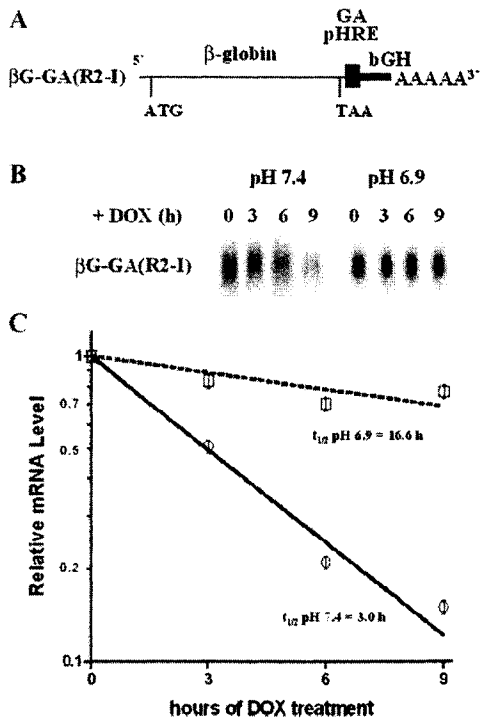

Fig. 4. Half-life analysis of βG-GA(R2-I) mRNA. *A*: βG-GA(R2-I) mRNA contains the coding region of the β-globin mRNA, a 29-bp segment of 3′-UTR of the GA mRNA containing the pHRE, and a short segment of the 3′-UTR of bGH mRNA that contains a polyadenylation site. *B*: Northern blot of RNA isolated from cells that stably express the pTRE-βG-GA(R2-I) construct. Cells were cultured in normal or acidic medium in the absence of Dox for 48 h and then transferred to media containing 1 μg/ml Dox. RNA was isolated at various times after addition of Dox and probed for βG-GA(R2-I) mRNA and 18S rRNA. *C*: level of βG-GA(R2-I) mRNA was divided by the corresponding level of 18S rRNA to correct for errors in sample loading. The log of the normalized data was then plotted vs. time of treatment with Dox. Values are means ± SE of data obtained from 3 separate determinations. The line represents the best-fit of the data points as determined by a KaleidaGraph program that weights each data point based on its standard deviation.

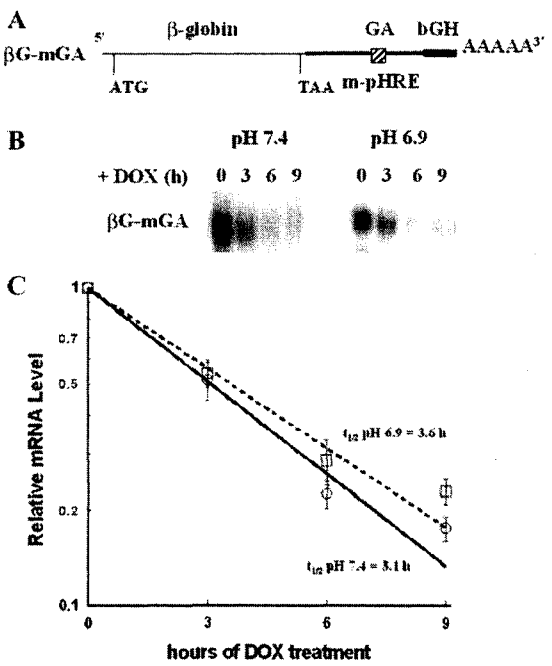

Fig. 5. Half-life analysis of βG-mGA mRNA. *A*: βG-mGA mRNA contains the coding region of the β-globin mRNA, a 960-bp segment of 3′-UTR of the GA mRNA in which the pHRE was mutated to the Mut3 sequence shown in Fig. 8 (m-pHRE), and a short segment of the 3′-UTR of bGH mRNA that contains a polyadenylation site. *B*: Northern analysis of RNA isolated from cells that stably express the pTREβG-mGA construct. Cells were cultured in normal or acidic medium in the absence of Dox for 48 h and then transferred to media containing 1 μg/ml Dox. RNA was isolated at various times after addition of Dox and probed for βG-mGA mRNA and 18S rRNA. *C*: level of βG-mGA mRNA was divided by the corresponding level of 18S rRNA to correct for errors in sample loading. The log of the normalized data was then plotted vs. time of treatment with Dox. Values are means ± SE of data obtained from 3 separate determinations. The line represents the best-fit of the data points as determined by a KaleidaGraph program that weights each data point based on its standard deviation.

cortex. Preincubation of the cytosolic extract with AUF1-specific antibodies results in the reproducible formation of a complex that exhibits a slightly slower electrophoretic mobility (Fig. 6*A*). No shift was observed when the cytosolic extract was preincubated with an equivalent amount of an unrelated antibody (data not shown). The observed shift suggests that AUF1 may bind to the GA(R2-I) RNA. Western blot analysis was performed to determine whether AUF1 is expressed in rat kidney cortex and in various proximal tubule cell lines (Fig. 6*B*). Jurkat cell extracts were used as a positive control (17). They express the four isoforms of AUF1 (p37, p40, p42, and p45) that are produced by alternative splicing of the initial AUF1 transcript (31). Rat kidney cortex contains significant levels of the p37, p40, and p42 isoforms of AUF1, whereas the LLC-PK$_1$-F$^+$ and WKPT (13) proximal tubule cells express differing amounts of the four isoforms.

The p40 AUF1 isoform is predominantly cytoplasmic (37) and hence was utilized in the following binding experiments. Increasing amounts of the purified recombinant p40 AUF1 form multiple complexes when incubated with the GA(R2-I) RNA (Fig. 7*A*). This pattern is characteristic of the fact that AUF1 forms dimers and larger oligomers on binding to AU-rich sequences (35). The observed binding of AUF1 is competed by increasing concentrations of unlabeled GA(R2-I) RNA, but not by a nonspecific RNA segment (pBSSK) that was transcribed from the multicloning site of pBluescript-SK(−) (Fig. 7*B*). Thus the observed binding interaction is specific. The complexes formed between AUF1 and the GA(R2-I) RNA are similar to those observed when AUF1 is incubated with a short RNA that contains the canonical AUUUA element (Fig. 8). AUF1 also binds to GA(R2-I) segments in which one of the two AU sequences is mutated to contain GC-nucleotides (Mut1 and Mut2). However, AUF1 does not bind to an GA(R2-I) segment in which both AU sequences are mutated (Mut3).

Scatchard analysis was performed to determine the dissociation constant (K_d) for AUF1 binding to the GA(R2-I) RNA. When 80 ng of recombinant AUF1 were incubated with 70 fmol of ^{32}P-labeled R-2I RNA, approximately one-third of the labeled probe formed a complex (Fig. 9*A*). The intensity of the shifted band decreased as the amount of unlabeled R-2I RNA was increased. The relative intensities of the bands that correspond to the bound and free probe were quantified by PhosphorImager analysis. These data along with the knowledge of the concentration of total probe in each sample were then used to calculate the concentrations of bound and free probe. The resulting values were plotted in the form of a Scatchard plot

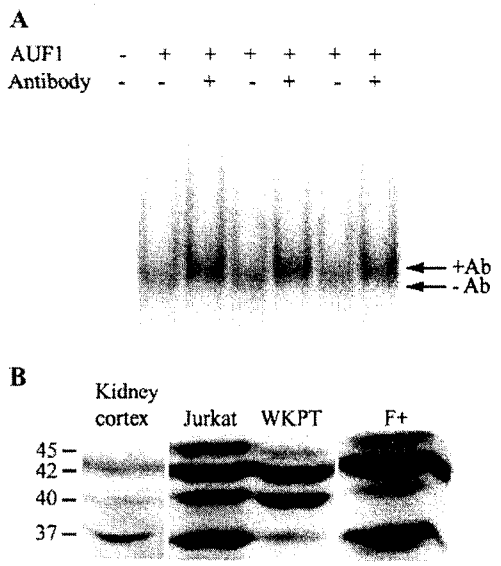

Fig. 6. Presence of AUF1 in kidney cell extracts. *A*: RNA gel-shift analysis of ^{32}P-GA(R2-I) RNA binding to a cystolic extract of rat kidney cortex. The kidney extract was preincubated in the absence (−) and presence (+) of AUF1-specific antibodies before addition of ^{32}P-GA(R2-I) RNA. The resulting complexes were subjected to nondenaturing polyacrylamide gel electrophoresis and visualized with a PhosphorImager. The arrows indicate the positions of the complexes that are formed in the presence (+Ab) and absence (−Ab) of AUF1 antibody. *B*: Western blot analysis of cytosolic extracts. Samples containing 20 μg of cytosolic proteins isolated from rat kidney cortex, from Jurkat cells, and from LLC-PK$_1$-F$^+$ and WKPT cells, porcine and rat renal proximal tubule-like cell lines, respectively, were fractionated on a 10% SDS-polyacrylamide gel and then probed with AUF1-specific antibodies.

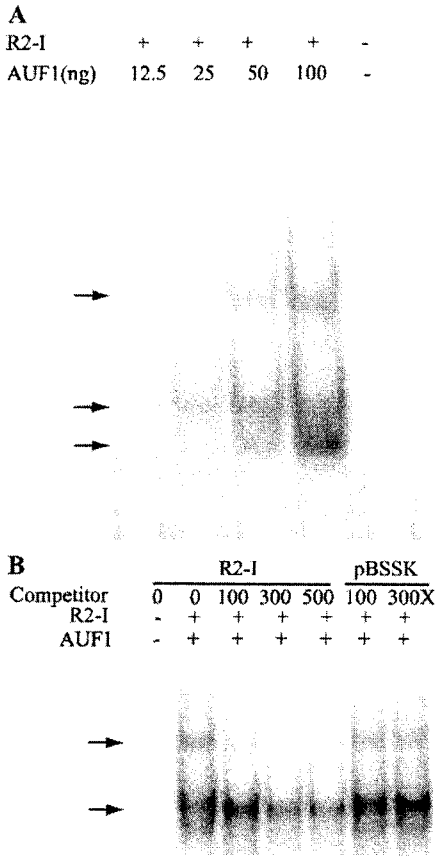

Fig. 7. Binding of recombinant AUF1 to GA(R2-I) RNA. *A*: ^{32}P-GA(R2-I) RNA was incubated with the indicated ng amounts of purified recombinant p40 AUF1. *B*: competition analysis was performed by incubating ^{32}P-GA(R2-I) RNA and recombinant p40 AUF1 in the absence and presence of the indicated fold-excess of unlabeled GA(R2-I) RNA or a nonspecific RNA transcribed from pBluescript-SK(-) (pBSSK). In both experiments, the resulting complexes were separated on a nondenaturing polyacrylamide gel and visualized with a PhosphorImager. The arrows indicate the positions of the protein/RNA complexes.

(Fig. 9*B*). Linear regression analysis of the plotted data indicated that the recombinant AUF1 binds the GA(R2-I) RNA with a K_d of ~2 μM.

DISCUSSION

A tetracycline-responsive expression (Tet-off) system (23) was used to characterize the potential role of deadenylation in the degradation of the GA mRNA. With this system, it is feasible to inhibit the synthesis of a single mRNA through the addition of a nontoxic level of Dox, instead of using 5–6 dichloro-1-β-ribofuranosylbenzimidazole (DRB), a general inhibitor of pol II transcription. Thus this approach avoids potential nonspecific effects that may be caused by the rapid decay of regulatory proteins or nucleases that participate in mRNA turnover. As a result, this protocol should also provide a more accurate quantification of the half-life of a mRNA.

When fully induced, the tetracycline-responsive promoter produced a significantly greater level of βG-GA mRNA than observed in previous experiments that used an RSV promoter to drive the synthesis of the reporter mRNA (12, 19). To avoid expression of very high levels of βG-GA mRNA that might exceed the amount of ζ-crystallin and/or other factors needed to accomplish a pH-responsive stabilization, a pulse-chase protocol was used to characterize the turnover of the βG-GA mRNA. With the use of this protocol, the levels of newly synthesized βG-GA mRNA were similar to those produced constitutively from the RSV promoter. None of the cell lines selected for stable expression of the βG-GA(R2-I) or βG-mGA mRNA produced the same rapid and pronounced increase, during a 3-h pulse, as observed with the 8C-2A line that expresses the βG-GA mRNA. As a result, it was not feasible to perform pulse-chase analysis with the truncated or mutated construct. However, the fully induced levels of the βG-GA(R2-I) and βG-mGA mRNAs were similar to that produced following a 3-h pulse of the βG-GA mRNA (data not shown). Thus all of the half-life analyses were performed using a similar level of expression of the reporter mRNA.

Using the pulse-chase protocol, the βG-GA mRNA was degraded with a half-life of 2.9 h in LLC-PK$_1$-F$^+$ cells that were maintained in normal medium and a 14-fold stabilization was observed when the cells were transferred to an acidic medium. In the previous study that used DRB to inhibit transcription, a half-life of 5.8 h and a 2.5-fold pH-responsive stabilization were observed for this construct (19). Therefore, data obtained using this less intrusive protocol both confirm and refine the previous conclusions that the 3′-UTR of the GA mRNA contains instability elements and confers a pH-responsive stabilization of the βG-GA mRNA under acidic conditions.

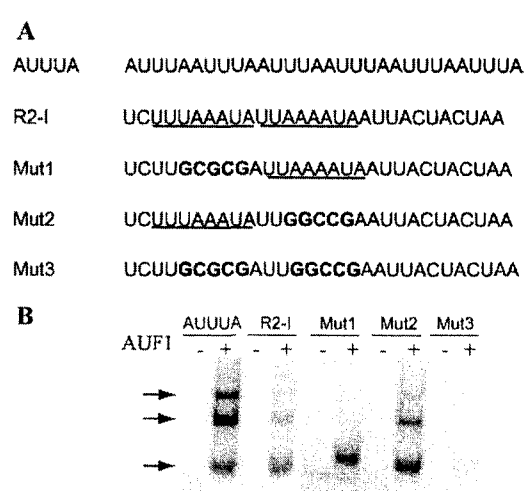

Fig. 8. Effect of mutation of the AU elements of binding of AUF1 to GA(R2-I) RNA. *A*: sequences of the AUUUA containing oligonucleotide of the GA(R2-I) RNA and the 3 mutant forms of GA(R2-I). *B*: purified recombinant p40 AUF1 was incubated with ^{32}P-labeled RNAs containing the canonical AUUUA element, the wild-type GA(R2-I) RNA, or GA(R2-I) RNAs in which the first (Mut1), second (Mut2), or both (Mut3) AU sequences were mutated to include GC-nucleotides. The resulting complexes were subjected to nondenaturing PAGE and visualized with a PhosphorImager. The arrows indicate the positions of the protein/RNA complexes.

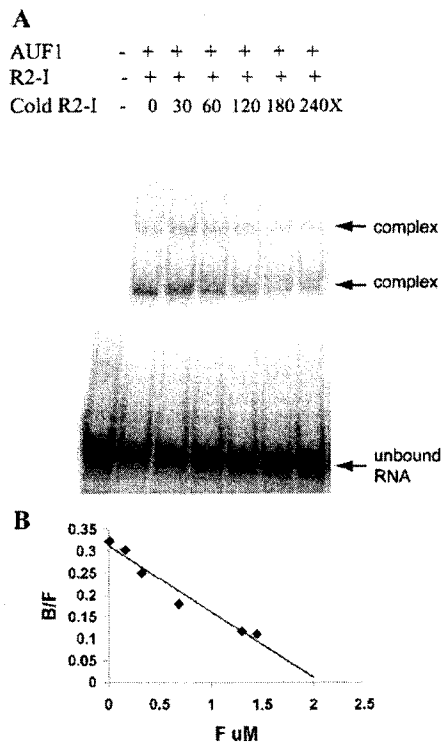

Fig. 9. Scatchard analysis of the binding of AUF1 to the GA(R2-I) RNA. *A*: samples containing 80 ng of purified recombinant p40 AUF1 and 70 fmol of ^{32}P-labeled GA(R2-I) were incubated in the presence of increasing amounts of unlabeled GA(R2-I) RNA. The resulting complexes were resolved on a nondenaturing polyacrylamide gel and imaged with a PhosphorImager. The arrows indicate the positions of the resulting complexes and the unbound RNA. *B*: relative intensities of the bands shown in *A* were quantified using ImageQuant software and the ratio of bound over free ^{32}P-labeled GA(R2-I) probe was plotted against the concentration of free probe present in each sample.

The total RNAs isolated from the transcriptional pulse analysis were also used to determine the mechanism of decay of the βG-GA mRNA. It was hypothesized that deadenylation would precede its decay as the 3′-UTR of GA contains AREs. Therefore, the isolated RNAs were incubated with a GA-specific oligonucleotide and digested with RNase H to produce a fragment of the 3′-UTR that was suitable for monitoring deadenylation (Fig. 3). Deadenylation of the βG-GA mRNA appeared to be synchronous under both normal and acidic conditions. Synchronous deadenylation is consistent with a distributive or nonprocessive ribonucleolytic removal of the poly(A) tail. Synchronous deadenylation has been observed in mRNAs containing both class I or class III ARE (2). Because the GA pH-RE lacks the canonical AUUUA sequence, it would be classified as a class III ARE. Thus the observation of distributive deadenylation by the βG-GA mRNA is consistent with the previous classification. However, when only synchronous deadenylation occurs, the body of the mRNA is not degraded until the mRNA is fully deadenylated. With the βG-GA mRNA, the body of the mRNA is degraded concomitant with the synchronous formation of a shortened, but not fully deadenylated poly(A) tail. Thus some of the βG-GA mRNA may undergo a more rapid, but processive, deadenylation to yield a fully deadenylated mRNA that is degraded as rapidly as it is produced. The latter process would determine the rate of turnover of the βG-GA mRNA.

When the LLC-PK$_1$-F$^+$ cells were transferred to acidic medium, both the rate and extent of deadenylation were significantly inhibited. This suggests that the factors that normally bind to the instability elements of the GA mRNA are either modified or displaced by alternative factors. As a result, the processive component of the deadenylation must be inhibited while the rate of synchronous deadenylation is also reduced significantly. Such changes in deadenylation would be sufficient to stabilize the GA mRNA. The observed changes in decay rates that were quantified with the βG-GA(R2-I) and βG-mGA mRNAs confirm the previous conclusion that the pH-RE is both sufficient and necessary to produce a pH-responsive stabilization (19). However, the observations that the βG-GA(R2-I) mRNA exhibits only a 5.5-fold stabilization, while the βG-mGA mRNA is degraded with a half-life similar to the βG-GA mRNA, strongly indicate that the 3′-UTR of the GA mRNA contains additional instability element(s) that may also participate in the pH-responsive stabilization. Additional experiments are needed to identify the remaining element(s) and the proteins that bind to these sequences.

ARE-mediated decay of mRNAs is usually proceeded by rapid deadenylation (2). AUF1 is a protein that binds to AREs within various mRNAs and enhances the rate of degradation (7, 33). Thus the observation that deadenylation occurs concomitantly with the rapid degradation of the βG-GA mRNA suggested that AUF1 may participate in this process. This hypothesis is supported by the observations that treatment with anti-AUF1 antibodies produces a slight supershift of the GA(R2-I) RNA/protein complex formed with a cytosolic extract of rat kidney and that recombinant p40 AUF1 exhibits specific binding to the pH-RE within the GA(R2-I) RNA. Analysis using the mutated GA(R2-I) RNAs indicates that a single 8-base AU-element is sufficient for AUF-1 binding. The same elements also bind ζ-crystallin with high affinity and specificity (28), suggesting that the two proteins may compete for binding. Unfortunately, the recombinant p40 AUF1 and the affinity-purified rat kidney ζ-crystallin form complexes that have identical mobility on a nondenaturing polyacryalamide gel (data not shown). Thus it was not feasible to test this hypothesis using the current RNA gel-shift protocol. However, previous studies demonstrating that AUF1 and HuR, an RNA-stabilizing protein, compete for binding to multiple AREs (16) support the feasibility of this hypothesis.

Scatchard analysis demonstrated that the interaction between recombinant p40 AUF1 and the GA(R2-I) RNA has a K_d of 2 μM. By contrast, fluorescence anisotropy measurements indicated that recombinant p40 AUF1 binds to the ARE of TNF-α mRNA with a 50-fold greater affinity (34). However, this same analysis demonstrated that phosphorylation of AUF1 affects the affinity and physical interaction between AUF1 and an ARE. With the use of Scatchard analysis, affinity-purified ζ-crystallin was also shown to bind to the GA(R2-I) RNA with a K_d of 20–40 nM (18). However, recombinant ζ-crystallin bound the GA(R2-I) RNA with an affinity similar to that of the recombinant p40 AUF1 (data not shown). Thus it will be important to determine whether the onset of acidosis alters the phosphorylation states of AUF1 and/or ζ-crystallin and

whether these changes affect their relative binding interaction with the pH-RE.

The combined observations support the following hypothesis for the mechanism by which changes in acid-base balance determine the stability of the GA mRNA. In normal acid-base balance, AUF1 preferentially binds to the pH-RE and recruits the protein complexes that account for the rapid removal of the poly(A) tail and promotes the subsequent degradation of the GA mRNA. The onset of acidosis is likely to activate a specific signaling mechanism (8, 22) that may result in covalent modification of ζ-crystallin and/or AUF1 and the preferential binding of ζ-crystallin to the pH-RE. As a result, the interaction of the deadenylase with the poly(A) tail is reduced. This results in the prolonged maintenance of the poly(A) tail and the increased stability of the GA mRNA. This hypothesis suggests numerous experiments that can be performed to further characterize the underlying mechanism and the regulation of this important adaptive response.

GRANTS

This work was supported by Public Health Service Grant DK-37124 from the National Institute of Diabetes and Digestive and Kidney Diseases.

REFERENCES

1. **Chen C and Okayama H.** High-efficiency transformation of mammalian cells by plasmid DNA. *Mol Cell Biol* 7: 2745–2752, 1987.
2. **Chen CY and Shyu AB.** AU-rich elements: characterization and importance in mRNA degradation. *Trends Biochem Sci* 20: 465–470, 1995.
3. **Curthoys NP and Gstraunthaler G.** Mechanism of increased renal gene expression during metabolic acidosis. *Am J Physiol Renal Physiol* 281: F381–F390, 2001.
4. **Curthoys NP and Lowry OH.** The distribution of glutaminase isoenzymes in the various structures of the nephron in normal, acidotic, and alkalotic rat kidney. *J Biol Chem* 248: 162–168, 1973.
5. **Curthoys NP and Watford M.** Regulation of glutaminase activity and glutamine metabolism. *Annu Rev Nutr* 15: 133–159, 1995.
6. **D'Alessio JM, Harris GH, Perna PJ, and Paule MR.** Ribosomal ribonucleic acid repeat unit of *Acanthamoeba castellanii*: cloning and restriction endonuclease map. *Biochemistry* 20: 3822–3827, 1981.
7. **DeMaria CT and Brewer G.** AUF1 binding affinity to A+U-rich elements correlates with rapid mRNA degradation. *J Biol Chem* 271: 12179–12184, 1996.
8. **Feifel E, Obexer P, Andratsch M, Euler S, Taylor L, Tang A, Wei Y, Schramek H, Curthoys NP, and Gstraunthaler G.** p38 MAPK mediates acid-induced transcription of PEPCK in LLC-PK$_1$-FBPase$^+$ cells. *Am J Physiol Renal Physiol* 283: F678–F688, 2002.
9. **Gao M, Fritz DT, Ford LP, and Wilusz J.** Interaction between a poly(A)-specific ribonuclease and the 5′ cap influences mRNA deadenylation rates in vitro. *Mol Cell* 5: 479–488, 2000.
10. **Gorman C, Padmanabhan R, and Howard BH.** High efficiency DNA-mediated transformation of primate cells. *Science* 221: 551–553, 1983.
11. **Gstraunthaler G and Handler JS.** Isolation, growth, and characterization of a gluconeogenic strain of renal cells. *Am J Physiol Cell Physiol* 252: C232–C238, 1987.
12. **Hansen WR, Barsic-Tress N, Taylor L, and Curthoys NP.** The 3′-UTR of rat renal glutaminase mRNA contains a pH-responsive stability element. *Am J Physiol Renal Fluid Electrolyte Physiol* 271: F126–F131, 1996.
13. **Hopfer U, Jacobberger JW, Gruenert DC, Eckert RL, Jat PS, and Whitsett JA.** Immortalization of epithelial cells. *Am J Physiol Cell Physiol* 270: C1–C11, 1996.
14. **Hwang JJ, Perera S, Shapiro RA, and Curthoys NP.** Mechanism of altered renal glutaminase gene expression in response to chronic acidosis. *Biochemistry* 30: 7522–7526, 1991.
15. **Kaiser S and Curthoys NP.** Effect of pH and bicarbonate on phosphoenolpyruvate carboxykinase and glutaminase mRNA levels in cultured renal epithelial cells. *J Biol Chem* 266: 9397–9402, 1991.
16. **Lal A, Mazan-Mamczarz K, Kawai T, Yang X, Martindale JL, and Gorospe M.** Concurrent versus individual binding of HuR and AUF1 to common labile target mRNAs. *EMBO J* 23: 3092–3102, 2004.
17. **Lapucci A, Donnini M, Papucci L, Witort E, Tempestini A, Bevilacqua A, Nicolin A, Brewer G, Schiavone N, and Capaccioli S.** AUF1 Is a bcl-2 A + U-rich element-binding protein involved in bcl-2 mRNA destabilization during apoptosis. *J Biol Chem* 277: 16139–16146, 2002.
18. **Laterza OF and Curthoys NP.** Effect of acidosis on the properties of the glutaminase mRNA pH-response element binding protein. *J Am Soc Nephrol* 11: 1583–1588, 2000.
19. **Laterza OF and Curthoys NP.** Specificity and functional analysis of the pH-responsive element within renal glutaminase mRNA. *Am J Physiol Renal Physiol* 278: F970–F977, 2000.
20. **Laterza OF, Hansen WR, Taylor L, and Curthoys NP.** Identification of an mRNA-binding protein and the specific elements that may mediate the pH-responsive induction of renal glutaminase mRNA. *J Biol Chem* 272: 22481–22488, 1997.
21. **Laterza OF, Taylor L, Unnithan S, Nguyen L, and Curthoys NP.** Mapping and functional analysis of an instability element in phosphoenolpyruvate carboxykinase mRNA. *Am J Physiol Renal Physiol* 279: F866–F873, 2000.
22. **Li S, Sato S, Yang X, Preisig PA, and Alpern RJ.** Pyk2 activation is integral to acid stimulation of sodium/hydrogen exchanger 3. *J Clin Invest* 114: 1782–1789, 2004.
23. **Loflin PT, Chen CY, Xu N, and Shyu AB.** Transcriptional pulsing approaches for analysis of mRNA turnover in mammalian cells. *Methods* 17: 11–20, 1999.
24. **Lowry OH, Rosebrough NJ, Farr AL, and Randall RJ.** Protein measurement with the Folin phenol reagent. *J Biol Chem* 193: 265–275, 1951.
25. **Parker RSH.** The enzymes and control of eukaryotic mRNA turnover. *Nat Struct Mol Biol* 11: 121–127, 2004.
26. **Porter D and Curthoys NP.** Use of thermostable and *Escherichia coli* RNase H in RNA mapping studies. *Anal Biochem* 247: 279–286, 1997.
27. **Schroeder JM, Liu W, and Curthoys NP.** pH-responsive stabilization of glutamate dehydrogenase mRNA in LLC-PK1-F$^+$ cells. *Am J Physiol Renal Physiol* 285: F258–F265, 2003.
28. **Tang A and Curthoys NP.** Identification of ζ-crystallin/NADPH:quinone reductase as a renal glutaminase mRNA pH response element-binding protein. *J Biol Chem* 276: 21375–21380, 2001.
29. **Tong J, Harrison G, and Curthoys NP.** The effect of metabolic acidosis on the synthesis and turnover of rat renal phosphate-dependent glutaminase. *Biochem J* 233: 139–144, 1986.
30. **Van Hoof A and Parker R.** The exosome: a proteasome for RNA? *Cell* 99: 347–350, 1999.
31. **Wagner BJ, DeMaria CT, Sun Y, Wilson GM, and Brewer G.** Structure and genomic organization of the human AUF1 gene: alternative pre-mRNA splicing generates four protein isoforms. *Genomics* 48: 195–202, 1998.
32. **Wilson GM and Brewer G.** Identification and characterization of proteins binding A + U-rich elements. *Methods* 17: 74–83, 1999.
33. **Wilson GM and Brewer G.** The search for *trans*-acting factors controlling messenger RNA decay. *Prog Nucleic Acid Res Mol Biol* 62: 257–291, 1999.
34. **Wilson GM, Lu J, Sutphen K, Suarez Y, Sinha S, Brewer B, Villanueva-Feliciano EC, Ysla RM, Charles S, and Brewer G.** Phosphorylation of p40AUF1 regulates binding to A + U-rich mRNA-destabilizing elements and protein-induced changes in ribonucleoprotein structure. *J Biol Chem* 278: 33039–33048, 2003.
35. **Wilson GM, Sun Y, Lu H, and Brewer G.** Assembly of AUF1 oligomers on U-rich RNA targets by sequential dimer association. *J Biol Chem* 274: 33374–33381, 1999.
36. **Wright PA and Knepper MA.** Phosphate-dependent glutaminase activity in rat renal cortical and medullary tubule segments. *Am J Physiol Renal Fluid Electrolyte Physiol* 259: F961–F970, 1990.
37. **Zhang W, Wagner BJ, Ehrenman K, Schaefer AW, DeMaria CT, Crater D, DeHaven K, Long L, and Brewer G.** Purification, characterization, and cDNA cloning of an AU-rich element RNA-binding protein, AUF1. *Mol Cell Biol* 13: 7652–7665, 1993.

9 REFERENCES

Ackerman, J.J., Lowry, M., Radda, G.K., Ross, B.D., and Wong, G.G. (1981). The role of intrarenal pH in regulation of ammoniagenesis: [31P]NMR studies of the isolated perfused rat kidney. J Physiol **319,** 65-79.

Aledo, J.C., Gomez-Fabre, P.M., Olalla, L., and Marquez, J. (2000). Identification of two human glutaminase loci and tissue-specific expression of the two related genes. Mamm Genome **11,** 1107-1110.

Aledo, J.C., Rosado, A., Olalla, L., Campos, J.A., and Marquez, J. (2001). Overexpression, purification, and characterization of glutaminase- interacting protein, a PDZ-domain protein from human brain. Protein Expr Purif **23,** 411-418.

Amasino, R.M. (1986). Acceleration of nucleic acid hybridization rate by polyethylene glycol. Anal Biochem **152,** 304-307.

Anderson, J.S., and Parker, R.P. (1998). The 3' to 5' degradation of yeast mRNAs is a general mechanism for mRNA turnover that requires the SKI2 DEVH box protein and 3' to 5' exonucleases of the exosome complex. Embo J **17,** 1497-1506.

Anderson, J.W. (1970). Pyruvate carboxylase and phosphoenolpyruvate carboxykinase in rat intestinal mucosa. Biochim Biophys Acta **208,** 165-167.

Antic, D., and Keene, J.D. (1997). Embryonic lethal abnormal visual RNA-binding proteins involved in growth, differentiation, and posttranscriptional gene expression. Am J Hum Genet **61,** 273-278.

Aruga, S., Wehrli, S., Kaissling, B., Moe, O.W., Preisig, P.A., Pajor, A.M., and Alpern, R.J. (2000). Chronic metabolic acidosis increases NaDC-1 mRNA and protein abundance in rat kidney. Kidney Int **58,** 206-215.

Atasoy, U., Watson, J., Patel, D., and Keene, J.D. (1998). ELAV protein HuA (HuR) can redistribute between nucleus and cytoplasm and is upregulated during serum stimulation and T cell activation. J Cell Sci **111 (Pt 21),** 3145-3156.

Bakheet, T., Frevel, M., Williams, B.R., Greer, W., and Khabar, K.S. (2001). ARED: human AU-rich element-containing mRNA database reveals an unexpectedly diverse functional repertoire of encoded proteins. Nucleic Acids Res **29,** 246-254.

Bartel, D.P., and Chen, C.Z. (2004). Micromanagers of gene expression: the potentially widespread influence of metazoan microRNAs. Nat Rev Genet **5,** 396-400.

Bernstein, B.W., Painter, W.B., Chen, H., Minamide, L.S., Abe, H., and Bamburg, J.R. (2000). Intracellular pH modulation of ADF/cofilin proteins. Cell Motil Cytoskeleton **47,** 319-336.

Bilang-Bleuel, A., Revah, F., Colin, P., Locquet, I., Robert, J.J., Mallet, J., and Horellou, P. (1997). Intrastriatal injection of an adenoviral vector expressing glial-cell-line-derived neurotrophic factor prevents dopaminergic neuron degeneration and behavioral impairment in a rat model of Parkinson disease. Proc Natl Acad Sci U S A **94,** 8818-8823.

Blackshear, P.J. (2002). Tristetraprolin and other CCCH tandem zinc-finger proteins in the regulation of mRNA turnover. Biochem Soc Trans **30,** 945-952.

Blaxall, B., Pende A, Wu SC Port JD. (2002). Correlation between intrinsic mRNA stability and the affinity of AUF1 (hnRNP D) and HuR for A+U-rich mRNAs. Mol Cell Biochem **232,** 1-11.

Bode, B.P. (2001). Recent molecular advances in mammalian glutamine transport. J Nutr **131,** 2475S-2485S; discussion 2486S-2477S.

Boden, D., Pusch O, Silbermann R, Lee F, Tucker L, Ramratnam B. (2004). Enhanced gene silencing of HIV-1 specific siRNA using microRNA designed hairpins. Nucleic Acids Res. **32,** 1154-1158.

Brennan, C.M., and Steitz, J.A. (2001). HuR and mRNA stability. Cell Mol Life Sci **58,** 266-277.

Brosnan, J.T., Lowry, M., Vinay, P., Gougoux, A., and Halperin, M.L. (1987). Renal ammonium production--une vue canadienne. Can J Physiol Pharmacol **65,** 489-498.

Brown, J.T., Bai, X., and Johnson, A.W. (2000). The yeast antiviral proteins Ski2p, Ski3p, and Ski8p exist as a complex *in vivo*. Rna **6,** 449-457.

Brummelkamp, T.R., Bernards, R., and Agami, R. (2002). A system for stable expression of short interfering RNAs in mammalian cells. Science **296,** 550-553.

Burch, H.B., Narins, R.G., Chu, C., Fagioli, S., Choi, S., McCarthy, W., and Lowry, O.H. (1978). Distribution along the rat nephron of three enzymes of gluconeogenesis in acidosis and starvation. Am J Physiol **235,** F246-253.

Caponigro, G., and Parker, R. (1995). Multiple functions for the poly(A)-binding protein in mRNA decapping and deadenylation in yeast. Genes Dev **9,** 2421-2432.

Carballo, E., Lai, W.S., and Blackshear, P.J. (1998). Feedback inhibition of macrophage tumor necrosis factor-alpha production by tristetraprolin. Science **281,** 1001-1005.

Carballo, E., Lai, W.S., and Blackshear, P.J. (2000). Evidence that tristetraprolin is a physiological regulator of granulocyte-macrophage colony-stimulating factor messenger RNA deadenylation and stability. Blood **95,** 1891-1899.

Carballo, E., Cao, H., Lai, W.S., Kennington, E.A., Campbell, D., and Blackshear, P.J. (2001). Decreased sensitivity of tristetraprolin-deficient cells to p38 inhibitors suggests the involvement of tristetraprolin in the p38 signaling pathway. J Biol Chem **276,** 42580-42587. Epub 42001 Sep 42586.

Carmell, M.A., and Hannon, G.J. (2004). RNase III enzymes and the initiation of gene silencing. Nat Struct Mol Biol **11,** 214-218.

Chen, C., and Okayama, H. (1987). High-efficiency transformation of mammalian cells by plasmid DNA. Mol Cell Biol **7,** 2745-2752.

Chen, C.Y., and Shyu, A.B. (1995). AU-rich elements: characterization and importance in mRNA degradation. Trends Biochem Sci **20,** 465-470.

Chen, C.Y., Gherzi, R., Ong, S.E., Chan, E.L., Raijmakers, R., Pruijn, G.J., Stoecklin, G., Moroni, C., Mann, M., and Karin, M. (2001). AU binding proteins recruit the exosome to degrade ARE-containing mRNAs. Cell **107,** 451-464.

Chen, Z., Hagler, J., Palombella, V.J., Melandri, F., Scherer, D., Ballard, D., and Maniatis, T. (1995). Signal-induced site-specific phosphorylation targets I kappa B alpha to the ubiquitin-proteasome pathway. Genes Dev **9,** 1586-1597.

Chiu, J.F., and Boeker, E.A. (1979). Cow brain glutaminase: partial purification and mechanism of action. Arch Biochem Biophys **196,** 493-500.

Chomczynski, P., and Sacchi, N. (1987). Single-step method of RNA isolation by acid guanidinium thiocyanate-phenol-chloroform extraction. Anal Biochem **162,** 156-159.

Chung-Bok, M.I., Vincent, N., Jhala, U., and Watford, M. (1997). Rat hepatic glutaminase: identification of the full coding sequence and characterization of a functional promoter. Biochem J **324 (Pt 1),** 193-200.

Cimbala, M.A., Lamers, W.H., Nelson, K., Monahan, J.E., Yoo-Warren, H., and Hanson, R.W. (1982). Rapid changes in the concentration of phosphoenolpyruvate carboxykinase mRNA in rat liver and kidney. Effects of insulin and cyclic AMP. J Biol Chem **257,** 7629-7636.

Curthoys, N.P. (1983). Role of gamma-glutamyltranspeptidase in the renal metabolism of glutathione. Miner Electrolyte Metab **9,** 236-245.

Curthoys, N.P. (1984). Glutamine metabolism in mammalian tissues. (Berlin).

Curthoys, N.P. (2001). Role of mitochondrial glutaminase in rat renal glutamine metabolism. J Nutr **131,** 2491S-2495S; discussion 2496S-2497S.

Curthoys, N.P., and Lowry, O.H. (1973). The distribution of glutaminase isoenzymes in the various structures of the nephron in normal, acidotic, and alkalotic rat kidney. J Biol Chem **248,** 162-168.

Curthoys, N.P., and Godfrey, S.S. (1976). Properties of rat kidney glutaminase enzymes and their role in renal ammoniagenesis. Curr Probl Clin Biochem **6,** 346-356.

Curthoys, N.P., and Watford, M. (1995). Regulation of glutaminase activity and glutamine metabolism. Annu Rev Nutr **15,** 133-159.

D'Alessio, J.M., Harris, G.H., Perna, P.J., and Paule, M.R. (1981). Ribosomal ribonucleic acid repeat unit of Acanthamoeba castellanii: cloning and restriction endonuclease map. Biochemistry **20,** 3822-3827.

Daugeron, M.C., Mauxion, F., and Seraphin, B. (2001). The yeast POP2 gene encodes a nuclease involved in mRNA deadenylation. Nucleic Acids Research **29,** 2448-2455.

Davidson, B.L., Allen, E.D., Kozarsk, K.F., Wilson, J.M., Roessler, B.J. (1993). A model system for *in vivo* gene transfer into the central nervous system using an adenoviral vector. Nat. Genet. **3,** 219-223.

Decker, C.J., and Parker, R. (1995). Diversity of cytoplasmic functions for the 3' untranslated region of eukaryotic transcripts. Curr Opin Cell Biol **7,** 386-392.

DeMaria, C.T., and Brewer, G. (1996). AUF1 binding affinity to A+U-rich elements correlates with rapid mRNA degradation. J Biol Chem **271,** 12179-12184.

Dember, L.M., Kim, N.D., Liu KQ, Anderson P. (1996). Individual RNA recognition motifs of TIA-1 and TIAR have different RNA binding specificities. J Biol Chem. **271,** 2783-2788.

Denis, C.L., and Chen, J. (2003). The CCR4-NOT complex plays diverse roles in mRNA metabolism. Prog Nucleic Acid Res Mol Biol **73,** 221-250.

Denli, A.M., Tops, B.B., Plasterk, R.H., Ketting, R.F., and Hannon, G.J. (2004). Processing of primary microRNAs by the Microprocessor complex. Nature **432,** 231-235.

Ding, L., Spencer, A., Morita, K., and Han, M. (2005). The developmental timing regulator AIN-1 interacts with miRISCs and may target the argonaute protein ALG-1 to cytoplasmic P bodies in C. elegans. Mol Cell **19,** 437-447.

Doench, J.G., and Sharp, P.A. (2004). Specificity of microRNA target selection in translational repression. Genes Dev **18,** 504-511.

Doench, J.G., Petersen, C.P., and Sharp, P.A. (2003). siRNAs can function as miRNAs. Genes Dev **17,** 438-442.

Elbashir, S., Harborth J, Weber K, Tuschl T. (2002). Analysis of gene function in somatic mammalian cells using small interfering RNAs. Methods. **26,** 199-213.

Elbashir, S.M., Martinez, J., Patkaniowska, A., Lendeckel, W., and Tuschl, T. (2001). Functional anatomy of siRNAs for mediating efficient RNAi in Drosophila melanogaster embryo lysate. Embo J **20,** 6877-6888.

Elgadi, K.M., Meguid, R.A., Qian, M., Souba, W.W., and Abcouwer, S.F. (1999). Cloning and analysis of unique human glutaminase isoforms generated by tissue-specific alternative splicing. Physiol Genomics **1,** 51-62.

Elgadi, K.M., W. W. Souba, and Abcouwer S. F. (1988). Evidence for a new glutaminase isoenzyme in rat tissues. *Surgical Forum* **44,** 52-54.

Feifel, E., Obexer, P., Andratsch, M., Euler, S., Taylor, L., Tang, A., Wei, Y., Schramek, H., Curthoys, N.P., and Gstraunthaler, G. (2002). p38 MAPK mediates acid-induced transcription of PEPCK in LLC-PK(1)-FBPase(+) cells. Am J Physiol Renal Physiol **283,** F678-688.

Feinberg, A.P., and Vogelstein, B. (1984). "A technique for radiolabeling DNA restriction endonuclease fragments to high specific activity". Addendum. Anal Biochem **137,** 266-267.

Frischmeyer, P.A., van Hoof, A., O'Donnell, K., Guerrerio, A.L., Parker, R., and Dietz, H.C. (2002). An mRNA surveillance mechanism that eliminates transcripts lacking termination codons. Science **295,** 2258-2261.

Gagna, C.E., Chen, J.H., Kuo, H.R., and Lambert, W.C. (1998). Binding properties of bovine ocular lens zeta-crystallin to right-handed B-DNA, left-handed Z-DNA, and single-stranded DNA. Cell Biol Int **22,** 217-225.

Gao, M., Fritz, D.T., Ford, L.P., and Wilusz, J. (2000). Interaction between a poly(A)-specific ribonuclease and the 5' cap influences mRNA deadenylation rates *in vitro*. Mol Cell **5,** 479-488.

Gao, M., Wilusz, C.J., Peltz, S.W., and Wilusz, J. (2001). A novel mRNA-decapping activity in HeLa cytoplasmic extracts is regulated by AU-rich elements. Embo J **20,** 1134-1143.

Garland, D., Rao, P. V., Del Corso, A., Mura, U., Zigler, J. S., Jr. (1991). zeta-Crystallin is a major protein in the lens of Camelus dromedarius. Arch Biochem Biophys **285,** 134-136.

Gherzi, R., Lee, K.Y., Briata, P., Wegmuller, D., Moroni, C., Karin, M., and Chen, C.Y. (2004). A KH domain RNA binding protein, KSRP, promotes ARE-directed mRNA turnover by recruiting the degradation machinery. Mol Cell **14,** 571-583.

Gil, J., and Esteban, M. (2000). Induction of apoptosis by the dsRNA-dependent protein kinase (PKR): mechanism of action. Apoptosis **5,** 107-114.

Goenka, S., Rao, C. M. (2001). Expression of recombinant zeta-crystallin in Escherichia coli with the help of GroEL/ES and its purification. Protein Expr Purif **21,** 260-267.

Gonzalez, P., Rao, P.V., and Zigler, J.S., Jr. (1994a). Organization of the human zeta-crystallin/quinone reductase gene (CRYZ). Genomics **21,** 317-324.

Gonzalez, P., Hernandez-Calzadilla, C., Rao, P.V., Rodriguez, I.R., Zigler, J.S., Jr., and Borras, T. (1994b). Comparative analysis of the zeta-crystallin/quinone reductase gene in guinea pig and mouse. Mol Biol Evol **11,** 305-315.

Good, D.W., and Burg, M.B. (1984). Ammonia production by individual segments of the rat nephron. J Clin Invest **73,** 602-610.

Gorman, C., Padmanabhan, R., and Howard, B.H. (1983). High efficiency DNA-mediated transformation of primate cells. Science **221,** 551-553.

Gossen, M., and Bujard, H. (1992). Tight control of gene expression in mammalian cells by tetracycline-responsive promoters. Proc Natl Acad Sci U S A **89,** 5547-5551.

Graham, F.L. (1977). Characteristics of a human cell line trnasformed by DNA from human adenovirus type 5. J. Gen. Virol. **36,** 59-72.

Greenberg, J.T., and Ausubel, F.M. (1993). Arabidopsis mutants compromised for the control of cellular damage during pathogenesis and aging. Plant J **4,** 327-341.

Gregory, R.I., Chendrimada, T.P., Cooch, N., and Shiekhattar, R. (2005). Human RISC couples microRNA biogenesis and posttranscriptional gene silencing. Cell **123,** 631-640.

Gregory, R.I., Yan, K.P., Amuthan, G., Chendrimada, T., Doratotaj, B., Cooch, N., and Shiekhattar, R. (2004). The Microprocessor complex mediates the genesis of microRNAs. Nature **432,** 235-240.

Gstraunthaler, G., and Handler, J.S. (1987). Isolation, growth, and characterization of a gluconeogenic strain of renal cells. Am J Physiol **252,** C232-238.

Gstraunthaler, G.J. (1994). Ammoniagenesis in renal cell culture. A comparative study on ammonia metabolism of renal epithelial cell lines. Contrib Nephrol **110,** 88-97.

Gueydan, C., Droogmans L, Chalon P, Huez G, Caput D, Kruys V. (1999). Identification of TIAR as a protein binding to the translational regulatory AU-rich element of tumor necrosis factor alpha mRNA. J Biol Chem. **274,** 2322-2326.

Guhaniyogi, J., and Brewer, G. (2001). Regulation of mRNA stability in mammalian cells. Gene **265,** 11-23.

Ha, I., Wightman, B., and Ruvkun, G. (1996). A bulged lin-4/lin-14 RNA duplex is sufficient for Caenorhabditis elegans lin-14 temporal gradient formation. Genes Dev **10,** 3041-3050.

Hajarnis, S., Schroeder, J.M., and Curthoys, N.P. (2005). 3'-Nontranslated region of phosphoenolpyruvate carboxykinase mRNA contains multiple instability elements that bind AUF1. Journal of Biolojical Chemistry **280.**

Haley, B., and Zamore, P.D. (2004). Kinetic analysis of the RNAi enzyme complex. Nat Struct Mol Biol **11,** 599-606.

Han, J., Lee, Y., Yeom, K.H., Kim, Y.K., Jin, H., and Kim, V.N. (2004). The Drosha-DGCR8 complex in primary microRNA processing. Genes Dev **18,** 3016-3027.

Hansen, W.R., Barsic-Tress, N., Taylor, L., and Curthoys, N.P. (1996). The 3'-nontranslated region of rat renal glutaminase mRNA contains a pH- responsive stability element. Am J Physiol **271,** F126-131.

Hanson, R., and Reshef, L. (1997). Regulation of phosphoenolpyruvate carboxykinase (GTP) gene expression. Annu Rev Biochem **66,** 581-611.

Haser, W.G., Shapiro, R.A., and Curthoys, N.P. (1985). Comparison of the phosphate-dependent glutaminase obtained from rat brain and kidney. Biochem J **229,** 399-408.

He, F., Li, X., Spatrick, P., Casillo, R., Dong, S., and Jacobson, A. (2003). Genome-wide analysis of mRNAs regulated by the nonsense-mediated and 5' to 3' mRNA decay pathways in yeast. Mol Cell **12,** 1439-1452.

He, T.C., Zhou, S., da Costa, L.T., Yu, J., Kinzler, K.W., and Vogelstein, B. (1998). A simplified system for generating recombinant adenoviruses. Proc Natl Acad Sci U S A **95,** 2509-2514.

Hentze, M. (1994). Enzymes as RNA-binding proteins: a role for (di)nucleotide-binding domains? Trends Biochem Sci.
19, 101-103.

Holcomb, T., Curthoys, N.P., and Gstraunthaler, G. (1995). Subcellular localization of PEPCK and metabolism of gluconeogenic substrains of renal cell lines. Am J Physiol **268,** C449-457.

Holcomb, T., Taylor, L., Trohkimoinen, J., and Curthoys, N.P. (2000). Isolation, characterization and expression of a human brain mitochondrial glutaminase cDNA. Brain Res Mol Brain Res **76,** 56-63.

Hollams, E.M., Giles, K.M., Thomson, A.M., and Leedman, P.J. (2002). MRNA stability and the control of gene expression: implications for human disease. Neurochem Res **27,** 957-980.

Hopfer, U., Jacobberger, J.W., Gruenert, D.C., Eckert, R.L., Jat, P.S., and Whitsett, J.A. (1996). Immortalization of epithelial cells. Am J Physiol **270,** C1-11.

Huang, Q.L., Russell, P., Stone, S. H., Zigler, J. S. (1987). Zeta-crystallin, a novel lens protein from the guinea pig. Curr Eye Res **6,** 725-732.

Hughey, R.P., Rankin, B.B., and Curthoys, N.P. (1980). Acute acidosis and renal arteriovenous differences of glutamine in normal and adrenalectomized rats. Am J Physiol **238,** F199-204.

Hwang, J.J., and Curthoys, N.P. (1991). Effect of acute alterations in acid-base balance on rat renal glutaminase and phosphoenolpyruvate carboxykinase gene expression. J Biol Chem **266,** 9392-9396.

Hwang, J.J., Perera, S., Shapiro, R.A., and Curthoys, N.P. (1991). Mechanism of altered renal glutaminase gene expression in response to chronic acidosis. Biochemistry **30,** 7522-7526.

Izquierdo, J.M. (2006). Control of the ATP synthase beta subunit expression by RNA-binding proteins TIA-1, TIAR, and HuR. Biochem Biophys Res Commun **348,** 703-711.

Jakymiw, A., Lian, S., Eystathioy, T., Li, S., Satoh, M., Hamel, J.C., Fritzler, M.J., and Chan, E.K. (2005). Disruption of GW bodies impairs mammalian RNA interference. Nat Cell Biol **7,** 1267-1274.

Jeon, S.a.L., P.F. (1995). Integration of human papillomavirus type 16 DNA into the human genome leads to increased stability of E6 and E7 mRNAs: implications for cervical carcinogenesis. *Proc. Natl Acad. Sci. USA* **92,** 1654-1658.

Jing, Q., Huang, S., Guth, S., Zarubin, T., Motoyama, A., Chen, J., Di Padova, F., Lin, S.C., Gram, H., and Han, J. (2005). Involvement of microRNA in AU-rich element-mediated mRNA instability. Cell **120,** 623-634.

Kaiser, S., and Curthoys, N.P. (1991). Effect of pH and bicarbonate on phosphoenolpyruvate carboxykinase and glutaminase mRNA levels in cultured renal epithelial cells. J Biol Chem **266,** 9397-9402.

Kaiser, S., Hwang, J.J., Smith, H., Banner, C., Welbourne, T.C., and Curthoys, N.P. (1992). Effect of altered acid-base balance and of various agonists on levels of renal glutamate dehydrogenase mRNA. Am J Physiol **262,** F507-512.

Karim, Z., Attmane-Elakeb, A., Sibella, V., and Bichara, M. (2003). Acid pH increases the stability of BSC1/NKCC2 mRNA in the medullary thick ascending limb. J Am Soc Nephrol **14,** 2229-2236.

Karinch, A.M., Lin, C.M., Wolfgang, C.L., Pan, M., and Souba, W.W. (2002). Regulation of expression of the SN1 transporter during renal adaptation to chronic metabolic acidosis in rats. Am J Physiol Renal Physiol **283,** F1011-1019.

Khvorova, A., Reynolds, A., and Jayasena, S.D. (2003). Functional siRNAs and miRNAs exhibit strand bias. Cell **115,** 209-216.

Kim, V.N. (2005). Small RNAs: classification, biogenesis, and function. Mol Cells **19,** 1-15.

Kiriakidou, M., Nelson, P.T., Kouranov, A., Fitziev, P., Bouyioukos, C., Mourelatos, Z., and Hatzigeorgiou, A. (2004). A combined computational-experimental approach predicts human microRNA targets. Genes Dev **18,** 1165-1178.

Klausner, R.D., Rouault, T.A., and Harford, J.B. (1993). Regulating the fate of mRNA: the control of cellular iron metabolism. Cell **72,** 19-28.

Kloosterman, W.P., Wienholds, E., Ketting, R.F., and Plasterk, R.H. (2004). Substrate requirements for let-7 function in the developing zebrafish embryo. Nucleic Acids Res **32,** 6284-6291.

Krebs, H. (1935). The synthesis of glutamine from glutamic acid and ammonia, and the enzymic hydrolysis of glutamine in animal tissues. Biochem. J. **29,** 1951-1969.

Kvamme, E., Tveit, B., and Svenneby, G. (1970). Glutaminase from pig renal cortex. I. Purification and general properties. J Biol Chem **245,** 1871-1877.

Lai, W., Carballo E, Strum JR, Kennington EA, Phillips RS, Blackshear PJ. (1999). Evidence that tristetraprolin binds to AU-rich elements and promotes the deadenylation and destabilization of tumor necrosis factor alpha mRNA. Mol Cell Biol **19,** 4311-4323.

Lal, A., Mazan-Mamczarz, K., Kawai, T., Yang, X., Martindale, J.L., and Gorospe, M. (2004). Concurrent versus individual binding of HuR and AUF1 to common labile target mRNAs. Embo J **23,** 3092-3102.

Landthaler, M., Yalcin, A., and Tuschl, T. (2004). The human DiGeorge syndrome critical region gene 8 and Its D. melanogaster homolog are required for miRNA biogenesis. Curr Biol **14,** 2162-2167.

Lapucci, A., Donnini, M., Papucci, L., Witort, E., Tempestini, A., Bevilacqua, A., Nicolin, A., Brewer, G., Schiavone, N., and Capaccioli, S. (2002). AUF1 Is a

bcl-2 A + U-rich element-binding protein involved in bcl-2 mRNA destabilization during apoptosis. J Biol Chem **277,** 16139-16146.

Laroia, G., Cuesta, R., Brewer, G., and Schneider, R.J. (1999). Control of mRNA decay by heat shock-ubiquitin-proteasome pathway. Science **284,** 499-502.

Laterza, O.F., and Curthoys, N.P. (2000a). Effect of acidosis on the properties of the glutaminase mRNA pH-response element binding protein. J Am Soc Nephrol **11,** 1583-1588.

Laterza, O.F., and Curthoys, N.P. (2000b). Specificity and functional analysis of the pH-responsive element within renal glutaminase mRNA. Am J Physiol Renal Physiol **278,** F970-977.

Laterza, O.F., Hansen, W.R., Taylor, L., and Curthoys, N.P. (1997). Identification of an mRNA-binding protein and the specific elements that may mediate the pH-responsive induction of renal glutaminase mRNA. J Biol Chem **272,** 22481-22488.

Laterza, O.F., Taylor, L., Unnithan, S., Nguyen, L., and Curthoys, N.P. (2000). Mapping and functional analysis of an instability element in phosphoenolpyruvate carboxykinase mRNA. Am J Physiol Renal Physiol **279,** F866-873.

Le Hir, H., Moore, M.J., and Maquat, L.E. (2000). Pre-mRNA splicing alters mRNP composition: evidence for stable association of proteins at exon-exon junctions. Genes Dev **14,** 1098-1108.

Leber, S., Yamagata M, Sanes JR. (1996). Gene transfer using replication-defective retroviral and adenoviral vectors. Methods Cell Biol. **51,** 161-183.

Lee, D.C., Gonzalez, P., and Wistow, G. (1994). Zeta-crystallin: a lens-specific promoter and the gene recruitment of an enzyme as a crystallin. J Mol Biol **236,** 669-678.

Lee, Y., Ahn, C., Han, J., Choi, H., Kim, J., Yim, J., Lee, J., Provost, P., Radmark, O., Kim, S., and Kim, V.N. (2003). The nuclear RNase III Drosha initiates microRNA processing. Nature **425,** 415-419.

Lejeune, F., Li, X., and Maquat, L.E. (2003). Nonsense-mediated mRNA decay in mammalian cells involves decapping, deadenylating, and exonucleolytic activities. Mol Cell **12,** 675-687.

Lewis, B.P., Burge, C.B., and Bartel, D.P. (2005). Conserved seed pairing, often flanked by adenosines, indicates that thousands of human genes are microRNA targets. Cell **120,** 15-20.

Li, S., Sato, S., Yang, X., Preisig, P.A., and Alpern, R.J. (2004). Pyk2 activation is integral to acid stimulation of sodium/hydrogen exchanger 3. J Clin Invest **114,** 1782-1789.

Linker, K., Pautz, A., Fechir, M., Hubrich, T., Greeve, J., and Kleinert, H. (2005). Involvement of KSRP in the post-transcriptional regulation of human iNOS expression-complex interplay of KSRP with TTP and HuR. Nucleic Acids Res **33,** 4813-4827.

Liu, J., Valencia-Sanchez, M.A., Hannon, G.J., and Parker, R. (2005). MicroRNA-dependent localization of targeted mRNAs to mammalian P-bodies. Nat Cell Biol **7,** 719-723.

Loflin, P., Chen, C.Y., and Shyu, A.B. (1999). Unraveling a cytoplasmic role for hnRNP D in the *in vivo* mRNA destabilization directed by the AU-rich element. Genes Dev **13,** 1884-1897.

Lowry, M., and Ross, B.D. (1980). Activation of oxoglutarate dehydrogenase in the kidney in response to acute acidosis. Biochem J **190,** 771-780.

Lowry, O.H., Rosebrough, N.J., Farr, A.L., and Randall, R.J. (1951). Protein measurement with the Folin phenol reagent. J Biol Chem **193,** 265-275.

Lund, E., Guttinger, S., Calado, A., Dahlberg, J.E., and Kutay, U. (2004). Nuclear export of microRNA precursors. Science **303,** 95-98.

Mahtani, K.R., Brook, M., Dean, J.L., Sully, G., Saklatvala, J., and Clark, A.R. (2001). Mitogen-activated protein kinase p38 controls the expression and posttranslational modification of tristetraprolin, a regulator of tumor necrosis factor alpha mRNA stability. Mol Cell Biol **21,** 6461-6469.

Makeyev, A.V., and Liebhaber, S.A. (2002). The poly(C)-binding proteins: a multiplicity of functions and a search for mechanisms. Rna **8,** 265-278.

Marcus, P.I., and Sekellick, M.J. (2001). Combined sequential treatment with interferon and dsRNA abrogates virus resistance to interferon action. J Interferon Cytokine Res **21,** 423-429.

Martinez, J.a.T.T. (2004). RISC is a 5' phosphomonoester-producing RNA endonuclease. Gene and Development **18,** 975-980.

Mazan-Mamczarz, K., Lal, A., Martindale, J.L., Kawai, T., and Gorospe, M. (2006). Translational repression by RNA-binding protein TIAR. Mol Cell Biol **26,** 2716-2727.

McGivan, J.D. (1988). In Glutamine and Glutamate in mammals. (Boca Baton).

Meister, A. (1975). Function of glutathione in kidney via the gamma-glutamyl cycle. Med. Clin. North Am. **59,** 649-666.

Min, H., Turck, C.W., Nikolic, J.M., and Black, D.L. (1997). A new regulatory protein, KSRP, mediates exon inclusion through an intronic splicing enhancer. Genes Dev **11,** 1023-1036.

Minamide L.S, Bamburg J.R. (1990): A filter paper dye-binding assay for quantitative determination of protein without interference from reducing agents or detergents. Anal Biochem. **190**, 66-70

Minamide, L.S.S.A., Sarmiere PD, Wiggan O, Maloney MT, Bernstein BW, Sneider JM, Gonzalez JA, Bamburg JR. (2003). Production and use of replication-deficient adenovirus for transgene expression in neurons. Methods Cell Biol. **71,** 387-416.

Mitchell, P., and Tollervey, D. (2003). An NMD pathway in yeast involving accelerated deadenylation and exosome-mediated 3'-->5' degradation. Mol Cell **11,** 1405-1413.

Moore, M.J. (2005). From birth to death: the complex lives of eukaryotic mRNAs. Science **309,** 1514-1518.

Muhlrad, D., Decker, C.J., and Parker, R. (1994). Deadenylation of the unstable mRNA encoded by the yeast MFA2 gene leads to decapping followed by 5'-->3' digestion of the transcript. Genes Dev **8,** 855-866.

Mukherjee, D., Gao, M., O'Connor, J.P., Raijmakers, R., Pruijn, G., Lutz, C.S., and Wilusz, J. (2002). The mammalian exosome mediates the efficient degradation of mRNAs that contain AU-rich elements. Embo J **21,** 165-174.

Neu, J., Shenoy, V., and Chakrabarti, R. (1996). Glutamine nutrition and metabolism: where do we go from here? Faseb J **10,** 829-837.

Niranjanakumari, S., Lasda, E., Brazas, R., and Garcia-Blanco, M.A. (2002). Reversible cross-linking combined with immunoprecipitation to study RNA-protein interactions *in vivo*. Methods **26,** 182-190.

Olalla, L., Aledo, J.C., Bannenberg, G., and Marquez, J. (2001). The C-terminus of human glutaminase L mediates association with PDZ domain-containing proteins. FEBS Lett **488,** 116-122.

Paddison, P.J., and Hannon, G.J. (2002). RNA interference: the new somatic cell genetics? Cancer Cell **2,** 17-23.

Paddison, P.J., Caudy, A.A., and Hannon, G.J. (2002). Stable suppression of gene expression by RNAi in mammalian cells. Proc Natl Acad Sci U S A **99,** 1443-1448.

Parker, J.S., Roe, S.M., and Barford, D. (2004). Crystal structure of a PIWI protein suggests mechanisms for siRNA recognition and slicer activity. Embo J **23,** 4727-4737.

Parker, R., and Song, H. (2004). The enzymes and control of eukaryotic mRNA turnover. Nat Struct Mol Biol **11,** 121-127.

Peltz, S.W., and Jacobson, A. (1992). mRNA stability: in *trans*-it. Curr Opin Cell Biol **4,** 979-983.

Peng, S.S., Chen, C.Y., Xu, N., and Shyu, A.B. (1998). RNA stabilization by the AU-rich element binding protein, HuR, an ELAV protein. Embo J **17,** 3461-3470.

Peng, Y., Amemiya, M., Yang, X., Fan, L., Moe, O.W., Yin, H., Preisig, P.A., Yanagisawa, M., and Alpern, R.J. (2001). ET(B) receptor activation causes exocytic insertion of NHE3 in OKP cells. Am J Physiol Renal Physiol **280,** F34-42.

Perera, S.Y., Chen, T.C., and Curthoys, N.P. (1990). Biosynthesis and processing of renal mitochondrial glutaminase in cultured proximal tubular epithelial cells and in isolated mitochondria. J Biol Chem **265,** 17764-17770.

Piecyk, M., S. Wax, A. R. Beck, N. Kedersha, M. Gupta, B. Maritim, S. Chen, C. Gueydan, V. Kruys, M. Streuli, and P. Anderson. (2000). TIA-1 is a translational silencer that selectively regulates the expression of TNF-. EMBO J **19,** 4154-4163.

Porter, D., and Curthoys, N.P. (1997). Use of thermostable and Escherichia coli RNase H in RNA mapping studies. Anal Biochem **247,** 279-286.

Porter, D., Hansen, W.R., Taylor, L., and Curthoys, N.P. (1995). Differential expression of multiple glutaminase mRNAs in LLC-PK1-F+ cells. Am J Physiol **269,** F363-373.

Preisig, P.A., and Alpern, R.J. (1988). Chronic metabolic acidosis causes an adaptation in the apical membrane Na/H antiporter and basolateral membrane Na(HCO3)3 symporter in the rat proximal convoluted tubule. J Clin Invest **82,** 1445-1453.

Quesada, A.R., Sanchez-Jimenez, F., Perez-Rodriguez, J., Marquez, J., Medina, M.A., and Nunez de Castro, I. (1988). Purification of phosphate-dependent

glutaminase from isolated mitochondria of Ehrlich ascites-tumour cells. Biochem J **255,** 1031-1035.

Raineri, I., Wegmueller, D., Gross, B., Certa, U., and Moroni, C. (2004). Roles of AUF1 isoforms, HuR and BRF1 in ARE-dependent mRNA turnover studied by RNA interference. Nucleic Acids Res **32,** 1279-1288. Print 2004.

Rao, P., and Zigler, J.S., Jr. (1992). Quinone induced stimulation of hexose monophosphate shunt activity in the guinea pig lens: role of zeta-crystallin. Biochim Biophys Acta **1116,** 75-81.

Rao, P.V., Krishna, C.M., and Zigler, J.S., Jr. (1992). Identification and characterization of the enzymatic activity of zeta-crystallin from guinea pig lens. A novel NADPH:quinone oxidoreductase. J Biol Chem **267,** 96-102.

Rao, P.V., Gonzalez, P., Persson, B., Jornvall, H., Garland, D., and Zigler, J.S., Jr. (1997). Guinea pig and bovine zeta-crystallins have distinct functional characteristics highlighting replacements in otherwise similar structures. Biochemistry **36,** 5353-5362.

Rodokanaki, A., Holmes, R. K., Borras, T. (1989). Zeta-crystallin, a novel protein from the guinea pig lens is related to alcohol dehydrogenases. Gene **78,** 215-224.

Romero, M.F., Douglas, J.G., Eckert, R.L., Hopfer, U., and Jacobberger, J.W. (1992). Development and characterization of rabbit proximal tubular epithelial cell lines. Kidney Int **42,** 1130-1144.

Ross, D.J., Koerner, S.K., Elashoff, J., Waxman, A.D., and Mohsenifar, Z. (1995). Isogravitational heterogeneity of perfusion after unilateral lung transplantation. Clin Sci (Colch) **89,** 285-291.

Ross, J. (1995). mRNA stability in mammalian cells. Microbiol Rev **59,** 423-450.

Sachs, A.B., and Deardorff, J.A. (1992). Translation initiation requires the PAB-dependent poly(A) ribonuclease in yeast. Cell **70,** 961-973.

Sahai, A., Laughrey, E., and Tannen, R.L. (1990). Relationship between intracellular pH and ammonia metabolism in LLC-PK1 cells. Am J Physiol **258,** F103-108.

Sajo, I.M., Goldstein, M.B., Sonnenberg, H., Stinebaugh, B.J., Wilson, D.R., and Halperin, M.L. (1981). Sites of ammonia addition to tubular fluid in rats with chronic metabolic acidosis. Kidney Int **20,** 353-358.

Sastrasinh, M., and Sastrasinh, S. (1990). Effect of acute pH change on mitochondrial glutamine transport. Am J Physiol **259,** F863-866.

Sastrasinh, S., and Sastrasinh, M. (1989). Glutamine transport in submitochondrial particles. Am J Physiol **257,** F1050-1058.

Schroeder, J.M. (2002). Characterization of the pH-responsive stabilization of glutamate de-hydrogenase and glutaminase messenger RNA. In Biochemistry and Molecular Biology (Fort Collins: Colorado State University).

Schroeder, J.M., Liu, W., and Curthoys, N.P. (2003a). pH-responsive stabilization of glutamate dehydrogenase mRNA in LLC-PK1-F+ cells. Am J Physiol Renal Physiol **285,** F258-265. Epub 2003 Apr 2008.

Schroeder, J.M., Liu, W., and Curthoys, N.P. (2003b). pH-responsive stabilization of glutamate dehydrogenase mRNA in LLC-PK1-F+ cells. Am J Physiol Renal Physiol **285,** F258-265.

Schroeder, J.M., Ibrahim, H., Taylor, L., and Curthoys, N.P. (2006). Role of deadenylation and AUF1 binding in the pH-responsive stabilization of glutaminase mRNA. Am J Physiol Renal Physiol **290,** F733-740.

Shafer, R.W., Chirgwin, K.D., Glatt, A.E., Dahdouh, M.A., Landesman, S.H., and Suster, B. (1991). HIV prevalence, immunosuppression, and drug resistance in patients with tuberculosis in an area endemic for AIDS. Aids **5,** 399-405.

Shapiro, R.A., Morehouse, R.F., and Curthoys, N.P. (1982). Inhibition by glutamate of phosphate-dependent glutaminase of rat kidney. Biochem J **207,** 561-566.

Shapiro, R.A., Haser, W.G., and Curthoys, N.P. (1985). The orientation of phosphate-dependent glutaminase on the inner membrane of rat renal mitochondria. Arch Biochem Biophys **243,** 1-7.

Shapiro, R.A., Haser, W.G., and Curthoys, N.P. (1987). Immunoblot analysis of glutaminase peptides in intact and solubilized mitochondria isolated from various rat tissues. Biochem J **242,** 743-747.

Shapiro, R.A., Farrell, L., Srinivasan, M., and Curthoys, N.P. (1991). Isolation, characterization, and *in vitro* expression of a cDNA that encodes the kidney isoenzyme of the mitochondrial glutaminase. J Biol Chem **266,** 18792-18796.

Shyu, A.B., Belasco, J.G., and Greenberg, M.E. (1991). Two distinct destabilizing elements in the c-fos message trigger deadenylation as a first step in rapid mRNA decay. Genes Dev **5,** 221-231.

Silbernagl, S. (1980). Tubular reabsorption of L-glutamine studied by free-flow micropuncture and microperfusion of rat kidney. Int J Biochem **12,** 9-16.

Sleeper, R.S., Vertuno, L.L., Strauss, F., and Preuss, H.G. (1978). Effects of acid challenge on *in vivo* and *in vitro* rat renal ammoniagenesis. Life Sci **22,** 1561-1571.

Smith, E.M., and Watford, M. (1990). Molecular cloning of a cDNA for rat hepatic glutaminase. Sequence similarity to kidney-type glutaminase. J Biol Chem **265,** 10631-10636.

Souba, W.W. (1991). Glutamine: a key substrate for the splanchnic bed. Annu Rev Nutr **11,** 285-308.

Soudais C, L.-B.C., Kissa K, Kremer E. J. (2001). Preferential transduction of neurons by canine adenovirus vectors and their efficient retrograde transport *in vivo*. FASEB
15, 2283-2285.

Squires, E.J., Hall, D.E., and Brosnan, J.T. (1976). Arteriovenous differences for amino acids and lactate across kidneys of normal and acidotic rats. Biochem J **160,** 125-128.

Steiger, M., Carr-Schmid, A., Schwartz, D.C., Kiledjian, M., and Parker, R. (2003). Analysis of recombinant yeast decapping enzyme. Rna **9,** 231-238.

Stoecklin, G., Colombi, M., Raineri, I., Leuenberger, S., Mallaun, M., Schmidlin, M., Gross, B., Lu, M., Kitamura, T., and Moroni, C. (2002). Functional cloning of BRF1, a regulator of ARE-dependent mRNA turnover. Embo J **21,** 4709-4718.

Sui, G., Soohoo, C., Affar el, B., Gay, F., Shi, Y., Forrester, W.C., and Shi, Y. (2002). A DNA vector-based RNAi technology to suppress gene expression in mammalian cells. Proc Natl Acad Sci U S A **99,** 5515-5520.

Svenneby, G., Torgner, I.A., and Kvamme, E. (1973). Purification of phosphate-dependent pig brain glutaminase. J Neurochem **20,** 1217-1224.

Symmons, M.F., Williams, M.G., Luisi, B.F., Jones, G.H., and Carpousis, A.J. (2002). Running rings around RNA: a superfamily of phosphate-dependent RNases. Trends Biochem Sci **27,** 11-18.

Tang, A., and Curthoys, N.P. (2001). Identification of zeta-crystallin/NADPH:quinone reductase as a renal glutaminase mRNA pH response element-binding protein. J Biol Chem **276,** 21375-21380. Epub 22001 Apr 21309.

Tange, T.O., Nott, A., and Moore, M.J. (2004). The ever-increasing complexities of the exon junction complex. Curr Opin Cell Biol **16,** 279-284.

Tannen, R.L., and Ross, B.D. (1979). Ammoniagenesis by the isolated perfused rat kidney: the critical role of urinary acidification. Clin Sci (Lond) **56,** 353-364.

Tanner, N.K., and Linder, P. (2001). DExD/H box RNA helicases: from generic motors to specific dissociation functions. Mol Cell **8,** 251-262.

Taylor, G.A., Thompson, M.J., Lai, W.S., and Blackshear, P.J. (1995). Phosphorylation of tristetraprolin, a potential zinc finger transcription factor, by mitogen stimulation in intact cells and by mitogen-activated protein kinase *in vitro*. J Biol Chem **270,** 13341-13347.

Tenenbaum, S.A., Lager, P.J. Carson, C.C. Keene, J.D. (2002). Ribonomics: identifying mRNA subsets in mRNP complexes using antibodies to RNA-binding proteins and genomic arrays. Methods. **26,** 191-198.

Tomari, Y., Matranga, C., Haley, B., Martinez, N., and Zamore, P.D. (2004). A protein sensor for siRNA asymmetry. Science **306,** 1377-1380.

Tong, J., Harrison, G., and Curthoys, N.P. (1986). The effect of metabolic acidosis on the synthesis and turnover of rat renal phosphate-dependent glutaminase. Biochem J **233,** 139-144.

Tucker, M., Staples, R.R., Valencia-Sanchez, M.A., Muhlrad, D., and Parker, R. (2002). Ccr4p is the catalytic subunit of a Ccr4p/Pop2p/Notp mRNA deadenylase complex in Saccharomyces cerevisiae. EMBO Journal **21,** 1427-1436.

Tucker, M., Valencia-Sanchez, M.A., Staples, R.R., Chen, J., Denis, C.L., and Parker, R. (2001). The transcription factor associated Ccr4 and Caf1 proteins are components of the major cytoplasmic mRNA deadenylase in Saccharomyces cerevisiae. Cell **104,** 377-386.

van Dijk, E., Le Hir, H., and Seraphin, B. (2003). DcpS can act in the 5'-3' mRNA decay pathway in addition to the 3'-5' pathway. Proc Natl Acad Sci U S A **100,** 12081-12086. Epub 12003 Oct 12081.

van Hoof, A., and Parker, R. (1999). The exosome: a proteasome for RNA? Cell **99,** 347-350.

van Hoof, A., Frischmeyer, P.A., Dietz, H.C., and Parker, R. (2002). Exosome-mediated recognition and degradation of mRNAs lacking a termination codon. Science **295,** 2262-2264.

Viswanathan, P., Chen, J., Chiang, Y.C., Denis, C.L., and Hiller, M. (2003). Identification of multiple RNA features that influence CCR4 deadenylation activity.Testis-specific TAF homologs collaborate to control a tissue-specific transcription program. Journal of Biological Chemistry **278,** 14949-14955.

Wagner, B.J., DeMaria, C.T., Sun, Y., Wilson, G.M., and Brewer, G. (1998). Structure and genomic organization of the human AUF1 gene: alternative pre-mRNA splicing generates four protein isoforms. Genomics **48,** 195-202.

Wilson, G.M., and Brewer, G. (1999a). Identification and characterization of proteins binding A + U-rich elements. Methods **17,** 74-83.

Wilson, G.M., and Brewer, G. (1999b). The search for *trans*-acting factors controlling messenger RNA decay. Prog Nucleic Acid Res Mol Biol **62,** 257-291.

Wilson, G.M., Sun, Y., Lu, H., and Brewer, G. (1999). Assembly of AUF1 oligomers on U-rich RNA targets by sequential dimer association. J Biol Chem **274,** 33374-33381.

Wilson, G.M., Lu, J., Sutphen, K., Suarez, Y., Sinha, S., Brewer, B., Villanueva-Feliciano, E.C., Ysla, R.M., Charles, S., and Brewer, G. (2003). Phosphorylation of p40AUF1 regulates binding to A + U-rich mRNA-destabilizing elements and protein-induced changes in ribonucleoprotein structure. J Biol Chem **278,** 33039-33048. Epub 32003 Jun 33019.

Wilusz, C.J., and Wilusz, J. (2004). Bringing the role of mRNA decay in the control of gene expression into focus. Trends Genet **20,** 491-497.

Wilusz, C.J., Gao, M., Jones, C.L., Wilusz, J., and Peltz, S.W. (2001). Poly(A)-binding proteins regulate both mRNA deadenylation and decapping in yeast cytoplasmic extracts. Rna **7,** 1416-1424.

Wright, P.A., and Knepper, M.A. (1990a). Phosphate-dependent glutaminase activity in rat renal cortical and medullary tubule segments. Am J Physiol **259,** F961-970.

Wright, P.A., and Knepper, M.A. (1990b). Glutamate dehydrogenase activities in microdissected rat nephron segments: effects of acid-base loading. Am J Physiol **259,** F53-59.

Wright, P.A., Burg, M.B., and Knepper, M.A. (1990). Microdissection of kidney tubule segments. Methods Enzymol **191,** 226-231.

Xu, N., Chen, C.Y., and Shyu, A.B. (1997). Modulation of the fate of cytoplasmic mRNA by AU-rich elements: key sequence features controlling mRNA deadenylation and decay. Mol Cell Biol **17,** 4611-4621.

Xu, N., Chen, C.Y., and Shyu, A.B. (2001). Versatile role for hnRNP D isoforms in the differential regulation of cytoplasmic mRNA turnover. Mol Cell Biol **21,** 6960-6971.

Xu, N., Loflin, P., Chen, C.Y., and Shyu, A.B. (1998). A broader role for AU-rich element-mediated mRNA turnover revealed by a new transcriptional pulse strategy. Nucleic Acids Res **26,** 558-565.

Yang, X., Amemiya, M., Peng, Y., Moe, O.W., Preisig, P.A., and Alpern, R.J. (2000). Acid incubation causes exocytic insertion of NHE3 in OKP cells. Am J Physiol Cell Physiol **279,** C410-419.

Yi, R., Qin, Y., Macara, I.G., and Cullen, B.R. (2003). Exportin-5 mediates the nuclear export of pre-microRNAs and short hairpin RNAs. Genes Dev **17,** 3011-3016.

Zeng, Y., Yi, R., and Cullen, B.R. (2003). MicroRNAs and small interfering RNAs can inhibit mRNA expression by similar mechanisms. Proc Natl Acad Sci U S A **100,** 9779-9784.

Zhang, T., Kruys, V., Huez, G., and Gueydan, C. (2002). AU-rich element-mediated translational control: complexity and multiple activities of *trans*-activating factors. Biochem Soc Trans **30,** 952-958.

Zhang, W.W., B. J., Ehrenman, K., Schaefer, A. W., DeMaria, C. T., Crater, D., DeHaven, K., Long, L., Brewer, G. (1993). Purification, characterization, and cDNA cloning of an AU-rich element RNA-binding protein, AUF1. Mol Cell Biol **13,** 7652-7665.